NEW APPROACHES TO THE PRODUCTION AND SEPARATION OF RECOMBINANT PROTEINS

By
Chia-Chang, Hsu

A thesis submitted to the University of Birmingham
for the degree of
DOCTOR OF PHILOSOPHY

School of Chemical Engineering
College of Engineering and Physical Sciences
May 2013

Thesis Abstract

Antibody fragments such as Fab fragments are invaluable for therapeutic and diagnosis purposes. Utilising the robust and relatively low cost *Escherichia coli* expression system for Fab production seems very promising. However, Fab production in *E. coli* currently suffers from issues including low yield and poor solubility of the Fab fragments. In this study, *E. coli* strain CLD048 was initially employed for the production of Fab D1.3 targeted into the periplasm with a target yield of ≥ 100 mg/L. Unfortunately, the fermentation was not successful. Thus, strategies for improving Fab production were explored, comprising lowering cultivation temperature, altering the timing of induction and harvest, and lowering the concentration of the inducer IPTG. The location of Fab D1.3 was shifted from extracellular to the periplasm, the overall Fab yield was increased 50-fold (from 1.4 mg/L to 48 mg/L) and the solubility of Fab D1.3 was improved. Subsequently, optimising release conditions for periplasmic proteins was investigated. Employing 0.1% sodium deoxycholate showed better protein release efficiency than the osmotic shock method. However, the overall titre of Fab D1.3 was not sufficient to meet the goal of ≥ 100 mg/L.

A successful fermentation was demonstrated by expressing A33 Fab′ in *E. coli* strain W3110, which produced 300 mg/L of A33 Fab′ in the periplasm. Various selective protein release methods (osmotic shock, SMALPs (poly(styrene-co-maleic acid) lipid particles) and heat treatment) were subsequently investigated. Heat treatment displayed the highest selectivity for A33 Fab′ release. Consequently, the method was applied to generate a large

quantity of crude *E. coli* periplasmic extract containing A33 Fab′, which was directly employed in the Aqueous Micellar Two-Phase System (AMTPS) for Fab' purification. The system successfully demonstrated the feasibility of continuous protein separation with a highly purified final product (~98%).

In other work, thermo-responsive polymer brush surface modified magnetic particles manufactured in our laboratories were benchmarked against Chelating Sepharose Fast Flow. Haemoglobin and His_6-GFP were employed to exploit the feasibility of thermally mediated target protein elution under binding conditions.

Acknowledgements

I am very grateful and indebted to my supervisor Professor Owen Thomas and Dr Eirini Theodossiou who have supported and challenged me throughout my PhD life. I have not only learnt the knowledge of science but also the attitude of research. I am also indebted to Dr. Tim Overton for guiding me with his broad knowledge in microbiology and consultancy on the *E.coli* fermentation.

I would like also to thank all the students and colleagues from the 'bio' group for their valuable assistance: Dr. Thomas Willett as a genuine advisor in chemistry, Dr. Yao Yu and Dr. Kalliopi Zourna for providing me with their experiences working with magnetic particles and polymer functionlisation (in chapter 6). Dr. Reza Jalalirad and Dr.Christine Müeller for sharing with me for the heavy loaded work during fermentation studies. and Ms Elaine Mittchel, for their willing assistance in the lab.

I am grateful to supervise and work with the Msc students David Valdés Peña, who has done excellent work in chapter 4 contributed to preliminary study with A33 Fab′ shake flask experiment which pre-define the growth condition for the A33 Fab′ fermentation.

Chapter 5 is a co-authorship research paper with Dr. Ingo Fischer and colleagues (KIT, Germany) published on Journal of Chromatography (A) in 2013. The aqueous micellar two-phase systems (AMTPS) was transported and operated by Dr. Ingo Fischer in the University of Birmingham (UK). We provided crude extract from *E.coli* with A33 Fab′ from 5L scale fermentation for demonstrating the feasibility of employing the AMTPS with the functionalised magnetic nanoparticles in continuous protein separation process. Also, we provided A33 Fab′ purification data by the

conventional chromatography (CEX and rProtein G columns) for benchmarking the purification efficiency on the newly developed system (AMTPS).

Finally, I would like to thank my parents for the financial supports and to make me believe I can achieve this milestone in my life.

Thanks

Contents and Appendices

List of Figures

List of Tables

1. Introduction

1.1. Background of the Project

All the research works have done in this thesis is part of the European Framework Programme 7 titled MagPro^{2}Life, which its broad aim is to address these barriers and demonstrate the use of fermenting *E.coli* for expressing recombinant antibody fragments and functionalised thermoresponsive polymer brush modified magnetic (nano) particle separation at pilot-scale for select feed, food and pharmaceutical products. The main objective of the MagPro^{2}Life project is to scale-up innovative nanotechnology based process to pilot-line-scale and demonstrate the feasibility of this technology (Fig. 1.1).

Fig. 1.1 Triangular diagram illustrating the starting point of the European Commission Project 7 and the objective of each working package (European Framework Programme 7).

The first phase of this Ph.D research project was focusing on Work Package 3 (WP3), starting with optimising growth condition for 5 litre scale fermentation of Anti-Hen Egg White Lysozyme Fab D1.3 (expressed from CLD048 *E.coli* strain provided by Avecia) and subsequently systematically examining selective periplasmic release method and applied different purification strategies. Key importance parameters of the *E.coli* fermentation have been altered such as, the cultivation temperature, induction timing and inducer concentration, we have managed to boost the overall production from the initial condition, and directing target protein into periplasm of *E.coli.* Also surprisingly discovered the solubility of Fab D1.3 was also improved. Taking the advantages of above successful example will lead to an easier purification process to perform. Despite the above merits, the overall Fab D1.3 titre was still insufficient to provide for the project partners (i.e. project goal is aiming for production titre with a minimum 100mg/L per batch of 5 L fermentation). Inevitable, another candidate *E.coli* strain was required for antibody fragment production to carry on the research for the project. UCB Celltech has kindly provided A33 Fab′ expressed from pTTOD A33gL4gH2Fab plasmid to us then transforming into W3110 *E.coli* strain to continue the research (Biopharma Line) for the MagPro^{2}Life project. We then employ recombinant A33 Fab′ for testing newly developed magnetic particles with functionalised ligands and other separations techniques (AMTPS), also evaluating the adsorption and desorption behaviour with the currently conventional chromatography support. In the end, two module proteins (Haemoglobin and His_6-GFP) were empolyed to study of recombinant protein purification on thermoresponsive polymer sureface modified magnetic particles and Chelating Sepharose Fast Flow.

1.2. **Antibodies**

Antibodies, often termed 'immunoglobulins', there are five chemically and physically distinct classes of antibody in humans (IgG, IgM, IgA, IgE,IgD) serve two functions: targeting foreign cells and macromolecules and to initiate key defence against pathogenic organisms and toxins (Huber, 1976; Kuby, 1997). The antibody repertoire is able to selectively bind molecules, so called ‘antigens’ recognised as foreign to the organism (Braden and Poljak, 1995; MacCallum *et al.*, 1996). In 1930’s, antibodies were identified as the protective agent in the serum (Kuby, 1997), from the late 1950's to early 1960's the basic structure of antibody was revealed by Gerald M Edelman and Rodney R Porter (Johnstone *et al.*, 1985; Raju, 1999). A key discovery from their fundamental research was able to locate the papain derived Fc and Fab fragments within a framework of light and heavy polypeptide chains and this led to the proposal of the basic four chain model of immunoglobulin G in 1962 (Johnstone *et al.*, 1985). ‘Polyclonal antibodies’ means the antibodies are a population of molecules, recognising many antigenic determinants or 'epitopes' on an antigen with a range of affinities (Kuby, 1997). Those are typically produced by inoculation of a suitable mammal, such as a mouse, rabbit or goat (Cooper and Paterson, 2001; Nakazawa *et al.*, 2010). An antigen is injected into the mammal. This induces the β-lymphocytes to produce IgG immunoglobulins specific for the antigen. This polyclonal IgG is purified from the mammal’s serum (Bak, 2004), and these antibodies are usually produced by immunisation of mammal, such as a mouse, rabbit or goat. Polyclonal antibodies have variety of applications. They can be exploited as a mean of inducing passive immunisation (e.g. for treatment against

Hepatitis A, snakebites and tetanus); they are also extensively employed in diagnostics, immunoturbidemetry, and immunohistochemistry (Bak, 2004). 'Monoclonal antibodies', developed by Kohler and Milstein (1975), to create cell lines producing predetermined, monospecific and monoclonal antibodies (mAB). An immortal cell (a myeloma tumour cell) was fused with a specific predetermined antibody-producing B cell from immunised animals or humans. The resulting hybridoma cell is immortal and synthesises homogeneous, specific mAB. They are identical antibodies identifying one epitope on antigen (Kuby, 1997). Because of their single epitope specificity, monoclonal antibodies have wide applications in diagnostics, research, and therapeutics, ranging from in vitro pregnancy tests against the hCG hormone to in vivo cancer treatments (Bak, 2004)

1.2.1. Structure of antibodies

Basic unit (Ig) is Y-shaped molecule composing four polypeptide chains. Featuring two identical heavy (H) of 50 kDa and two identical light (L) of 25 kDa chains held together by non-covalent interactions and disulphide bridges (Fig. 1.2).

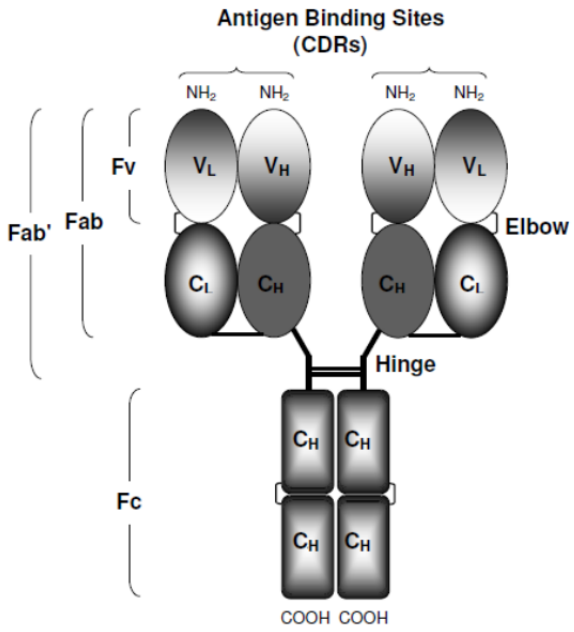

Fig. 1.2 Structure of the immunoglobulin G (IgG). Showing the two heavy chain comprising three constant domains C_H1-3 and V_H, and two light chains containing once constant region (C_L) and one variable region (V_L).(Adopted from Jalalirad, 2010)

Antibody are composed of several globular domains that are rich in β-sheet and have a conserved disulphide bond. The Ig folds are connected by short interdomain linkers, named as elbow, or longer linkers known as hinges. Each variable region has three hypervariable loops (complementary determining regions, CDRs) allows millions of antibodies with different tip structures, that together form a common six-loop antigen binding site. (Padlan, 1994; Halaby *et al.*, 1999; Humphreys, 2007)

1.2.2. Antibody Expression history

The history of antibody has been heavily involved with the testing and production of therapeutic proteins in mammalian tissue culture, most notably using CHO cells (derived from Chinese Hamster Ovaries (Chadd and Chamow, 2001).

The demand for new and improved antibody production systems has arisen in recent years. Many researchers have been working towards alternative antibody expression systems such as yeasts (Saccharomyces or Pichia), filamentous fungi, transgenic plants, and *E. coli* (Harrison and Keshavarz-Moore, 1996; Peeters *et al.*, 2001; Holliger and Hudson, 2005; Farid, 2007; Steinmeyer and McCormick, 2008).

Until Simmons and colleagues (2002) was able to expressed the first full-length immunoglobulins in *Escherichia coli*, the application of *E. coli* expression systems was limited mainly to the production of the fragment antigen binding (Fab fragment) and the portion of the antibody responsible for binding the target antigen. The applications for Fab fragments are frequently used in diagnostic applications, therapeutics, and in testing variable regions slated for reincorporation into full-length monoclonal antibodies (Boleti *et al.*, 1995; Spiridon *et al.*, 2004; Quintero-Hernández *et al.*, 2007; Weisser and Hall, 2009).

Antigen-binding antibody fragments can also be produced by proteolysis of whole antibodies (Johnstone *et al.*, 1985; Raju, 1999). The protease papain digests the full-length IgG and releases the four N-terminal domains and has a molecular weight around 50 kDa. Pepsin cleaves the heavy chains slightly after hinge; thus, the dimeric Fab' fragment, or F(ab)', is produced (Fig. 1.3). Both enzymes release the C-terminal four domains or Fc fragment, which is glycosylated in the C_H2 domain and has effector functions such as serum half-life, complement activation, and recruitment of immune cells (Holliger and Hudson, 2005; Humphreys, 2007).

On the other hand, the smallest fragment (~30 kDa) contains the whole antigen binding site of a whole IgG antibody, which is composed of both the variable heavy chain (V_H) and variable light chain (V_L) domains. This heterodimer fragment, called Fv fragment (for fragment variable), is still capable of binding the antigen, but native Fv fragments are unstable because the non-covalently associated V_L and V_H domains tends to dissociate from each other (Boleti *et al.*, 1995; Braden and Poljak, 1995; Holliger and Hudson, 2005).

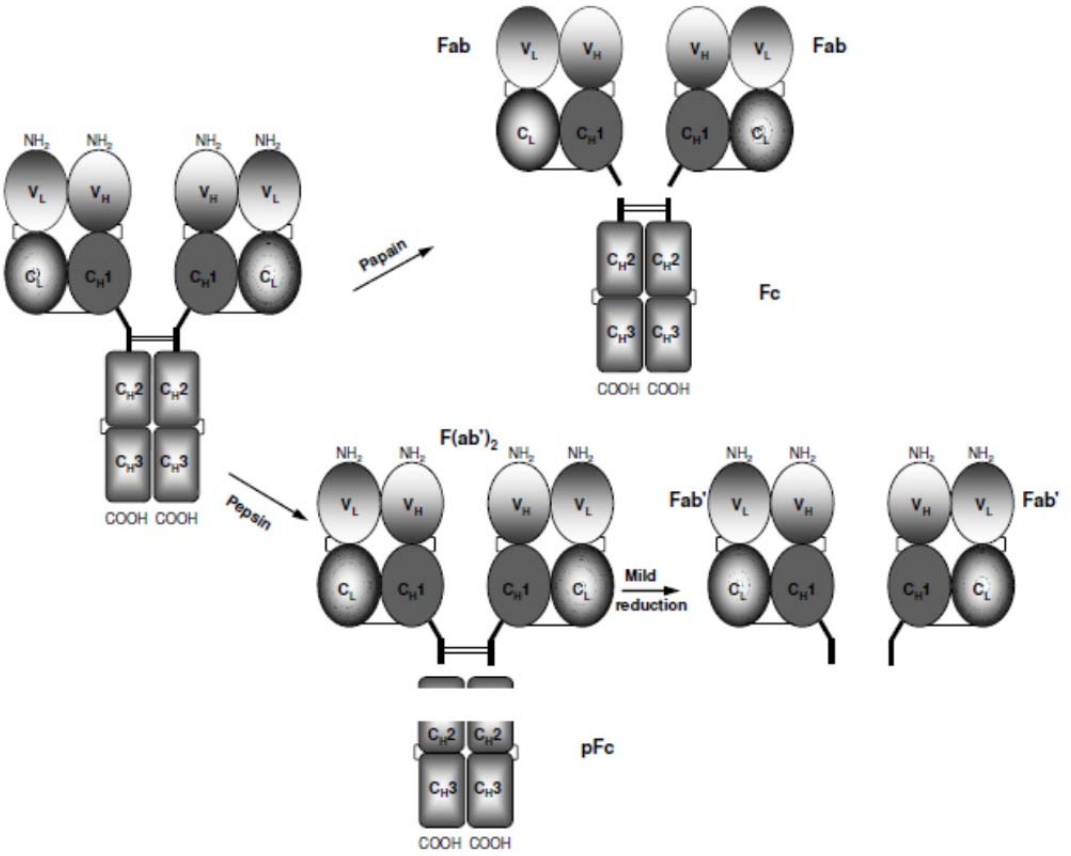

Fig. 1.3 Chemical treatment to digest a Full-length antibody. Papain digestion results in cleavage of the immunoglobulin into Fab and Fc fragments, and pepsin digestion causes cleavage of the IgG molecule into F(ab)'2. Pepsin also digests the Fc regions into fragments.(Adopted from Jalalirad, 2010)

1.2.3. Current state of Fab production

In recent years, various forms of antibody fragment (i.e. Fab, Fv, scFv, V_Hs, diabodies, triabodies, etc.) has been successfully produced in *E.coli* (Humphreys, 2003; Holliger and Hudson, 2005). These smaller fragments have various features (e.g., monomeric binding, lack of effector functions, rapid systemic clearance, and rapid tissue penetration). However, the production of single domain antigen binding fragment (V_Hs) in soluble form is difficult, due to the sticky behaviour of the fragment which would cause aggregation plus low thermal stability. (Huston *et al.*, 1993; Nieba *et al.*, 1997; Arndt *et al.*, 1998). An recent example demonstrated by Quintero-Hernández and his co-workers (2007) in obtaining scFv fragment from a neutralizing mouse antibody (BCF2) was used to produce three derived scFvs. Only one of them was neutralising, however when expressed as Fab, all of them became neutralising fragments in vivo. In striking contrast, the stability of the four Fabs derived from their respective scFvs was improved when tested in the presence of guanidinium chloride. This result has shown by changing the protein conformation from scFv to Fab can improve the functional stability and avoid additional maturation steps. Hence, the antigen-binding fragment (Fab) has been considered a more functionally stable version of recombinant antibodies than single chain antibody fragments (scFvs) (Wörn and Plückthun, 1999, 2001; Humphreys, 2007). Since then, the recombinant antibodies are increasingly popular over a broad spectrum of therapeutic and research applications. In the clinic, antibodies can be fused to species such as tumour, cancer targeting, clot imaging, enzymes, viruses, radionuclides and toxins for drug therapy (Humphreys *et al.*, 1997; Hudson, 1998; Wörn and Plückthun,

2001; Jurado *et al.*, 2002; Natarajan *et al.*, 2008). Several successful applications by fusion a functional protein with a Fab in *E. coli* have reported (Boleti *et al.*, 1995; Dennis *et al.*, 2002; Kellner *et al.*, 2011). The antigen targeting-specific Fab region is fused to a functional protein sequence, thus creating targeted therapeutics with enhanced cell killing. In human medicine, a new concept was developed by fusion of an effector protein onto an antigen recognising antibody fragment for specifically targeting on tumour treatments, called 'magic bullet' (Spooner *et al.*, 1994; Boleti *et al.*, 1995). The effector protein gene directly fused to the gene of an antibody fragment, resulting in new bi-functional recombinant proteins (Neuberger *et al.*, 1984). An example is the employment of cancer-specific bi-functional antibodies targeting cytotoxic molecules to tumour cells and consequently eliminates these tumour cells without harming healthy cells (Boleti *et al.*, 1995). In the laboratory, antibodies have been widely used in immuonoblotting, enzyme-linked immunosorbent assay (ELISA), and affinity purification. The increasing demand for recombinant antibodies has been driving the development towards a multi production systems as can be in yeasts, mammalian cells, transgenic plants and animals, and *Escherichia coli* (Hudson, 1998; Joosten *et al.*, 2003; Andersen and Reilly, 2004). In comparison to other expression systems, *E. coli* has taken the advantage of offering substantially low-cost and robust protein expression, based on well understand with the genetics, physiology and regulatory systems of this organism. A considerable defect of in *E.coli* was lack of post-glycosylation and high-level expression in producing recombinant protein has been resolved by the genetically engineered of the host. For example, there has been reported on production of aglycosylated

Fc-containing antibody in the periplasm of *E. coli* (Simmons *et al.*, 2002). Although, it is deemed that manufacturing of full-length antibody is very difficult in *E. coli* because this organism is not especially well-adapted for the expression of very large, disulphide bond-rich and multimeric proteins. Nevertheless, for many of the mentioned applications, the presence of glycosylation in the Fc constant regions is unnecessary; thus, in these applications, aglycosylated full-length antibodies or smaller antibody fragments can be employed (Andersen and Reilly, 2004). As a type of antibody fragments, the Fab fragment of an antibody contains the antigen-binding site and the four domains (i.e. V_H, C_H1, V_L and C_L); V_H and V_L domains are fused to the following constant antibody domains C_H and C_L, respectively (Fig. 1.2). The smaller size of Fab is more suitable for applications such as tumour penetration and imaging (Boleti *et al.*, 1995), and Fab exhibits a shorter half-life than full-length Manufacture of recombinant proteins in *E. coli*. immunoglobulin G molecules (Andersen and Reilly, 2004), resulting in the faster clearance of the toxic labelled antibody fragments from the circulation in normal organ (Joosten *et al.*, 2003). However, from therapeutic point of view, the short circulating half-life of Fab fragment would be a drawback, but this constraint can be addressed by approaches by employing polyethylene glycol (PEG) attach to Fab fragment (Chapman *et al.*, 1999; Leong *et al.*, 2001; Chapman, 2002) and albumin-binding peptide (Dennis *et al.*, 2002), which have been proved to increase the circulating half-life. In contrast to some of the heavily engineered antibody fragments, the Fab has native sequence; subsequently, it is less likely for the Fab to be immunogenic when used as therapy. The remarkable feature of Fab' is

thermal (> 60°C) and chemical (> 2 M guanidine hydrochloride) stability which makes it resistant to harsh conditioning and purification processes in downstream (Weir and Bailey, 1995; Humphreys, 2007).

1.2.4. Anti − Hen Egg White Lysozyme (HEWL) Fab

Since high-resolution structures complexes of HEWL protein with Fab D1.3 and Fv D1.3 fragments are available (Amit *et al.*, 1985, 1986; Fischmann *et al.*, 1991; Bhat *et al.*, 1994), the conformation of Fab D1.3 has been defined in great details, which is around 50 kDa size protein containing one disulphide bond to link heavy and light chains (Ginnette *et al.*, 1986; Kenett *et al.*, 1987; Fischmann *et al.*, 1991). Apart from their intrinsic interest, antigen–antibody complexes represent a valuable model for the study of protein interactions (Kenett *et al.*, 1987; MacCallum *et al.*, 1996) because (1) the size of the interface typically falls in the standard category (B ≈ 1290 $Å^2$, measured in the HEWL–Fab D1.3 complex) (Fischmann *et al.*, 1991), and (2) negligible conformational changes are expected upon complex formation (the measured RMSD between free and complexed HEWL is 0.64 Å) (Amit *et al.*, 1986; Braden and Poljak, 1995). This allows Fab D1.3 becoming a great tool as an useful mean for the identification of contact surfaces between proteins, based on a general photochemical modification of the polypeptide chain with methylene carbine.

1.2.5. A33 Fab'

Thermo stable A33 Fab' has different toleration profiles when expressed in *E.coli* compared with Fab D1.3 (Humphreys, 2007). It is a disulphide bonded protein with hinge around ~55 kDa and binding to a tumour-associated (human colorectal carcinoma) antigen. The importance of maximising the possible yield is to find the right expression conditions. In an early work, Fab' was expressed with human protein disulphide isomerise (PDI) to increase the yield of antibody fragment in the periplasm of *E. coli* (Humphreys *et al.*, 1996). However, this approach proved to be only helpful with Fab' where inappropriate intra-domain disulphide bonds could be formed (ibid). Moreover, the co-expression of PDI can have a negative effect in overall Fab' production as over-production of chaperone can add to the metabolic burden of the cell, leading to even more decreased growth rates and reduced final biomass (Martínez-Alonso *et al.*, 2010). The production system used in the present work was optimised to deliver a balanced expression of the light (LC) and heavy (HC) chains, which gave the highest Fab′ yield. A small excess of LC is allowed, otherwise the HC is surpassed by the LC's hoard of the folding and secretion machinery (Humphreys *et al.*, 2002).

It is advantageous to target the product to the periplasm rather than the cytoplasm as it accumulates vast majority of host proteins plus DNA and RNA (Hockney, 1994) Furthermore, less degradation, the oxidising environment promotes disulphide bond formation required in the hinge of the Fab' and downstream processing is facilitated (Mücke *et al.*, 2009). Relevant factors affecting secretion through the *Sec* pathway (the protein translocation pathway from the cytoplasm across the cytoplasmic membrane) are culture

medium, amino acid composition, size of protein and signal peptide, where in the present work the LC and HC are preceded by the OmpA signal peptide (Mori and Ito, 2001; Humphreys, 2007; Mergulhão and Monteiro, 2007). Leakage to the culture broth is also not desired as the viscosity of the culture broth is increased and this negatively affects operations such as filtration and centrifugation and Fab' from the supernatant may be degraded or incorrectly folded. Leaking cells are less robust and they could lyse during recovery or periplasmic extraction, increasing the level of contaminants for the subsequent downstream processing steps (Flaschel and Friehs, 1993; Choi *et al.*, 2006).

The reasons for failure to produce high yields of recombinant protein are well known, mostly due to the accumulation of incorrectly folded proteins caused by the overwhelming expression rates which provoke saturation of the post-translational modifications machinery (N-terminal, C-terminal and cross-linking modifications, glycosylation, etc) (Sevastsyanovich *et al.*, 2009). This causes a toxic effect on the cell that triggers stress responses that lead to growth arrest, loss of cultivability and ultimately death and lysis. Not only does stress affect cellular physiology, it can also have negative effects on recombinant protein quantity and quality caused by increased proteolysis and/or mistranslation of the product (Ramírez and Bentley, 1995; Hoffmann and Rinas, 2004). Since it is desired to partition Fab′ in the soluble form to the periplasm, accumulation of the product is achieved through a long period of induction during which expression is done at moderate levels to reduce stress. This permits growth to higher biomass concentrations and thus higher quantities of Fab′.

1.2.6. Expression Fab in E.coli periplasm

There are three locations for the manufacture of soluble proteins in *E. coli*: the cytoplasm, the periplasm, and leak into the culture media. The periplasm is preferable for expression of soluble antibodies, mainly because it is the naturally oxidizing environment to facilitates the formation of disulphide bonds, accurately cleaved N-terminal extension "signal peptide" to form correct N-terminus, and the exposure to extracellular chemical agents (<500 Da in size) which aid the folding and modification of antibodies. Key importance of locating proteins in the periplasm can prevent highly diluted when leak to culture media and avoid contamination with DNA or RNA in cytoplasm, with careful considered harvest and extraction can result in very useful concentration of the periplasm proteins (Humphreys, 2007). A diversity of approaches, including optimising the expression of light and heavy chains to obtain augmented titres of antibody fragments (Humphreys *et al.*, 2002), host cell engineering to hinder proteolysis of the light chain (Chen *et al.*, 2004), and co-expression of chaperones to ameliorate folding or disulphide bond formation (Ramm and Plückthun, 2000; Humphreys *et al.*, 2002) have been implemented to enhance the periplasmic production level of antibody fragments up to 2 g/L using the *E. coli* system (Carter *et al.*, 1992; Chen *et al.*, 2004). Having achieved desirable levels of expression in the periplasm, it is required to develop the extraction processes to release the maximise amount of the recombinant protein while minimising the release of other host proteins and biomolecules. At large scale, the prevalent technique for purifying proteins from periplasm includes breaking the cytoplasmic membrane and the outer membrane and discharging the entire content of the bacterial cells. In as

much as approximately 80% of the total cellular protein is located in the cytoplasm, this method of non-selective-protein release makes the purification process burdensome (Pugsley, 1993). in the laboratory scale, the methods frequently used for cell fractionation and isolating periplasmic fraction are spheroplasting and osmotic shock treatment (Neu and Heppel, 1965; Neu *et al.*, 1967), but these techniques are not capable to deal with the culture volume over 10 litres (Neu and Heppel, 1965). Directing Fab into periplasm and looking for cell disruptions techniques which is selective and effective at large scale and smooth the subsequent protein recovery processes is still a goal to be achieved.

1.3. Strategies for improving Fab accumulation in *E.coli* periplasm

1.3.1. Influence of cultivation temperature and shifting temperature upon induction for Fab expression

E.coli can maintain balanced growth between 20°C and 37°C. Raising the temperature above 40°C or lowering it below 20°C results in progressively slower growth, until growth ceases at the maximum temperature of growth, 49°C, or the minimum, 8°C (Jones *et al.*, 1987). Comprehensive studies on the factors that influence expression conditions and product yield are still required for full process development (Yee and Blanch, 1992; Yoon *et al.*, 1994; Ramírez and Bentley, 1995; Corisdeo and Wang, 2004; Pelegrine and Gasparetto, 2005; Wunschel *et al.*, 2005). An early example of applying low temperature resulting in higher yield of soluble Fd' fragment production, which

was expressed with a complementary ƙ light chain fragment in order to form of Fab fragment. The higher yield of active, soluble Fab fragments was obtained at 21°C and 30°C then at 37°C (Cabilly, 1989). A study was done by (Pinsach *et al.*, 2008) showed a group of *E.coli* fed-batch fermentation was conducted under different temperature (37°C, 33°C and 28°C). The effects of lowering the temperature were analysed by the specific enzyme active and protein content. Reduction of the specific activity loss was observed when the process temperature was decreased to 28°C. Lower plasmid copy number and specific production rates probably alleviated the metabolic load on host cell during recombinant protein overexpression. More recently (Rodríguez-Carmona *et al.*, 2012) has also investigated the influence of temperature (37°C, 33°C and 28°C) on recombinant Fab expression and secretion to periplasm in *E. coli*. The results has shown that biomass yield was not affected within this temperature range whilst product yield increased as temperature decreased, but the decrease of temperature might lead to the protein leakage into culture broth. Above results have proven that carefully choosing the cultivation temperature would massively affect on the protein activity and its yield and also the location of recombinant proteins.

Temperature obviously is a very crucial factor to control the proteolysis by preventing the possible stress response (heat stress and induction stress), which might lead to increase protein production yield due to reduce the degree of proteolysis associated with chaperons and proteolysis proteins. (Enfors, 1992). It has been examined the usefulness fermentation and strain engineering approaches in circumventing the problem of csp*A* promoter repression following prolonged incubation at low temperature. Temperature

cycling and successive temperature downshift in fermentors are found to only marginally improve yield. Vasina and coworkers in 1998 investigated whether successive temperature downshifts could be used to maximise the yields of β-galactosidase. This approach appeared feasible since temperature drops as small as 7°C have been shown to be sufficient to induce the cspA promoter in shake flask cultures. Meanwhile, in 2.5-L batch fermentors were transferred from 37°C to 29°C, about 4000 U of activity accumulated within 1 h before becoming diluted as a result of biomass increase, which is a rather simple tactic of controlling of proteolysis on cultivation level. Further, it has been reported lowering the bacterial growth temperature could decrease periplasmic aggregation and increase the yield of soluble antibody protein (Skerra and Plückthun, 1991). Moreover, protein degradation rate will decrease with decreased temperature in accordance to the Arrhenius' Law, and protein misfolding often occurs at high temperatures due to either heat damage or due to an increase of protein synthesis rate (Enfors, 1992). For these reasons, the most straightforward as well as promising strategy to improve the quality for Fab fragment production in *E.coli* was to identify the optimal process temperature for recombinant protein production.

1.3.2. Influence of inducer concentration (Isopropyl β-D-1-thiogalactopyranoside)

Genes are either expressed constitutively or regulated. Two different classes of regulators have been described, transcriptional repressors and transcriptional activators. Repressors bind to operators located either within the promoter region or immediately downstream from it and, in most cases,

prevent RNA polymerase promoter binding or act as a road-block. To relieve repression, the repressor has to dissociate from its operator. In some cases, an inducer will be either synthesised by the cell or taken up from the environment which binds to the repressor causing dissociation from its operator (Schumann and Ferreira, 2004). Isopropyl β-D-1-thiogalactopyranoside (IPTG) a very commonly inducer for expression recombinant protein in *E.coli* system, often working in the combination ranges of promoter which regulate tightly and strongly for the protein expression (Yansura and Henner, 1984; Weickert *et al.*, 1996; Jeong and Lee, 2000).The disadvantage of using IPTG as an inducer is the high metabolic load imposed by it, often causing the stress response from cells and leads to inhibit protein production (Kilikian *et al.*, 2000). When compared with lactose induction, as assessed by the cell protein content and stability, indicates that lactose is probably the most appropriate inducer for the synthesis of this heterologous protein (Neubauer *et al.*, 1992; Donovan *et al.*, 1996; Gombert and Kilikian, 1998). However, unlike IPTG as an enzyme cannot be consumed, lactose gets metabolised by the cells, depletion of lactose eventually would cause transcriptional response decreases, also change the pH of the medium which might potentially influence protein expression and bacterial growth. A generic improving protocol for recombinant protein production in *E.coli* was developed by (Sevastsyanovich *et al.*, 2009). By using a C-terminal green fluorescent protein (GFP) fusion to a model target protein, *Escherichia coli* CheY, was exploited both as a reporter of the accumulation of soluble recombinant protein, and to develop a generic approach to optimise protein yields. Eight micro mole of [IPTG] as inducer suggested obtaining the optimal

product yields. The improved protocol was shown to be suitable for process scale-up and intensification.

1.4. Selective release of periplasmic proteins and purification techniques

1.4.1. Release methods

1.4.1.1. Cold osmotic shock

This is by far the best and easiest method for do fractionation of periplasmic, cytoplasmic and membrane. However, it is rather labour intense and only practical in the small scale. Cell pellets obtained from 1 mL fermentation samples were resuspended in an osmotic shock solution (designated OS1) containing 20 mM Tris-HCl buffer, pH 8.0, supplemented with 2.5 mM EDTA and 20% sucrose. The use of adding sucrose here was to stabilise the inner membrane for preventing leakage from cytoplasm. After a static incubation on ice for 600 s, the cells were harvested by centrifugation (15,800 *g*, 120 s) and the supernatants were immediately frozen at −20°C. The resulting cell pellets (spheroplasts) were then resuspended in a second osmotic shock solution (designated OS2) without adding sucrose (i.e. 20 mM Tris-HCl buffer pH 8.0, containing 2.5 mM EDTA) and incubated on ice for 600 s. Following centrifugation (15,800 *g*, 120 s), the supernatants were then removed and stored at −20°C until required (Neu and Heppel, 1965; Neu *et al.*, 1967; Humphreys, 2007; Jalalirad, 2010).

1.4.1.2. Heat treatment

This method is only applicable to the thermally stable protein, such as Fab'. The extraction buffer comprises 100 mM Tris, 10 mM EDTA, pH 7.4. The ratio of sample to resuspension buffer is 1:1 (i.e. 1mL fermentation pellet resuspend with 1mL extraction buffer) Incubation was performed at 60°C for 16 h. The elevated temperature will ensure the removal of any incorrectly folded non-disulphide Fab′ and truncated Fab′ species, as well as to pre clean a substantial percentage of host proteins, thereby resulting in enrichment of heterologous protein (Weir and Bailey, 1995; Humphreys *et al.*, 1997; Popplewell *et al.*, 2005; Humphreys, 2007).

1.4.1.3. Poly(styrene-co-maleic acid) lipid particles- SMALPs

In order to study the structure and function of a protein, it is generally required that the protein in question is purified away from all others. For soluble proteins, this process is greatly aided by the lack of any restriction on the free and independent diffusion of individual protein particles in three dimensions (Jamshad *et al.*, 2011). This is not the case for membrane proteins, as the membrane itself forms a continuum that joins the proteins within the membrane with one another. The membrane therefore needs to be disrupted in order to separate and hence purification of membrane proteins. The recent advances in the methods employed to separate membrane proteins before purification generally moves away from solubilisation methods based on the use of small surfactants, which have been shown to suffer from significant practical problems(Froner *et al.*, 2011; Jamshad *et al.*, 2011). On contrast, the poly(styrene-co-maleic acid) lipid particles (SMALPs) is created from one of

the nanotechnology that uses a range of reagents that fragment the membrane into nanometre-scale particles to surround the protein completely with the local membrane environment and encapsulate the membrane protein in a 10 nm disc-like structure (Jamshad *et al.*, 2011). Moreover, the amphipathic polymer poly(styrene-co-maleic acid) is reversible via a pH dependent conversion (Knowles *et al.*, 2009), which makes this polymer more applicable in different environment conditions. More importantly, SMA has been proved can be used for *in vivo* administration which makes it ideally suits to purification and further biochemical study (Froner *et al.*, 2011).

1.4.2. Newly developed separation techniques- Mix brushes smart polymers on magnetic particles (thermo responsive)

1.4.2.1. Magnetic particles and adsorbents

Nowadays, there are two ways to get magnetic particles either synthesis in the laboratory, or commercially available products can be found on the market. The properties of magnetic particle such as superparamagnetism, magnetite content, the specific surface area, diameter size distribution, porosity, disparity and functionalisation possibilities, are very important to the selection of desirable applications. Although many of the particles are available behave like superparamagnetic and only responding to an external magnetic field, but not interacting themselves in the absence of magnetic field is suitable for High Gradient Magnetic Fishing (HGMF), because the magnetic particles can be

easily resuspended and avoid agglomeration thereby remaining in suspension for a long time (Teotia and Gupta, 2001).

Traditional chromatography supports with immobilised affinity ligands are enabling magnetic separation to bind specific target molecular, such as, antibodies, protein A and Protein G are used most often in the cases of proteins and peptides isolation (Cuatrecasas, 1971). Magnetic particles can also serve as generic solid phases to which native or modified affinity ligands immobilisation (i.e. protein A, protein G or antibodies) (Weetall and Lee, 1989). It is also feasible to immobilise other ligands of interest to both commercial and laboratory made magnetic particles then used as an affinity chromatography in HGMF system (Heebøll-Nielsen *et al.*, 2003). The polyvinyl alcohol magnetic beads (M−PVA) manufactured by Chemagen Biopolymer Technologie AG (Baesweiler, Germany) were used to carry out all studies in this thesis (Fig. 1.4)

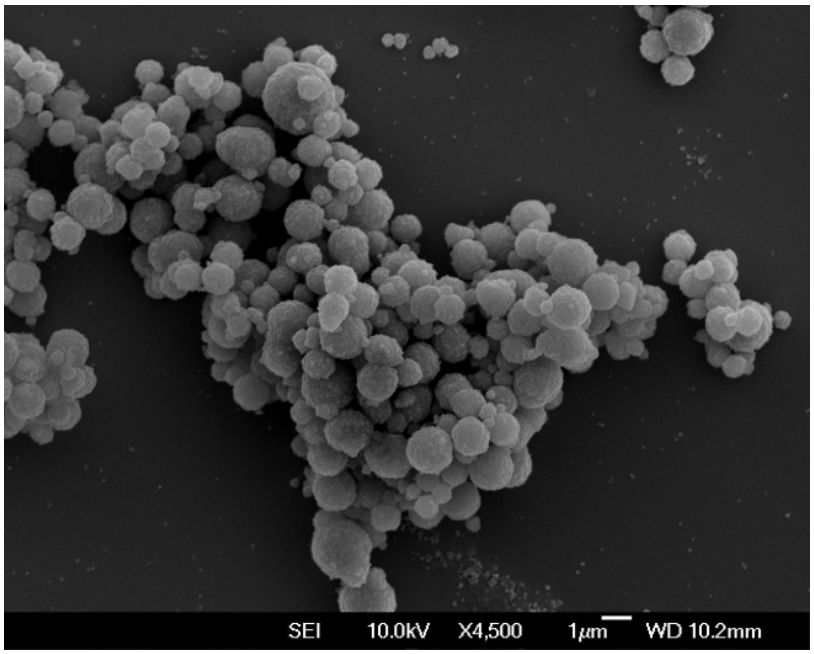

Fig. 1.4 SEM reveals the m-PVA particles from the batch number R2-109027 supplied from Chemagen Biopolymer Technologie AG (Baesweiler, Germany), with magnetite content 50-60%, sized distribution: 1-3 µm, Mr: 130,000, degree of hydrolysis: 86.7-87.8%, and specific surface area: ca. 40 m2/g.

These beads have been developed by an innovative suspension-based production process, which is patented worldwide and allows a very economical production of biocompatible magnetic beads based on polyvinyl alcohol. The main advantages of these magnetic beads are the hydrophilicity of the PVA surface, the biocompatibility, which enables the use of M−PVA beads in medical therapy, the individually tunable sizes of the M−PVA beads, and depending on the application, the chemical functionality of the matrix can be used for the most different modifications (www.chemagen.de). These advantages lead to excellent magnetic particles applicable in a huge variety of separation and purification processes.

1.4.2.2. 'Smart' polymers-Thermoresponsive

'Smart' or stimulus-responsive polymers undergo strong conformational changes when only small changes in the environment (e.g. pH, temperature, ionic strength, electric or magnetic field, or other parameters) occur. They are also named 'intelligent' or 'environmental' polymers, and they undergo fast, reversible changes in microstructure from a hydrophilic to a hydrophobic state (Galaev and Mattiasson, 2007).

Since 10 years ago, smart polymeric materials have become to widely apply in biotechnology in numerous ways. Since the term "smart polymeric materials" encompasses a wide spectrum of different compounds with huge potential for bioseparation applications, scientists have grown great interest in generating and manipulating these compounds (Roy and Gupta, 2003). Recently a group of polymers has been described and characterised by their unique properties. The solubility decreases when the temperature is increased by few degrees. The phenomenon as such may not be unique, but this property started to attract attention among biotechnologists for developing further applications. Temperature is absolutely critical for these class of polymers due to the phase transition occurring when the temperature reaches the lower critical solution temperature (LCST) (Fig. 1.5). For example the most commonly used thermoresponsive polymer, poly(*N*-Isopropylacrylamide) (p(NIPAAm)) possesses inverse solubility upon heating, a property contrary to the behaviour of most polymers in organic solvents under atmospheric pressure near room temperature. Its macromolecular transition from a hydrophilic to hydrophobic structure occurs suddenly at the lower critical

solution temperature (LCST), which experimentally lies between 30°C and 35°C (Schild, 1992).

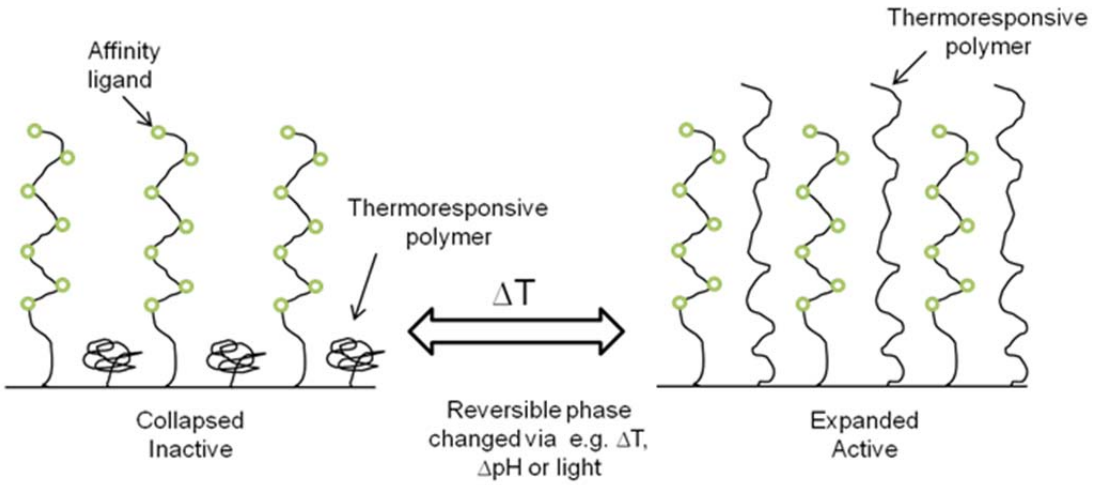

Fig. 1.5 Schematic presentation of the mechanism of collapsed and expanded smart polymers.

The concept of using metal chelates in affinity techniques presents a milestone in bioseparation (Porath *et al.*, 1975). Immobilised metal affinity (IMA) techniques (Andersson *et al.*, 1991; Arnold, 1991), IMA-chromatography (IMAC) and metal chelate affinity precipitation (MCAP) (Galaev *et al.*, 1997; Kumar *et al.*, 1998), are now being widely applied in protein purification, particularly when dealing with products requiring high purity. The technique offers a number of important advantages over other type affinity techniques for protein purification, especially subject to the binding capacity, ligand stability, matrix regeneration and protein recovery (Arnold, 1991). The technique is based on the selective interaction between the electron donor groups on the proteins and on the transition-metal ions [Cu(II), Ni(II), Zn(II) or Co(II)] which are loaded on the chelating ligands coupled to a solid support. The amino acids histidine, cysteine, tryptophan, and arginine have strong

electron donor groups in their side chains, the position of those amino acids on protein and the presence of such exposed residues are important factors for the success of proteins interaction with chelated metal ion ligands. Various ligands like protease inhibitors, antibodies, nucleotides, carbohydrates, and triazine dyes have been successfully used in affinity precipitation (Gupta and Mattiasson, 1994). Chelating metal ions offer many advantages over classical biological affinity types, as they are small molecules, inexpensive, chemically and physically tolerant, and easily coupled on matrices at high density resulting in high binding capacity adsorbents.

The metal chelating ligand, poly-vinylimidazole, p(VI) has been proposed for metal chelate affinity precipitation of proteins (Galaev *et al.*, 1997). When it is copolymerised with p(NIPAAm), the mixed polymer brushes of p(VI + NIPAAm) forms a complex with metal ions in such a way that two to three imidazole residues coordinate with a single metal ion (Kumar *et al.*, 1998). This is possible since the flexible p(VI + NIPAAm) copolymer in solution can have a conformation in which imidazole groups are close enough to coordinate with the same metal ion. It is therefore an unusual but excellent behaviour for downstream separation, by grafting thermoresponsive polymers with metal chelated ligands on magnetic particles to create an intellectual polymer brush layers on magnetic particle used in High-Gradient Magnetic Fishing (HGMF).

1.5. **Aim of this thesis.**

The broad objective of this thesis has been to design an improved new process for periplasmic recombinant protein production and demonstrate the feasibility of newly innovated purification technology.

Initially, recombinant proteins. *E. coli* CLD048 expresses anti hen egg white lysozyme Fab (so called Fab D1.3) in the periplasm. Due to the nature of this particular Fab, lysozyme is prohibited during cell lysis must be accepted. The aim of chapter 2 was to optimise the fermentation process for Fab D1.3 production from *E. coli* strain (CLD048), and to improve production titre, location and solubility by altering fermentation conditions (i.e. temperature, induction concentration, timing for induction and harvest during fed-batch cultivation).

The aim of chapter 3 was to investigate periplasmic protein release by examining different extraction method and condition systematically to identify better/optimum condition applied for periplasmic proteins release. Subsequently, exploring the possibilities of direct capturing Fab D1.3 from the culture broth and periplasmic fraction (i.e. supernatant from osmotic shock 1 solution) by employing cation exchange (HiTrap SP_XL) and affinity chromatography (HiTrap rProtein G).

The aim of chapter 4 was to employ an alternative periplasmically expressed A33 Fab′ for large quantity Fab production (> 100 mg/L). Due to the poor yield of Fab D1.3 from fermentations and problematic conditioning occurring in the chromatography purification steps, the stain was forced to abandon. Initially,

the preliminary shake flask result was to identify the potential growth condition and production of the A33 Fab′ fermentation. Later, three selective periplasmic release methods (i.e. osmotic shock, heat treatment and SMALPs) were investigated to determine which method is more suitable to apply for extracting A33 Fab′ from the periplasm.

The aim of chapter 5 was to demonstrate direct capture of the antibody fragment A33 Fab´ from a crude *E. coli* periplasmic extract on CEX functionalised magnetic nano-particle sorbents with two aqueous micellar systems (ATPS). Also it was benchmarking with commercial available chromatographic columns (HiTrap rProtein G and Fractogel EMD SO3 cation exchanger) to evaluate the purification performance. We also investigated the feasibility of using ATPS in continuous protein separation.

The aim of chapter 6 was to employ two model proteins with rich histidine (GFP-His_6, Haemoglobin) to study the kinetic of protein adsorption and desorption behaviour on the thermoresponsive polymer brush surface modified M-PVA particle created by Ce(IV) reaction. Further investigation the influence of additives on the temperature induced phase transition of ungrafted polymers (i.e. poly(*N*-vinylimidazole), poly(*N*-isopropylacrylamide)) in solution.

.

1.6. **References**

Amit, A., Mariuzza, R., Phillips, S., and Poljak, R. (1986). Three-dimensional structure of an antigen-antibody complex at 2.8 A resolution. Science (80-.). *233*: 747–753.

Amit, A.G., Mariuzza, R.A., Phillips, S.E. V., and Poljak, R.J. (1985). Three-dimensional structure of an antigen–antibody complex at 6 Å resolution. Nature *313*: 156–158.

Andersen, D.C., and Reilly, D.E. (2004). Production technologies for monoclonal antibodies and their fragments. Curr. Opin. Biotechnol. *15*: 456–62.

Andersson, L., Sulkowski, E., and Porath, J. (1991). Immobilized metal ion affinity chromatography of serum albumins. Bioseparation *2*: 15–22.

Arndt, K.M., Müller, K.M., and Plückthun, A. (1998). Factors influencing the dimer to monomer transition of an antibody single-chain Fv fragment. Biochemistry *37*: 12918–26.

Arnold, F.H. (1991). Metal-Affinity Separations: A New Dimension in Protein Processing. Biotechnology. (N. Y). *9*: 151–6.

Bak, H. (2004). New downstream processes for antibodies: From rabbit serum to Ig-fraction. Technical University of Denmark.

Bhat, T.N., Bentley, G.A., Boulot, G., Greene, M.I., Tello, D., Dall'Acqua, W., Souchon, H., Schwarz, F.P., Mariuzza, R. a, and Poljak, R.J. (1994). Bound water molecules and conformational stabilization help mediate an antigen-antibody association. Proc. Natl. Acad. Sci. U. S. A. *91*: 1089–93.

Boleti, E., Deonarain, M.P., Spooner, R.A., Smith, A.J., Epenetos, A.A., and George, A.J.T. (1995). Construction, expression and characterisation of a single chain anti-tumour antibody (scFv)-IL-2 fusion protein. Ann. Onc. *6*: 945–947.

Braden, B.C., and Poljak, R.J. (1995). Structural features of the reactions between antibodies and protein antigens. FASEB J. *9*: 9–16.

Cabilly, S. (1989). Growth at sub-optimal temperatures allows the production of functional, antigen-binding Fab fragments in Escherichia coli. Gene *85*: 553–557.

Carter, P., Kelley, R.F., Rodrigues, M.L., Snedecor, B., Covarrubias, M., Velligan, M.D., Wong, W.L., Rowland, A.M., Kotts, C.E., and Carver, M.E. (1992). High level Escherichia coli expression and production of a bivalent humanized antibody fragment. Biotechnology. (N. Y). *10*: 163–7.

Chadd, H.E., and Chamow, S.M. (2001). Therapeutic antibody expression technology. Curr. Opin. Biotechnol. *12*: 188–194.

Chapman, a P., Antoniw, P., Spitali, M., West, S., Stephens, S., and King, D.J. (1999). Therapeutic antibody fragments with prolonged in vivo half-lives. Nat. Biotechnol. *17*: 780–3.

Chapman, A.P. (2002). PEGylated antibodies and antibody fragments for improved therapy: a review. Adv. Drug Deliv. Rev. *54*: 531–545.

Chen, C., Snedecor, B., Nishihara, J.C., Joly, J.C., McFarland, N., Andersen, D.C., Battersby, J.E., and Champion, K.M. (2004). High-level accumulation of a recombinant antibody fragment in the periplasm of Escherichia coli requires a triple-mutant (degP prc spr) host strain. Biotechnol. Bioeng. *85*: 463–74.

Choi, J.H., Keum, K.C., and Lee, S.Y. (2006). Production of recombinant proteins by high cell density culture of Escherichia coli. Chem. Eng. Sci. *61*: 876–885.

Cooper, H.M., and Paterson, Y. (2001). Production of polyclonal antisera. Curr. Protoc. Cell Biol. *Chapter 16*: Unit 16.2.

Corisdeo, S., and Wang, B. (2004). Functional expression and display of an antibody Fab fragment in Escherichia coli: study of vector designs and culture conditions. Protein Expr. Purif. *34*: 270–9.

Cuatrecasas, P. (1971). Affinity chromatography. Annu. Rev. Biochem. *40*: 259–78.

Dennis, M.S., Zhang, M., Meng, Y.G., Kadkhodayan, M., Kirchhofer, D., Combs, D., and Damico, L.A. (2002). Albumin binding as a general strategy for improving the pharmacokinetics of proteins. J. Biol. Chem. *277*: 35035–43.

Donovan, R.S., Robinson, C.W., and Glick, B.R. (1996). Review: optimizing inducer and culture conditions for expression of foreign proteins under the control of the lac promoter. J. Ind. Microbiol. *16*: 145–54.

Enfors, S.-O.O. (1992). Control of in vivo proteolysis in the production of recombinant proteins. Trends Biotechnol. *10*: 310–5.

Farid, S.S. (2007). Process economics of industrial monoclonal antibody manufacture. J. Chromatogr. B. Analyt. Technol. Biomed. Life Sci. *848*: 8–18.

Fischmann, T.O., Bentley, G.A., Bhat, T.N., Boulot, G., Mariuzza, R.A., Phillips, S.E., Tello, D., and Poljak, R.J. (1991). Crystallographic refinement of the three-dimensional structure of the FabD1.3-lysozyme complex at 2.5-A resolution. J. Biol. Chem. *266*: 12915–20.

Flaschel, E., and Friehs, K. (1993). Improvement of downstream processing of recombinant proteins by means of genetic engineering methods. Biotechnol. Adv. *11*: 31–77.

Froner, E., D'Amato, E., Adamo, R., Prtljaga, N., Larcheri, S., Pavesi, L., Rigo, A., Potrich, C., and Scarpa, M. (2011). Deoxycholate as an efficient coating agent for hydrophilic silicon nanocrystals. J. Colloid Interface Sci. *358*: 86–92.

Galaev, I., and Mattiasson, B. (2007). Smart Polymers: Applications in Biotechnology and Biomedicine (CRC Press).

Galaev, I.Y., Kumar, A., Agarwal, R., Gupta, M.N., and Mattiasson, B. (1997). Imidazole—a new ligand for metal affinity precipitation. Appl. Biochem. Biotechnol. *68*: 121–133.

Ginnette, B., Carlos, R., Bentley, G.A., Poljak, R.J., Barbier, E., Guern, C. Le, and Cazenave, P.-A. (1986). Preliminary Crystallographic Sttidy of a Complex Between the Fab Fragment of a Monoclonal Anti-lysozyme Antibody (D1 . 3) and the Fab Fragment from an. J. Mol. Biol. 577–579.

Gombert, a K., and Kilikian, B. V (1998). Recombinant gene expression in Escherichia coli cultivation using lactose as inducer. J. Biotechnol. *60*: 47–54.

Gupta, M.N., and Mattiasson, B. (1994). Affinity precipitation. In Highly Selective Separations in Biotechnology, G. Street, ed. (Dordrecht: Springer Netherlands), pp 7–33.

Halaby, D.M., Poupon, A., and Mornon, J. (1999). The immunoglobulin fold family: sequence analysis and 3D structure comparisons. Protein Eng. *12*: 563–71.

Harrison, J.S., and Keshavarz-Moore, E. (1996). Production of antibody fragments in Escherichia coli. Ann. N. Y. Acad. Sci. *782*: 143–58.

Heebøll-Nielsen, A., Choe, W.-S., Middelberg, A.P.J., and Thomas, O.R.T. (2003). Efficient inclusion body processing using chemical extraction and high gradient magnetic fishing. Biotechnol. Prog. *19*: 887–98.

Hockney, R.C. (1994). Recent developments in heterologous protein production in Escherichia coli. Trends Biotechnol. *12*: 456–63.

Hoffmann, F., and Rinas, U. (2004). Stress induced by recombinant protein production in Escherichia coli. Adv. Biochem. Eng. Biotechnol. *89*: 73–92.

Holliger, P., and Hudson, P.J. (2005). Engineered antibody fragments and the rise of single domains. Nat. Biotechnol. *23*: 1126–36.

Huber, R. (1976). Antibody structure. Trends Biochem. Sci. *1*: 174–178.

Hudson, P.J. (1998). Recombinant antibody fragments. Curr. Opin. Biotechnol. *9*: 395–402.

Humphreys, D.P. (2003). Production of antibodies and antibody fragments in Escherichia coli and a comparison of their functions, uses and modification. Curr. Opin. Drug Discov. Devel. *6*: 188–96.

Humphreys, D.P. (2007). Periplasmic Expression of Antibody Fragments. In The Periplasm, (American Society for Microbiology), pp 361–388.

Humphreys, D.P., Carrington, B., Bowering, L.C., Ganesh, R., Sehdev, M., Smith, B.J., King, L.M., Reeks, D.G., Lawson, A., and Popplewell, A.G. (2002). A plasmid system for optimization of Fab' production in Escherichia coli: importance of balance of heavy chain and light chain synthesis. Protein Expr. Purif. *26*: 309–20.

Humphreys, D.P., Chapman, a P., Reeks, D.G., Lang, V., and Stephens, P.E. (1997). Formation of dimeric Fabs in Escherichia coli: effect of hinge size and isotype, presence of interchain disulphide bond, Fab' expression levels, tail piece sequences and growth conditions. J. Immunol. Methods *209*: 193–202.

Humphreys, D.P., Weir, N., Lawson, a, Mountain, a, and Lund, P. a (1996). Co-expression of human protein disulphide isomerase (PDI) can increase the yield of an antibody Fab' fragment expressed in Escherichia coli. FEBS Lett. *380*: 194–7.

Huston, J.S., McCartney, J., Tai, M.S., Mottola-Hartshorn, C., Jin, D., Warren, F., Keck, P., and Oppermann, H. (1993). Medical applications of single-chain antibodies. Int. Rev. Immunol. *10*: 195–217.

Jalalirad, R. (2010). Improving the recovery of "difficult to release" periplasmically-expressed products from recombinant E. coli. University of Birmingham.

Jamshad, M., Lin, Y.-P., Knowles, T.J., Parslow, R. a, Harris, C., Wheatley, M., Poyner, D.R., Bill, R.M., Thomas, O.R.T., Overduin, M., and Dafforn, T.R. (2011). Surfactant-free purification of membrane proteins with intact native membrane environment. Biochem. Soc. Trans. *39*: 813–8.

Jeong, K.J., and Lee, S.Y. (2000). Secretory production of human leptin in Escherichia coli. Biotechnol. Bioeng. *67*: 398–407.

Johnstone, A.P.P., Kerr, M.A. a, and Turner, M.W.W. (1985). Rodney Robert Porter (1917-1985). J. Immunol. Methods *85*: 1–4.

Jones, P.G., Vanbogelen, R.A., and Neidhardt, F.C. (1987). Induction of proteins in response to low temperature in Escherichia coli. J. Bacteriol. *169*: 2092–2095.

Joosten, V., Lokman, C., Hondel, C.A. Van Den, and Punt, P.J. (2003). The production of antibody fragments and antibody fusion proteins by yeasts and filamentous fungi. Microb. Cell … *15*: 1.

Jurado, P., Ritz, D., Beckwith, J., Lorenzo, V. de, and Fernández, L.A. (2002). Production of functional single-chain Fv antibodies in the cytoplasm of Escherichia coli. J. Mol. Biol. *320*: 1–10.

Kellner, C., Bleeker, W.K., Lammerts van Bueren, J.J., Staudinger, M., Klausz, K., Derer, S., Glorius, P., Muskulus, A., Goeij, B.E.C.G. de, Winkel, J.G.J. van de, Parren, P.W.H.I., Valerius, T., Gramatzki, M., and Peipp, M. (2011). Human kappa light chain targeted Pseudomonas exotoxin A--identifying human antibodies and Fab fragments with favorable characteristics for antibody-drug conjugate development. J. Immunol. Methods *371*: 122–33.

Kenett, D., Fleminger, G., Katchalski-Katzir, E., and Poljak, R.J. (1987). Lysozyme bound to the D1.3 monoclonal antibody retains enzymatic activity in assays using N-acetylglucosamine oligomers as substrate. Mol. Immunol. *24*: 313–6.

Kilikian, B.V., Suárez, I.D., Liria, C.W., and Gombert, A.K. (2000). Process strategies to improve heterologous protein production in Escherichia coli under lactose or IPTG induction. Process Biochem. *35*: 1019–1025.

Knowles, T.J., Finka, R., Smith, C., Lin, Y.-P., Dafforn, T., and Overduin, M. (2009). Membrane proteins solubilized intact in lipid containing nanoparticles bounded by styrene maleic acid copolymer. J. Am. Chem. Soc. *131*: 7484–5.

Kohler, G., and Milstein, C. (1975). Continuous cultures of fused cells secreting antibody of predefined specificity. Nature *256*: 495–497.

Kuby, J. (1997). Immunology (W H Freeman & Co (Sd)).

Kumar, A., Galaev, I., and Mattiasson, B. (1998). Metal chelate affinity precipitation: a new approach to protein purification. Bioseparation 185–194.

Leong, S.R., DeForge, L., Presta, L., Gonzalez, T., Fan, a, Reichert, M., Chuntharapai, a, Kim, K.J., Tumas, D.B., Lee, W.P., Gribling, P., Snedecor, B., Chen, H., Hsei, V., Schoenhoff, M., Hale, V., Deveney, J., Koumenis, I., Shahrokh, Z., McKay, P., Galan, W., Wagner, B., Narindray, D., Hébert, C., and Zapata, G. (2001). Adapting pharmacokinetic properties of a humanized anti-interleukin-8 antibody for therapeutic applications using site-specific pegylation. Cytokine *16*: 106–19.

MacCallum, R.M., Martin, a C., and Thornton, J.M. (1996). Antibody-antigen interactions: contact analysis and binding site topography. J. Mol. Biol. *262*: 732–45.

Martínez-Alonso, M., García-Fruitós, E., Ferrer-Miralles, N., Rinas, U., and Villaverde, A. (2010). Side effects of chaperone gene co-expression in recombinant protein production. Microb. Cell Fact. *9*: 64.

Mergulhão, F.J., and Monteiro, G.A. (2007). Analysis of factors affecting the periplasmic production of recombinant proteins in Escherichia coli. J. Microbiol. Biotechnol. *17*: 1236–41.

Mori, H., and Ito, K. (2001). The Sec protein-translocation pathway. Trends Microbiol. *9*: 494–500.

Mücke, M., Ostendorp, R., and Leonhartsberger, S. (2009). E. coli Secretion Technologies Enable Production of High Yields of Active Human Antibody Fragments. BioProcess Tech.

Nakazawa, M., Mukumoto, M., and Miyatake, K. (2010). Production and purification of polyclonal antibodies. Methods Mol. Biol. *657*: 63–74.

Natarajan, A., Xiong, C.-Y., Gruettner, C., DeNardo, G.L., and DeNardo, S.J. (2008). Development of multivalent radioimmunonanoparticles for cancer imaging and therapy. Cancer Biother. Radiopharm. *23*: 82–91.

Neu, H.C., and Heppel, L. a (1965). The release of enzymes from Escherichia coli by osmotic shock and during the formation of spheroplasts. J. Biol. Chem. *240*: 3685–92.

Neu, H.C., James, A., and Chou, J. (1967). Release of Surface Enzymes in Enterobacteriaceae by Osmotic Shock. J. Bacteriol. *94*: 1934–1945.

Neubauer, P., Hofmann, K., Holst, O., Mattiasson, B., and Kruschke, P. (1992). Maximizing the expression of a recombinant gene in Escherichia coli by manipulation of induction time using lactose as inducer. Appl. Microbiol. Biotechnol. *36*:

Neuberger, M.S., Williams, G.T., and Fox, R.O. (1984). Recombinant antibodies possessing novel effector functions. Nature *312*: 604–608.

Nieba, L., Honegger, a, Krebber, C., and Plückthun, a (1997). Disrupting the hydrophobic patches at the antibody variable/constant domain interface: improved in vivo folding and physical characterization of an engineered scFv fragment. Protein Eng. *10*: 435–44.

Padlan, E.A.E. (1994). Anatomy of the antibody molecule. Mol. Immunol. *31*: 169–217.

Peeters, K., Wilde, C. De, Jaeger, G. De, Angenon, G., and Depicker, a (2001). Production of antibodies and antibody fragments in plants. Vaccine *19*: 2756–61.

Pelegrine, D.H.G., and Gasparetto, C. a. (2005). Whey proteins solubility as function of temperature and pH. LWT - Food Sci. Technol. *38*: 77–80.

Pinsach, J., Mas, C. de, López-Santín, J., Striedner, G., and Bayer, K. (2008). Influence of process temperature on recombinant enzyme activity in Escherichia coli fed-batch cultures. Enzyme Microb. Technol. *43*: 507–512.

Popplewell, A.G., Sehdev, M., Spitali, M., and Weir, a N.C. (2005). Expression of antibody fragments by periplasmic secretion in Escherichia coli. Methods Mol. Biol. *308*: 17–30.

PORATH, J., CARLSSON, J., OLSSON, I., and BELFRAGE, G. (1975). Metal chelate affinity chromatography, a new approach to protein fractionation. Nature *258*: 598–599.

Pugsley, a P. (1993). The complete general secretory pathway in gram-negative bacteria. Microbiol. Rev. *57*: 50–108.

Quintero-Hernández, V., Juárez-González, V.R., Ortíz-León, M., Sánchez, R., Possani, L.D., and Becerril, B. (2007). The change of the scFv into the Fab format improves the stability and in vivo toxin neutralization capacity of recombinant antibodies. Mol. Immunol. *44*: 1307–15.

Raju, T.N. (1999). The Nobel chronicles. 1972: Gerald M Edelman (b 1929) and Rodney R Porter (1917-85). Lancet *354*: 1040.

Ramírez, D.M., and Bentley, W.E. (1995). Fed-batch feeding and induction policies that improve foreign protein synthesis and stability by avoiding stress responses. Biotechnol. Bioeng. *47*: 596–608.

Ramm, K., and Plückthun, A. (2000). The periplasmic Escherichia coli peptidylprolyl cis, trans-isomerase FkpA II. Isomerase-independent chaperone activity in vitro. J. Biol. Chem. *275*: 17106–13.

Rodríguez-Carmona, E., Cano-Garrido, O., Dragosits, M., Maurer, M., Mader, A., Kunert, R., Mattanovich, D., Villaverde, A., and Vázquez, F. (2012). Recombinant Fab expression and secretion in Escherichia coli continuous culture at medium cell densities: Influence of temperature. Process Biochem. *47*: 446–452.

Roy, I., and Gupta, M.N. (2003). Smart polymeric materials: emerging biochemical applications. Chem. Biol. *10*: 1161–71.

Schild, H.G. (1992). Poly(N-isopropylacrylamide): experiment, theory and application. Prog. Polym. Sci. *17*: 163–249.

Schumann, W., and Ferreira, L.C.S. (2004). Production of recombinant proteins in Escherichia coli. Genet. Mol. Biol. *27*: 442–453.

Sevastsyanovich, Y., Alfasi, S., Overton, T., Hall, R., Jones, J., Hewitt, C., and Cole, J. (2009). Exploitation of GFP fusion proteins and stress avoidance as a generic strategy for the production of high-quality recombinant proteins. FEMS Microbiol. Lett. *299*: 86–94.

Simmons, L.C., Reilly, D., Klimowski, L., Raju, T.S., Meng, G., Sims, P., Hong, K., Shields, R.L., Damico, L.A., Rancatore, P., Yansura, D.G., and Shantha Raju, T. (2002). Expression of full-length immunoglobulins in Escherichia coli: rapid and efficient production of aglycosylated antibodies. J. Immunol. Methods *263*: 133–147.

Skerra, A., and Plückthun, A. (1991). Secretion and in vivo folding of the Fab fragment of the antibody McPC603 in Escherichia coli: influence of disulphides and cis-prolines. Protein Eng. *4*: 971–9.

Spiridon, C.I., Guinn, S., and Vitetta, E.S. (2004). A comparison of the in vitro and in vivo activities of IgG and F(ab')2 fragments of a mixture of three monoclonal anti-Her-2 antibodies. Clin. Cancer Res. *10*: 3542–51.

Spooner, R.A., Murray, S., Rowlinson-Busza, G., Deonarain, M.P., Chu, A., and Epenetos, A.A. (1994). Genetically engineered antibodies for diagnostic pathology. Hum. Pathol. *25*: 606–14.

Steinmeyer, D.E., and McCormick, E.L. (2008). The art of antibody process development. Drug Discov. Today *13*: 613–8.

Teotia, S., and Gupta, M.N. (2001). Purification of alpha-amylases using magnetic alginate beads. Appl. Biochem. Biotechnol. *90*: 211–220.

Vasina, J.A., Peterson, M.S., and Baneyx, F. (1998). Scale-up and optimization of the low-temperature inducible cspA promoter system. Biotechnol. Prog. *14*: 714–21.

Weetall, H.H., and Lee, M.J. (1989). Antibodies immobilized on inorganic supports. Appl. Biochem. Biotechnol. *22*: 311–30.

Weickert, M.J., Doherty, D.H., Best, E.A., and Olins, P.O. (1996). Optimization of heterologous protein production in Escherichia coli. Curr. Opin. Biotechnol. *7*: 494–499.

Weir, A.N.C.A., and Bailey, N.A.N. (1995). Process for obtaining antibodies utilizing heat treatment (US).

Weisser, N.E., and Hall, J.C. (2009). Applications of single-chain variable fragment antibodies in therapeutics and diagnostics. Biotechnol. Adv. *27*: 502–20.

Wörn, A., and Plückthun, a (1999). Different equilibrium stability behavior of ScFv fragments: identification, classification, and improvement by protein engineering. Biochemistry *38*: 8739–50.

Wörn, A., and Plückthun, a (2001). Stability engineering of antibody single-chain Fv fragments. J. Mol. Biol. *305*: 989–1010.

Wunschel, D.S., Hill, E.A., McLean, J.S., Jarman, K., Gorby, Y.A., Valentine, N., and Wahl, K. (2005). Effects of varied pH, growth rate and temperature using controlled fermentation and batch culture on matrix assisted laser desorption/ionization whole cell protein fingerprints. J. Microbiol. Methods *62*: 259–71.

Yansura, D.G., and Henner, D.J. (1984). Use of the Escherichia coli lac repressor and operator to control gene expression in Bacillus subtilis. Proc. Natl. Acad. Sci. U. S. A. *81*: 439–43.

Yee, L., and Blanch, H.W. (1992). Recombinant Protein Expression in High Cell Density Fed-Batch Cultures of Escherichia Coli. Bio/Technology *10*: 1550–1556.

Yoon, S.K., Kang, W.K., and Park, T.H. (1994). Fed-batch operation of recombinant Escherichia coli containing trp promoter with controlled specific growth rate. Biotechnol. Bioeng. *43*: 995–9.

2. Controlling the location and solubility of Fab D1.3

2.1. Abstract

The periplasm of *E. coli* has shown several important features to be an ideal location for accumulating recombinant proteins. The oxidative environment aids protein folding and correct disulphide bond formation. Since less than 10% of total cellular proteins accumulate in the periplasmic space, employing selective release methods (such as osmotic shock) would simplify subsequent downstream purification. Avoiding direct contact with DNA and RNA in the cytoplasm or chemical reagents in culture broth are especially beneficial when localising the desired recombinant protein product in the periplasm of *E. coli*. Despite these merits, there are still some issues that need to be addressed. The antibody fragment (Fab D1.3) employed in this work can easily leak from the periplasm into the culture broth, also a high percentage of the target protein is likely to be retained within the cytoplasm, possibly in insoluble form. In the worst case, cells lysed a few hours after induction, the target proteins mixing with cell components, resulting in a very difficult situation for product recovery. In this work, Preliminary shake flask experiments were conducted to identify the factors (such as temperature, IPTG concentration and induction timing determined by OD_{600} reading) effect on the *E. coli* growth and location of recombinant protein production. The best result of Fab production in the periplasm was achieved with 50 μM [IPTG] for induction at OD_{600}~1 at 25°C. We then demonstrate that considerable control over the location and solubility

of the Fab product can also be achieved in 5 L feb-batch fermentation process through systematic variation of growth and induction temperature, inducer concentration and points of induction and cell harvest. At different times during fed-batch cultivation, cells were centrifugally separated from the suspending broth and subjected to osmotic shock procedures. The Fab concentration in the resulting fractions (broth, periplasmic and cytoplasmic) was then measured by ELISA, SDS-PAGE and Western blotting. We describe how changes in all of the above fermentation parameters influence product titre, location, and solubility. We have obtained total ~ 48 mg/L of Fab D1.3 mainly in the culture broth (21.09 mg/L) and OS1 (25.08 mg/L, periplasmic fraction). The optimum condition for Fab D1.3 production was cultivated at 25°C and decreased to 20°C upon induction. The induction was performed at OD_{600} ~ 20 with 0.2 mM of [IPTG]. Cells were harvested at 18.15 h post-induction. Furthermore, the ratio of soluble to insoluble was 60% to 40%, which suggested the majority of Fab D1.3 was soluble. Despite the above merits, the titre of Fab D1.3 was not sufficient to meet our goal (require ~100 mg/L of releasable Fab D1.3)

2.2. **Introduction**

E. coli is one of the microorganisms being studied and commonly used for production of recombinant proteins because of the thorough understanding of its cell structure and genomic information. Indeed, through modern genetic technology, gene alteration offers a wide range of possibilities to produce desired products (Hockney, 1994; Weickert *et al.*, 1996; Baneyx, 1999; Jana and Deb, 2005; Sørensen and Mortensen, 2005; Chen, 2011). By inserting a genetically modified plasmid into hosts, it enables bacteria to produce proteins according to the recombinant gene sequence from the plasmid (Cheah *et al.*, 1987; Humphreys *et al.*, 2002; Carton *et al.*, 2007). The flexible scale of fermentation process in *E. coli* provides a robust and rapid production of invaluable recombinant protein for the biopharmaceutical industry (Harrison and Keshavarz-Moore, 1996; Chadd and Chamow, 2001; Farid, 2007). The current bottleneck is the linkage between the upstream production (fermentation) and the downstream purification. Export of large quantities of recombinant protein into the culture broth could allow simple recovery but the initial purity would be low therefore requiring many steps of concentration and clarification. In comparison, periplasmic targeting of recombinant protein could result in higher purity and fewer conditioning steps required, although the yield may be less and protein extraction from the periplasm is still required (Houdebine, 2002; Kelley, 2009; Mücke *et al.*, 2009; Rosa *et al.*, 2010; Chen, 2011). This means producing good purity and higher yield of the target protein as a feedstock for downstream process and subsequent chromatography purification needs to be well balanced (i.e. high yield but low purity or low yield but high purity) for optimising whole production.

Targeting recombinant protein into the periplasm seems to be an good solution for proteins which require disulfide bonds and avoid exposing to extracellular chemical agents (Humphreys, 2007). In addition, utilising the periplasm for protein accumulation could simplify the downstream process. Although an outer membrane disruption step is required, only around ten per cent of soluble cellular protein is in the periplasm; this also avoids contamination from DNA or RNA (Van Wielink *et al.*, 1990; Humphreys *et al.*, 2004; Humphreys, 2007). Several studies have provided possible solutions for improvement of protein production and accumulation in the periplasm. A very common strategy is by boosting the titre of target product with a stronger promoter (Sockolosky and Szoka, 2012). In particularly, to increase the yield of Fab production in the periplasm, human protein disulphide isomerase can be co-expressed, or a Eukaryotic Signal Peptide can be used at the 5′ end of the coding sequence to effectively target protein in the periplasm (Humphreys *et al.*, 1996, 2000) .

Changing the growth media and cultivation conditions are the easiest and simplest method to achieve above the goals, improving the production titre and recombinant protein folding state. In addition, it can also aid recombinant protein localisation of the desired products to the periplasm, subsequently helping downstream extraction and purification steps (Schein and Noteborn, 1988; Wunschel *et al.*, 2005; Sevastsyanovich *et al.*, 2009; Rodríguez-Carmona *et al.*, 2012). This may be achieved by manipulating the timing of induction (Neubauer *et al.*, 1992; Vila *et al.*, 1997), and using different inducers (i.e. lactose) (Gombert and Kilikian, 1998). Furthermore, specific growth rate (μ) controlled by fed batch feeding has also been shown to impact

on the quality and quantity of desired products. In some case, cell growth phase and protein synthesis phases are separated, so a faster specific growth rate helps in achieving higher biomass before induction thereby increasing the quantity of the products (Curless *et al.*, 1990). Another proposal raised by Riesenberg and co-workers (1990) suggested the opposite idea, combining the cell growth and protein synthesis phases by slowing the specific growth rate ($0.02\ h^{-1} < \mu < 0.4\ h^{-1}$), aiding protein synthesis after induction therefore generating more soluble product. The same result has been demonstrated by Sevastsyanovich and co-workers (2009); a C-terminal green fluorescent protein (GFP) fusion to a model target protein *E. coli* CheY expressed from a pET20 vector. Using very low IPTG concentrations (8 μM), which avoids growth arrest and loss of culturability post-induction, the recombinant protein accumulated to 30% of the total protein content of the bacteria. In addition to above, there are other factors that also have great influence towards intracellular protein production and accumulation, such as temperature (Jones *et al.*, 1987; Daniel and Gottschalk, 1992; Wunschel *et al.*, 2005; Sevastsyanovich *et al.*, 2009; Rodríguez-Carmona *et al.*, 2012) and concentration of inducer (IPTG in those cases) (Kilikian *et al.*, 2000; Lin *et al.*, 2008; Sevastsyanovich *et al.*, 2009).

In this study we aimed to produce a minimum titre of 100 mg/L Anti-Hen Egg White Lysozyme antibody Fab fragment (so-called Fab D1.3) ideally in the periplasm for use in screening and testing high binding capacity cation exchange ligands on magnetic particles, and subsequently apply feedstock with magnetic particles to high gradient magnetic fishing (HGMF) or continuous magnetic separation devices developed by other project partners.

We demonstrated that alteration of the cultivation temperature, timing of induction and inducer (IPTG) concentration could be a generic method to partially control the location of the target protein accumulation to benefit the protein release and purification processes, and simultaneously increase the ratio of soluble to insoluble protein for higher percentages of soluble protein.

2.3. **Material and methods**

2.3.1. Materials

The tetracycline resistant *E. coli* CLD048 harbouring pAVE046 (Hodgson *et al.*, 2007), expressing the antibody fragment Fab D1.3 (targeting as heavy and light chains into the periplasm, codes for signal peptide is not availbe due to the company privacy) was provided by Avecia Biotechnology (Billingham, UK). Nutrient agar and phosphate buffered saline (PBS) were purchased from Oxoid (Basingstoke, Hampshire, UK). Yeast extract and tryptone were obtained from Becton, Dickinson and company (BD) (Sparks, MD, USA). Sodium dodecyl sulphate (SDS) and Laemmli electrophoresis and running buffers were obtained from Bio-Rad Laboratories (Hercules, CA, USA). Ammonium hydroxide, phosphoric acid, magnesium sulphate, calcium chloride dihydrate, manganese (II) sulphate four hydrate and HPLC grade methanol were purchased from Fisher Scientific (Loughborough, Leicestershire, UK). Bugbuster Protein extraction reagent was purchased from Merck Chemicals Ltd (Nottingham, UK). TMB microwell peroxidase substrate (2-C) and TMB membrane peroxidase substrate system (3-C) were obtained from KPL (Gaithersburg, MD, USA). Hybond-P PVDF membrane

was obtained from Amersham Biosciences (Uppsala, Sweden). Bicinchoninic acid (BCA) protein assay kit and Isopropyl β-D-1-thiogalactopyranoside (IPTG) were purchased from Thermo Scientific (Rockford, IL, USA). Tetramethylethylenediamine (TEMED) was supplied by Melford Laboratories (Suffolk, UK). SimplyBlue Safe Stain and SeeBlue Plus2 Pre-Stained Standard were purchased from Invitrogen (Paisley, UK). Ammonium sulphate, glycerol, potassium phosphate monobasic and dibasic, citric acid, ferrous sulphate heptahydrate, zinc sulphate, sodium molibdate dihydrate, copper (II) sulphate, boric acid, tetracycline, sodium chloride, sodium hydroxide, Tween 20, ethylenediaminetetraacetic acid (EDTA), sucrose, Trizma-base, sodium phosphate monobasic, sodium phosphate dibasic, sodium carbonate, sodium hydrogen carbonate, glycine for electrophoresis, chicken egg white lysozyme (HEWL), albumin from bovine serum (BSA), and anti-human IgG (Fab specific) - peroxidise antibody produced in goat, as well as all other chemicals used in this study were obtained from Sigma-Aldrich Co. (St. Louis, MO, USA).

2.3.2. Methods

2.3.2.1. Initial Fed-batch fermentation

E. coli strain CLD048 was stored at −80°C in 20% LB and 80% glycerol and propagated on Nutrient agar plates supplemented with 15mg/L tetracycline and incubated at 37°C overnight. The initial inoculum was prepared in a 500 mL conical flask by inoculating 100 mL of Luria Bertani (LB) broth (comprising 1% NaCl, 0.5% yeast extract and 1% tryptone) containing 15 mg/L tetracycline with a fresh single colony of *E. coli* CLD048 and shaking at 37°C

and 200 rpm for 13 h. The inoculum was transferred into a complex medium (composition provided by Avecia Biotechnology; Table 2.1). Fermentation was conducted using a 5 L Electrolab fermentor (Tewkesbury, UK) equipped with 6-bladed rushton turbine impellers and four baffles located around the edge of the vessel. The vessel containing 3 L of medium (Table 2.1) was sterilised at 121°C for 0.5 h then cooled down to set temperature; post sterilisation and trace metal additions (Table 2.1 and Table 2.2) were added after cooling.

Table 2.1 Culture medium composition, the grey part indicates the components needed to be added after sterilisation and cooling of the medium to 37°C prior to inoculation of the fermentor.

Component of medium	Concentration
$(NH_4)_2\ SO_4$	14 g/L
Glycerol	35 g/L
Yeast extract	20 g/L
KH_2PO_4	2 g/L
K_2HPO_4	16.5 g/L
Citric acid	7.5 g/L
Conc. H_3PO_4	1.5 mL/L
1 M $MgSO_4.7H_2O$ solution	10 mL/L
1 M $CaCl_2.2H_2O$ solution	2 mL/L
Antifoam AF204	0.2 mL/L
15 mg/mL Tetracycline	1 mL/L

Table 2.2 Trace metal composition, 34 mL solution was sterilised through a 0.22 μm sterile filter into a suitable sterile container and added into 1 L medium in the fermentor.

Component	Concentration
$FeSO_4.7H_2O$	3.36 g/L
$ZnSO_4.7H_2O$	0.84 g/L
$MnSO_4.H_2O$	0.51 g/L
$Na_2MoO_4.2H_2O$	0.25 g/L
$CuSO_4.5H_2O$	0.12 g/L
H_3BO_3	0.36 g/L
Conc. H_3PO_4	48 mL/L

Table 2.3 Glycerol and magnesium sulphate feed composition.

Component of medium	Concentration
Glycerol	714 g/L
1 M Mg $SO_4.7H_2O$	30 mL/L

The pH of the medium was adjusted to 7.0 using ammonium hydroxide. The fermentor was inoculated with 100 mL (ca. 3% inoculum/medium ratio) from the overnight shake flask inoculum, and initially operated in batch mode. The starting conditions were: temperature 37°C; agitator speed 200 rpm; air-flow rate 1.0 VVM; pH 7.0. Agitation rate was increased according to dissolved oxygen level in the medium (up to maximum value of 1000rpm), to sustain the DOT set point of 30%. The pH was maintained at 7.0 throughout the fermentation by the automatic addition of NH_4OH (10% v/v). Once carbon source was depleted, indicated by an increased reading of dissolved oxygen measured in the fermentor, the glycerol/magnesium sulphate feed (Table 2.3) was initiated at a constant rate of 9.0 ± 2.0 (g glycerol/h).

2.3.2.2. Bugbuster for fractionation of soluble (S) and insoluble (I) protein from cell pellets

Routinely, the cells were separated from 1mL of fermentation sample by centrifugation (15,800 *g* 600 s). The supernatants were discarded and the cell pellets resuspended in Bugbuster protein extraction reagent; the volume of reagent (μL) employed was determined using the Manufacturer's formula:

Reagent volume (μL) = ((OD_{600} value) x (sample volume (mL)) x 100) /1.5

Following gentle mixing by inversion, the reagent / cell cocktail was incubated at room temperature for 300 s, before centrifuging at 15,800 *g* at 4°C for 20 minutes. Soluble proteins were in the supernatant, and insoluble proteins remained in the pellet. Ten microlitre portions of the supernatant fractions were mixed with equal volumes of Laemmli sample buffer. The pellet fractions

were washed with 160 μL PBS buffer, before centrifuging at 15,800 *g* for 600 s at 4°C, carefully discarding the supernatants and resuspending in Laemmli buffer (the volume used was equal to that of the Bugbuster reagent initially employed). Both sample types (10 μL for soluble and 5 μL for insoluble fraction) were then boiled for 600 s and pulse centrifuged for 10 s at 15,800 *g* before loading onto 14% polyacrylamide gels and performing SDS-PAGE for protein separation.

2.3.3. Improved protocol

2.3.3.1. Coupled shake flask experiments

E. coli strain CLD048 was stored at −80°C in 20% LB and 80% glycerol and propagated on Nutrient agar plates supplemented with 15mg/L tetracycline and incubated at 37°C overnight. A fresh single colony of *E. coli* CLD048 was cultivated in a 500 mL conical flask with 100 mL of Luria Bertani (LB) broth (comprising 1% NaCl, 0.5% yeast extract and 1% tryptone) containing 15 mg/L tetracycline. The first set of experiment was cultivated at 30°C and 25°C and shaking at 200 rpm, induction was performed with 8 μM and 20 μM of [IPTG] at OD_{600}~0.5, respectively. The second set of experiment was cultivated at 25°C and shaking at 200 rpm. IPTG concentration was increased to 20 μM and 50 μM for induction when OD_{600} reached 0.5 and 1, respectively. All samples were collected at 24 h post-induction employing osmotic shock to extract proteins from periplasm and cytoplasm, ELISA to analyse the [Fab] in the culture broth, periplasmic fraction (OS1) and cytoplasmic fraction (OS2).

2.3.3.2. 5 litre fed batch fermentation experiment with improved protocol

Fermentation conditions applied were subject to the results of the shake flask experiments. The same medium as initial fed-batch fermentation was employed, but the temperature was set at 25°C, inducer concentration varied between 0.008 mM to 0.2 mM, timing of induction was decided by OD_{600nm} value between 1 and 20. Fed batch feeding strategy was to increase the feeding rate according to the increase of biomass (i.e. OD_{600} reading) thus controlling the specific growth rate (*μ)*. Feeding rate was calculated with exponential feeding for the fed batch fermentation (Yee and Blanch, 1992; Equation 2.1) with set *E. coli* specific growth rate (*μ*=0.3) and maximum flowrate was 54 mL/h (Jalalirad, 2010).

$$F = \left(\frac{1}{\mathrm{S}}\right) \times \left(\frac{\mu}{\mathrm{Y_{XS}}} + \mathrm{m}\right) \times \mathrm{X_0} \times \mathrm{e}^{\mu t} \times 60$$

Equation 2.1

$$X_0 = OD_{600nm} \times V \times 0.4$$

Equation 2.2

Where, *F*, the feeding rate into the bioreactor (mL/h); X_0, initial biomass (g); V, the initial volume of medium (L); *μ*, specific growth rate (1/h); t, time (h); S, glycerol concentration in the feeding solution (g/L); Y_{xs}, cell yield on glycerol (g/g) and m, the maintenance coefficient for glycerol (g of the substrate per g of cell per h)., Every parameter in Equation 2.1 were used as following, S = 0.714 g/L, V = 3 L, Y_{xs} = 0.6167 g/g, maintenance coefficient = 0.003683 (Wallace *et al.*, 1986) , *μ* = 0.3 1/h. X_0 was calculated following the Equation 2.2

2.3.4. Osmotic shock

Cell pellets harvested by centrifugation (15,800 *g*, 180 s) from 1 mL fermentation samples were re-suspended in an osmotic shock solution (designated OS1) made of 20 mM Tris-HCl buffer (pH 8.0) supplemented with 2.5 mM EDTA and 20% sucrose. After a static incubation on ice for 600 s, the cells were harvested by centrifugation (15,800 *g*, 180 s) and the supernatants (periplasm) were immediately decanted and frozen at −20°C. The resulting cell pellets (spheroplasts) were then re-suspended in a second osmotic shock solution (comprising 20 mM Tris-HCl buffer pH 8.0 2.5 mM EDTA) and incubated on ice for 600 s. Following centrifugation (15,800 *g*, 180 s), the supernatants (cytoplasm) and pellets (unbroken cells) were then separated and stored at −20°C for further analysis.

2.3.5. Analysis

2.3.5.1. Optical density

OD_{600nm} measurements were done in a Uvikon spectrophotometer 922 (NorthStar Scientific, UK). Sterile 'production medium' was used as reference for calibration. The instrument was re-calibrated with PBS solution prior to every measurement. When required, samples were diluted in PBS solution to obtain readings within the working range of the instrument.

2.3.5.2. BCA Assay

Protein concentrations of Culture broth, OS1 and OS2 supernatant fractions were measured with the Pierce® BCA Protein Assay Kit (Thermo Scientific,

2011a). Twenty-five microlitres of 2 mg/mL BSA (standard) and unknown samples were loaded into microplate wells. Two hundred microlitres of the kit's working reagent were added to each well and pipette mixed at least 10 times. Microplates were covered and incubated for at 37°C and 300 rpm in microplate shaker (Infors AG, Switzerland) for 0.5 h. Microplates were cooled to room temperature; absorbance was measured at 562 nm on a GloMax®-Multi Detection System (Promega, UK).

2.3.5.3. DPA Assay

The amount of DNA present in the samples was measured by a modified diphenylamine (DPA) assay. Standards were prepared from calf thymus DNA (Deoxyribonucleic acid sodium salt from calf thymus) dissolved in Tris/EDTA solution pH 8 to the final concentration of 1 mg/mL and incubated at 2-8°C overnight for dissolving DNA thoroughly. Chromogenic reagent was mixed with 0.5 mL of acetaldehyde diluted in 25 mL of distilled water and 1.5 g diphenylamine was dissolved in 100 mL of glacial acetic acid with 1.5 mL concentrated sulphuric acid and then stored at 4°C. Reference standards were made with 150, 100, 75, 50, 25, 20, 15, 10, 5 and 0 μL of the original DNA stock solution (1mg/mL) and filled up with Tris/EDTA pH 8 solution to the final volume of 175 μL. Aliquots (175 μL) of samples and calf thymus DNA standards were pipetted into screw capped starstedt tubes. To these, 5 μL portions of BSA (2 mg/mL, dissolved in distilled water) and 200 μL aliquots of 0.4 M perchloric acid (PCA) were added. The tubes were sealed and after vortex mixing incubated at 4°C for 0.5 h.

After incubation, each sample was centrifuged at 15,800 *g* for 20 minutes and the supernatant discarded. 250 μL of 1 M PCA was added to each pellet, vortexed and incubated at 70°C for 0.5 h, then cooled down to room temperature and 500 μL of freshly prepared chromogenic reagent was added to each well. Samples and standards were incubated at 37°C overnight followed by centrifugation at 15,800 *g* for 600 s. Two hundred microlitres of each supernatant was transferred into a 96-well flat bottom micro plate and the absorbance was measured at 600_{nm}.

2.3.5.4. SDS-polyacrylamide gel electrophoresis (SDS-PAGE) for Fab D1.3 separation

Proteins were separated using 14% polyacrylamide gels at 150 V/20 mA for 2.5 h using Laemmli electrophoresis and running buffers (Bio-Rad). Prior to electrophoresis, all samples were diluted 1:1 with the Laemmli Sample Buffer (65.8 mM Tris-HCl, pH 6.8, 2.1% SDS, 26.3% (w/v) glycerol, 0.01% bromophenol blue), boiled at 110°C for 600 s, and then centrifuged in a microcentrifuge (7,000 *g* 15 s), before loading into the wells of the gel. SeeBlue Plus2 Pre-Stained Standard was used for estimation of molecular weight of protein bands on the gel. Following electrophoresis, gels were rinsed three times with 100 mL of distilled water and then stained with sufficient Simply Blue Safe Stain (5 mL/cm^2) to cover the gel, for 1 h at room temperature with gentle shaking. The stain was discarded and the gel was subsequently washed twice with 100 mL of distilled water for 1 h with gentle shaking.

2.3.5.5. Western Blotting Fab D1.3

For Western blotting, SDS-PAGE gels were not stained. The stacking gel was removed and the resolving gel was soaked in protein transfer buffer (3.03 g/L Trizma-base, 14.4 g/L glycine and methanol (20% v/v)) for 0.5 h. Hybond-P PVDF membrane (GE Healthcare, RPN303F) and 5 mm thick filter paper were cut according to the dimensions of the gel, soaked in 100% (v/v) methanol for 10 s, washed in distilled water for 300 s, and equilibrated in the protein transfer buffer for 0.5 h. The electroblotting cassette was assembled and placed between the electrodes in the blotting unit according to the manufacturer's instructions (Mini Trans-Blot electrophoretic Transfer Cell, Bio-Rad, CA, USA). The band-transfer was carried out initially for 1 h at 100 V, with cold transfer buffer at 4°C, and was then perpetuated at 4°C, at 30 V, overnight. Following transfer, the membrane was removed from the blotting cassette, the orientation of the gel on the membrane was marked, and the membrane was rinsed briefly in phosphate buffered saline (PBS; 11.5 g/L di-sodium hydrogen orthophosphate, 2.96 g/L sodium dihydrogen orthophosphate, and 5.84 g/L sodium chloride; pH 7.5).

For immuno-detection, gentle shaking was applied throughout the whole process. Non-specific binding sites on the membrane were blocked using 3% (w/v) BSA made in PBS, for 1 h, and then rinsed for 300 s twice with PBS containing 0.1% (v/v) Tween 20. The blot was washed with an excess volume of PBS containing 0.1% (v/v) Tween 20 for 300 s and incubated with anti-human IgG (Fab specific) - peroxidise antibody (diluted down in PBS 10,000-fold) for 1 h. The blot was washed three times with PBS/Tween 20, and 15mL of the enzyme substrate for each PVDF membrane (TMB membrane

peroxidise substrate system (3-C)) solution was added to the blot and incubated at room temperature until the desired band intensity was achieved. Subsequently distilled water was used to stop the reaction; blots were dried in air then stored at 4°C for further analysis.

2.3.5.6. Sandwich ELISA method for Fab D1.3

Each well of a 96-well microplate was coated overnight at 4°C with 100 μL of 0.1% hen egg white lysozyme, made in coating buffer (1.59 g/L Na_2CO_3 and 2.93 g/L $NaHCO_3$). Two hundred microlitres of PBS-BSA (1 PBS tablet with 1 g BSA in 100mL distilled water) was added to block unspecific binding, with shaking (500 rpm) in a microplate incubator shaker (Infors AG type AK120, Infors HT, Bottmingen Switzerland) for 1 h, at 37°C. The wells were then washed three times with 300 μL wash buffer (1 PBS tablet and 100 μl Tween 20 in 100 mL of distilled water) per well and tap dried. Both standards and samples (100 μL), having been diluted in PBS on a separate plate, were transferred to the washed ELISA plate, incubated at 37°C, 500 rpm for 1 h, washed again with the wash buffer three times and tap dried. The plate was then loaded with 100 μL anti-human IgG (Fab specific) - peroxidase antibody produced in goat, which was diluted 10000-fold in the blocking buffer, incubated at 37°C, 500 rpm for 1 h, and then washed three times with the wash buffer and tap dried, before 100 μL of peroxidase substrate was added to each well. The reaction was stopped after 600 s by adding 100 μL of 1 M H_3PO_4 to each well, and the plate was read at the wavelength of 450 nm using a microplate reader (Promega Glomax-Multi detection system, Turner BioSystems Inc., Sunnyvale, CA, USA).

2.4. **Results and discussions**

2.4.1. Fab D1.3 fermentation at 37°C, induced at OD_{600nm}~40 with 0.1 mM IPTG.

Five litre scale fermentations were performed with CLD048 *E. coli* strain. We aimed to produce recombinant Fab D1.3 with a minimum concentration of 100 mg/L for the MagPro^{2}Life project (European Framework 7) partners; also, for experiments conducted on the newly designed cation exchange ligands on the magnetic particles in a continuously magnetic separation device. According to the fermentation protocol described in (Hodgson *et al.*, 2007; Jalalirad, 2010) the titre of Fab D1.3 was estimated at around 70-120 mg/L in the culture broth by the end of fermentation process (ca. ~8−12 h post-induction). The result of the first fermentation is shown in Fig. 2.1 (Batch No.1). The fermentation was inoculated with 100 mL of overnight culture of *E. coli* strain CLD048, cultivation temperature was set at 37°C, pH 7, the dissolved oxygen was maintained at 30% and the initial agitation rate at 250 rpm. Agitation rate was increased subject to the percentage of dissolved oxygen. The maximum speed was limited to 1000 rpm. The feed was started at 8 h after inoculation. For induction, 0.1 mM IPTG was added 8 h after inoculation at an OD_{600} of around 45. Data in Fig. 2.1(a) was automatically recorded by Electro Lab software. Fermentation samples were manually taken every 2 h after induction. Cells were harvested when a decrease in the OD reading was observed after induction (8 h post-induction).

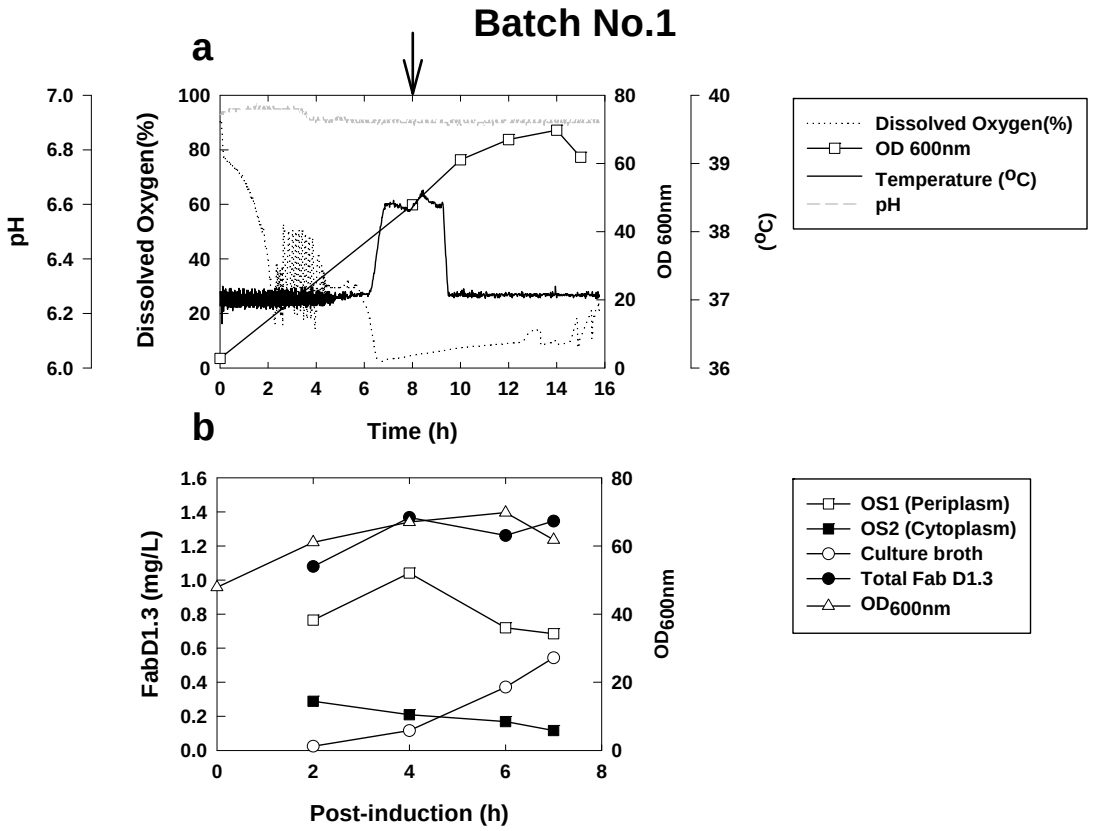

Fig. 2.1 Fed-batch fermentative production (initial volume 3 L) of Fab D1.3 (anti lysozyme) in recombinant *E. coli* at 37°C. Induction (arrow) was performed with 0.1 mM IPTG at OD_{600}~ 47.9. **(a)** Fermentation parameters (Dissolved oxygen%, Temperature and pH value) were recorded by software, optical density was measured by photospectrometer at 600nm wavelength. The arrow indicated the point of induction. **(b)** Concentration of active Fab D1.3 measured by ELISA from three subcellular locations.

Result from Fig. 2.1(a) showed important parameters (e g. pH, dissolved oxygen percentage (DOT), temperature) and the OD_{600} measured during the fermentation process. In the first 2 h after inoculation, cells were growing steadily to the conditions in the fermentation indicated by a steady decrease of DOT from 95% to the set point of 30%. Then a fluctuation was observed in DOT suggested that cells were demanding more oxygen therefore agitation speed was changing rapidly. Further decrease of DOT was detected at 6 h after inoculation because of the maximum agitation speed was reached (1000rpm) could not enable sufficient oxygen to be dissolved to reach a DOT

of 30%. Induction was performed at 8 h after inoculation with 0.1M IPTG at OD_{600} of 47.9. A steady increase of OD was shown every 2 h post-induction and reached a peak at 6 h post-induction at an OD_{600} of around 70. Cell harvesting was performed at 7 h post-induction when a decrease in OD_{600} was observed (from 70 to 61.8).

Unexpectedly, applying the same conditions as described in (Hodgson *et al.*, 2007; Jalalirad, 2010) in this first fermentation was not successful. Analysis of culture broth, periplasmic and cytoplasmic fractions at different time points showed a much lower titre than previously reported Fig. 2.1 b). Between 2 to 4 h post-induction, the majority of Fab was detected in the periplasm (OS1) at a concentration of around 0.9 mg/L, and 0.2 mg/L of Fab was in the cytoplasm (OS2). Almost no Fab was detected in culture broth in the first 4 h after induction shown in Fig. 2.1(b). By the end of process, the [Fab] in culture broth increased to 0.4 mg/L but still the periplasm held the most Fab. In total, approximately 1.3 mg/L of Fab was produced across three locations. However, there was ~11.5 g/L of total protein measured in the culture broth at the end of fermentation (see below Table 2.4). This was very poor purity (0.005%) for the Fab and very difficult to use it as an initial feedstock for purification. As the result, the priority at this stage was to increase Fab titre in the culture broth.

A lot of research has demonstrated that when recombinant protein production from a certain gene sequence cannot be achieved, lowering the fermentation temperature might be an effective solution to improve the yield of the recombinant protein and the ratio of soluble to insoluble protein. Decreasing the temperature for *E. coli* cultivation is likely to slow the protein synthesis process therefore preventing the stress response from the cells for better

quality of recombinant protein production in terms of protein solubility (Daniel and Gottschalk, 1992; Weickert *et al.*, 1996; Panda, 2003; Vallejo and Rinas, 2004; Singh and Panda, 2005; Wunschel *et al.*, 2005; Ventura and Villaverde, 2006; Gasser *et al.*, 2008). Recently, Pinsach and co-workers (2008) investigated the effects of cultivation temperature reduction in *E. coli* from 37°C to 33°C and 28°C and suggested that further reduction to 28°C showed success in improving the yield of final product. Therefore, it is reasonable to reduce temperature from 37°C to 30°C to apply on the next fermentation for trying increase the yield of Fab D1.3.

Table 2.4 Summary of the [Fab], [total protein] and [DNA] in batch No.1 and No.2.

Batch No.	Temperature (°C)	Induction OD_{600nm}	IPTG (mM)	Fab (mg/L)				Total Protein (g/L)			Purity of Fab in different location (%)			DNA[1] in culture broth (mg/L)
				CB[1]	OS1[1]	OS2[1]	Total	CB[1]	OS1[1]	OS2[1]	CB[1]	OS1	OS2	
1	37	47.9	0.1	0.582	0.686	0.117	1.385	11.568	-	-	0.005	-	-	-
2	30	42.3	0.1	28.038	4.700	0.242	32.98	7.780	-	-	0.36	-	-	0.985

[1] All samples were measured in the end of fermentation (harvest). Fab was measured using ELSIA, total protein using BCA assay and DNA using DPA assay. CB= Culture broth

2.4.2. Fab D1.3 fermentation at 30°C, induced at OD_{600nm}~40 with 0.1 mM IPTG.

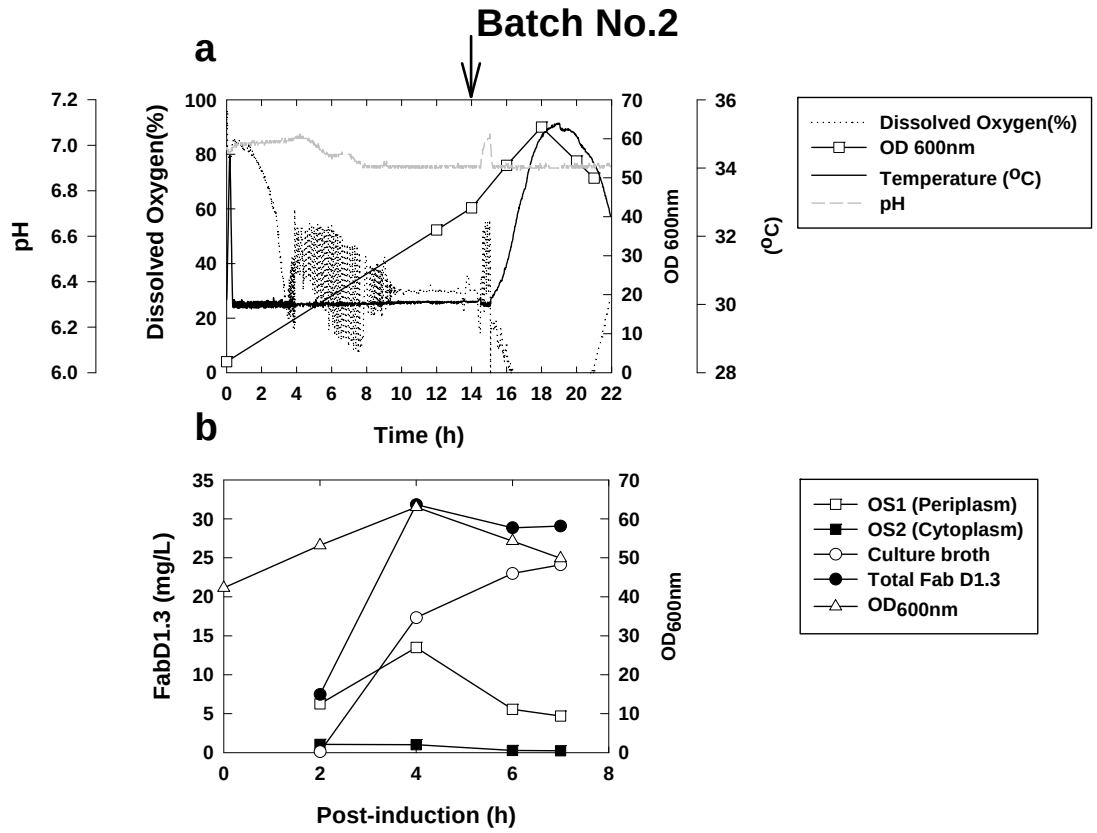

Fig. 2.2 Fed-batch fermentative production (initial volume 3 L) of Fab D1.3 (anti lysozyme) in recombinant E. coli at 30°C. Induction (arrow) was performed with 0.1 mM IPTG at OD~ 42.3. . **(a)** Fermentation parameters (Dissolved oxygen%, Temperature and pH value) were recorded by software, optical density was measured by photospectrometer at 600nm wavelength. The arrow indicated the point of induction. **(b)** Concentration of active Fab D1.3 measured by ELISA from three subcellular locations.

The same fermentation procedures were followed from previous experiments, overnight inoculum was added into 5L fermentation vessel with 3L initial medium for the fermentation. Cultivation parameters were as described in Batch 1 (Fig. 2.1), except that the temperature was set at 30°C. As the temperature was decreased to 30°C, the cells grew much slower to adapt to the colder environment compared with the previous batch (see Fig. 2.1 a).

0.1mM IPTG was added 14 h after inoculation, at an OD_{600} of around 42.3. Unfortunately, there was an uncontrolled temperature increase occurring 2 h post-induction, which could potentially compromise the yield of the Fab. Results in Fig. 2.2 (b) indicate that Fab rapidly accumulated; at 2 h post-induction, the majority of Fab was detected in the periplasm (~5 mg/L) and there was a barely detectable amount of Fab in the cytoplasm and culture broth. At 4 h post-induction, [Fab] had increased 2 fold in periplasm and significantly in culture broth (~15 mg/L). This implied that only 40% of Fab was retained in the periplasm, while 60% of the Fab had leaked into culture broth. At this stage, the overall yield of Fab reached a peak of 31.8 mg/L (Fig. 2.2 b). Noticeably, Fab concentrations did not increase after 4 h post-induction; the overall [Fab] in the periplasm decreased and that in the culture broth increased. This might be explained by the decrease in OD_{600} after 4 h post-induction, indicating that cell integrity was decreased. Despite the fact that the majority of Fab was detected in the culture broth (ca. ~82%) at the point of harvest, and the rest was in the periplasm, nearly no Fab was detected in the cytoplasm. This fermentation proved that decreasing the temperature successfully improved the yield of Fab around 30-fold in comparison to batch No.1, (Fig. 2.1 b and Fig. 2.2 b). Furthermore, the total protein concentration of the culture broth was measured to compare the purity between batches 1 and (Table 2.4). The [total protein] was 33% lower in the culture broth of batch 2 compared to batch 1 (i.e. from 7.8 g/L versus 11.6 g/L), and along with the increased Fab concentration in the culture broth of batch 2, the culture broth Fab purity increased from 0.005% in batch 1 to 0.36% in batch 2. Because of the harvest was 2 h further delayed compared to batch 1, the [DNA] in the

culture broth was measured in order to understand the relationship between the decrease in OD_{600} and the culture broth DNA concentration, indicating cell lysis. Table 2.4 indicates that [DNA] in batch 2 culture broth was nearly 1 mg/L, which may be problematic for downstream purification. The batch 2 culture broth contained a high concentration of total protein (7.8 g/L) and high salt concentration leading to high conductivity (~35 mS/cm), with a very high DNA concentration (~1 mg/L). One of the most commonly used techniques for antibody fragment capture is Cation Exchange Chromatography (CEX). Lacki *et al.* (2007) demonstrated the effect of feedstock conditions (i.e. pH, conductivity) on the binding capacity of Fab using CEX. Their results suggested that ideal feedstock conditions for CEX are low pH (3-5) and low conductivity (~5 mS/cm). Unfortunately, the culture broth generated from batch 2 would need extensive conditioning to meet those conditions, and as a consequence it would be expected that the Fab concentration would decrease during these conditioning steps.

As mentioned in the introduction, the periplasm can offer a much better environment for protein targeting compared to the extracellular environment (Humphreys, 2007). More importantly, cells can be concentrated by centrifugation then disrupted with a generic chemical method (e g. osmotic shock). This would potentially provide a better feedstock for downstream processing when compared to culture broth. In order to localise the Fab into the periplasm for resolving the above problems and identifying the operational window for Fab D1.3 production, a series of shake flask experiments were conducted by systematically examining the effects of each cultivation

parameter, (i.e. temperature, induction timing and IPTG concentration) to fulfil our goals.

2.4.3. Identification of conditions for Fab D1.3 production and optimisation by coupled shake flasks experiments

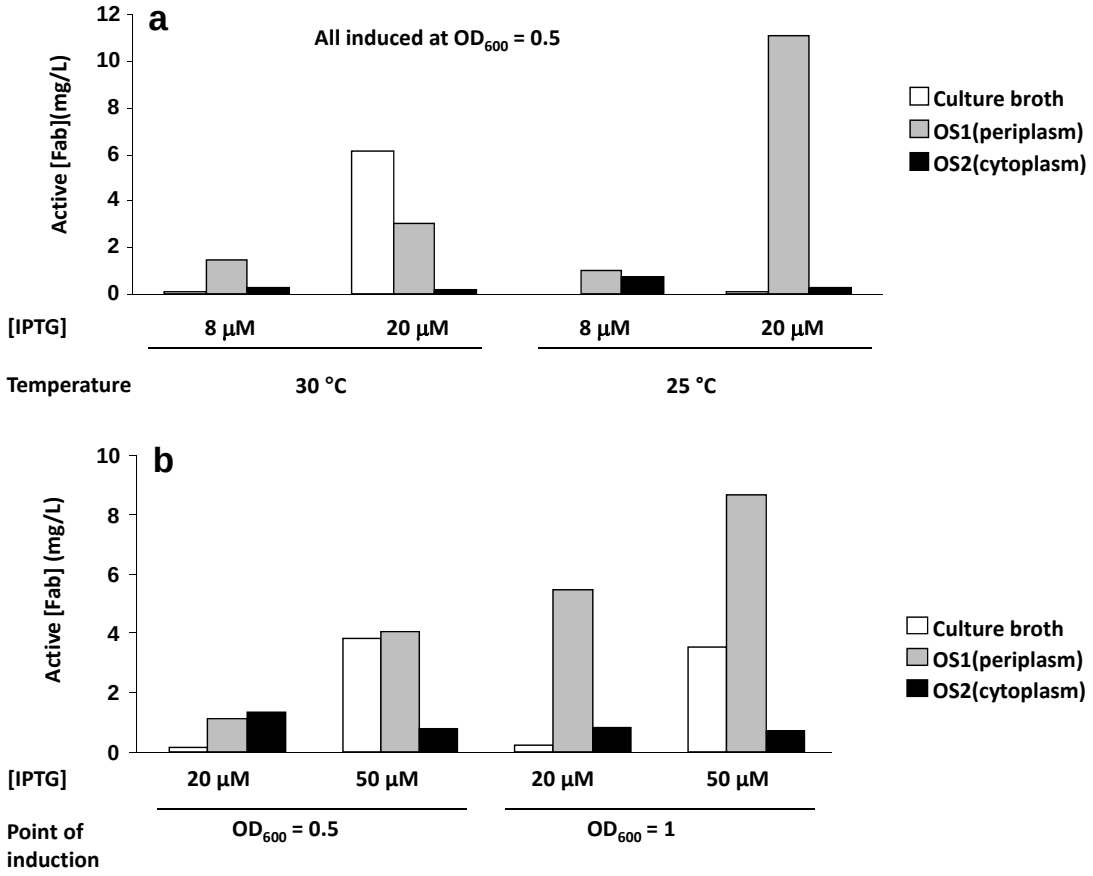

Fig. 2.3 ELISA analysis shows the active [Fab] in the culture broth, OS1 and OS2 from coupled growth & DSP optimisation – shake flask experiments. **(a)** Effects of decrease in incubation temperature and increase in [IPTG] for induction on Fab production in three different locations. **(b)** Effects of Induction at different of OD_{600nm} value and increase in [IPTG] for induction on Fab production in three different locations.

We adopted a similar strategy to Sevastsyanovich *et al.* (2009), to investigate this particular *E. coli* strain CLD048 for determining operation conditions and

the production window to produce an acceptable titre of periplasmic Fab D1.3 (~100 mg/L). Fig. 2.3 shows results from a series of scoping shake flask experiments. One hundred millilitres of LB media in 500mL shake flasks was used to cultivate *E. coli* strain CLD048 at either 25°C or 30°C to the desired OD_{600} (i.e. 0.5 or 1). At this point, cultures were induced with different concentrations of IPTG; 8 μM, 20 μM or 50 μM). Samples from all the shake flask experiments were harvested at 24 h post-induction. Samples were centrifuged to separate cells and culture broth, and then periplasmic (OS1) and cytoplasmic (OS2) fractions were extracted from the cells using osmotic shock. Active Fab concentration in different locations (periplasm, cytoplasm and culture broth) was measured by ELISA (Fig. 2.3). From Fig. 2.3 (a), it was observed that decreasing incubation temperature and [IPTG] aided periplasmic Fab production. At 30°C, increasing [IPTG] from 8 μM to 20 μM increased overall Fab titre, but the majority of Fab leaked into the culture broth at the higher inducer concentration. In striking contrast, decreasing the growth temperature to 25°C maintained a high Fab titre but also allowed periplasmic accumulation. Corisdeo and Wang (2004) compared Fab production in *E. coli* at three different temperatures (16°C, 25°C and 37°C), the result suggesting that although cultures at 37°C generated more Fab, it was mostly in the culture broth. Cultures at 25°C generated Fab in the cells. This is in agreement with the results here. Moreover, regardless of the decrease in temperature, using 20 μM of IPTG to induce Fab production was shown to generate more Fab than 8 μM induction. Cultivation at 25°C generated at least 2 fold more Fab in the periplasm when compared to 30°C, which is the desired location for the Fab accumulation.

Since higher [IPTG] and decreased cultivation temperature were effective in improving the yield of Fab, the lower temperature (25°C) and higher [IPTG] (i.e. 20 μM and 50 μM) were selected for the next experiments (Fig. 2.3 b).The goal was to investigate Fab production in relation to induction at different biomass concentrations (OD_{600} of 0.5 versus 1). Earlier result in Fig. 2.3 (a) showed higher [IPTG] (20 μM) at an induction point of OD_{600}=0.5 generated more Fab compared to 8 μM IPTG, but increased the proportion of Fab leaking into the culture broth at 30°C. Inducing at an OD_{600} of 1 with the same [IPTG] generated more periplasmic Fab. Here, in Fig. 2.3 (b) shows the positive impact of the point of induction in relation to biomass with increasing inducer concentrations from 20 μM to 50 μM on Fab production and location. Cells induced at higher biomass showed a significant increase of the overall Fab titre, 50% higher than induction at OD_{600nm}~0.5. Noticeably, although use of a higher concentration of inducer generated an increased yield of Fab, between 40% and 50% of total Fab leaked into culture broth. This might imply that *E. coli* cannot grow and produce this recombinant Fab simultaneously and that growth and production phases must be separated, or that cells at a higher OD_{600} are more capable of generating Fab.

Several groups (Kosinski *et al.*, 1992; Miao and Kompala, 1992; Donovan *et al.*, 1996; Kilikian *et al.*, 2000) have reported that when induced with relatively high [IPTG], cells might lyse after a certain period of cultivation time. As results showed from above experiments, many factors are important for growing *E. coli* to generate correctly folded recombinant protein with directing to the desired location, such as temperature, inducer concentration and induction timing subject to biomass. The investigation by conducting shake

flask experiments has identified those parameters which will be crucial for Fab D1.3 fermentation.

2.4.4. Adapting improved protocol to Fab D1.3 fermentations

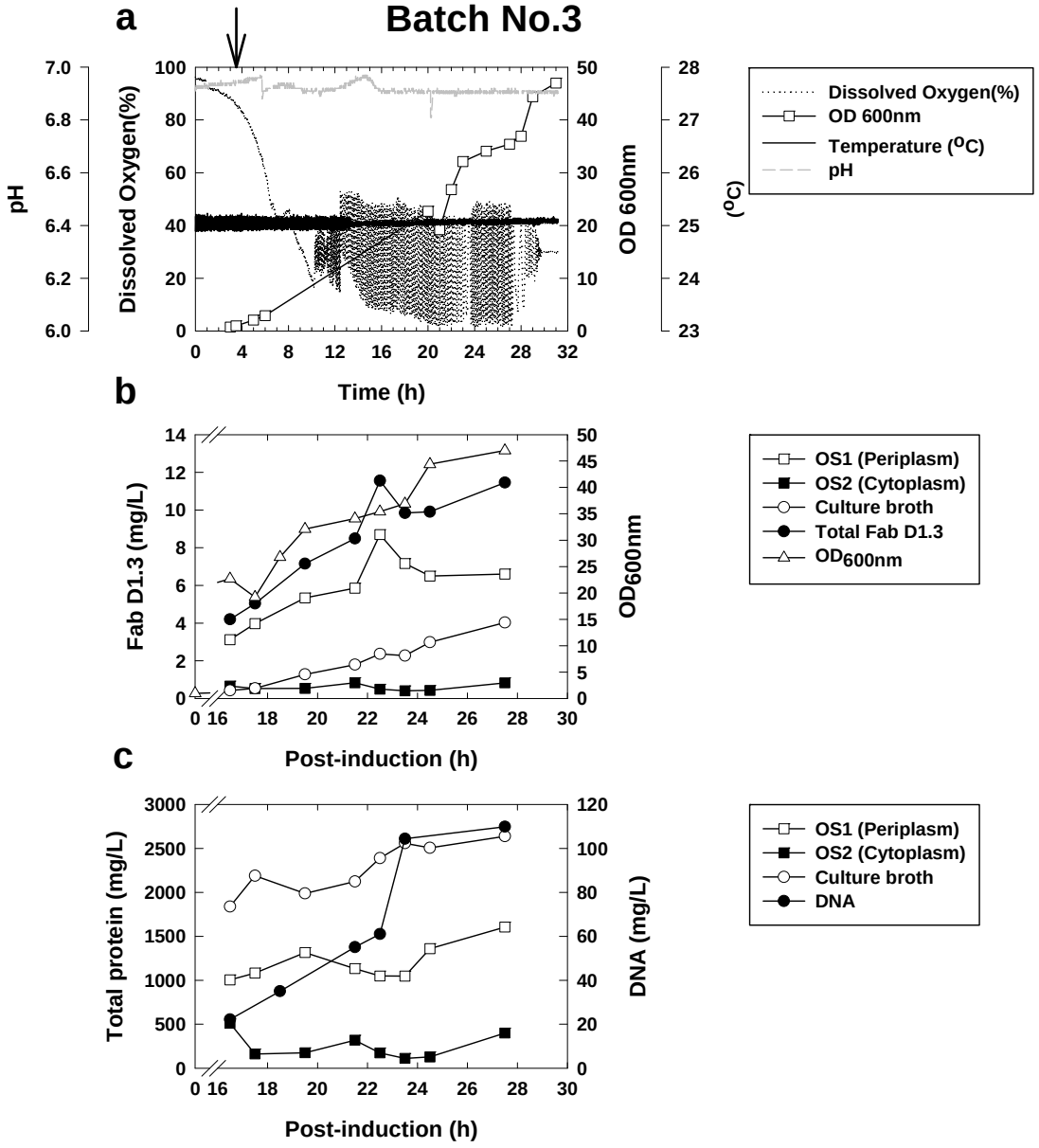

Fig. 2.4 Fed-batch fermentative production (initial volume 3 L) of Fab D1.3 (anti lysozyme) in recombinant *E. coli* at 25°C. Induction (arrow) was performed with 0.02 mM IPTG at OD_{600}~ 1. **(a)** Dissolved oxygen %, Temperature and pH value were recorded by computer, optical density was measured by photospectrometer at 600nm wavelength. The arrow indicated the point of induction. **(b)** Concentration of active Fab D1.3 measured by ELISA in three subcellular fractions from osmotic shock treatment **(c)** [total protein] was measured by BCA assay in the three subcellular fractions and [DNA] in culture broth was measured by DPA assay.

According to the studies done by (Corisdeo and Wang, 2004; Sevastsyanovich *et al.*, 2009) and the results of the shake flask experiments (Fig. 2.3), the cultivation temperature was set at 25°C for the batch No.3 fermentation (Fig. 2.4 a). Fab production was induced with 0.02 mM of IPTG when the OD_{600} reached 1. The other parameters were the same as batch No.2 fermentation. The improved protocol of (Sevastsyanovich *et al.*, 2009) was applied to minimise stress, attempt to increase the titre and solubility of Fab, and to shift the majority of Fab into the periplasm. The strategy here was to induce with a low concentration of IPTG (0.02 mM) at very early growing phase (OD_{600}~1), guided by the results of shake flask experiments (Fig. 2.3 b). Cells were harvested after 31.5 h cultivation time, when the final OD_{600} reached 47. A great advantage of applying fed-batch feeding in fermentation is the higher biomass that can be achieved in comparison with shake flask growth. Although the final OD_{600} reading was much higher than the shake flask, the overall yield of Fab was only 11 mg/L (Fig. 2.4 b). This is possible because of the induction was performed at low biomass or the [IPTG] was too low (Miao and Kompala, 1992).

Result in Fig. 2.4 (b) was observed a similar behaviour of Fab production to the shake flask experiments (Fig. 2.3 b), that the majority of Fab accumulated in the OS1 (periplasm fraction). In addition, the [DNA] detected in the culture broth at the end of fermentation was significantly reduced when compared to batches 1 and 2 to 0.11 mg/L (Table 2.4 Fig. 2.4 c). The [Fab] in the culture broth very slowly increased, which suggested that the cells were still mainly intact at the harvest stage, therefore the majority of Fab was kept inside of cells. In contrast, batch No. 2 showed (Fig. 2.2 b) that [Fab] in culture broth

increased rapidly (0.1 mg/L to 17.3 mg/L) at 2 to 4 h post-induction with nearly 1 mg/L DNA detected in the culture broth at the end of fermentation. More importantly, the concentration of total protein was around 1.6 g/L in the OS1 fraction (Fig. 2.4 c) in the end of fermentation, which was almost 80% less than batch No.2 (7.5 g/L in culture broth). This would hugely simplify CEX purification.

In terms of improving the yield of Fab D1.3, the result from batch No.3 was not successful, but invaluable experience was gained from the earlier shake flask results (Fig. 2.3 b) and this batch to realise that an induction at higher biomass could be a strategy to increase protein production (Kilikian *et al.*, 2000; Lin *et al.*, 2008; Sevastsyanovich *et al.*, 2009). Therefore, the next fermentation was induced at a higher OD_{600} of around 20 with the same concentration of IPTG (20 μM) and temperature (25°C).

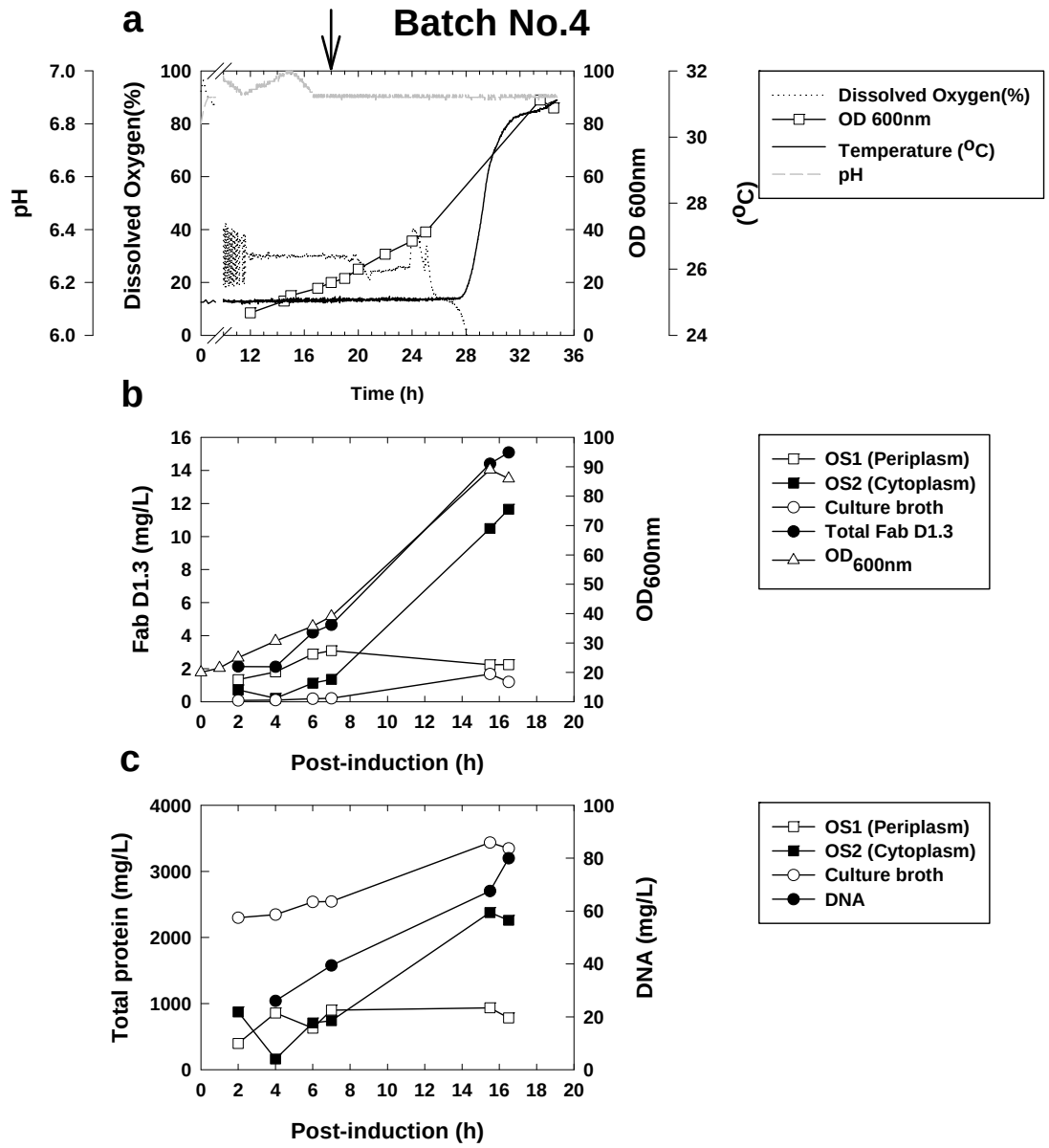

Fig. 2.5 Fed-batch fermentative production (initial volume 3 L) of Fab D1.3 (anti lysozyme) in recombinant E. coli at 25°C. Induction (arrow) was performed with 0.02 mM IPTG at OD~ 20. **(a)** Dissolved oxygen %, Temperature and pH value were recorded by computer, optical density was measured by spectrometer at 600nm wavelength. The arrow indicated the point of induction. **(b)** Concentration of active Fab D1.3 measured by ELISA in three subcellular fractions from osmotic shock treatment **(c)** [total protein] was measured by BCA assay in the three subcellular fractions and [DNA] in culture broth was measured by DPA assay.

Cultivation conditions applied in this fermentation was the same as described in batch 3 (Fig. 2.4), except that induction was delayed until an OD_{600} of 20. In this fermentation, Fig. 2.5 (a) illustrates that each parameter applied to this fermentation was stably controlled at pH 7 but temperature increased by 5°C

near the end of fermentation due to the failure of cooling system. Induction was performed with 0.02 mM of IPTG at OD_{600}~20 18 hours after inoculation. Cells were harvested after a total of 34.5 h cultivation time at a final OD_{600} of 86. The earlier results in shake flask experiment showed that inducing with the same concentration of IPTG (i.e. 0.02 mM) at higher biomass concentration resulted in an increase of overall protein production (Fig. 2.3 b). The first 8 h post-induction did not show any significant Fab production in any compartment of *E. coli*. Noticeably, from 7 to 17 h post-induction nearly 75 % of Fab was produced and accumulated in cytoplasm. This showed Fab was made in cytoplasm, but was not transported to the periplasm, resulting in a very low overall titre of Fab production. However, the overall Fab production still had a slight increase compared with batch No.3 (from 11 mg/L to 15 mg/L), which was induced at a much lower biomass (OD_{600} of 1). The result might explain the positive effect by delaying induction with higher biomass was compromised by insufficient [IPTG] per cell, resulting in overall low titre of Fab production. Therefore, this was not a consistent result from the above findings.

Miao and Kompala (1992) has concluded that [IPTG] of higher than 0.1 mM should be used to overcome culture instability during induction at midexponential phase. However, induction with 50 μM [IPTG] should occur at low cell density (OD_{600}~1) to allow the cells have enough time for protein synthesis. This might explain our results in batch No.4 that induction with 20 μM [IPTG] at OD_{600}~20 resulted in insufficient [IPTG] per cell to trigger rapid protein synthesis, hence most Fab was still in the cytoplasm. Because of low protein synthesis rate and much higher biomass in the end of fermentation were observed, which could indicate stress response causing by producing

recombinant proteins was not significant, thereby leading the low Fab production in this fermentation. In addition, the [DNA] in the culture broth was even lower than the previous result (0.08 mg/L). This suggests that when the low [IPTG] (20 μM) was applied for induction, cells would keep intact resulting in low [DNA] in culture broth (Fig. 2.4 and Fig. 2.5). Whereas high [IPTG] (e.g. 0.1 mM [IPTG] in batch No.2) was applied resulting in cell lysis thereby increase of [DNA] in culture broth was detected (i.e. batch No.2, 0.985 mg/L [DNA] was detected in the culture broth Table 2.4).

Comparing batches 3 and 4, induction was performed at higher biomass in batch 4 (OD_{600}~20), therefore the [IPTG] per cell was diluted 20 fold between batches 3 and 4. Thereafter, increasing [IPTG] induction should be a logical way to improve Fab titre with current fermentation conditions for the next batch.

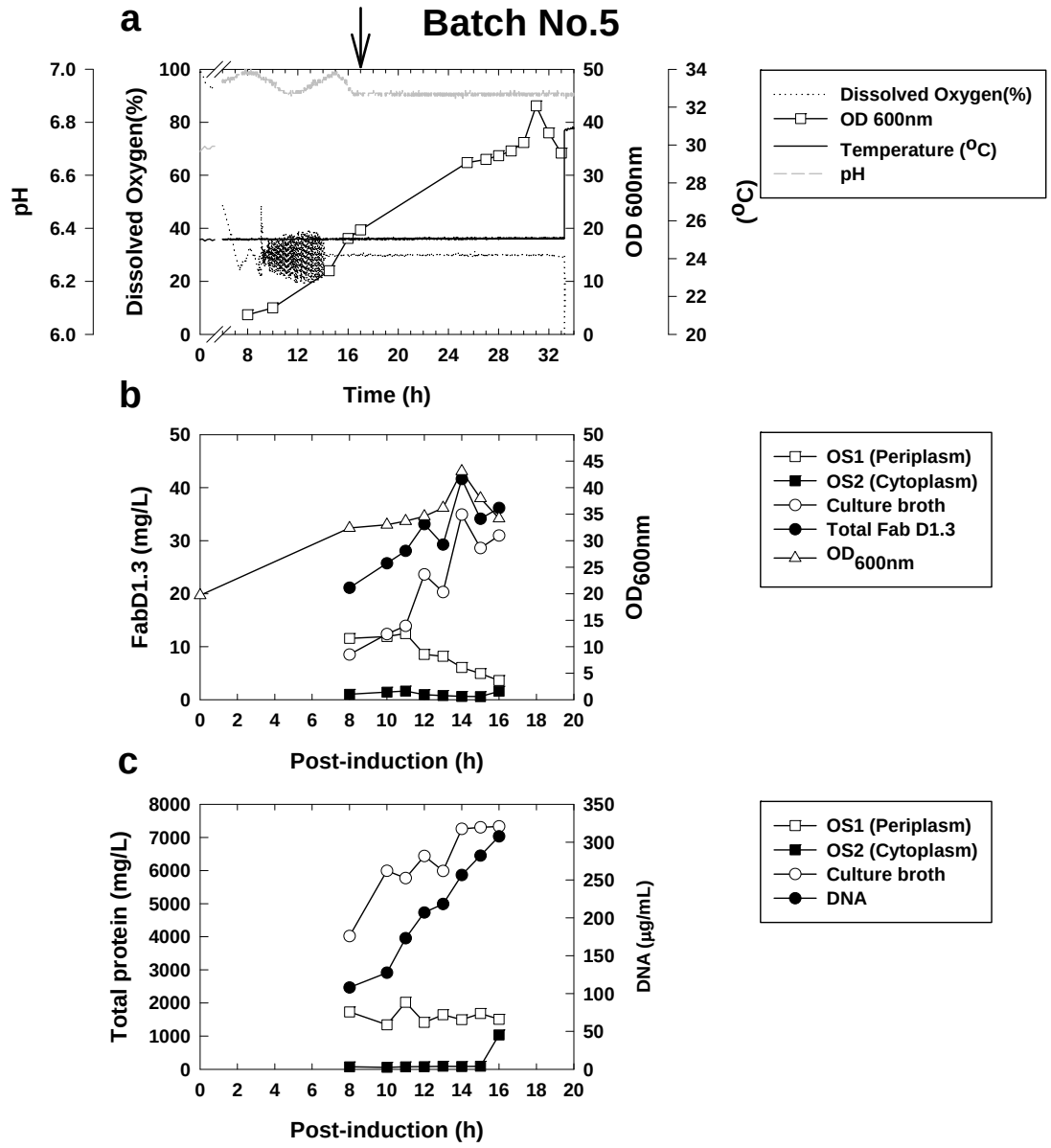

Fig. 2.6 Fed-batch fermentative production (initial volume 3 L) of Fab D1.3 (anti lysozyme) in recombinant E. coli at 25°C. Induction (arrow) was performed with 0.1 mM IPTG at OD~ 20. **(a)** Dissolved oxygen %, Temperature and pH value were recorded by computer, optical density was measured by spectrometer at 600nm wavelength. The arrow indicated the point of induction. **(b)** Concentration of active Fab D1.3 measured by ELISA in three subcellular fractions from osmotic shock treatment **(c)** [total protein] was measured by BCA assay in the three subcellular fractions and [DNA] in culture broth was measured by DPA assay.

Cultivation conditions applied in this fermentation was the same as described in batch No.4, except an increase of [IPTG] from 0.02 mM to 0.1 mM. Fig. 2.6 (a) illustrates the each parameter applied to this fermentation, seeming stable for pH and temperature maintained at 7 and 25°C respectively. Unlike the

previous batch, induction was performed with 0.1 mM IPTG at OD_{600} around 20; then the fermentation was left overnight (8 h). Thus, the first sample was collected at 8 h post-induction then every 2 h until the end of fermentation. Cells were harvested after total 33 h cultivation, the final OD_{600} was 34.2.

Clearly, the highest OD_{600} value in this batch (43.11) was only half of the previous batch (89). This was because the high [IPTG] caused a significant reduction in cell growth rate; this has been observed by many research groups (Miao and Kompala, 1992; Jeong and Lee, 1999; Choi *et al.*, 2000, 2006).

With similar length of cultivation time after Induction, a much lower OD_{600} value was reached in this batch compared to batch No.4 (Fig. 2.5 a). In striking contrast, the results in Fig. 2.6 (b), showed a dramatic increase for the overall [Fab] in the end of fermentation, which was 2 fold higher than Fig. 2.5 No. 4 (Fig. 2.5 b). Furthermore, the majority of Fab production was in the culture broth in this fermentation instead of cytoplasm. There was not any obvious increase of [Fab] observed in cytoplasm, but Fab accumulated in the periplasm (to a maximum concentration of 12 mg/L) then gradually decreased after 11 h post-induction. The total [Fab] was 36.17 mg/L at the end of fermentation, but only 10% was in the periplasm (3.61 mg/L) and 4% was in the cytoplasm (1.6 mg/L); more than 85% of [Fab] was detected in the culture broth (31 mg/L). Unfortunately, there was no sample collected between induction and 8 h post-induction, so we could only speculate based on results (Fig. 2.4 and Fig. 2.5). Previously, Batch No.4 showed that when the cells were intact at the end of fermentation, [DNA] and [total protein] in the culture broth were measured around 80 mg/L and around 3500 mg/L, respectively.

Following the same principle, in Batch 5, between 0 to 8 h post-induction or earlier Fab was initially synthesised in cytoplasm then transported and accumulated in the periplasm. Cells were still intact, implied by the [DNA] (ca. 108 mg/L) and [total protein] (ca. 4000 mg/L) in the culture broth, not significantly higher than the corresponding results in batch 4. In addition, the [Fab] measured at 8 h post-induction in the periplasm (11.5 mg/L) was slight higher than in the culture broth (8.5 mg/L) in the fermentation. Taking collectively, before 8 h post-induction, most Fab was stored in the periplasm. However, Fab leaked into the culture broth; between 8 and 10 hours post-induction, there was more Fab in the Culture broth than the periplasmic fraction (Fig. 2.6b). Despite this, Fab was still being generated by the cells up to the point of harvest.

Results in Fig. 2.6 (c) show a rapid increase of [DNA] and [total protein] in the culture broth after 8 h post-induction, this implied that cell integrity was decreasing over time, resulting in [Fab], [total protein] and [DNA] increasing in the culture broth. Consequently, although *E. coli* was still producing Fab but fewer and fewer cells were able to retain the Fab in the cell thereby a decrease of [Fab] in the periplasm and increase of [Fab] in culture broth. This was also observed in batch No.2 (Fig. 2.2), where the same [IPTG] (0.1 mM) for induction was performed at 30°C but with higher biomass at OD_{600} around 40 (Fig. 2.2 a). Although the temperature had been decreased by 5°C, the cells were still not able to maintain the Fab in the periplasm but in the culture broth due to cell lysis. This might suggest that the concentration of IPTG per cells for induction was still too high. However, in terms of Fab purity in the culture broth, this is a promising result compared with previous batch No.4.

Even though the total protein concentration in the culture broth was 2 fold higher than batch.4 (7.3 g/L *cf.* 3.3 g/L), batch 5 generated 3 litres of culture broth containing around 99 mg of Fab and 21.9 g of total protein in the end of fermentation, the Fab purity in the culture broth was much higher than batch 4 which had 3.6 mg of Fab within 9.9 g of total protein. As the result, the purity of Fab in culture broth has increased over 10 fold (0.42% *cf.* 0.036%).

Interestingly, the peak OD_{600} (~43.11) corresponded to the peak overall Fab production (41.6 mg/L) and [Fab] in the culture broth (34.9 mg/L) at 14 hours post induction, which might indicate there were correlations between biomass and the yield of Fab. Thus, if high cell density fermentation can be achieved with high [IPTG] induction, then cells could be harvested before lysis. This might offer an opportunity to exploit the optimum conditions and operation window to improve the Fab production and retain the product in the periplasm.

Thus far, the yield of Fab in culture broth had been improved over 50-fold compared with the initial conditions in batch No.1 (30.97 mg/L *cf.* 0.58 mg/L). The only comparable result was generated in batch No.2 (ca. 28 mg/L), which was very difficult to apply on CEX due to the nature of the feedstock composition (i.e. pH, conductivity and total protein concentration). Unfortunately, although we have successfully produced a slightly higher titre of Fab in batch No.5 (ca. in total 36.18 mg/L), but 85% of Fab was in the culture broth, which will encounter the same problems as batch No.2 for the feedstock clarification and in conditioning for CEX. As mentioned from the introduction, temperature plays an extremely important role for *E. coli* cultivation, many studies (Daniel and Gottschalk, 1992; Holt *et al.*, 2000; Ramos *et al.*, 2001; Corisdeo and Wang, 2004; Ami *et al.*, 2009) have

suggested further reduction of temperature to decrease periplasmic misfolded proteins and soluble aggregates as an effective means to increase the yield of soluble protein and improve the cell stability thereby benefitting the quality of protein folding and production. It might be sensible to take the advantage of lowering the temperature upon induction for prolonging the cell viability thereby increasing the overall titre of Fab and allowing better translocation into the periplasm.

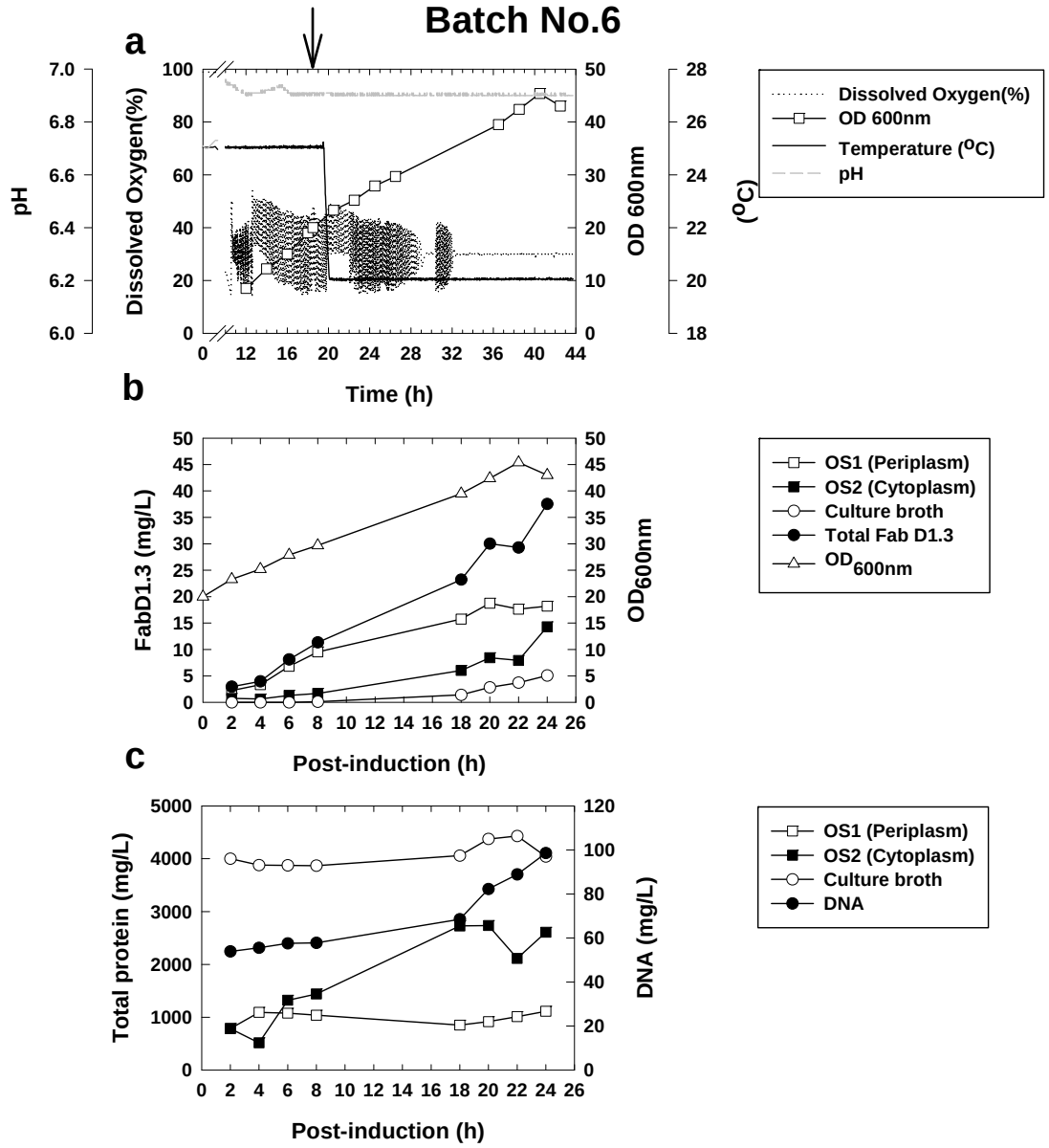

Fig. 2.7 Fed-batch fermentative production (initial volume 3 L) of Fab D1.3 (anti lysozyme) in recombinant E. coli at 25°C then decreased to 20°C upon induction. Induction (arrow) was performed with 0.1 mM IPTG at OD~ 20. **(a)** Dissolved oxygen %, Temperature and pH value were recorded by computer, optical density was measured by spectrometer at 600_{nm} wavelength. Arrow indicated the point of induction. **(b)** Concentration of active Fab D1.3 measured by ELISA in three subcellular fractions from osmotic shock treatment **(c)** [total protein] was measured by BCA assay in the three subcellular fractions and [DNA] in culture broth was measured by DPA assay.

Cultivation conditions applied in this fermentation were the same as described in batch No.5, except that the temperature was reduced by 5°C upon induction to 20°C. Fig. 2.7 (a) shows the each parameter applied to this

fermentation, pH was controlled at 7. Induction was performed with 0.1 mM IPTG at 18.5 h after inoculation when the OD_{600} was around 20, cells were harvested after 42.5 h total cultivation, and the final OD_{600} was 43. Fig. 2.7 (b) shows clearly that most Fab accumulated in the periplasm (OS1), followed by the cytoplasm (OS2) and finally the culture broth. The Fab concentration in each fraction increased along with the increase of the OD_{600} value, which matched with the observation in batch .5 that the yield of Fab increased concurrently with biomass when a sufficient quantity of inducer was added. Noticeably only a little Fab leaked out into the culture broth 18 h post-induction. Fig. 2.7 (c) shows the same result of DNA content in the culture broth started to increase 18 h after post-induction. Those results indicated that to prevent periplasmic Fab leaking into culture broth and to preserve the integrity of cells, harvesting should be earlier than 18 h post-induction. Thus we have effectively defined the harvest window. Furthermore, in combination of Fig. 2.7 (b and c) compared with batch No.5 (Fig. 2.6 b and c) show the Fab purity in the periplasmic fraction (OS1) at the end of fermentation had been greatly improved (1.6% *cf.* 0.24%). As mentioned in batch.5, there was a certain period of time during fermentation when the majority of Fab was retained in the periplasm (e.g. at 8 h post-induction); because the [total protein] was much lower in the periplasm compared to the culture broth (1.7 g/L *cf.* 4 g/L), hence the purity of Fab in the periplasm was higher than the culture broth (0.67% *cf.* 0.21%). In order to maximise the Fab purity and yield in the periplasm, the current decision for cell harvest needs to be revised. We need to investigate the optimal timing for harvesting not depending on the decrease

of OD value. Therefore we can determine the “operation window” for the fermentation.

Fig. 2.7 (b and c) illustrate that the purity of Fab in the periplasmic fraction (OS1) was 1.85% at 18 h post-induction, 2 h later hit a peak of 2% then decreased nearly 0.2% every 2 h; at 24 h post-induction it was 1.63%. Further, the [Fab] in culture broth increased from 1.4 mg/L to 5 mg/L (18 h to 24h post-induction). Likewise, Fig. 2.7 (c) shows that [DNA] was just above 60 mg/L in the culture broth 18 h post-induction, then gradually increased every 2 h and was nearly 100 mg/L in the end of fermentation. The above suggest that from 18−24 h post-induction, some cells began to lyse but fortunately most Fab was still in the periplasm. Noticeably, a distinct difference was observed; in batch No.5 the most of Fab leaked out into culture broth, but in batch No.6 most Fab accumulated in the periplasm. The result suggested that further lowering the cultivation temperature upon induction had effectively slowed down the protein synthesis process (compare total [Fab] in Fig. 2.6 and Fig. 2.7), thereby prolonging the duration of protein production meanwhile maintaining both the cells integrity and protein accumulation in the desired compartment. This can be seen as a means to manipulate the location of Fab. However, this strategy can neither prevent cell lysis after 18 h post-induction, which was indicated by the increase in [DNA] in the culture broth, nor increase the overall titre, which was similar to batch No.5. Although reducing temperature upon induction seems to be effective in controlling the location for accumulation, the overall titre was still not competitive with the result mentioned in Hodgson *et al.* (2007) and Jalalirad, (2010).

The results from shake flask experiments have shown an increase in overall titre by increasing the [IPTG] when induced at the same biomass. To increase the Fab production and extend the operation window, in the next fermentation we doubled the concentration of inducer and harvested cells earlier, allowing simultaneous cell growth and production and harvest before cells lysis occurred (Kilikian *et al.*, 2000).

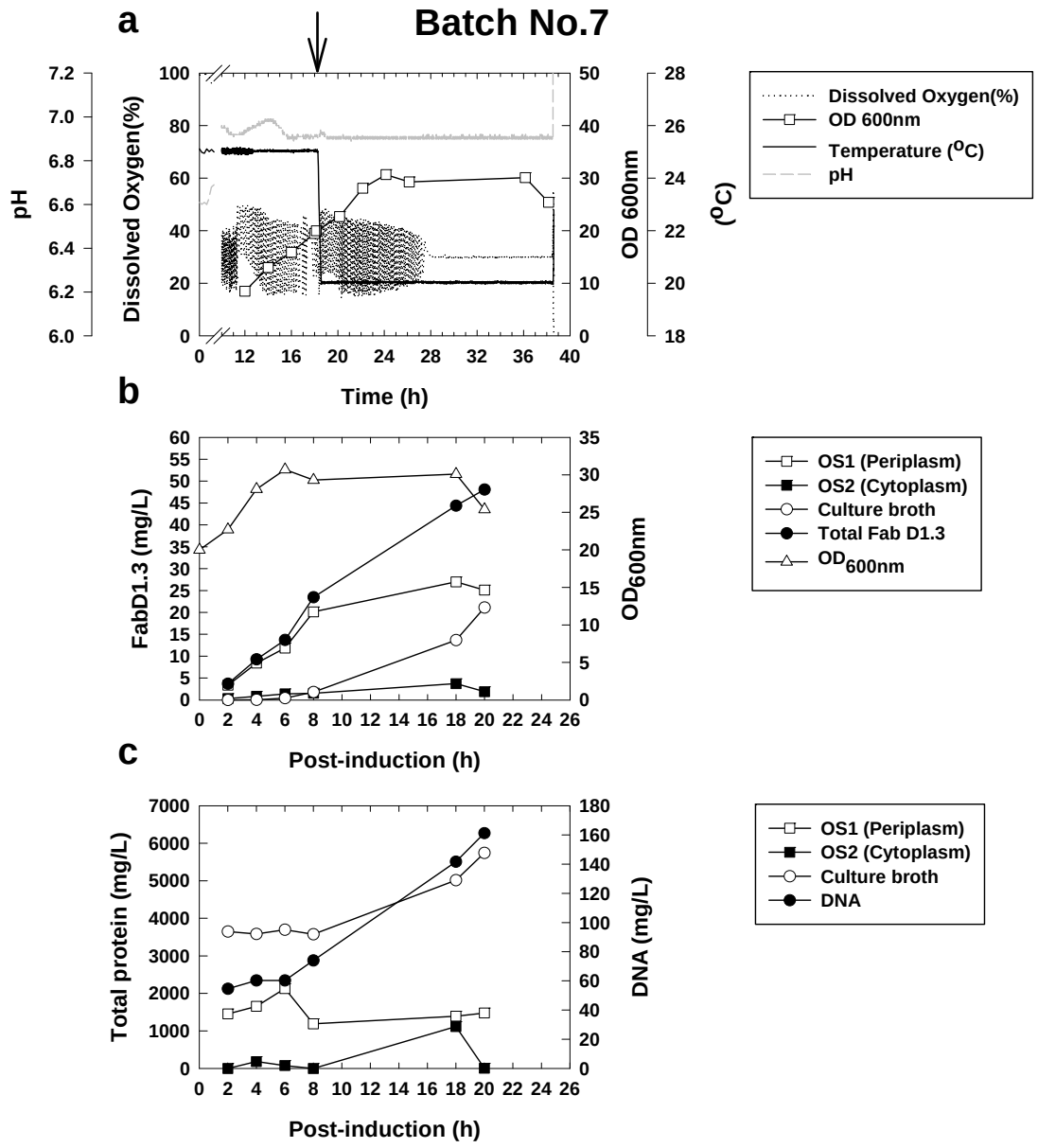

Fig. 2.8 Fed-batch fermentative production (initial volume 3 L) of Fab D1.3 (anti lysozyme) in recombinant E. coli at 25°C then decreased to 20°C upon induction. Induction (arrow) was performed with 0.2 mM IPTG at OD~ 20. **(a)** Dissolved oxygen %, Temperature and pH value were recorded by computer, optical density was measured by spectrometer at 600_{nm} wavelength. Arrow indicated the point of induction. **(b)** Concentration of active Fab D1.3 measured by ELISA in three subcellular fractions from osmotic shock treatment **(c)** [total protein] was measured by BCA assay in the three subcellular fractions and [DNA] in culture broth was measured by DPA assay.

Cultivation conditions applied in this fermentation was the same as described in batch No.6, except that 0.2 mM IPTG was applied for induction. Fig. 2.8 (a) showed the each parameter applied to this fermentation stably maintained at pH 7 and temperature was set at 25°C then decreased to 20°C upon induction,

the level of dissolved oxygen was decreased when the biomass was increased, 0.2 mM IPTG was added 18.15 h after inoculation when the OD_{600} was 20 and cells were harvested after 38.15 h cultivation, the final OD_{600} being 25.4. Compared to the previous fermentation (batch No.6) (Fig. 2.7 and Fig. 2.8), cultivation time to reach OD_{600}~20 was very similar (batch No.6 was 18.5 h *cf.* batch No.7 was 18.15 h) but the growth rate after induction was much slower than batch No.6, resulting in lower final OD_{600} value (ca. ~25.4). Not surprisingly, the reduction of cell growth rate was due to the higher [IPTG] of 0.2 mM (Miao and Kompala, 1992; Jeong and Lee, 1999; Choi *et al.*, 2000, 2006)

Both Fig. 2.8(b) and Fig. 2.7(b) show a steady increase of Fab accumulated in the OS1 fraction during the first 8 h post-induction. Notably, increase in [IPTG] from 0.1 mM to 0.2 mM has received a positive effect on the overall Fab yield at the end of the fermentation increased by 22% compared with batch No.6 (48 mg/L in batch No.7 *cf.* 37.5 mg/L in batch No.6). At the end of fermentation, Fab yield in the OS1 fraction (periplasm) increased by 28% (25 mg/L in batch No.7 *cf.* 18 mg/L in batch No.6). Further, the Fab production rate at first 8 h post-induction was 2 times faster in batch No.7, which suggested using high [IPTG] for induction might be possible to accumulated significant amounts of the recombinant proteins in the cell (Kilikian *et al.*, 2000).

However, the consequence was an overall increase in [DNA] and [total protein] in culture broth between 8 h post-induction and harvest (Fig. 2.8 c), which imply the optimum production duration should be no longer than 8 h post-induction and that cell harvesting should be no later than 6 to 8 h post-

induction. Also, this might indicate that *E. coli* strain CLD048 was not capable of growing and producing this recombinant Fab simultaneously. A better strategy to apply on this strain for Fab production would be separating the cell growth phase and protein expression phase. First to achieve relatively high biomass and induction is performed with 0.1~0.2 mM [IPTG], then harvesting in a short period of time after induction, as seen in batches 6 and 7. Another speculation was mentioned in (Stock *et al.*, 1977; Van Wielink *et al.*, 1990) that the periplasmic space of *E. coli* is of limited physical size (i.e. between 20% to 40% of the total cell volume) and therefore has a specific capacity for proteins. Although the overall titre of Fab was systematically increased over the process, it might be possible that we have reached the natural limit for proteins accumulated in the periplasm in *E. coli*. Thus far, although the overall Fab titre was increased massively from 1 to 50 (mg/L) with partially controlling the location of Fab accumulation, the fermentation system still did not meet the goal we set to achieve at the beginning (≥ 100 mg/L of releasable Fab D1.3). As the results, an alternative strain is required from UCB Celltech to express A33 Fab′ (Chapter 4) to carry on further research and provide to project partners as initial feedstock for testing on the aqueous micellar two phase systems for continuously protein separation (Chapter 5).

2.4.5. Summary of the shake flasks experiments and fermentation results

In this section, the condition changes for the fermentations are summarised in Table 2.5 and Table 2.6 list all the conditions applied to different batches of fermentation to illustrate the change on the different parameters and the

subsequent effect on the Fab 1.3 production in periplasm, cytoplasm and culture broth. In addition, the purity of Fab in each location was calculated from the concentration of Fab dived by concentration of total protein to allow comparing feedstock conditions for the following purification. Initially, our goal in this study was to employ *E. coli* strain CLD048 to produce a minimum 100 mg/L of the releasable anti-Hen Egg White Lysozyme antigen binding fragment (anti-HEWL Fab D1.3) in the culture broth or from intracellular (ca. 40 mg/L could be potential yield from the periplasm) as a model feedstock for screening and testing the high binding capacity cation exchange ligand coupled on magnetic particles.

Table 2.5 Summary of cultivation conditions applied to 3L *E. coli* fermentations for (Anti-HEWL) Fab D1.3 production.

Batch	Temperature (°C)	OD_{600} at induction	IPTG (mM)	Cultivation time to induction (hours)	Post- induction (hours)	Total cultivation time (hours)	Final OD_{600}
1	37	47.9	0.1	8	7	15	61.8
2	30	42.3	0.1	14	7	21	49.9
3	25	1	0.02	3.5	27.5	31	47
4	25	20	0.02	18	16.5	34.5	86
5	25	20	0.1	17	16	33	34.2
6	25 → 20	20	0.1	18.5	24	42.5	43
7	25 → 20	20	0.2	18.15	20	38.15	25.4

Table 2.6 Summary of the [Fab], [total protein] and [DNA] in different condition fermentations.

Batch No.	Temperature (°C)	Induction OD_{600nm}	IPTG (mM)	Fab (mg/L)				Total Protein(g/L)			Purity of Fab in different location (%)			DNA[2] in culture broth (mg/L)
				CB[2]	OS1[2]	OS2[2]	Total	CB[2]	OS1[2]	OS2[2]	CB	OS1	OS2	
1	37	47.9	0.1	0.582	0.686	0.117	1.385	11.568	-	-	0.005	-	-	-
2	30	42.3	0.1	28.038	4.700	0.242	32.98	7.780	-	-	0.36	-	-	0.985
3	25	1	0.02	4.027	6.600	0.828	11.455	2.637	1.605	0.400	0.153	0.411	0.207	0.11
4	25	20	0.02	1.196	2.246	11.64	15.082	3.347	0.782	2.260	0.036	0.287	0.515	0.08
5	25	20	0.1	30.968	3.610	1.597	36.175	7.329	1.510	1.037	0.422	0.239	0.154	0.307
6	25->20	20	0.1	5.05	18.19	14.31	37.55	4.040	1.113	2.609	0.125	1.634	0.548	0.099
7	25->20	20	0.2	21.09	25.08	1.89	48.06	5.744	1.477	1.116	0.367	1.698	0.169	0.161

[2] All samples were measured in the end of fermentation (harvest). Fab was measured using ELSIA, total protein using BCA assay and DNA using DPA assay. CB= Culture broth, OS1= Supernatant of osmotic shock 1 solution (periplasmic fraction), OS2= Supernatant of osmotic shock 2 solution (cytoplasmic fraction)

In batch No.1, cultivation temperature was set at 37°C and induction was performed with 0.1 mM IPTG at OD_{600}~ 45 which resulted in a very short production phase overlapping with severe cell lysis. More than 40% of the active and soluble Fab leaked into the culture broth, which has a total protein concentration of 11.57 g/L (Table 2.6). Following by temperature reduction cultivation at 30°C in batch 2, although the overall Fab titre was improved hugely (ca. ~33 mg/L), however the most of Fab was again in the culture broth, which was heavily contaminated with DNA (ca. ~1 g/L) and over 7 mg/L of total protein. Because of the complex media used for *E. coli* strain CLD048, the ionic strength of the culture broth was around 35 mS/cm at the end of fermentation. Therefore, it was very difficult to purify Fab directly from the complex and heavily contaminated culture broth by CEX (Lacki *et al.*, 2007). Jalalirad (2010) mentioned that a dialysis process would be necessary if trying to purify Fab from the culture broth, but more than 50% of the Fab product was lost during the process. Therefore, directing Fab into the periplasm would be more suitable for this study (Humphreys, 2007). Coupled shake flask experiments were conducted based on the concept provided from Sevastsyanovich *et al.* (2009) to investigate the effects on growth temperature, IPTG concentration and timing of induction for the Fab production and location (i.e. cytoplasm, periplasm or culture broth). The results suggested that decreased cultivation temperature (i.e. 30°C to 25°C) with an increase of [IPTG] (i.e. 8 μM to 50 μM) improved the overall Fab production. Further, induction with higher biomass (OD_{600} ~ 0.5 *cf.* OD_{600} ~ 1) showed increase in the total Fab production too. Noticeably, induction with higher [IPTG] per cell result in Fab leaking into the culture broth (Fig. 2.3).

According to results from the shake flask experiment along with the improved protocol of Sevastsyanovich *et al.* (2009), batch No.3 (Fig. 2.4) was induced with 0.02 mM of IPTG at OD_{600} of 1 at 25°C. Noticeably, the overall Fab production was decreased 65% compared to batch No.2 (11.45 mg/L *cf.* 32.98 mg/L) but 60% of the Fab was detected in OS1 fraction (periplasm) (Table 2.6). The result indicates that induction was performed at low [IPTG] (0.02 mM) and low biomass (OD_{600}~1) allowed Fab accumulated in the periplasm and avoided leaking into the culture broth even with the longest cultivation time (27.5 h post-induction) compared with the other fermentations (Table 2.5), the cells remained intact. Therefore, low [DNA] was detected in the culture broth (0.11 mg/L) at the end of fermentation. The possible reason for low titre of Fab production is because of the induction at low biomass (OD_{600}~1), which is also observed from the result of the shake flask experiments (Fig. 2.3). Therefore, in the next fermentation induction was performed at OD_{600}~20 (Fig. 2.5).

Surprisingly, Table 2.6 shows the induction with 0.02 mM of [IPTG] at OD_{600} of 20 did not result in a significant increase in overall Fab production compared with batch No.3 (15 mg/L *cf.* 11.45 mg/L). In striking contrast, around 77% of Fab was accumulated in cytoplasm, which suggested that: (i) although Fab was synthesised after induction, it was not translocated into periplasm; and (ii) a low [DNA] (~0.08 mg/L) was detected in the culture broth with high final OD value (~86) which suggested that cells were as intact as in the previous fermentation. In order to improve the yield of Fab, Miao and Kompala (1992) suggested higher than 0.1 mM [IPTG] should be used to overcome culture instability when induction at midexponential phase. Therefore, we have increased [IPTG] to 0.1 mM for induction.

Comparing between batches No.5 and No.4, the increase in [IPTG] for induction seems to be an effective strategy that increased the total yield of Fab more than 2 fold (36.2 mg/L *cf.* 15.1 mg/L), despite of fact that majority of Fab (ca. 85%) was detected in the culture broth in the end of fermentation batch No. 5 (Table 2.6). Similar result was observed in batch No.2 (Table 2.6) that the most Fab (ca. 85%) leaked into culture broth indicated that cells after induction were not able to kept protein the Fab within the cells. Furthermore, shake flask results (Fig. 2.3), demonstrated that the majority of Fab was shifted from the culture broth to the periplasm when the temperature was decreased from 30°C to 25°C. Therefore, we decided to decrease the cultivation temperature from 25°C to 20°C upon induction, in order to keep the majority of Fab in the periplasm.

The last two fermentations (batch No.6 and No.7) were considered successful examples. Using the same [IPTG] (0.1 mM) in batches No.5 and No.6 (Table 2.5) did not increase the overall Fab titre but decrease in temperature from 25°C to 20°C upon induction in batch.6 has successfully directed the Fab to accumulate in the periplasm and the cytoplasm (Table 2.6). The majority of Fab was in OS1 (18.19 mg/L) and OS2 (14.31 mg/L) fraction by the end of fermentation (Table 2.6). Similar Fab production behaviour was also observed in batch No.4 (Fig. 2.5 b) that cytoplasm contained higher amount of [Fab] suggesting that a further increase [IPTG] was feasible to increase the yield of Fab. Since targeting the Fab accumulation in the periplasm and adopting the improved protocol from Sevastsyanovich *et al.* (2009), we have improved the purity of Fab in the periplasmic fraction (OS1) by 4 times (0.41% *cf.* 1.63%), compared with the result obtained in batch No.3 (Table 2.6). Therefore, we

have tried to double the [IPTG] for induction in batch No.7 for increase the overall titre of Fab and allocate the majority of Fab into the periplasm.

As expected, the overall titre of Fab increased 30% (ca. 48 mg/L) in batch No.7 compared with batch No.6 by doubling the [IPTG] for induction. In addition, periplasm (ca. 52%) and culture broth (ca. 43%) are two main locations where Fab was detected for batch.7 (Table 2.6). Not only the yield of Fab in the periplasm was increased, but also the purity of Fab in the periplasm slightly increased to nearly 1.7%, which was the highest purity compared to the other batches (Table 2.6). Further, it can be noticed that [Fab] in the periplasm increased in the first 8 h post-induction, whereas after 8 hours only increased slightly. Whereas [DNA] and [Fab] in the culture broth increased after 8 h post-induction until in the end of fermentation, which might suggest to maintain the cell integrity and avoid Fab leakage from the periplasm into the culture broth, the operation window for cell harvesting should be done in the early stage after induction (i.e. 8 h post-induction).

2.4.6. Improvement of solubility of target protein

As demonstrated by the above fermentation data, adapting the improved protocol from Sevastsyanovich *et al.* (2009) appears to improve the overall Fab titre and enable us to partially control the location of Fab. To extend the study in order to investigate Fab solubility, Bugbuster was employed to isolate soluble and insoluble proteins from cell pellets collected from each fermentation batch. Soluble and insoluble fractions were separated by 14% polyacrylamide gel electrophoresis, transferred to PVDF membrane and Fab D1.3 was detected using Western blotting. Utilising densitometry software

"ImageJ" allowed us to compare the ratio of soluble to insoluble Fab in each fermentation (Fig. 2.9).

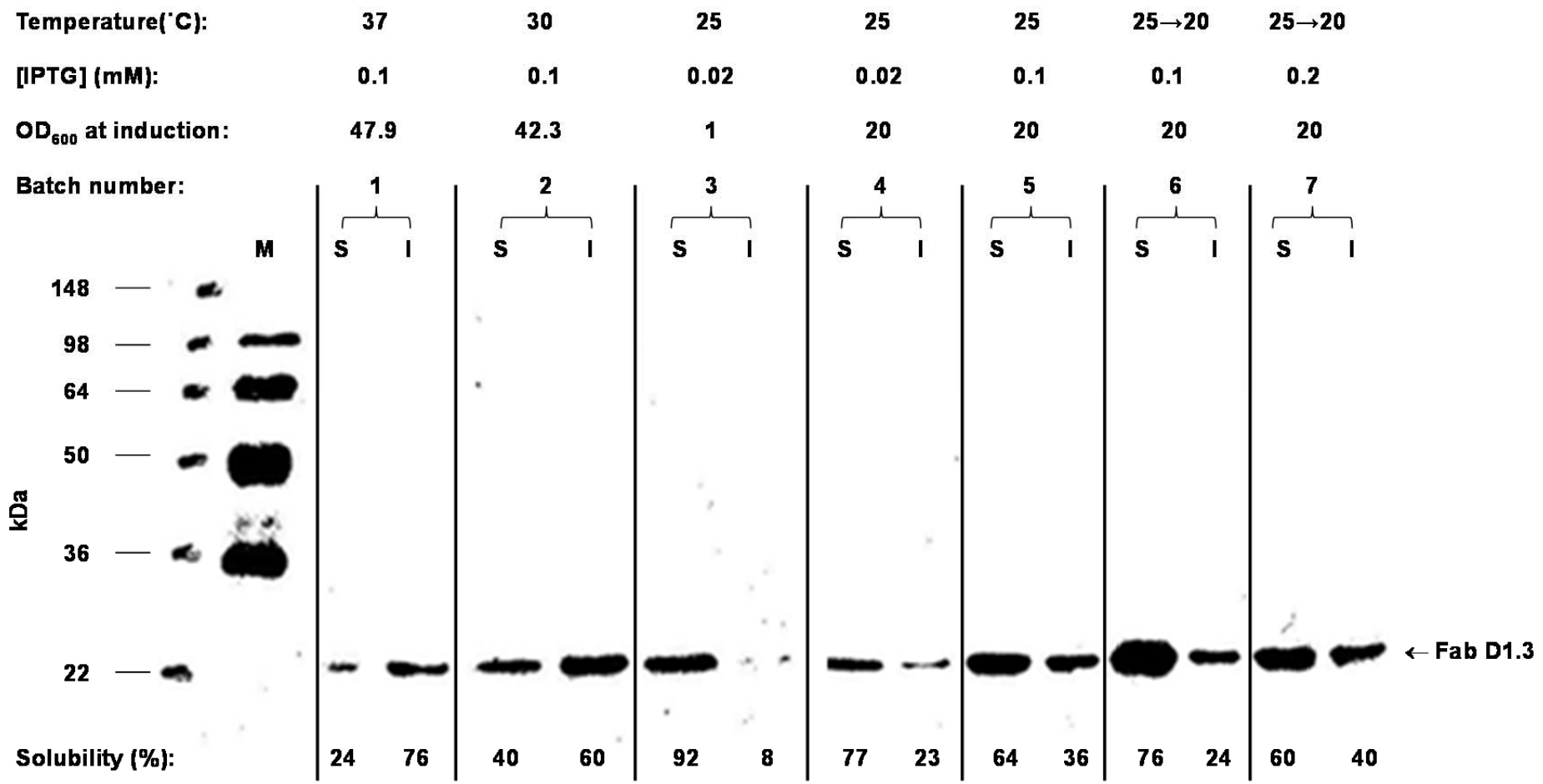

Fig. 2.9 Western blot analysis of soluble **(S)** and insoluble **(I)** samples arising from Bugbuster fractionation. Whole cell pellet (1 mL) fraction derived from Bugbuster was washed in PBS buffer, centrifuged, and the obtained soluble and insoluble samples. Prior to Western blotting, samples were subjected to 14% reducing SDS-PAGE. Conditions applied to different fermentation batches were described above, arrow indicates the protein band of Fab D1.3.

In the first two batches (No.1 and 2) showed more than 50% of Fab was in insoluble form, while in batches where the growth temperature was decreased to 25°C (i.e. batch No.3 thereafter), a significant change was observed in favour of soluble Fab production. Although the total Fab production was not promising in batch No.3 (11.45 mg/L), it showed that 92% of the Fab was soluble, only 8% insoluble form was detected, which was the best result among those conditions. The results suggest the ratio of soluble to insoluble was highly related to temperature, [IPTG] and timing of induction (Schein and Noteborn, 1988; Vera, 2007; Sevastsyanovich *et al.*, 2009). Comparing batches No.3 and 4, where induction was performed at higher biomass (OD_{600}~20), resulted in an increase in the quantity of insoluble Fab, yet still 77% of Fab produced in the cell remained soluble.

Increase in [IPTG] showed significant increase in the overall yield of Fab in batch No.5, but the ratio of soluble to insoluble decreased more than 10% compared to batch No.4. Fernández-Castané and co-workers (2012) suggested that the rate of IPTG intake by cells increases when higher [IPTG] was supplied for induction, thereby increasing the protein synthesis rate. Consequently, a lower ratio of soluble to insoluble Fab was observed in batch No. 5.

In batch No.6, decrease temperature upon induction from 25°C to 20°C aided Fab retaining in the cell (i.e. periplasm and cytoplasm, total [Fab] was 32.5 mg/L), but also increased the ratio of soluble to insoluble (from 64% to 76%) compared with batch No.5. The result implied that temperature effect on protein synthesis rate was greater than additional IPTG, therefore slowing the rate of protein synthesis, and then improving Fab solubility. Taking

advantages of altering cultivation conditions in terms of temperature and induction timing, batch No.6 has shown the completely opposite soluble to insoluble ratio versus batch.1 suggested that the cultivation strategy adopted from the improved protocol (Sevastsyanovich *et al.*, 2009) is applicable to this expression system, thereby increasing the correct folding of Fab D1.3.

In the last batch of fermentation (batch No.7), 0.2 mM of [IPTG] was used for induction. Not surprisingly, a decrease in solubility of Fab was observed when [IPTG] was increased (60%), which was similar to batch No.5 (ca. 64%). Yet again, the Fab titre increased to 48.06 mg/L, mainly being present in the periplasm (ca. 25 mg/L) and culture broth (ca. 21 mg/L). Taken collectively, batch No.7 might not have the highest ratio of soluble to insoluble, but the total yield of Fab was the best, especially in periplasmic fraction. Whereas batch No.3 had the highest ratio of soluble to insoluble (ca. 92%) but the total Fab production was too low (ca. 11.455 mg/L). As the result, carefully balance between the titre of Fab and solubility is crucial to enable more soluble active Fab.

2.5. **Conclusions**

Shake flask experiments coupled to osmotic shock extraction helped us to identify suitable cultivation condition for the production of Fab D1.3. Following a systematic improved protocol (Sevastsyanovich *et al.*, 2009) we investigated the impact of temperature, induction timing and inducer concentration on the titre, location and solubility of Fab.

From the last two fermentations we have also determined the growth conditions suitable for this strain and the Fab production window should be between 6 to 8 h post-induction for harvesting. If the cells were harvested later than this stage, the Fab began to leak out into culture broth. In conclusion, we have demonstrated substantial control over the length of the production phase, Fab D1.3 distribution and form, and the level of contamination by DNA also identifying the optimal conditions for maximising the accumulation of Fab D1.3 in periplasm, which is using a cultivation temperature of 25°C then decreasing to 20°C upon induction at OD_{600} of 20 with 0.2 mM of [IPTG] and harvest between 6 to 8 h after induction. However, it was not possible to accumulate all of the soluble Fab D1.3 in the periplasm and the titres achieved are low (≤ 25 mg/L of original culture, 1.7% initial Fab purity in the periplasmic fraction) (Table 2.6, batch No.7). Furthermore, cell integrity appears to be poor, even after low temperature growth and induction and early harvesting. Evidence for this comes from the overly high protein and DNA content of OS1 (data not shown). The unexpectedly heavy contamination of OS1 seriously compromises the subsequent separation performance. Taken collectively, the unsuccessful fermentation for Fab D1.3 production was due to the nature of this strain. Despite all the progress we have achieved thus far, the basic and the most important issue still remains unsolved; the titre of Fab is still far too low to meet our goal (≥ 100 mg/L of releasable Fab D1.3). As the result, we have decided to abandon this strain and looked for an alternative strain, which will be provided from the UCB Celltech to express A33 Fab′ in periplasm.

2.6. **References**

Ami, D., Natalello, a, Schultz, T., Gatti-Lafranconi, P., Lotti, M., Doglia, S.M., and Marco, A. de (2009). Effects of recombinant protein misfolding and aggregation on bacterial membranes. Biochimica et Biophysica Acta *1794*: 263–9.

Baneyx, F. (1999). Recombinant protein expression in *Escherichia coli.* Current Opinion in Biotechnology *10*: 411–421.

Carton, J.M., Sauerwald, T., Hawley-Nelson, P., Morse, B., Peffer, N., Beck, H., Lu, J., Cotty, A., Amegadzie, B., and Sweet, R. (2007). Codon engineering for improved antibody expression in mammalian cells. Protein Expression and Purification *55*: 279–86.

Chadd, H.E., and Chamow, S.M. (2001). Therapeutic antibody expression technology. Current Opinion in Biotechnology *12*: 188–194.

Cheah, U.E., Weigand, W. a, and Stark, B.C. (1987). Effects of recombinant plasmid size on cellular processes in *Escherichia coli*. Plasmid *18*: 127–34.

Chen, R. (2011). Bacterial expression systems for recombinant protein production: E. coli and beyond. Biotechnology Advances 1–6.

Choi, J.H., Jeong, K.J., Kim, S.C., and Lee, S.Y. (2000). Efficient secretory production of alkaline phosphatase by high cell density culture of recombinant *Escherichia coli* using the Bacillus sp. endoxylanase signal sequence. Applied Microbiology and Biotechnology *53*: 640–5.

Choi, J.H., Keum, K.C., and Lee, S.Y. (2006). Production of recombinant proteins by high cell density culture of *Escherichia coli*. Chemical Engineering Science *61*: 876–885.

Corisdeo, S., and Wang, B. (2004). Functional expression and display of an antibody Fab fragment in *Escherichia coli*: study of vector designs and culture conditions. Protein Expression and Purification *34*: 270–9.

Curless, C., Pope, J., and Tsai, L. (1990). Effect of preinduction specific growth rate on recombinant alpha consensus interferon synthesis in *Escherichia coli*. Biotechnology Progress *6*: 149–52.

Daniel, R., and Gottschalk, G. (1992). Growth temperature-dependent activity of glycerol dehydratase in *Escherichia coli* expressing the Citrobacter freundii dha regulon. FEMS Microbiology Letters *79*: 281–5.

Donovan, R.S., Robinson, C.W., and Glick, B.R. (1996). Review: optimizing inducer and culture conditions for expression of foreign proteins under the control of the lac promoter. Journal of Industrial Microbiology *16*: 145–54.

Farid, S.S. (2007). Process economics of industrial monoclonal antibody manufacture. Journal of Chromatography. B, Analytical Technologies in the Biomedical and Life Sciences *848*: 8–18.

Fernández-Castané, A., Caminal, G., and López-Santín, J. (2012). Direct measurements of IPTG enable analysis of the induction behavior of E. coli in high cell density cultures. Microbial Cell Factories *11*: 58.

Gasser, B., Saloheimo, M., Rinas, U., Dragosits, M., Rodríguez-Carmona, E., Baumann, K., Giuliani, M., Parrilli, E., Branduardi, P., Lang, C., Porro, D., Ferrer, P., Tutino, M.L., Mattanovich, D., and Villaverde, A. (2008). Protein folding and conformational stress in microbial cells producing recombinant proteins: a host comparative overview. Microbial Cell Factories *7*: 11.

Gombert, a K., and Kilikian, B. V (1998). Recombinant gene expression in *Escherichia coli* cultivation using lactose as inducer. Journal of Biotechnology *60*: 47–54.

Harrison, J.S., and Keshavarz-Moore, E. (1996). Production of antibody fragments in *Escherichia coli*. Annals of the New York Academy of Sciences *782*: 143–58.

Hockney, R.C. (1994). Recent developments in heterologous protein production in *Escherichia coli*. Trends in Biotechnology *12*: 456–63.

Hodgson, I., Lennon, C., and Kara, V. (2007). Expression system.

Holt, J.G., Krieg, N.R., Sneath, P.H.A., Staley, J.T., and Williams, S.T. (2000). Facultatively anaerobic gram-negative rods, group 5. Bergeys Manual of Determinitive Bacteriology (New York: Lippen- cott Williams and Wilkins).

Houdebine, L.-M. (2002). Antibody manufacture in transgenic animals and comparisons with other systems. Current Opinion in Biotechnology *13*: 625–629.

Humphreys, D.P. (2007). Periplasmic Expression of Antibody Fragments. In The Periplasm, (American Society for Microbiology), pp 361–388.

Humphreys, D.P., Carrington, B., Bowering, L.C., Ganesh, R., Sehdev, M., Smith, B.J., King, L.M., Reeks, D.G., Lawson, A., and Popplewell, A.G. (2002). A plasmid system for optimization of Fab' production in *Escherichia coli*: importance of balance of heavy chain and light chain synthesis. Protein Expression and Purification *26*: 309–20.

Humphreys, D.P., Heywood, S.P., King, L.M., Bowering, L.C., Turner, J.P., and Lane, S.E. (2004). Engineering of *Escherichia coli* to improve the purification of periplasmic Fab' fragments: changing the pI of the chromosomally encoded PhoS/PstS protein. Protein Expression and Purification *37*: 109–18.

Humphreys, D.P., Sehdev, M., Chapman, A.P., Ganesh, R., Smith, B.J., King, L.M., Glover, D.J., Reeks, D.G., and Stephens, P.E. (2000). High-level periplasmic expression in *Escherichia coli* using a eukaryotic signal peptide: importance of codon usage at the 5' end of the coding sequence. Protein Expression and Purification *20*: 252–64.

Humphreys, D.P., Weir, N., Lawson, a, Mountain, a, and Lund, P. a (1996). Co-expression of human protein disulphide isomerase (PDI) can increase the yield of an antibody Fab' fragment expressed in *Escherichia coli*. FEBS Letters *380*: 194–7.

Jalalirad, R. (2010). Improving the recovery of "difficult to release" periplasmically-expressed products from recombinant E. coli. University of Birmingham.

Jana, S., and Deb, J.K. (2005). Strategies for efficient production of heterologous proteins in *Escherichia coli*. Applied Microbiology and Biotechnology *67*: 289–98.

Jeong, K.J., and Lee, S.Y. (1999). High-level production of human leptin by fed-batch cultivation of recombinant *Escherichia coli* and its purification. Applied and Environmental Microbiology *65*: 3027–32.

Jones, P.G., Vanbogelen, R.A., and Neidhardt, F.C. (1987). Induction of proteins in response to low temperature in *Escherichia coli*. J. Bacteriol. *169*: 2092–2095.

Kelley, B. (2009). Industrialization of mAb production technology: the bioprocessing industry at a crossroads. mAbs *1*: 443–52.

Kilikian, B.V., Suárez, I.D., Liria, C.W., and Gombert, A.K. (2000). Process strategies to improve heterologous protein production in *Escherichia coli* under lactose or IPTG induction. Process Biochemistry *35*: 1019–1025.

Kosinski, M., Rinas, U., and Bailey, J. (1992). Isopropyl-β-d-thiogalactopyranoside influences the metabolism of *Escherichia coli*. Applied Microbiology and Biotechnology *36*:

Lacki, K.M., Mueller, J., Harinarayan, C., Reis, R. Van, Fahrner, R., Alstine, J.M. Van, Healthcare, G.E., Ab, B., Uppsala, S.-, Ljunglöf, A., Reis, R. van, and Alstine, J.M. Van (2007). Ion exchange chromatography of antibody fragments. Biotechnology and Bioengineering *96*: 515–24.

Lin, B., Renshaw, M.W., Autote, K., Smith, L.M., Calveley, P., Bowdish, K.S., and Frederickson, S. (2008). A step-wise approach significantly enhances protein yield of a rationally-designed agonist antibody fragment in E. coli. Protein Expression and Purification *59*: 55–63.

Miao, F., and Kompala, D.S. (1992). Overexpression of cloned genes using recombinant *Escherichia coli* regulated by a T7 promoter: I. Batch cultures and kinetic modeling. Biotechnology and Bioengineering *40*: 787–96.

Mücke, M., Ostendorp, R., and Leonhartsberger, S. (2009). E. coli Secretion Technologies Enable Production of High Yields of Active Human Antibody Fragments. BioProcess Technical.

Neubauer, P., Hofmann, K., Holst, O., Mattiasson, B., and Kruschke, P. (1992). Maximizing the expression of a recombinant gene in *Escherichia coli* by manipulation of induction time using lactose as inducer. Applied Microbiology and Biotechnology *36*:

Panda, A.K. (2003). Bioprocessing of therapeutic proteins from the inclusion bodies of *Escherichia coli*. Advances in Biochemical Engineering/biotechnology *85*: 43–93.

Pinsach, J., Mas, C. de, López-Santín, J., Striedner, G., and Bayer, K. (2008). Influence of process temperature on recombinant enzyme activity in *Escherichia coli* fed-batch cultures. Enzyme and Microbial Technology *43*: 507–512.

Ramos, J.L., Gallegos, M.-T.T., Marqués, S., Ramos-González, M.-I.I., Espinosa-Urgel, M., and Segura, A. (2001). Responses of Gram-negative bacteria to certain environmental stressors. Current Opinion in Microbiology *4*: 166–71.

Riesenberg, D., Menzel, K., Schulz, V., Schumann, K., Veith, G., Zuber, G., and Knorre, W. (1990). High cell density fermentation of recombinant *Escherichia coli* expressing human interferon alpha 1. Applied Microbiology and Biotechnology *34*:

Rodríguez-Carmona, E., Cano-Garrido, O., Dragosits, M., Maurer, M., Mader, A., Kunert, R., Mattanovich, D., Villaverde, A., and Vázquez, F. (2012). Recombinant Fab expression and secretion in *Escherichia coli* continuous culture at medium cell densities: Influence of temperature. Process Biochemistry *47*: 446–452.

Rosa, P. a J., Ferreira, I.F., Azevedo, a M., and Aires-Barros, M.R. (2010). Aqueous two-phase systems: A viable platform in the manufacturing of biopharmaceuticals. Journal of Chromatography. A *1217*: 2296–305.

Schein, C.H., and Noteborn, M.H.M. (1988). Formation of Soluble Recombinant Proteins in *Escherichia coli* is Favored by Lower Growth Temperature. Bio/Technology *6*: 291–294.

Sevastsyanovich, Y., Alfasi, S., Overton, T., Hall, R., Jones, J., Hewitt, C., and Cole, J. (2009). Exploitation of GFP fusion proteins and stress avoidance as a generic strategy for the production of high-quality recombinant proteins. FEMS Microbiology Letters *299*: 86–94.

Singh, S.M., and Panda, A.K. (2005). Solubilization and refolding of bacterial inclusion body proteins. Journal of Bioscience and Bioengineering *99*: 303–10.

Sockolosky, J.T., and Szoka, F.C. (2012). Periplasmic production via the pET expression system of soluble, bioactive human growth hormone. Protein Expression and Purification *87*: 129–135.

Sørensen, H.P., and Mortensen, K.K. (2005). Advanced genetic strategies for recombinant protein expression in *Escherichia coli*. Journal of Biotechnology *115*: 113–28.

Stock, J.B., Rauch, B., and Roseman, S. (1977). Periplasmic space in Salmonella typhimurium and *Escherichia coli*. J. Biol. Chem. *252*: 7850–7861.

Vallejo, L.F., and Rinas, U. (2004). Strategies for the recovery of active proteins through refolding of bacterial inclusion body proteins. Microbial Cell Factories *3*: 11.

Ventura, S., and Villaverde, A. (2006). Protein quality in bacterial inclusion bodies. Trends in Biotechnology *24*: 179–85.

Vera, A. (2007). The conformational quality of insoluble recombinant proteins is enhanced at low growth temperatures. Biotechnology And *96*: 1101–1106.

Vila, P., Corchero, José LuisCubarsi, R., and Villaverde, A. (1997). Enhanced fitness of recombinant protein synthesis in the stationary phase of *Escherichia coli* batch cultures. BIOTECHNOLOGY LETTERS *3*: 225–228.

Wallace, R.J.R., Holms, W.W.H., Letters, F.M., and Fem, E. (1986). Maintenance coefficients and rates of turnover of cell material in *Escherichia coli* ML308 at different growth temperatures. FEMS Microbiology Letters *37*: 317–320.

Weickert, M.J., Doherty, D.H., Best, E.A., and Olins, P.O. (1996). Optimization of heterologous protein production in *Escherichia coli*. Current Opinion in Biotechnology *7*: 494–499.

Wielink, J.E. Van, Duine, J.A.J.J.A., and Wielink, J. Van (1990). How big is the periplasmic space? Trends in Biochemical Sciences *15*: 136–137.

Wunschel, D.S., Hill, E.A., McLean, J.S., Jarman, K., Gorby, Y.A., Valentine, N., and Wahl, K. (2005). Effects of varied pH, growth rate and temperature using controlled fermentation and batch culture on matrix assisted laser desorption/ionization whole cell protein fingerprints. Journal of Microbiological Methods *62*: 259–71.

Yee, L., and Blanch, H.W. (1992). Recombinant Protein Expression in High Cell Density Fed-Batch Cultures of *Escherichia coli*. Bio/Technology *10*: 1550–1556.

3. Periplasmic release for Fab D1.3 from *E.coli* cells

3.1. Abstract

Sample obtained from a fermentation batch (cultivation temperature 25°C then decreasing to 20°C upon induction at OD_{600nm}~20, with 0.1 mM IPTG.) described in chapter 2 was used in this chapter for the selectivity periplasmic release experiment. Following by purification by affinity and ion exchange chromatography were used in order to purify Fab D1.3 from culture broth and/or osmotic shock fluid samples. In the release experiments suggested that the optimum condition for releasing protein from periplasm should be using 0.1% Sodium deoxycholate (Doc) with shaking for either 0.5 or 2 h, with ratio of cell concentration to buffer between 0.5 to 1. However, due to the issue of large amount of DNA also being released by 0.1% Doc, the osmotic shock was more suitable and employed for the later purification experiments. Impact of feedstock conditioning towards Fab loss and subsequent chromatographic purification with 5 mL HiTrap SP Sepharose XL columns was also examined. A small (~10%) loss in Fab occurred following dilution of cell-free broth (~10 mS/cm), pH adjustment (to pH 5) and clarification (filtration through a 0.2 μm membrane); however, this was offset by a greater loss in contaminating host protein (~ 30%), resulting in improved feedstock quality (1.2 fold purification of Fab). Breakthrough studies conducted with conditioned cell-free broth (lacking benzonase) and OS1 revealed extremely low capacity Fab binding to the SP Sepharose XL. The purity of Fab eluates

coming off OS1 loaded columns were roughly twice those eminating from columns supplied with conditioned broth (10% cf. 5%). The presence of non-proteinaceous material (nucleic acids, LPS) plus high protein contamination likely contribute to the disappointing CEX purification peformance observed with both conditioned broth and OS1 feedstocks. Attempts to purify Fab D1.3 from these same feedstocks by Protein G affinity chromatography also proved unsuccessful.

3.2. **Introduction**

Periplasmic release has received much attention in recent decades for exploring protein production and purification in *E.coli* (Ito *et al.*, 1981; Khosla and Bailey, 1989; Naglak and Wang, 1990; Van Wielink *et al.*, 1990; French *et al.*, 1996; Link *et al.*, 1997; Pierce *et al.*, 1997; Chen *et al.*, 2004a; Liu *et al.*, 2004). This offers a great potential for production, purification and protection of recombinant protein compared with protein secretion into culture broth, which was mentioned briefly in the Chapter 2. In this study, Fab D1.3 (anti-HEWL antibody fragment) has been used throughout all the experiments.

Fab D1.3 is one of the many antibody that requires disulfide bonds for the final folded state for which it is translocated across the cytoplasmic membrane into the periplasm in *E.coli* where it interact with enzymes, mainly DsbA, DsbB, DsbC and DsbD that catalyse the formation and isomerisation of disulfide bonds (Akiyama *et al.*, 1992; Wunderlich and Glockshuber, 1993; Jeong and Lee, 2000; Nakamoto and Bardwell, 2004). The disulfide bond formation occurs due to an oxidative process, where the thiol (SH) groups of two cysteines are joined together by a covalent force (Ehrmann, 2006). In the early 1990s, scientists (Bardwell *et al.*, 1991; Akiyama *et al.*, 1992; Peek and Taylor, 1992) discovered the periplasmic DsbA (disulfide bond binding) protein in *E.coli* which illustrated a clearer mechanism of disulfide bond formation, where enzymes were catalysts crucial for disulfide bonds formation. Generally speaking, *E.coli* does not secrete proteins to culture broth, but extra signal sequences can be inserted upstream of genes for periplasmic targeting (de Marco, 2009), which provides a much cleaner environment for the proteins than the cytoplasm. Further, cells often exposed to a series of

variable threats from the surrounding environment, for example, a sudden change of pH, temperature, salt concentration and the presence of proteases or detergents, where store the invaluable proteins in the periplasmic space can protect them from degradation or denatured in comparison to the outer membrane environment. Another factor taken into account is the size of the periplasm, which was mentioned by Schlegel (1986) that periplasmic layer was only 7 nm wide. This would only occupy approximately 4.5% of the total cell volume, which is very small space for the protein accumulation, especially for the titre up to a few hundred grams per litre production. However, Van Wielink and co-worker (1990) suggested the periplasmic layer, which was believed to be ~7 nm wide, as 4.5% of cell volume was rather underestimated. The actual space for the periplasm determined by electron microscopy comparises 20-40% of the cell volume is between 32 to 71nm wide (Stock *et al.*, 1977). There should be sufficient space in the periplasm for the protein accumulation.

Much research has looked into methods of selectively and effectively release proteins from the periplasm, such as osmotic shock, chemical permeabilisation using surfactants (anionic, cationic, non-ionic), chelators and chaotropic agents or organic solvents (Pierce *et al.*, 1997; Chen *et al.*, 2004b; Jalalirad, 2010), heat treatments (Katsui *et al.*, 1982; Weir and Bailey, 1995). Taking consideration of scalable and generality, osmotic shock seems the better option among the other methods for protein release from the periplasm. Because it does not require detergent uses nor high temperature, which might cause conformation change for some proteins or losing its function (Argos *et al.*, 1979; Digel *et al.*, 2006). A well balance between

selectivity and efficiency are equally important for the protein release and subsequent downstream process; the former provides better purity. Consequently, the feedstock may not require many clarification steps (i.e. multiple cycles of high speed centrifugation, filtration), leading to higher overall yield and less loss of the target product. It also would ease the conditioning process for the initial feedstock when purification is performed on chromatographic system. The latter offers higher titre for the target protein, surely this is the general goal for the protein production, but without selectively release, the product might be heavily contaminated with other protein spices or nucleic acid when the cell is completely burst. As the result, we should strive the optimise condition for both effective and selective protein release in the periplasm. The standard osmotic protocol (Neu *et al.*, 1967) states cells were harvested during late exponential or stationary phase then re-suspended in osmotic shock buffer (concentrated sucrose, EDTA and Tris buffer). The mixture was incubated at low temperature (ca ~4°C) for a short period of time. After liquid-solid separation by centrifugation, the supernatant was collected as the released protein from the periplasm. Here, cells are shrinking due to the high osmotic strength from sucrose solution, EDTA works as a cation chelator to destabilise the cell envelope thereby releasing lipopolysaccharide (LPS), therefore increasing the permeability of the outer membrane. The cold environment can rapidly increase the cell size and aid the protein release from periplasm simultaneously (Chen *et al.*, 2004b). In contrast to osmotic shock, chemical permeabilisation relies on purely on the functions of chemical interactions between the reagents and cell wall. Unlike the requirement of accurate temperature control (~4°C) and time consuming

routine procedure of osmotic shock, chemically releasing is a robust method to apply on protein release. However, due to the nature of protein and use of reagents, it has certain disadvantages, such as causing protein unfolding, degradation, more importantly the toxicity of using surfactants might not be acceptable for the final products. Although heat treatment has been identified as a more effective technique for periplasmic protein release, due to its own limitations, many proteins are not able to tolerate the high temperature environment for long period of time (ca.~ 60°C, 16 h), resulting in protein degradation, changes to conformation or loss of activity. Therefore, this method would only be possible when the target protein is thermally stable.

In this chapter, we have focus on investigating the periplasmic protein release mechanism. All the samples were taken from a single batch of fermentation, which produced was 40 μg/mL Fab D1.3 in the periplasm. For evaluation purposes, release methods were tested by modifying the conditions of the standard osmotic shock (i.e. incubation time, static or with vortex, buffer concentration) to identify the optimum conditions for periplasmic release, also comparing the selectivity of release between osmotic shock and chemical permeabilisation (0.1% Sodium deoxycholate, so called 0.1% Doc). Subsequently, culture broth and OS1 fraction (extraction from periplasm) were used as feedstock with SP_XL HiTrap (CEX) and HiTrap rProteinG (Affinity) columns following protocols described in Ljunglöf et al., (2007) to obtain preliminary purification results.

3.3. **Material and methods**

3.3.1. Materials

All the materials were carried out from Chapter 2. Experiment samples were obtained from fed-batch fermentation described in Chapter 2 (section 2.4.3. Fig. 2.8). Prior to the release experiments by various osmotic shock and sodium deoxycolate (0.1% Doc) conditions, all the fermenation samples were centrifuged at 15,800 *g* for 600 s to remove the culture medium.

3.3.2. Methods

3.3.2.1. Modified osmotic shock for periplasmic protein release

Initially, a large proportion of cell pellet was resuspended in PBS buffer to OD~25. One millilitre fermentation aliquot sample was centrifuged for 600 s at 15,800 *g*. Supernatant was removed and kept for further analysis. Different volumes of osmotic shock solution (0.5, 1, 2, 3 mL) were mixed with the pellets and incubated for 10 or 30 minutes on the ice statically or shaking (1000 rpm).

3.3.2.2. 0.1% sodium deoxycholate for periplasmic protein release

Initially, a large proportion of cell pellet was resuspended in PBS buffer to OD~25. One millilitre fermentation aliquot sample was centrifuged for 600 s at 15,800 *g*. Supernatant was removed and kept for further analysis. Different volumes of 0.1% Doc solution (0.5, 1, 2 mL) were mixed with the pellets on

the shaker (1000 rpm) and incubated for various time length (i.e. 900s, 1 and 2 h) at the room temperature.

3.3.2.3. Pre-treatment with Benzonase Nuclease

Samples pre-treated with Benzonase nuclease (9025-65-4, Sigma) was adding 9 U/mL was added according to the suggesting concentration by manual. The samples were incubated at 37°C overnight for the best performance of Benzonase, no additional separation was for the enzyme removal for further purification or analysis processes.

3.3.2.4. Fab D1.3 purification

Purification from osmotic shock fluid and culture broth sample obtained from a fed-batch fermentation, described in chapter 2 (Fig 2.8, batch No.7), was used in this chapter for the purification studies.

3.3.2.4.1. Fab D1.3 purification on HiTrap SP Sepharose XL

Purification from culture broth sample was performed on a 5-mL HiTrap SP_XL Sepharose column. Prior to application of cell-free culture fluid onto the column, the feedstock was extensively dialysed overnight against 15 mM sodium acetate, pH 5.0, at 4°C with changing the buffer in order to reduce both the conductivity (from ca. 40 to 5.0 mS/cm) by dilution and pH (from 7.0 to 5.0) by using 15 mM sodium acetate at pH 5 for optimal sorption of the Fab on the cation exchange (CEX) matrix. The 6-fold dilution buffer was added into culture broth sample for reduction conductivity to desire value. Sample was re-centrifuged (9390 *g* for 30 minutes) and filtered through 0.45 and

subsequently 0.22 μm Millipore filters. The sample (1200 mL) was then loaded at a flow rate of 2.5 mL/minute on the HiTrap SP_XL column which was pre-equilibrated with 15 mM sodium acetate buffer, pH 5.0. Following wash step was done at the same flow velocity with the equilibration buffer for 25 mL (5 column volumes, CVs). Finally the elution was achieved by employing 20 mM MES (2- morpholinoethanesulfonic acid, 4.5 mM sodium MES, 1.5 M NaCl, pH 5.5) to elute the binding Fab for 5 CVs. Eluted fractions containing Fab D1.3 from chromatography on HiTrap SP_XL was store at −20°C for further analyse. The amount of Fab D1.3 and total protein in various fractions was measured by ELISA and BCA assay, respectively.

3.3.2.4.2. Fab D1.3 purification on HiTrap rProtein G column

For this purpose, 1 mL HiTrap rProtein G was equilibrated with 20 mM sodium phosphate buffer, pH 7.0. The culture broth sample (50 mL) from fed-batch fermentation was centrifuged at 9390 *g* for 600 s (Sigma 3K30, SciQuip, Shropshire, UK) and clarified by filtration through 0.45 and subsequently 0.22 μm syringe filters (Millipore, MA, USA). The sample (pH 7.0) was put through the HiTrap rProtein G column using an AKTA explore system (GE Healthcare, Life Sciences, Buckinghamshire, UK) at a flow velocity of 1 mL/minute. After loading, the column was extensively (5 CVs) washed with 20 mM sodium phosphate buffer, pH 7.0, and elution (10 CVs) was made with 0.1 M glycine-HCl, pH 2.7 at the same flow rate. The eluate was instantaneously neutralised with 1 M Tris-HCl, pH 9.0, and stored at 4°C. The amount of Fab D1.3 in various fractions was measured using ELISA.

3.4. **Results and discussions**

3.4.1. Releasing Fab D1.3 by modified osmotic shock and 0.1% Sodium deoxycholate (Doc) in various conditions.

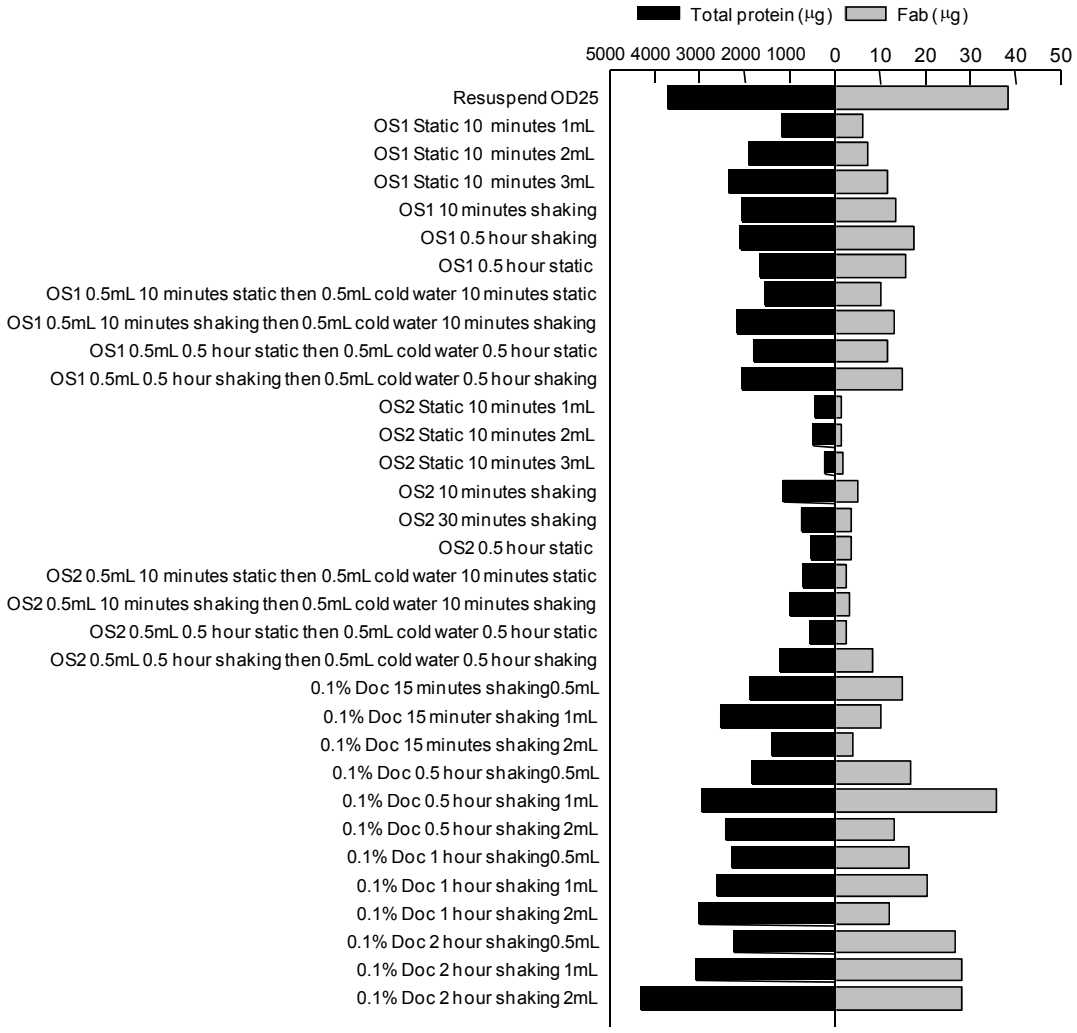

Fig. 3.1. The impact of total protein and Fab D1.3 released by various conditions of osmotic shock and 0.1% Doc. In case of the osmotic shock treatment variable time and volume of the OS solution was used also incorporated with vortex to enhance the protein release. For 0.1% Doc, time variable and volume of the solution were tested. On the left side of the graph, total protein released was measured by BCA assay and right side was the amount of Fab released in different conditions, both data had already expressed in the same volume.

This chapter described the further release experiment of Fab D1.3 from periplasmic space. As demonstrated in Chapter 2, partially controlled location of target protein to accumulate in the periplasm is feasible. Subsequently, the extraction procedures can be achieved by different means, namely osmotic shock and chemical permeability. Alteration the conditions of osmotic shock standard protocol (Neu *et al.*, 1967) suggested more selective and better efficiency of the protein releasing. The amount of total protein and Fab D1.3 released by two different techniques were shown in the Fig. 3.1 (osmotic shock and 0.1% Doc). Interestingly, the most release was measured in the supernatant of cell re-suspension. There are two possible explanations. Firstly, It could be that the cells were frozen after 24 h. Due to the repeat freezing and thawing (Johnson and Hecht, 1994), and the formation of ice crystals in the cells, the cells perforates and releases the majority of contains. Secondly, the integrity of the cells at harvesting stage could be another reason, as already discussed in Chapter 2. Although the titre of Fab D1.3 was boosted up to 40 mg/L in the periplasm, however the cells were incapable of holding intact shape, which was suggested by the increase of the DNA concentration in the culture broth over time. As shown in Fig. 3.1, most of the target product was released during the first re-suspension step (ca ~38 μg). Not surprisingly, the following osmotic shock could only extract a very little remaining target protein within the cells (ca ~5 μg). When double or triple the resuspension buffer, slightly increase of Fab release was observed (up to 11 μg), which also led more DNA leaking into the extractions, possibly because the outer membrane had been severely damaged after repeating disrupting the cells with sudden temperature changes. Comparing various length of incubation time with 0.1%

Doc to release protein at shaking condition, despite of the volume increase of extraction solutions, the length of incubation time shows significant effect on protein releasing. Especially doubling the length of incubation time, which increased from 15 to 30 minutes with shaking, almost increases 2 fold of protein release. As mentioned in the introduction section, that ETDA acting as a cation chelator to un-stabilised the outer membrane thereby releasing protein from periplasm. When the incubation time is more than 2 h, mixing seemed to enhance the interaction between ETDA and outer membrane therefore improving the permeability, which showed above 30 μg of Fab D1.3 was released regardless the length of incubation time for the case of 0.1% Doc was employed.

As suggested by Neu *et al.*, (1967) osmotic shock can be accomplished by adding cold water or magnesium solution. Here, 0.5 mL of cold water was added to final 1:1 ratio for the final cell concentration in various incubation conditions. The results illustrated that incubation with shaking had better release than static, in average shaking was 30% more efficient. Up to 0.5 h, both conditions showed similar release profile, which implied that shaking movement was effectively shorten the length of incubation to achieve that same magnetite of protein release in contrast to statically incubation. However, it could very much depend on the cell concentration of re-suspension, the high OD value might require longer time for incubation in both cases. The profiles of protein release from OS2 (cytoplasm) illustrate that only very little protein remained in the cells, causing by the first re-suspension damaged the cell wall and primarily target proteins accumulated in periplasm. Employing 0.1% Doc as a chemical mean to penetrate bacterial membrane seems to be a more

effective method of protein release in comparison of osmotic shock. Only by giving minimum 0.5 h to incubate at shaking condition, it was possible to release at least 10 μg or more regardless different cell concentrations in the re-suspension. In particular, the optimum condition, which was 0.1% Doc with shaking and 1:1 ratio of cell concentration nearly, matched the amount of Fab being released by the first re-suspended step with Tris buffer.

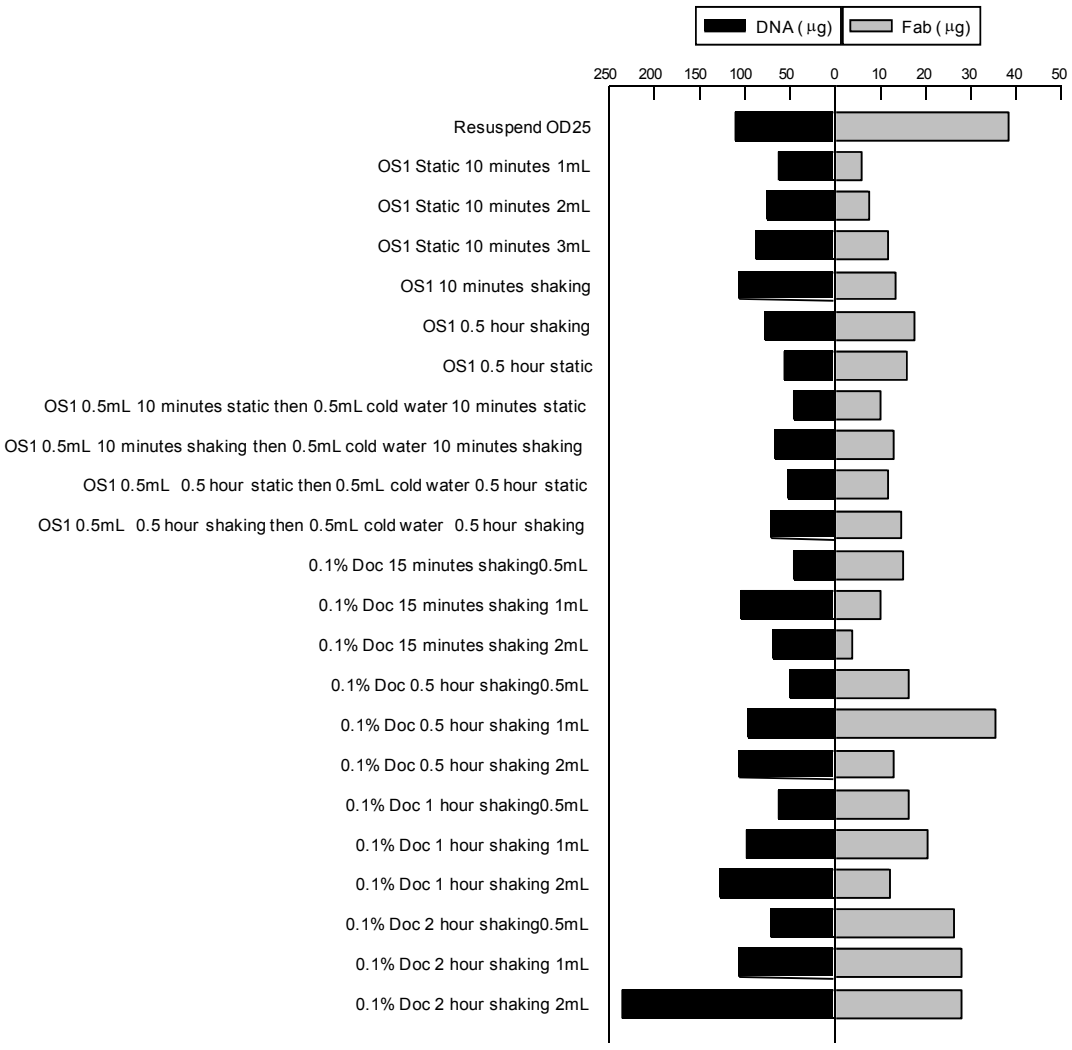

Fig. 3.2. The impact of DNA and Fab D1.3 released by various conditions of osmotic shock and 0.1% Doc. In case of the osmotic shock treatment variable time and volume of the OS solution was used also incorporated with vortex to enhance the protein release. For 0.1% Doc, time variable and volume of the solution were tested. On the left side of the graph, total protein released was measured by BCA assay and right side was the amount of Fab released in different conditions, both data had already expressed in the same volume.

Combining Fig. 3.1 Fig. 3.2 shows the more effective on protein release with the higher DNA leakage from cells. Because the main interests in this chapter focus on understanding the protein release from periplasm, therefore OS2 fraction (cytoplasm) was not measured and compared. As shown on Fig. 3.2, the average amount of DNA being released by osmotic shock was less than 0.1% Doc, because the large DNA molecular seemingly acts as large cation adsorbents under low pH condition, therefore competing with the cation exchange resin of the functional groups of the chromatography material. To prevent the aggregation forming and subsequently clogging chromatograph column, the less amount of DNA in the feed stock would definitely be better to start with chromatographic purification procedure. For the reason, although the optimum release condition from periplasmic protein should be using 0.1% Doc with shaking for either 0.5 or 2 h, with cell concentration could be between 0.5-1 to its original sample volume, but osmotic shock was selected for protein extraction method.

3.4.2. Releasing Fab D1.3 with Benzonase pre-treatment in different pH value conditions.

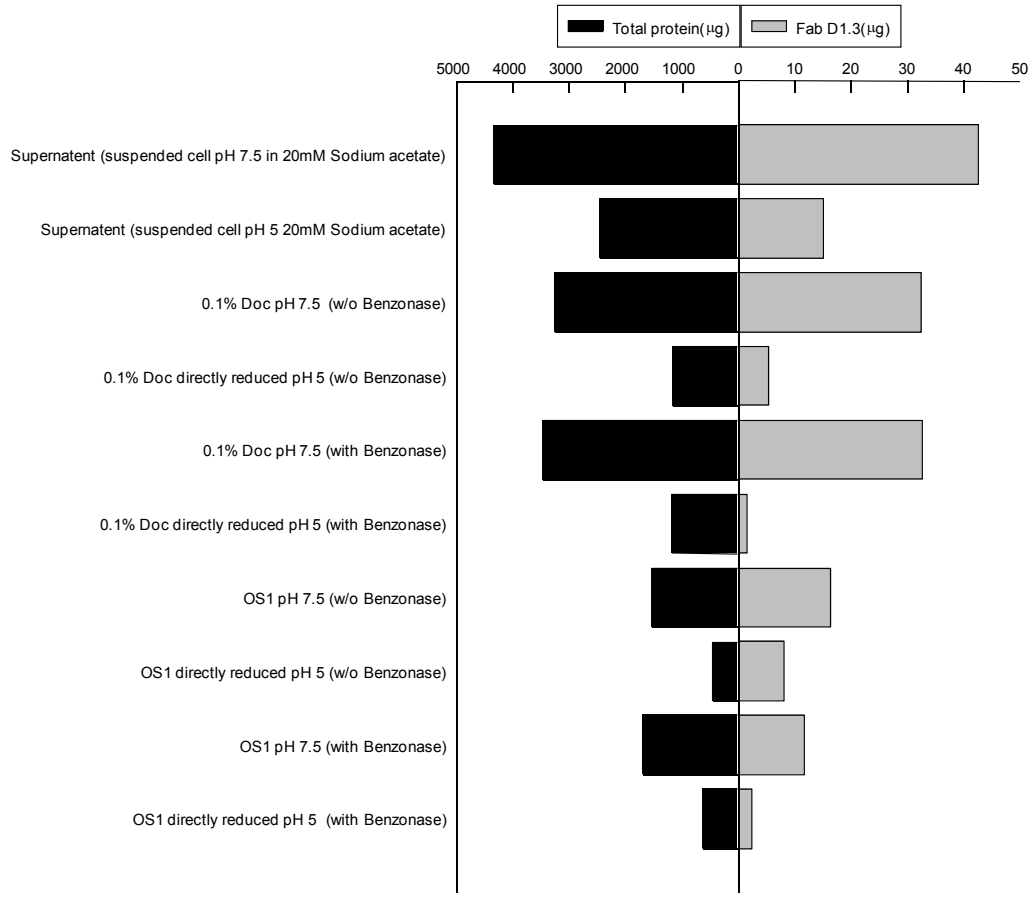

Fig. 3.3 The effects on pH adjustment of osmotic shock 1 solution for protein release and the impact on total protein and Fab release after applying Benzonase with samples. On the left side of the graph, DNA released was measured by DPA assay and right side was the amount of Fab released in different conditions.

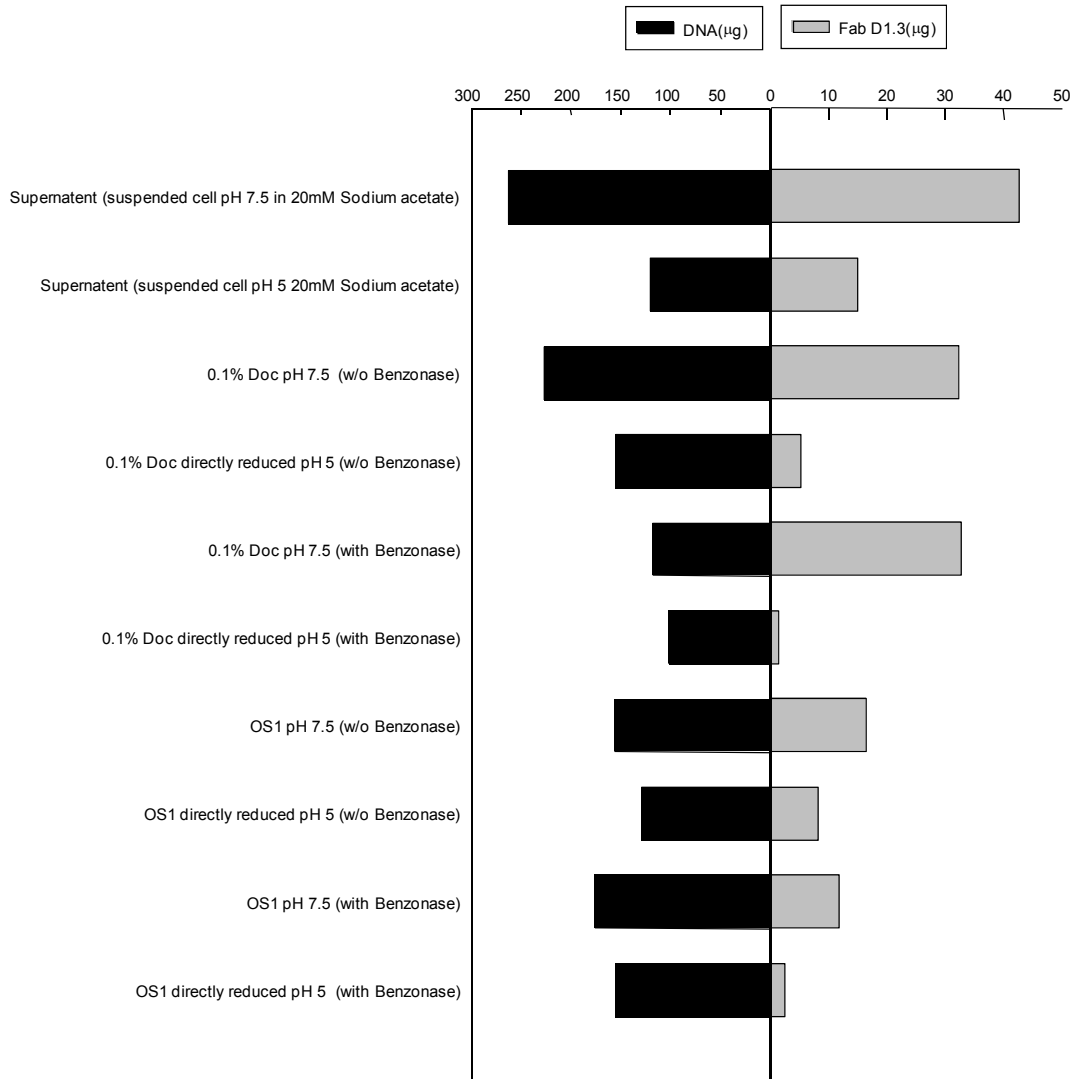

Fig. 3.4 The effects on pH adjustment of osmotic shock 1 solution for protein release and the impact on total protein and Fab release after applying Benzonase with samples On the left side of the graph, total protein released was measured by BCA assay and right side was the amount of Fab released in different conditions.

The cells were first re-suspended with 20 mM sodium acetate buffer to the same optical density value as harvest (OD_{600nm}~25.4). One millilitre of mixture was aliquot to 1.5 mL eppendorf tube and centrifuged (15,800 *g*, 120 s), the supernatant was stored for further analyse. Cell pellets were used for the osmotic shock or 0.1% Doc chemical release. All the supernatants were measured by ELISA (active Fab D1.3 concentration), BCA assay (total protein concentration) and DPA assay (DNA concentration) to obtain the results in Fig.

3.3 and Fig. 3.4. Benzonase was employed here as a pre-treatment to reduce the concentration of DNA in the supernatant by cutting it into small fragments. Benzonase was added into supernatant and incubated at 37°C for overnight.

A speculation reason for the large molecular DNA would eventually acting as a cation adsorbent at low pH condition to capture the Fab D1.3 and other proteins, whose isoelectric point is higher than 8, would possess positive charge on the surface when the pH is below 8. This experiment was designed to understand the effect of pH towards releasing efficiency of osmotic shock and 0.1% Doc, also to investigate whether DNA was the potential issue for the loss of target protein during the pH adjustment.

It is very clear that the major release occurred at the first step of cells re-suspension (~40 μg/mL), 0.1% Doc could also release around 30 μg of Fab when applied with the optimum condition. In total, there was nearly 70 μg of Fab released from 1mL cell pellet, which suggests that the total of Fab is very likely underestimated due to the insufficiently releasing ability of osmotic shock. Likewise, using 0.1% Doc or osmotic shock for extraction protein from the cells observed similar behaviour, not surprisingly, the more protein released along with more Fab. However, neither extraction methods showed high purity for the Fab release, only 0.6~0.9% of the total protein, which was measured regardless the benzonase pre-treatment was performed (Fig. 3.3).This suggests DNA may not be the reason of Fab loss during the protein extraction from the cells because benzonase should eliminate possibility of DNA acting as cation exchanger to bind Fab. Further, at pH 7.5, the efficiency of release are very similar for both methods, but there is 40% decrease of

DNA concentration with pre-treated benzonase sample by using 0.1% Doc extraction method. This again has implied that loss of Fab may not be the large negative charged DNA group to bind proteins. It is more likely due to the precipitation occurred prior to pH adjustment, which showed in Fig. 3.3 and Fig. 3.4 that both results with pH 5 condition had much lower amount of Fab regardless the benzonase pre-treatment was applied.

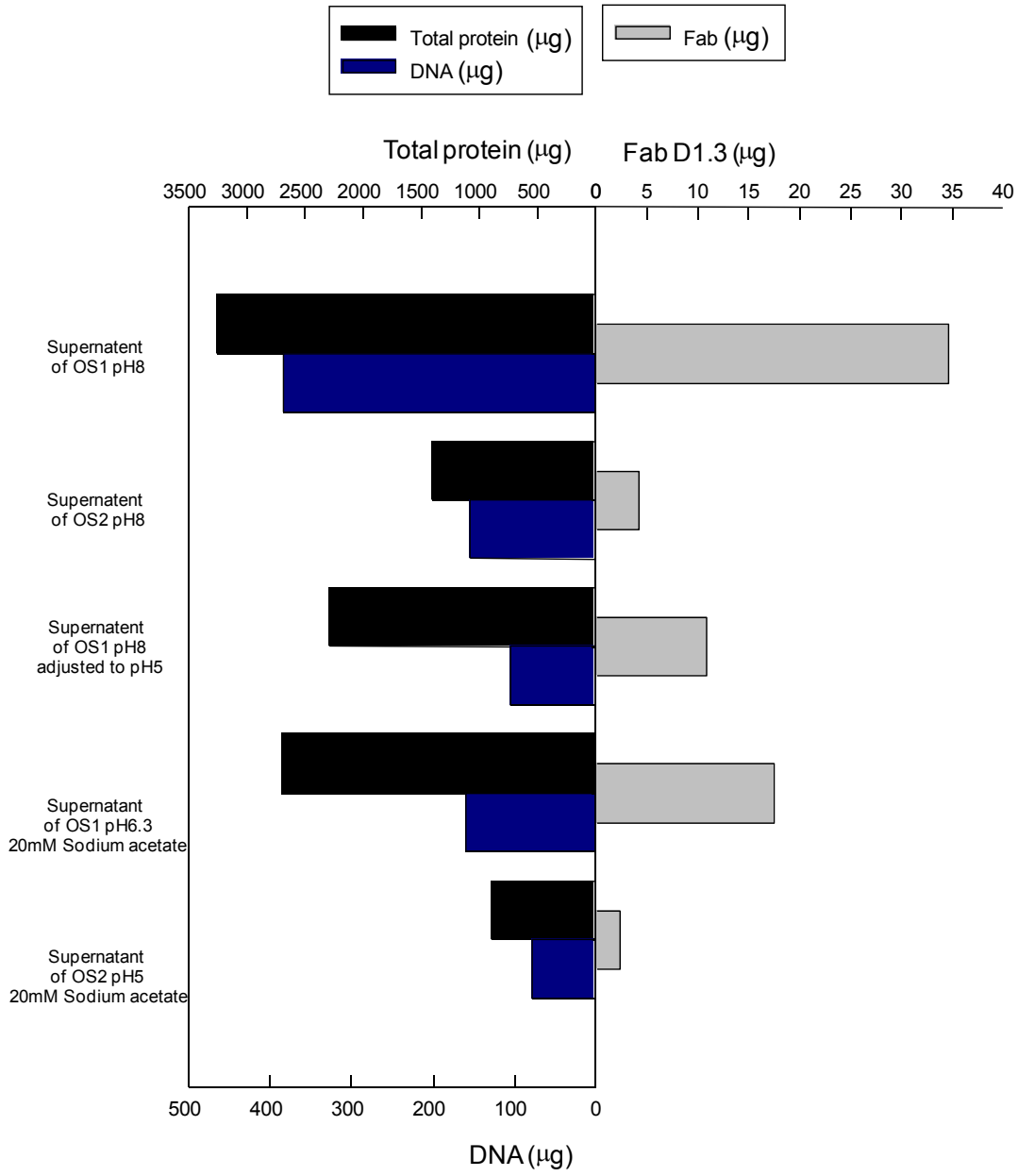

Fig. 3.5 The effects on using different pH for osmotic shock and afterwards pH adjustment for total protein, DNA and Fab release. Data showed in left side was amount of total protein and DNA measured in each condition, amount of Fab was shown in right.

In order to prove adjusting pH could be the potential reason of losing Fab D1.3 more than the cause of DNA-protein binding mechanism, a step-wise pH adjustment was conducted to reveal the story behind it. Differently, this was done by directly re-suspended with OS 1 and 2 (1:1 ratio) with 1 mL cell pellet. Obviously, the majority of Fab was accumulated in OS1 (periplasm), only little

in the OS2 (cytoplasm). Unlike the previous results, OS 1 fraction extracted nearly 35 μg of Fab D1.3 from 1 mL pellet, but the purity still remained unchanged (0.9%). Close to 400 μg of DNA was also released, which is the combination amount of DNA from the supernatants of suspended cell at pH 7.5 in 20 mM sodium acetate and OS1 pH 7.5 (without Benzonase pre-treatment). This implied the there was no selective release from osmotic in this condition, and cell integrity after frozen-thaw and re-suspension process were severely compromised. Taken collectively, osmotic shock and 0.1% Doc did not perform well at pH 5, only around 10 μg or less of Fab was released, whereas at pH 8, both can release ~30 μg of Fab from 1 mL re-suspended cell pellet. Further reduction on pH from 8 to 5 causes a significant lost (~30%) of Fab in both cases (Fig. 3.5).

3.4.3. Fab D1.3 purification on cation exchange and affinity chromatography

3.4.3.1. Breakthough study of Fab D1.3 purification on HiTrap SP Sepharose XL with culture broth

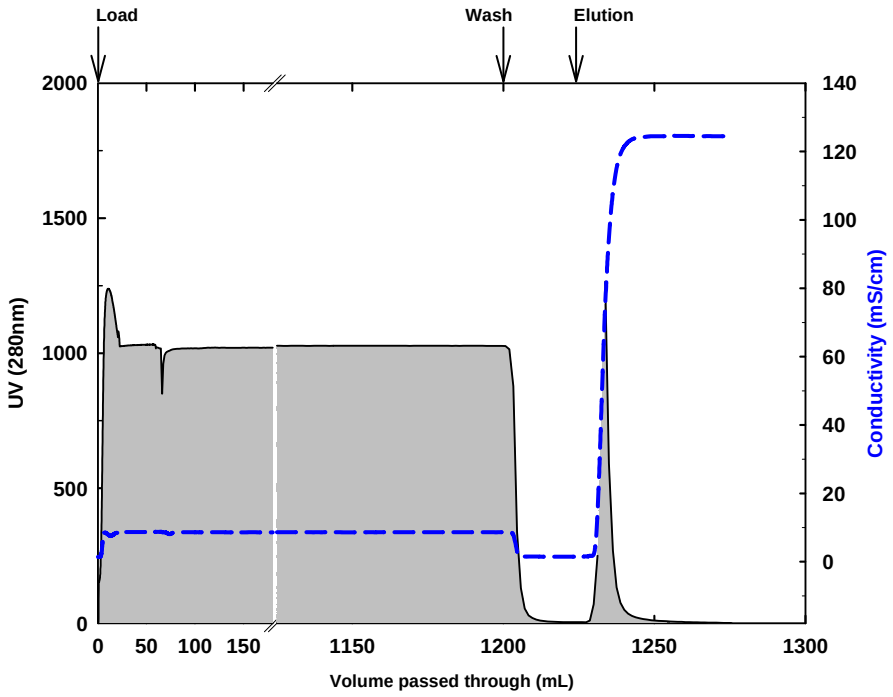

Fig. 3.6 Chromatogram for the purification of Fab using HiTrap SP_XL (CEX) column. The conductivity was reduced from 35 mS/cm to 10 mS/cm and pH was reduced from 7 to 5, 1200mL of sample from culture broth was loaded.

Table 3.1 Amount of total protein and Fab D1.3 measured by BCA assay and ELISA from each step of CEX purification.

	Volume (mL)	Fab D1.3 (mg)	Total protein (mg)	Target yield (%)	Total protein yield (%)	Purity (%)	Purification factor
Load	1200.00	7.77	1996.34	100.00	100.00	0.39	1.00
FT	1200.00	6.55	1968.78	84.35	98.62	0.33	
Wash	25.00	0.04	7.52	0.48	0.38	0.49	
Elution	50.00	1.18	20.04	15.18	1.00	5.88	15.18

Following by the release experiments, it is important to know whether the feed stock is suitable for chromatography purification. For the capture purpose, cation exchange chromatography (CEX) is very commonly used. Especially, the isoelectric point of Fab D1.3 is 8.7, so simply adjust the pH and conductivity of feed stock to binding condition should reveal how the Fab behaving under binding condition in CEX. Breakthrough experiment is to determine the dynamic binding capacity of feed stock applied to CEX. More than 1 litre of culture broth was applied to CEX column (HiTrap SP_XL 5mL) with pH adjusted from 7 to 5 and reduced conductive from 35 to 10 by 5 time dilutions. Culture broth then passed through 0.45 and 0.22 μm syringe filters for further clarification. 1200 mL of conditioned culture broth on HiTrap SP_XL 5 mL CEX column with a flow rate of 150 mL/h, then 5 CVs of equilibration buffer for washing and 20 CVs of elution buffer for linear elution were applied. The chromatogram showed in Fig. 3.6, the binding action occurred before loading 100mL of feedstock, which indicated by the slightly fluctuated UV_{280} reading. This also suggested that column were quickly saturated by proteins in the feedstock. Theoretically commercial CEX column would have minimum 100-150 mg/L of protein binding capacity which was much higher than the amount of total from the elution step (Table 3.1). Another speculation was due to the pH adjustment, proteins were precipitating slowly over the loading process, which was observed from samples stored overnight in the fridge at 4°C. While loading the culture broth into the column, the protein precipitation was quickly formed due to higher pressure, consequently clogged the channels between adsorbents and proteins, thereby preventing protein

binding occurs. As the result, the binding capacity of column was dramatically decreased.

3.4.3.2. Fab D1.3 purification on HiTrap SP Sepharose XL with OS 1 fraction

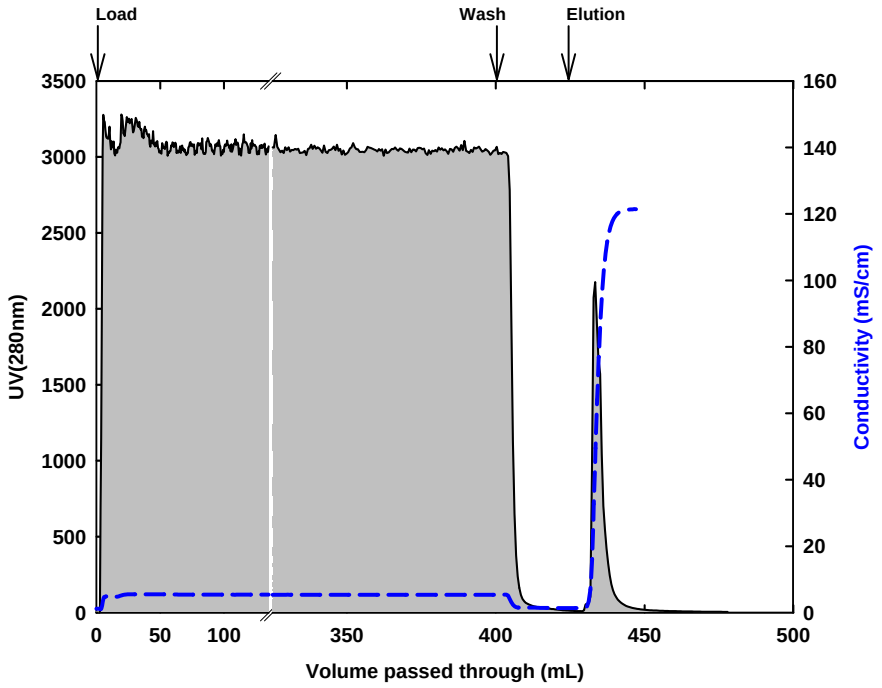

Fig. 3.7 Chromatogram for the purification of Fab using HiTrap SP_XL (CEX) column. The pH was reduced from 7 to 5, and conductivity was 5 mS/cm without conditioning, 400mL of sample from OS1 supernatant was loaded.

Table 3.2 Amount of total protein and Fab D1.3 measured by BCA assay and ELISA from each step of CEX purification.

	Volume (mL)	Fab D1.3 (mg)	Total protein (mg)	Target yield (%)	Total protein yield (%)	Purity (%)	Purification factor
Load	400.00	24.91	1450.03	100.00	100.00	1.72	1.00
FT	400.00	21.43	1399.72	86.01	96.53	1.53	
Wash	25.00	0.37	16.90	1.47	1.17	2.17	
Elution	50.00	3.12	33.41	12.52	2.30	9.34	5.43

From the earlier release experiments shown, it could be featured that the extract from periplasm (OS1 fraction) is a much better feedstock to start with downstream purification in terms of Fab purity, DNA concentration and conductivity. There is no requirement for additional dilution to reduce conductivity, but still a pH adjustment is required. From previous breakthrough experiment, it was noticed that slowly precipitation could be a potential issue for chromatography, thereby loading less amount of feedstock from OS1 fraction would be enough to determine the binding capacity of 5 mL HiTrap SP_XL column in relation to use OS1 as feed stock. The purification applied 400 mL OS1 extract with adjusted pH to 5 after releasing, following by 10 CVs of wash phase with equilibration buffer and then 20 CVs of linear elution strategy, which can be seen in Fig. 3.7.

In striking contrast, the protein concentration was higher than in previous experiment according to the UV reading, which suggested majority of proteins were in the flow through but not bound to the column or the column was not blocked due to the condition of feed stock. Furthermore, Table 3.1 illustrates that 62% more Fab had been eluted despite of less amount of Fab was loaded to the column initially. This was possible due to much cleaner environment of periplasm, lower concentration of DNA (See results from Chapter 2) and higher purity of Fab, comparing Table 3.1Table 3.2, shows the significant improve of initial purity of Fab between culture broth and OS1 (periplasm). Although a huge lost (ca. 60%) of Fab during the pH adjustment (showed in Fig. 3.5) could be detected, but extraction from periplasm seems offering a promising result for purification via chromatography system.

3.4.3.3. Effect of Benzonase pre-treatment for Fab D1.3 purification on HiTrap SP Sepharose XL.

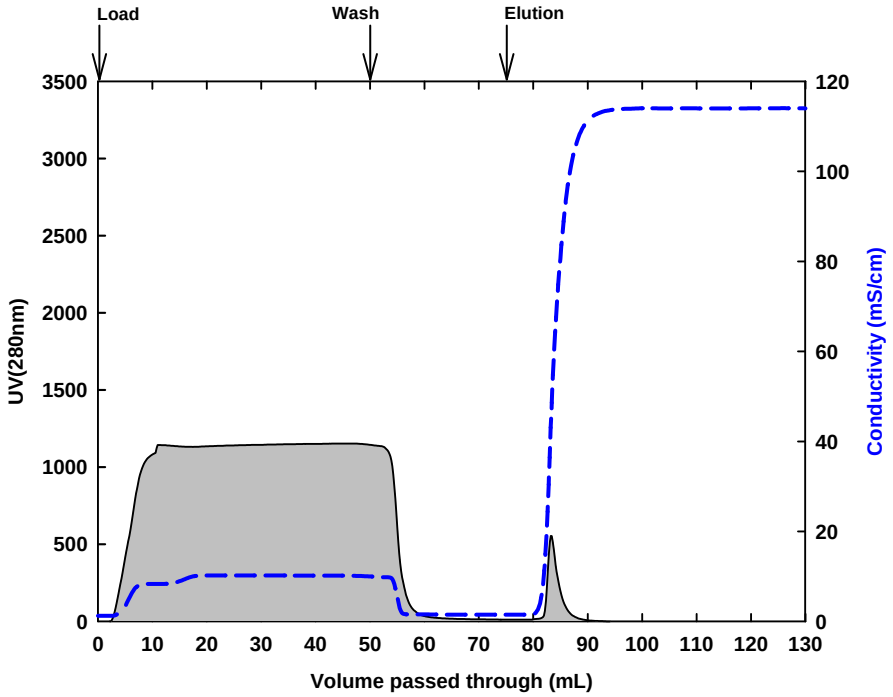

Fig. 3.8 Chromatogram for the purification of Fab using HiTrap SP_XL (CEX) column. 50 mL culture broth conditioned to conductivity of 10 mS/cm, pH 5 was applied.

Table 3.3 Amount of total protein and Fab D1.3 measured by BCA assay and ELISA from each step of CEX purification.

	Volume (mL)	Fab D1.3 (mg)	Total protein (mg)	Target yield (%)	Total protein yield (%)	Purity (%)	Purification factor
Load	50.00	0.21	82.48	100.00	100.00	0.25	1.00
FT	50.00	0.01	72.85	6.28	88.33	0.02	
Wash	25.00	0.01	5.17	5.80	6.27	0.23	
Elution	50.00	0.18	4.45	87.92	5.40	4.09	16.29

The presence of DNA influence on protein purification from above experiments remained unknown. This could be the issue of causing precipitation during pH adjustment, thereby resulting to the loss of Fab as DNA molecular acted as a large cation exchange adsorbent to bind and drag

positive charge protein forming precipitation also clogging the column while loading the feedstock into it. In order to reveal the mechanism for inhibition of protein binding, a control experiment was performed by loading 50mL of culture broth on the CEX column followed by 5 CVs of wash and 10 CVs of elution. Although elution phase was observed very similar between Fig. 3.6 and. Fig. 3.8, proteins in the loading phase very quickly occurred in flowthrough fraction based on the UV reading. This showed either the column was instantly saturated by the protein loaded onto it even though with much less amount of feed stock loading, or at the pressure and tiny space condition, the column was quickly been clogged because of the precipitation formed much quicker than the room temperature condition, which could be a possible scenario that precipitation was observed when feed stock left statically in the room temperature over a period of 1 hour. Despite all the drawbacks from the feedstock condition, the purification factor was 16.29 implied more effective on Fab purification than previous two trails (Table 3.1, purification factor: 15.18; Table 3.2, purification factor: 5.43). Further experiment was conducted to check whether adding Benzonase would be an effective solution to resolve the binding problem.

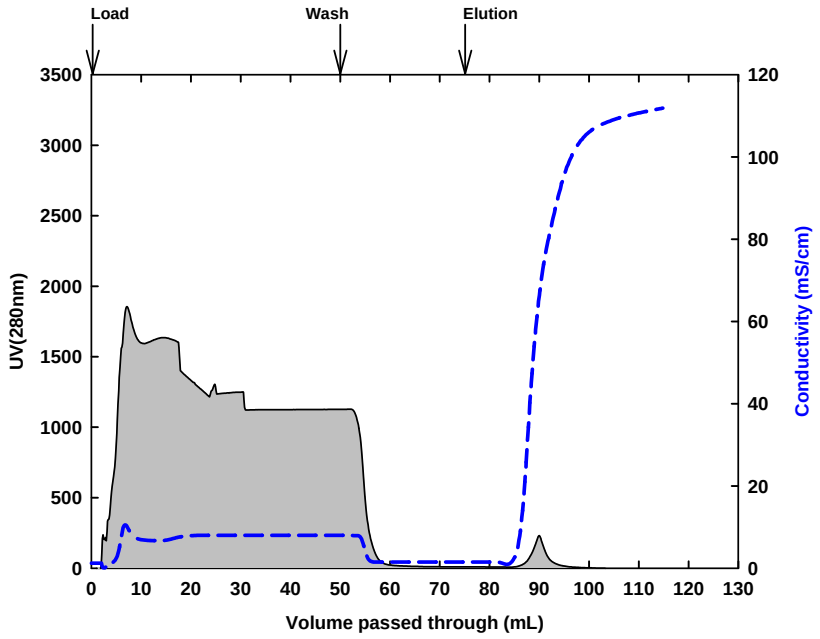

Fig. 3.9 Chromatogram for the purification of Fab using HiTrap SP_XL (CEX) column. 50 mL culture broth with benzonase pre-treatment then conditioned to conductivity of 10 mS/cm, pH 5 was applied.

Table 3.4 Amount of total protein and Fab D1.3 measured by BCA assay and ELISA from each step of CEX purification.

	Volume (mL)	Fab D1.3 (mg)	Total protein (mg)	Target yield (%)	Total protein yield (%)	Purity (%)	Purification factor
Load	50.00	0.24	80.81	100.00	100.00	0.29	1.00
FT	50.00	0.12	73.64	52.10	91.13	0.17	
Wash	25.00	0.00	5.40	0.84	6.68	0.04	
Elution	50.00	0.11	1.77	47.06	2.19	6.33	21.50

To identify the binding was inhibited by the presence of DNA at low pH condition; 50 mL culture broth was pre-treated with benzonase and incubated at 37°C for overnight, following by centrifugation and filtrations for loading on the CEX column. Notably, at the first half loading phase (~25 mL) showed much higher UV reading in comparison with Fig. 3.8. This suggested that benzonase was effectively cutting large DNA molecular to small fragments

thereby preventing proteins bound to it, as the result more proteins detected in the flow through, a peak was clearly spotted at very early of loading phase.

Although the yield of target protein dropped below 50% by treating sample with benzonase, the final purity of Fab and the purification factor had increased 2% and 5, respectively. Nevertheless, the elution peak seemed smaller than one of the previous results (Fig. 3.8), but the Fab purity was increased from 4 to 6.3%, this could be the due to the pre-treatment of benzonase. An inference can be drawn from the above result that the presence of DNA might not be the major reason for competing protein binding onto CEX absorbents, so pre-treatment with benzonase did not improve the binding efficiency significantly. The ultimate solution should be to prevent precipitation after the pH adjustment so that cation exchange chromatography becomes a feasible tool in the capture step. However, because of the nature of the feedstock composition, either the binding condition was not ideal or the dynamic binding capacity was too low to accommodate the feed stock, resulting in a rapid saturation of the column. Although we mentioned using HiTrap Protein G column for the Fab purification, but the purification was not successful, results showed no binding and elution (Data no shown). Even though affinity adsorption is not affected by the conductivity of feedstock, but the HiTrap Protein G column has failed to bind any Fab, possibly due to the same reason as CEX, that precipitation was quickly occurring while the feedstock being loaded onto column. Despite of all the efforts so far, such as prolonged the Fab production phase, directing accumulation of Fab into periplasm by altering growth conditions (temperature, induction timing, IPTG concentration) and seeking optimisation of releasing methods and conditions

(osmotic shock and 0.1% Doc), still faced many unsolved problems in the downstream purification process. An alternative *E.coli* strain producing antibody fragment will be necessary for further research.

3.5. **Conclusions**

Growth at 25°C and induction at 20°C resulted in the greatest accumulation of FabD1.3 within the periplasmic space (Chapter 2). Under these conditions the Fab represented 1.5 –1.7% of the total soluble protein. A distinct advantage of the periplasmic processing route is minimal conditioning of the OS1 fraction (ionic strength <6 mS/cm, pH ~7.5) prior to CEX adsorption of the Fab (simple pH adjustment is required). Feedstock conditioning and Fab D1.3 recovery were examined to seek for the optimum release condition and minimal feedstock conditioning. From the above results suggested optimal condition for releasing Fab from periplasm should be using 0.1% Doc with shaking for either 0.5 or 2 h, with 0.5-1 ratio of the cell concentration to the original sample volume. However, the DNA leakage proves to be a potential issue in the subsequent chromatographic purification. Therefore, osmotic shock was still proven to be a more suitable extraction method.

The following feedstock conditioning on composition of feedstock results showed that small (~10%) loss in Fab occurred following dilution of cell-free broth (~ 10 mS/cm), pH adjustment (~ pH 5) and clarification (filtration through a 0.2 μm membrane) however, this was offset by a greater loss in contaminating host protein (~30%), resulting in improved feedstock quality (1.2 fold purification of Fab). Prior treatment of the cell-free broth with benzonase was expected to prevent protein aggregation with large DNA

molecular therefore avoiding Fab loss altogether (26% loss; resulting in ~1.4 fold enhanced Fab purity), and increased ease of clarification by filtration by reducing the degree of precipitation. However, benefits on CEX purification performance were mixed, i.e. higher degree of purification (step PF of 22 cf. 16 and final purity of 7.1% cf. 4.1%), but lower step yield (50% cf. 88%).

Furthermore, a breakthrough studies was conducted with conditioned cell-free broth (lacking benzonase) and OS1 to discover extremely low capacity Fab binding (0.4 mg/mL cf. 0.6 mg/mL for conditioned cell-free broth and OS1 respectively) to the SP Sepharose XL. The purity of Fab eluates coming off OS1 loaded columns were roughly twice those eminating from columns supplied with conditioned broth (10% cf. 5%). The presence of non-proteinaceous material (nucleic acids, LPS) plus high protein contamination likely contribute to the disappointing CEX purification performance observed with both conditioned broth and OS1 feedstocks. Attempting to purify Fab D1.3 directly from culture broth by rProtein G affinity chromatography was proved unsuccessful (Fab failed to bind), but highly pure (98-99%) Fab D1.3 was obtained when PD10 desalted CEX elution pools were applied to rProtein G Sepharose columns (Jalalirad, 2010).

Thus far, despite the clear results obtained from the release experiment suggested the total yield of Fab D1.3 could be underestimated (ca. $\leq$ 70 mg/L) and applying 0.1% Doc might be the better the option for Fab release compared with the osmotic shock, but all the subsequent chromatographic purification with conditioned culture broth and OS1 supernatant (CEX and rProteinG) results were unsuccessful. Regrettably to say, even though the

titre of Fab D1.3 could be improved to meet our goal (~100 mg/L), but the following purification would be very troublesome and nearly impossible to proceed.

It is therefore an alternative *E.coli* strain for robust anti-body fragment production (A33 Fab′), which is kindly offered from UCB Celltech (Humphreys *et al.*, 1996, 2002), will be employed for the next chapter and hopefully provide workable feedstock for European Framework 7 project partners to test newly designed magnetic particles and devices (chapter 5) .

3.6. **References**

Akiyama, Y., Kamitani, S., Kusukawa, N., and Ito, K. (1992). In vitro catalysis of oxidative folding of disulfide-bonded proteins by the *Escherichia coli* dsbA (ppfA) gene product. J. Biol. Chem. *267*: 22440–22445.

Argos, P., Rossmann, M.G., Grau, U.M., Zuber, H., Frank, G., and Tratschin, J.D. (1979). Thermal stability and protein structure. UCLA Forum in Medical Sciences 159–69.

Bardwell, J.C., McGovern, K., and Beckwith, J. (1991). Identification of a protein required for disulfide bond formation in vivo. Cell *67*: 581–9.

Chen, C., Snedecor, B., Nishihara, J.C., Joly, J.C., McFarland, N., Andersen, D.C., Battersby, J.E., and Champion, K.M. (2004a). High-level accumulation of a recombinant antibody fragment in the periplasm of *Escherichia coli* requires a triple-mutant (degP prc spr) host strain. Biotechnology and Bioengineering *85*: 463–74.

Chen, Y.-C., Chen, L.-A., Chen, S.-J., Chang, M.-C., and Chen, T.-L. (2004b). A modified osmotic shock for periplasmic release of a recombinant creatinase from *Escherichia coli*. Biochemical Engineering Journal *19*: 211–215.

Digel, I., Maggakis-Kelemen, C., Zerlin, K.F., Linder, P., Kasischke, N., Kayser, P., Porst, D., Temiz Artmann, A., and Artmann, G.M. (2006). Body temperature-related structural transitions of monotremal and human hemoglobin. Biophysical Journal *91*: 3014–21.

Ehrmann, M. (2006). The Periplasm (ASM Press).

French, C., Keshavarz-Moore, E., and Ward, J.M. (1996). Development of a simple method for the recovery of recombinant proteins from the *Escherichia coli* periplasm. Enzyme and Microbial Technology *19*: 332–338.

Humphreys, D.P., Carrington, B., Bowering, L.C., Ganesh, R., Sehdev, M., Smith, B.J., King, L.M., Reeks, D.G., Lawson, A., and Popplewell, A.G. (2002). A plasmid system for optimization of Fab' production in *Escherichia coli*: importance of balance of heavy chain and light chain synthesis. Protein Expression and Purification *26*: 309–20.

Humphreys, D.P., Weir, N., Lawson, a, Mountain, a, and Lund, P. a (1996). Co-expression of human protein disulphide isomerase (PDI) can increase the yield of an antibody Fab' fragment expressed in *Escherichia coli*. FEBS Letters *380*: 194–7.

Ito, K., Bassford, P.J., and Beckwith, J. (1981). Protein localization in E. coli: is there a common step in the secretion of periplasmic and outer-membrane proteins? Cell *24*: 707–17.

Jalalirad, R. (2010). Improving the recovery of “difficult to release” periplasmically-expressed products from recombinant E. coli. University of Birmingham.

Jeong, K.J., and Lee, S.Y. (2000). Secretory production of human leptin in *Escherichia coli*. Biotechnology and Bioengineering *67*: 398–407.

Johnson, B.H., and Hecht, M.H. (1994). Recombinant Proteins Can Be Isolated from E. coli Cells by Repeated Cycles of Freezing and Thawing. Bio/technology (Nature Publishing Company) *12*: 1357–1360.

Katsui, N., Tsuchido, T., Hiramatsu, R., Fujikawa, S., Takano, M., and Shibasaki, I. (1982). Heat-induced blebbing and vesiculation of the outer membrane of *Escherichia coli*. Journal of Bacteriology *151*: 1523–31.

Khosla, C., and Bailey, J.E. (1989). Evidence for partial export of Vitreoscilla hemoglobin into the periplasmic space in *Escherichia coli*. Implications for protein function. Journal of Molecular Biology *210*: 79–89.

Lacki, K.M., Mueller, J., Harinarayan, C., Reis, R. Van, Fahrner, R., Alstine, J.M. Van, Healthcare, G.E., Ab, B., Uppsala, S.-, Ljunglöf, A., Reis, R. van, and Alstine, J.M. Van (2007). Ion exchange chromatography of antibody fragments. Biotechnology and Bioengineering *96*: 515–24.

Link, A.J., Carmack, E., Yates, J.R., and Iii, J.R.Y. (1997). A strategy for the identification of proteins localized to subcellular spaces: Application to E. coli periplasmic proteins. International Journal of Mass Spectrometry and Ion Processes *160*: 303–316.

Liu, Y., Fu, X., Shen, J., Zhang, H., Hong, W., and Chang, Z. (2004). Periplasmic proteins of *Escherichia coli* are highly resistant to aggregation: reappraisal for roles of molecular chaperones in periplasm. Biochemical and Biophysical Research Communications *316*: 795–801.

Marco, A. de (2009). Strategies for successful recombinant expression of disulfide bond-dependent proteins in *Escherichia coli*. Microbial Cell Factories *8*: 26.

Naglak, T.J., and Wang, H.Y. (1990). Recovery of a foreign protein from the periplasm of *Escherichia coli* by chemical permeabilization. Enzyme and Microbial Technology *12*: 603–611.

Nakamoto, H., and Bardwell, J.C.A. (2004). Catalysis of disulfide bond formation and isomerization in the *Escherichia coli* periplasm. Biochimica et Biophysica Acta *1694*: 111–9.

Neu, H.C., James, A., and Chou, J. (1967). Release of Surface Enzymes in Enterobacteriaceae by Osmotic Shock. J. Bacteriol. *94*: 1934–1945.

Peek, J.A., and Taylor, R.K. (1992). Characterization of a periplasmic thiol:disulfide interchange protein required for the functional maturation of secreted virulence factors of Vibrio cholerae. Proceedings of the National Academy of Sciences of the United States of America *89*: 6210–4.

Pierce, J.J., Turner, C., Keshavarz-Moore, E., and Dunnill, P. (1997). Factors determining more efficient large-scale release of a periplasmic enzyme from E. coli using lysozyme. Journal of Biotechnology *58*: 1–11.

Schlegel, H.G. (1986). General Microbiology (Cambridge University Press).

Stock, J.B., Rauch, B., and Roseman, S. (1977). Periplasmic space in Salmonella typhimurium and *Escherichia coli*. J. Biol. Chem. *252*: 7850–7861.

Weir, A.N.C.A., and Bailey, N.A.N. (1995). Process for obtaining antibodies utilizing heat treatment (US).

Wielink, J.E. Van, Duine, J.A.J.J.A., and Wielink, J. Van (1990). How big is the periplasmic space? Trends in Biochemical Sciences *15*: 136–137.

Wunderlich, M., and Glockshuber, R. (1993). In vivo control of redox potential during protein folding catalyzed by bacterial protein disulfide-isomerase (DsbA). The Journal of Biological Chemistry *268*: 24547–50.

4. Production and release of periplasmic A33 Fab′

4.1. Abstract

A plasmid produced A33 Fab′ was kindly provided from UCB Celltech. One of the main advantages employing this plasmid is to express Fab′ into periplasm in *E.coli.* A preliminary study on shake flask experiments first to confirm the higher protein expression titre over the Fab D1.3. In combinations of improved and company supplied protocols generated around 0.3 g/L releasable Fab′ from a single batch of 3 litre fermentation. Following by a systematically investigation of release methods and conditions, which was comparing the osmotic shock, heat treatment and SMALPs ([poly(styrene-co-maleic acid) lipid particles]) to release A33 Fab′ from periplasm in various conditions. Despite the osmotic shock has been widely accepted for the protein release, but in this particular case, heat treatment exhibited highly selective and effective for A33 Fab′ extraction. Although SMALPs has been proven successfully in few applications for the proteins extraction and possible designed for *in vivo* uses but the release ability was not significant as heat treatment in this study. It is therefore, heat treatment was selected to carry out further optimisation. The result indicated that maximum protein release occurred in buffer to cells ratio at 0.5 to 1 (i.e. cell density ~ 27% w/v), which compared with the standard protocol (provided by UCB Celltech) 1 to 1 ratio (i.e. cell density ~ 13% w/v), was 10% more effective in terms of [total protein] release.

4.2. . Introduction

4.2.1. A33 Fab′

There are many forms of antibodies can be produced by *E.coli*, in previous case, Anti-HEWL Fab D1.3 was used as a model protein for assessing production titres by altering growth temperature, IPTG concentration and timing of induction (see chapter 2). Despite the significant improvements on the quality of Fab D1.3 in terms of solubility and purity from crude extract, the overall titre of Fab D1.3 was still too low to meet requirements, which minimum was aiming no less than 100mg/L of [Fab] per batch of fermentation. For this reason, another antibody plasmid was enquired and kindly supplied by UCB Celltech.

Monoclonal antibodies (MAb) can be effective for the treatment of a wide range of diseases, dealing with illnesses from cancer to infections (Mücke *et al.*, 2009). Typically MAbs are produced by the mammalian cells due to its complex polypeptide structure also needing post-translational modification after expression, mainly N-linked and O-Linked glycosylation are identical modification which discovered in humans. However, production in mammalian cells require high standard of research for building the cell line, time consuming cultivation and expensive media, also pathogenic viral clearance is required the human therapy.

Fig. 4.1 shows the Fab′ as a therapeutic molecule derived from an antibody in which the effector functions (receptor blockade, receptor activation/cross-linking, antigen blockade) are not required, but the therapeutic activity is

retained (Humphreys *et al.*, 2002). The main disadvantage of using Fab′ for the therapeutic purpose is the short half-life in the human circulation system. The solution was proposed by Chapman (2002) by coupling polyethylene glycol in specific sites will effectively extend the half-life of Fab′. Because of glycosylation is not required for Fab′ to improve its half-life which offers a very attractive choice *Escherichia coli* for more robust Fab production in comparison with mammalian cell (Humphreys *et al.*, 2002). There are many advantages considering using this production system including the wide genomic knowledge available, the easiness of gene manipulation, availability of expression vectors, adaptability to express a wide range of recombinant proteins, the speed of development and the short fermentation cycle (Ramírez and Bentley, 1995; Baneyx, 1999; Simmons *et al.*, 2002; Fountoulakis and Gasser, 2003; Hu *et al.*, 2007).

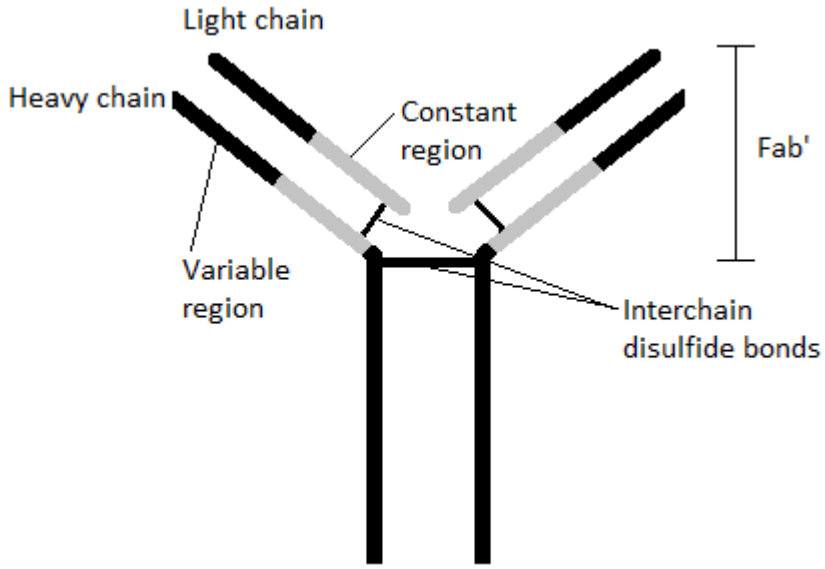

Fig. 4.1 Structural representation of an antibody and its basic regions (Adapted from Lydyard et al., 2004)

One important consideration when producing recombinant proteins such as Fab′ is the design of the expression vector that will carry the foreign gene to be expressed by the bacteria. In this case the expression vector consists of a plasmid carrying the genes for the light and heavy chains of the Fab′ as well as for tetracycline resistance, used for selection and preventing empty host out growing the containing cell during the production(Lee and Edlin, 1985; Ratledge and Kristiansen, 2006). The choice of using tetracycline has been made because it has been reported that tetracycline resistance marker offers less plasmid loss during recombinant protein production unlike ampicillin (Novagen, 1999).

A low copy number of plasmid system is advantageous for expression the recombinant protein as the metabolic burden will not overly loaded for the cells (Hoffmann and Rinas, 2004). This allows separate the growth phase from the production phase as the plasmid's genes will not be expressed until the Isopropyl *β*-D-1-thiogalactopyranoside (IPTG) or other inducer (i.e. lactose) is applied to inhibit the repressor and start the transcription for making recombinant proteins. IPTG is an allolactose analogue that activates the *Lac* operon. As it cannot be metabolised by *E. coli* the concentration remains constant, thus the *lac* controlled genes have a steady expression rate throughout the experiment (Ratledge and Kristiansen, 2006). Furthermore, it is also important to use strains in-cooperate with few mutations for the protease deficiencies and temperature adaptation, which would enhance higher yields of Fab′ (reviewed by Weickert *et al.*, 1996).

4.2.2. SMALPs [poly(styrene-co-maleic acid) lipid particles]

In the plastic industry, SMALPs [poly(styrene-*co*-maleic acid) lipid particles] is broadly used for numerous applications. This pH responsive/dependent polymer has brought huge interests to bioengineers recently, especially in drug delivery applications (Maeda *et al.*, 2009) due to its amphipathic properties. It is because various ratios of combining Maleic acid (hydrophilic) and styrene (hydrophobic) make the polymer itself amphipathic. Depending on the either composition, the richer constituent decides the character of the polymer. Low molecular mass polymer is soluble at neutral pH, under pH 6, the maleic acid group dominate positive charge, the polymer becoming insoluble.

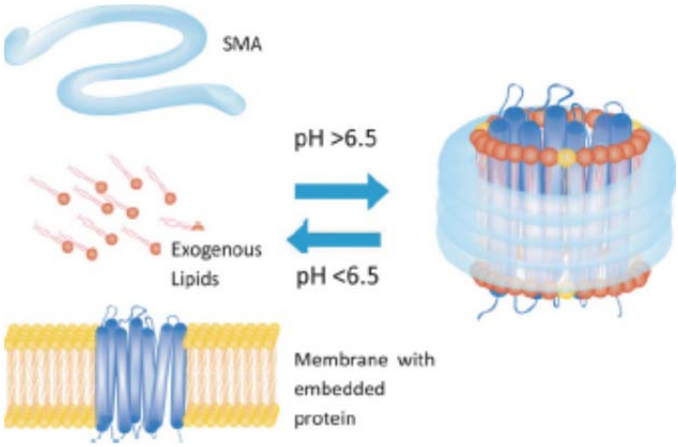

Fig.4.2 Mechanism of SMA form a disc with membrane protein. Adopt from (Jamshad *et al.*, 2011)

Researchers (Knowles *et al.*, 2009) have shown that, SMA will auto assemble a disc form in the presence of lamellar membrane that contain a lipid interior surrounded by an SMA annulus. This behaviour closely matches of the other nano-encapsulation methods offering the opportunity to use the material for

membrane protein purification. It was because the process produces a remarkably homogenous particle with a diameter between 9 and 11 nm. A purification example of applying SMA directly to bilayers without any additional treatment with surfactant, which contain the naturally abundant proteins bacteriorhodopsin and PagP has demonstrated the great potential for the protein purification. In each case, the SMA clarified the turbid membrane solution and was amenable to conventional protein purification methods. A method for directly solubilising proteins from their native environment into a form that is highly amenable to many downstream studies (Jamshad *et al.*, 2011). Seemingly, SMALPs has great potential as a generic mean dor periplasmic protein release by destabilising the membrane and encapsulating the proteins providing similar native surrounding environment but its specificity remains unclear. It is therefore we would like to ultilise SMALPs in this study to investigate the efficiency on periplasmic protein and any specificity for A33 Fab′ release.

Humphreys *et al.* (2002) have shown development to achieve high Fab′ production (580 mg/L) targeting in the periplasm. This would be very promising for us to employ similar strain provided by UCB Celltech to production substantial quantity of the A33 Fab′. By conducting preliminary study on shake flasks cultivate the W3110 *E.coli* harbouring pTTOD A33gL4gH2Fab plasmid to express periplasmic A33 Fab′ for investing the effect of IPTG concentration and temperature on cell growth and recombinant protein production. Based on the information gathers from shake flask experiment, 5 L scale fermentation will be performed to obtain sufficient amount of Fab′ (≥ 100 mg/L) for further investigation on protein release

methods, namely osmotic shock, heat treatment extraction and SMALPs. Depending on which method gives the best result, a systematically study will be carried out for seeking the optimum operation condition.

4.3. **Material and methods**

4.3.1. E. coli transformation and cell bank production

The A33 Fab′ expression plasmid DNA (pTTOD A33gL4gH2Fab) was received from UCB Celltech (UCB Celltech, Slough, UK). 100 μl of W3110 *E.coli* competent cell suspension were mixed with 3 μl of Fab′ expression plasmid and incubated on ice for 1 h. Bacteria were treated with heat shock at 42°C for 120 s to stimulate plasmid uptake. 0.5 mL of super-optimal catabolite repression (SOC) medium was added to treated cells and the suspension was incubated at 37°C for 1 h. Cells were harvested by centrifugation (Centrifuge 5415D, Eppendorf AG, Germany), re-suspended in 100 μL of SOC medium (2% tryptone, 0.5% yeast extract, 10 mM sodium chloride, 2.5 mM potassium chloride, 10 mM magnesium chloride, 10 mM magnesium sulphate, 20 mM glucose), spread on nutrient agar (NA) plates with tetracycline (10 μg/mL) and incubated at 37°C overnight (Laboratory oven, LTE-Scientific Ltd, UK).

A single colony was collected and cultivated in 80 mL LB broth with tetracycline (10 μg/mL) at 37°C, 200rpm overnight (Cooled orbital incubator, Gallenkamp, UK). After growing bacteria 20 mL sterile glycerol was added to flask and mixed gently. Culture was loaded into Eppendorf tubes with 0.5 mL and stored at −80°C until required.

4.3.2. Inoculum culture

Twenty millilitre of 'SM6E' production media (5.2 g/L $(NH_4)_2SO_4$, 4.14 g/L $NaH_2PO_4 \cdot H_2O$, 4.025 g/L KCl, 1.04 g/L $MgSO_4 \cdot 7H_2O$, 5.20 g/L citric acid, 31.111 g/L glycerol, 0.0522 g/L $CaCl_2 \cdot 2H_2O$, 0.0206 g/L $ZnSO_4 \cdot 7H_2O$, 0.0272 g/L $MnSO_4 \cdot 4H_2O$, 8.1 mg/L $CuSO_4 \cdot 5H_2O$; 4.2 mg/L $CoSO_4 \cdot 7H_2O$, 0.1006 g/L $FeCl_3 \cdot 6H_2O$, 0.3 mg/L H_3BO_3, 0.2 mg/L $Na_2MoO_4 \cdot 2H_2O$, pH adjusted to 6.95 with NH_4OH, and 0.1 mg/L tetracycline were seeded with 3% (v/v) cell bank suspension (Humphreys *et al.*, 2002). Inoculum cultures were shaken overnight (20−22 h) at 200 rpm and 30°C.and the final OD_{600nm} was around 5.2.

4.3.3. *Shake flask experiments*

Four per cent of inoculum culture was added to 100mL 'production medium' in 500mL flasks and incubated at 200rpm, 30°C and 25°C. Initial OD_{600nm} ~0.25., at OD_{600nm} 0.5, [IPTG] was added at 0, 8, 50, 100, 150, 200 and 500μM to induce Fab′ expression. Experiments were carried out in duplicates. Double samples were taken every 2 h and up to 24 h post induction as indicated in the figures. Fresh samples were centrifuged at 15,800 *g* for 300 s. The supernatant was recovered and stored in sterile tubes. The supernatant and cell pellets were stored at −20°C until required.

4.3.4. Modified UCB Celltech and improve protocol

One hundred millilitre of the overnight inoculum was add into 2 L "SM6E" media (Humphreys *et al.*, 2002) in a 5 L Electrolab fermentor (Tewkesbury,

UK) to continue culture till reached OD_{600nm} ~30, the glycerol (714 g/L 99.9% glycerol, 30 mL 1M $(NH_4)_2SO_4$) feed was started with feb-batch feeding rate (Chapter2, section 2.3.3.2, Equation 2.1) until the end of the fermentation process, induction was made with [IPTG] of 0.5 mM when OD_{600nm} reached 80, temperature was decreased from 30°C to 25°C upon induction. Samples were taken every 2 h to measure optical density and harvest at 24 h post-induction.

4.3.5. Protein release methods

4.3.5.1. Osmotic shock

Protocol was the same as described in Chapter 2 (methods section 2.3.4).

4.3.5.2. Heat treatment

The heat treatment employed was recommended by UCB Celltech Ltd and (Weir and Bailey, 1995; Humphreys *et al.*, 2002). Routinely, the cell pellets were resuspended in 1 mL of 100 mM Tris buffer pH 7.4 supplemented with 10 mM EDTA. 4). Incubate the suspension at 60°C for ~16 h (overnight), with agitation at 200 rpm, clarify the supernatant by applying centrifugation at 15,800 *g* for 10 minutes, and the supernatants were immediately frozen at −20°C for further A33 Fab′ analysis.

4.3.5.3. Preparation of SMALPs [poly(styrene-co-maleic acid) lipid particles]

Weighing 25 g of poly(styrene-co-maleic acid polymer and transferred to a 500 ml round bottom flask then gently mixed with 250 ml 1 M NaOH for overnight at room temperature on a magnetic stirrer. In a Fume hood, removing magnetic flea and added a few anti bumping granules then placing round bottom flask on a heating mantle with a condenser attached and turned maximum heat level until polymer and NaOH solution reached boiling point, turned heat down to continue gentle reflux for 2 h. Ensure the condenser was connected to water supply and there was flow allowing polymer/NaOH to cool to room temperature in Fume hood with the condenser still connected and water flowing. The percentage of polymer content was re-calculated by the remaining mixture volume content of the polymer. Carefully aliquot 5mL into labelled tubes with volume of aliquot and percentage polymer content and store aliquots frozen at −20°C for further use.

For use the polymer, first thaw sample at room temperature then dialysing against buffer (50 mM Tris buffer pH 8.0 or 50 mM Phosphate buffer pH 8.0). At least 3 changes of buffer were required over a period of 24 h for ensuring there was the least possible space above the polymer to the clip or knot in the tubing or the volume would swell too much and too low a percentage of polymer achieved. Using at least 1 L buffer per change for 40 to 50 ml of polymer dialyse. Measuring volume of dialysate and re-calculate polymer content percentage and store dialysed Polymer in the fridge but used at room temperature

The 2.5% SMALPs was prepared from the above dialysed stock with 1 % lipid in 50 mM Tris pH 8.0 at room temp for periplasmic release (2.5% SMALPs solution was kindly provided Prof. Tim Dufforn, School of Bioscience, University of Birmingham, UK).

4.3.6. Systematically periplasmic release experiment

A systematic release experiment was conducted with various release methods and conditions. Heat treatment, 2.5% SMALPs in 50mM Tris buffer pH 8.0 and 50 mM Tris buffer pH 8.0 were employed to extract the protein from periplasm in *E.coli*. Each cell pellet (1 mL fermentation sample harvested at 24 h post-induction) was added 1mL or 3 mL of different releasing buffers then incubating and vortexing at 200 rpm at room temperature for 2 h or overnight, only the heat treatment was performed at 60°C

4.3.6.1. Heat treatment release on various cell density

Various ratios of the heat treatment buffer were applied 4, 2, 1, 0.5, 0.4, 0.3 and 0.2 mL to re-suspend 1mL cell pellet (24 h post-induction), then Incubated the suspension at 60°C for ~16 h (overnight), agitated at 200 rpm. Clarifying the supernatant by centrifugation at 15,800 *g* for 10 minutes, and the supernatants were immediately stored and frozen at −20°C for A33 Fab′ analysis.

4.3.7. Analysis

Optical density, BCA assay and DPA assay were done as described in Chapter 2 (section 2.3.5.1−3).

4.3.7.1. Colony forming units

Serial dilutions of fermentation samples were prepared aseptically in PBS for viability counts. One hundred microlitres aliquots of serial dilutions were plated onto LB agar plates supplemented with 15 mg/L tetracycline, and following overnight incubation at 37°C, the number of colony forming units (CFU) was measured by counting colonies on plates containing less than 300 colonies according to following formula.

$$\text{CFU/mL} = \text{No. of colonies} \times \text{dilution factor} \times 10$$

4.3.7.2. 14 % SDS-poly-acrylamide gel electrophoresis (SDS-PAGE) for A33 Fab′ protein separation

The resolving gel was prepared with 3.86 mL dH_2O; 3.75 mL 1.5M Tris, pH 8.8; 150 μL 10% SDS; 7.15 mL Ultra Pure Protogel (National Diagnostics, UK); 75 μL 15% APS; and 15 μL TEMED to a total 15 mL solution sufficient for casting 4 mini gels. The stacking gel was made by adding 3 mL dH_2O; 1.25 mL 0.5M Tris, pH 6.8; 50 μL 10% SDS; 625 μL Ultra Pure Protogel; 25 μL 15% APS; and 5 μL TEMED to a total 5mL solution enough for casting 4 mini gels. Cell pellet samples were re-suspended in sample buffer according to the OD (Laemmli sample buffer (Bio-Rad Laboratories, USA); with β-mercaptoethanol. Samples were boiling at 110°C for 15 minutes in the Dry

block heating system (Grant Instruments (Cambridge) Ltd, UK). Samples were spun down at 15,800 *g* for 10 minutes. Ten microlitre of the sample's supernatant were loaded per well. Five microlitre of See Blue® Plus2 Prestained Standard (Invitrogen, USA) was loaded as marker/reference. SDS-PAGE tray was filled with Tris-Glycine-SDS-PAGE (TGS) buffer (Fisher Scientific Ltd). Gels were run at 50V for 0.5 h, followed by 2 h at 100V (OmniPAC MIDI, Geneflow, UK). Gels were stained with Simply Blue™ SafeStain (Invitrogen, USA) for 1 h and left in dH_2O overnight for distaining and washing.

4.3.7.3. Sandwich ELISA for A33 Fab′

ELISA plates were coated at 4°C overnight with 2 μg/L sheep anti-human IgG (The Binding Site, UK) in PBS solution. The coating buffer was discarded and wells were loaded with 200 μL of blocking PBS-BSA solution (prepared by adding 1 PBS tablet and 1 g of BSA in 100mL dH_2O) and incubated at 37°C, 250 rpm for 1h in plate shaker. The blocking buffer was discarded and ELISA plates washed three times with 300 μL wash buffer (prepared by adding 5 PBS tablets and 50 μL of Tween−20 in 500 mL dH_2O) then tap dried. ELISA plates were loaded with 100 μL of unknown samples (CB, OS1 and OS2 fractions) and standard (purified Fab′) samples. Four consecutive 1/4 serial dilutions were performed per unknown sample and eight consecutive 1/3 dilutions were carried out for the standards to develop the standard curve for estimating [Fab′]. ELISA plates were loaded with diluted sample and standards then incubated at 37°C, 250 rpm for 1 h. The sample solution was discarded and the plates were washed three times with 300 μL wash buffer

and tap dried. One hundred microlitre of detection antibody solution, made from 20 mL of blocking buffer containing 2 μL of goat anti-human Fab peroxidase conjugate (Sigma-Aldrich, UK), were loaded into ELISA plates and incubated at 37°C, 250 rpm for 1 h. The detection antibody solution was discarded and the plates were washed three times with 300 μL wash buffer and tap dried. One hundred microlitre of TMB Microwell Peroxidase Substrate System (2-C) (Insight Biotechnology Ltd, UK) were loaded per well and incubated at room temperature, at 250 rpm for 10 minutes. The reaction was stop by adding 100 μL of 1 M H_3PO_4 per well. The absorbance was measured at 450nm in GloMax®-Multi Detection System. ((Humphreys *et al.*, 1996, 2002)

4.3.7.4. Western blotting for A33 Fab′

Protein samples were separated using gel electrophoresis as described in the SDS-PAGE section. Proteins were transferred onto Hybond-P PVDF membrane (Amersham, UK) following the manufacturer's blotting protocol in the Mini Trans-Blot® Electrophoretic Transfer Cell module (BioRad, USA). Membrane was incubated with Mouse Anti-Human Kappa-HRP (Southern Biotech, USA) as primary antibody (1/10,000). Colorimetric detection was used for blotting development by addition of TMB Membrane Peroxidase Substrate System (3-C) (KPL, USA) according to product's instructions.

4.4. **Results and discussions**

4.4.1. Growth & DNA profiles from shake flask cultivations performed at 30°C with different IPTG concentrations

The preliminary shake flask experiment was conducted according to the protocol suggested by the UCB Celltech to verify the plasmid (pTTOD A33gL4gH2Fab) was correctly transformed into *E.coli* W3110 strain. Based on the previous results (see chapter 2) and the improved protocol (Sevastsyanovich *et al.*, 2009), different concentrations of IPTG for induction were tested at 30°C, 200 rpm cultivation condition. Samples were taken every 2 h after induction and 24 h post induction to measure optical density, and plated on agar plates for the colony form unit (CFU) to observe the cell viability throughout the cultivation. DNA concentration in culture broth was measured by DPA assay as an indicator for cell status over the period of cultivation. When the DNA concentration increases in the culture broth meaning more cell lysis were occurring during the cultivation process, meanwhile CFU would decrease to reflex the loss of cell viability. Therefore, there would be a potential risk of losing Fab′ into culture broth when the cell integrity is compromised thereby containing the target protein with DNA and other protein species, eventually causing the same problems we have encounter with Fab D1.3 in the purification process.

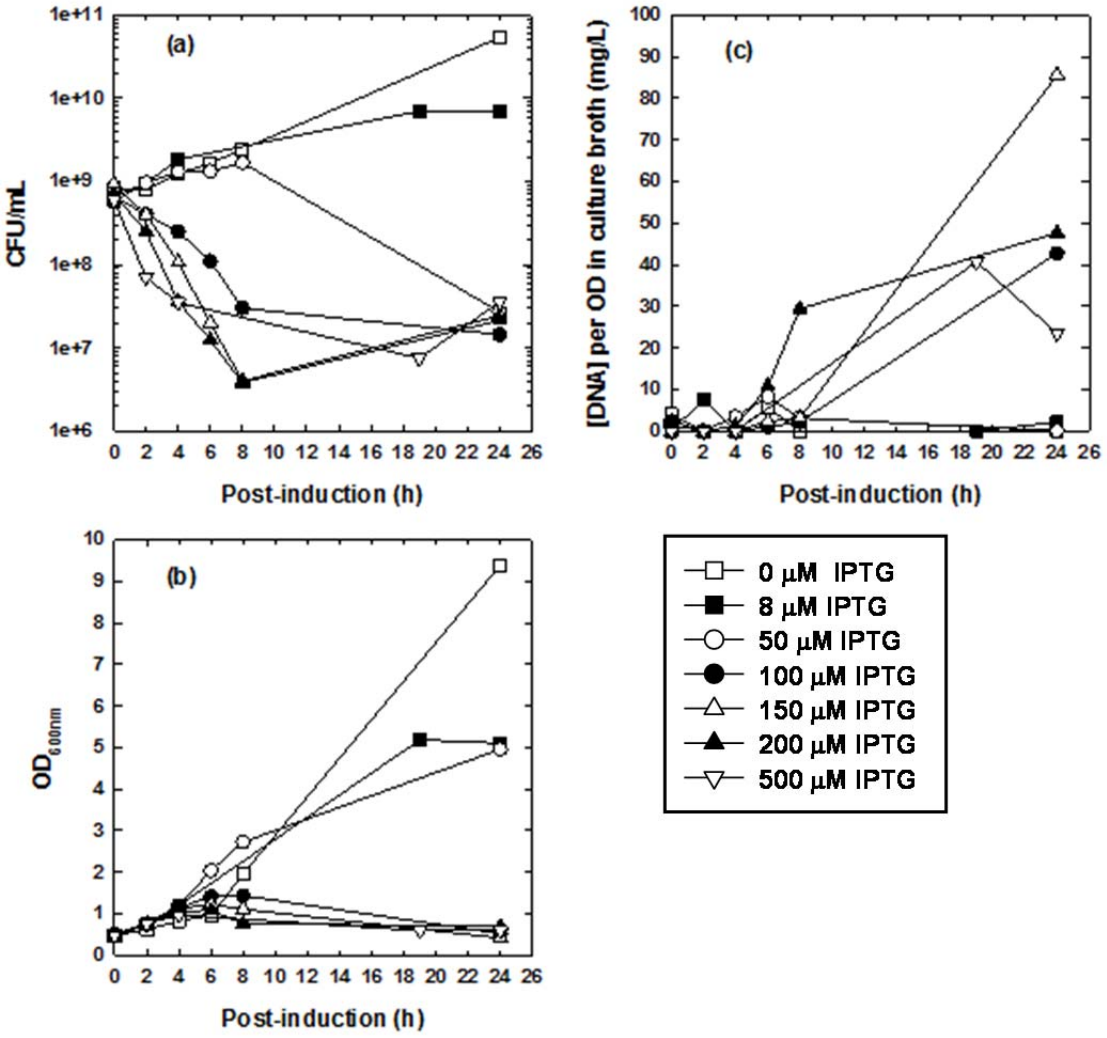

Fig. 4.3 Results of impacts on [IPTG] for the cell viability and DNA leakage to culture broth from various time points. a Plot of the colony form unit with different [IPTG] induction. b Optical density readings after induction with different [IPTG] c [DNA] in culture broth measured by DPA assay.

The CFU data from Fig. 4.3a illustrates the effects of induction with different concentration of IPTG on the cell viability. There are two separated group can be observed. Clearly, applied 100 μM and above IPTG for induction have strongly negative impact on the cell viability which can be seen the CFU counts are decreasing in every sampling point. On the other hand, the negative control and low concentration of IPTG (8 and 50 μM) have consistently increased of CFU counts within the first 8 h post induction but

decreased in the end of cultivation. The result has suggested the balance for induction at low biomass (OD_{600}~0.5) but not affected on cell viability was between 50 to 100 μM IPTG. Higher amount of IPTG could cause cell stress response and damage on cell metabolism thereby preventing the recombinant protein production (Kosinski *et al.*, 1992; Miao and Kompala, 1992; Donovan *et al.*, 1996; Kilikian *et al.*, 2000).

Similar tendency of results observed in the Fig. 4.3b, which illustrates the higher biomass achieved by inducing with lower concentration of IPTG. Whereas the higher concentration of IPTG shows flatted on the OD_{600} reading (~1). Further, Fig. 4.3 (a and b) have confirmed with each other when applied the IPTG concentration above 100 μM resulted OD~1 thereby CFU count at 24 h post induction was around 10 to 7^{th} power. This has proven that cells could not tolerate under high concentration of inducer as compared to the negative control and 8 μM IPTG applied. Both have ended with higher final OD reading also higher CFU counts (Fig. 4.3 a and b). Although using 50 μM IPTG has reached final OD around 4 but the CFU count was similar to other higher concentration IPTG applied. This implies the real living cells were much less than it showed on OD reading, cell debris could be the factor to misleading the actual biomass estimated by the optical density reading.

Measurements of DNA concentration in culture broth per OD reading gave the information regarding to the cell condition shows in Fig. 4.3c. Induction with IPTG below 50 μM, there was nearly untraceable amount of DNA in the culture broth. Surprisingly, applied 100 μM and 150 μM IPTG resulted 42 mg/L and 85 mg/L of DNA leaked into culture broth, whereas the higher

concentration IPTG did not lead to higher amount DNA in the culture broth. This might be linked with cell viability as mentioned above that cells were not able to tolerate under such high concentration of IPTG. Because the surviving cells were much less with high concentration IPTG applied compared with other conditions, subsequently decrease of DNA concentration in culture broth can be observed after reaching the peak with 150 μM IPTG condition. Overall, the above results have suggested that induction with IPTG higher than 150 μM was unsuitable as those conditions might over-stress the cells to the point of death and lysis. The optimum concentration for induction seemed to be between 50 and 100 μM to balance the cell viability and DNA leakage to the culture broth at 30°C. For this purpose, those two conditions were selected for further optimisation as it seemed to be on the borderline of cell tolerability.

4.4.2. SDS-PAGE and western blotting analysis for shake flask experiments conducted at 30°C with different [IPTG].

The molecular weight of A33 Fab′ recombinant protein is estimated around 25 kDa (Humphreys *et al.*, 2002). Protein samples were pre-treated with β-mercaptoethanol and boiling at 110°C for 10 minutes to reduce disulphide bond prior to loading on 14% SDS-gel for protein separation.

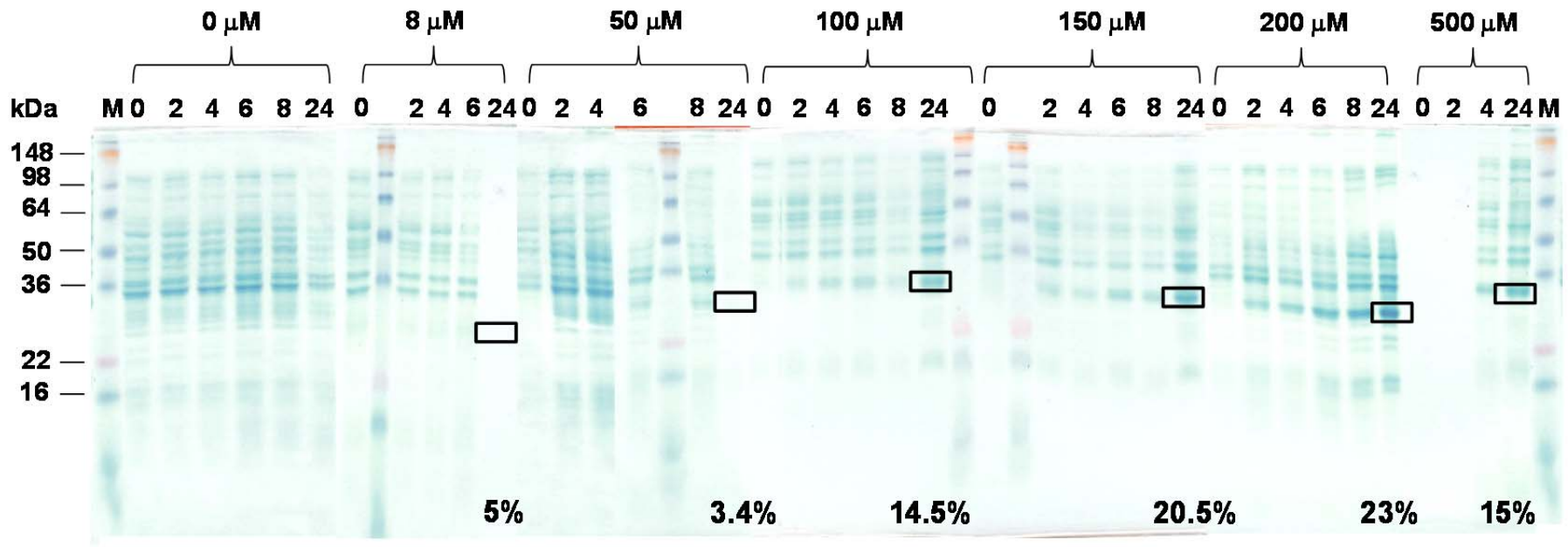

Fig. 4.4 Reducing 14% SDS-PAGE analysis shows shake flask cultivations performed at 30°C with different IPTG concentrations. Samples were 1 mL cell pellets collected in different time points after induction as showed on each lane. Black boxes indicate the protein band of A33 Fab′ on the gel. The numbers below the gels show the relative amount of Fab′ (measured by area analysis using ImageJ software).

Previously in Fig. 4.3 studied on the impact of IPTG concentration to the cell integrity and viability. Subsequently it is important to investigate the recombinant protein expression in relation to the inducer concentration. The 1mL cell pellets were collected from different timing and loaded on 14% SDS-PAGE to separate proteins in the cells. Analysing the intensity on the gel for A33 Fab′ by ImageJ, a colorimetric method, compared from 0 to 500 μM IPTG applied for the Fab′ induction. As can been seen the result in Fig. 4.4, there are no clear protein express of A33 Fab′ for 0,8 and 50 μM IPTG, even at 24 h post induction. Although the software has detected very minor signal from the gels, but is not possible to see. Induction with higher concentration IPTG (i.e. 100 μM of IPTG and above) have clearly showed a band just slightly above 22 KDa protein marker at 24 h post induction. Furthermore, the protein band intensities measured by colorimetry have shown huge increase between 100 μM and 200 μM of IPTG from 14.5% to 23% of A33 Fab′.

Studies by Donovan *et al.* (1996) has review several factors (i.e. temperature, IPTG concentration, type of inducer lactose or IPTG, timing of induction, growth media and duration of induction phase) for optimising the protein production in *E.coli*. When induced with IPTG for recombinant protein production, will allow the separation of cell growth phase and protein synthesis phase, therefore when the higher biomass is achieved, the higher yield of protein could be produced. In addition, Kosinski and co-workers (1992) designed the H35 stress response protein in *E.coli* to demonstrate the stress response when the IPTG was applied for the foreign protein production and also suggested that IPTG might cause the decrease in specific growth rate.

It is therefore we can explain the reason of the highest IPTG concentration (500 μM) did not continuously increase yield of Fab′ but only had 15% compared with other conditions. The results in Fig. 4.4 have suggested that there is a limit to use IPTG for protein expression in *E.coli*. The higher IPTG concentration might offer higher yield of Fab production. However, with excessive amount of inducer (e g. 500 μM) will cause negative effect on the protein production (Kosinski *et al.*, 1992; Donovan *et al.*, 1996). Based on the analysis of colorimetry, the strongest band intensity of Fab′ occurred with 200 μM IPTG applied; also steady increase of Fab′ expression was observed of induction from 50 μM to 200 μM IPTG. From the results of the preliminary shake flask experiments allowed us to understand the limitation of this Fab strain and the possible operation window for the following fermentation.

A specific and efficient protein detecting procedure after transferring from SDS electrophoresis to a PVDF membrane (Burnette, 1981). Due the nature of the immunology, A33 Fab′ specifically reacts with anti Fab than other protein species on the gel. This method allows us to clarify and confirm the type of proteins separated on the SDS-PAGE.

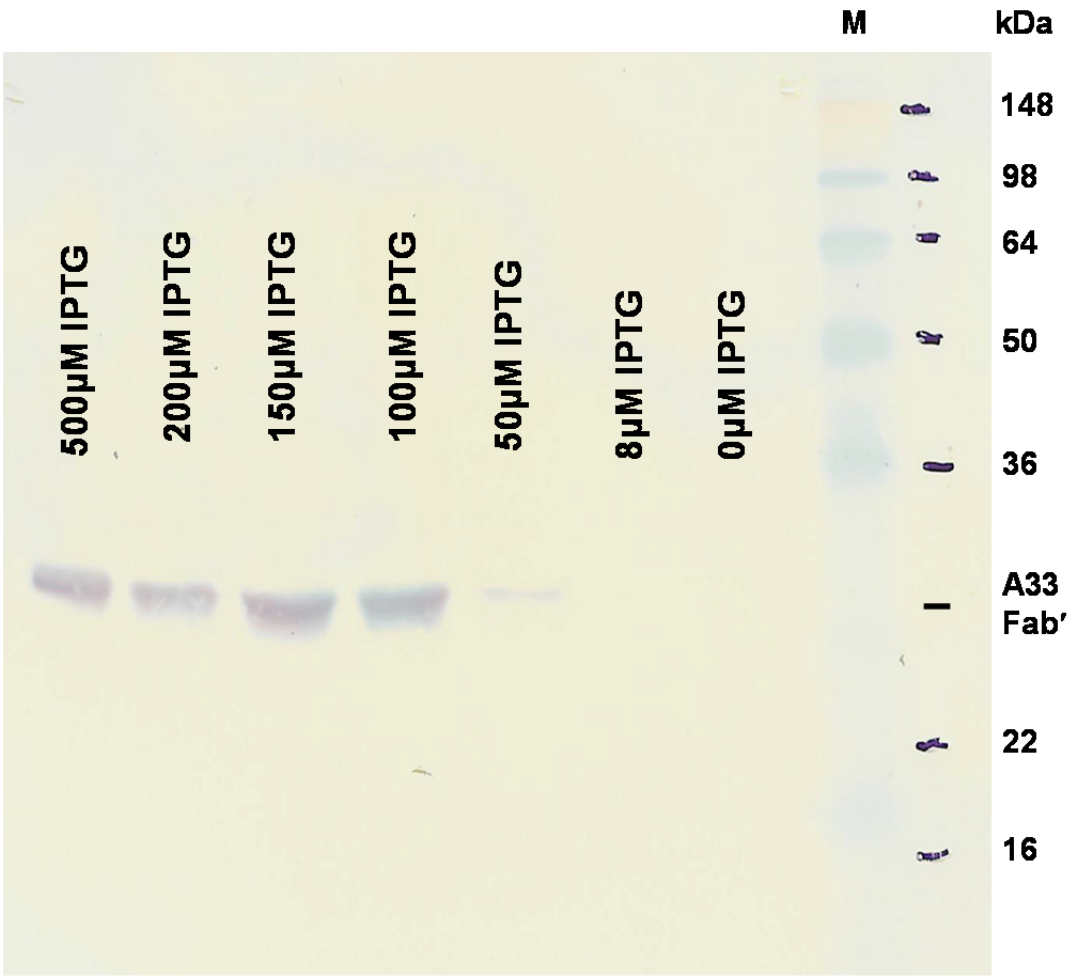

Fig. 4.5 Western Blot analysis shows the effect of [IPTG] on A33 Fab′ production in shake flask experiments at 30°C. Loading sample of 1 mL cell pellet (24 h post-induction), separated by 14% SDS-PAGE, followed by wet transferring to PVDF membrane for western blotting with IgG specific anti Fab produced in Goat.

Undoubtedly, the result in Fig. 4.5 confirms the A33 Fab′ was correctly expressed in the shake flask experiments. Strikingly, there is strong signal observed from 100 μM and above conditions. A very minor band barely shows on the membrane for the 50 μM IPTG condition. Analysing the four strong bands by colorimetry, the results suggests the maximum production obtained with 150 μM IPTG for induction which is around 10% higher than the 100 μM. For the higher IPTG concentration (200 and 500 μM) were down to 55~60% of Fab production compared to the optimal results. Despite of the higher

production with applying 150 μM IPTG to induce, but the overall cell viability is poor compared with 100 μM IPTG applied (Fig. 4.3 a and b). The CFU and OD reading was much lower in the higher IPTG condition, also the increasing amount of nuclear acids leaked into the culture broth. Taken collectively, we have selected using 50 μM and 100 μM of IPTG for the further optimisation experiment.

4.4.3. Cultivating A33 Fab′ with temperature downshift (30°C to 25°C) upon induction in shake flask

Taking a step forward from above results and experiences of adopting improve protocol (Sevastsyanovich *et al.*, 2009), lowering the temperature would be a viable strategy to apply for increase the Fab production and maintaining the use of high concentration IPTG for impulse expression. Therefore, cultivation temperature was decreased from 30°C to 25°C in this set of shake flask experiment. The reason of lowing temperature upon induction was minimising the stress response caused by inducer (Vera, 2007; Pinsach *et al.*, 2008) thereby prolonging the protein production phase. In addition, lower the chance of incorrect protein folding; simultaneously prevent a sudden shock to the cells leading death and lysis. Fig. 4.6 was the cell pellet sampled in different time intervals after induction with 0, 50 μM and 100 μM IPTG separated by 14% SDS-PAGE, when compared the results from Fig. 4.4 and Fig. 4.6.

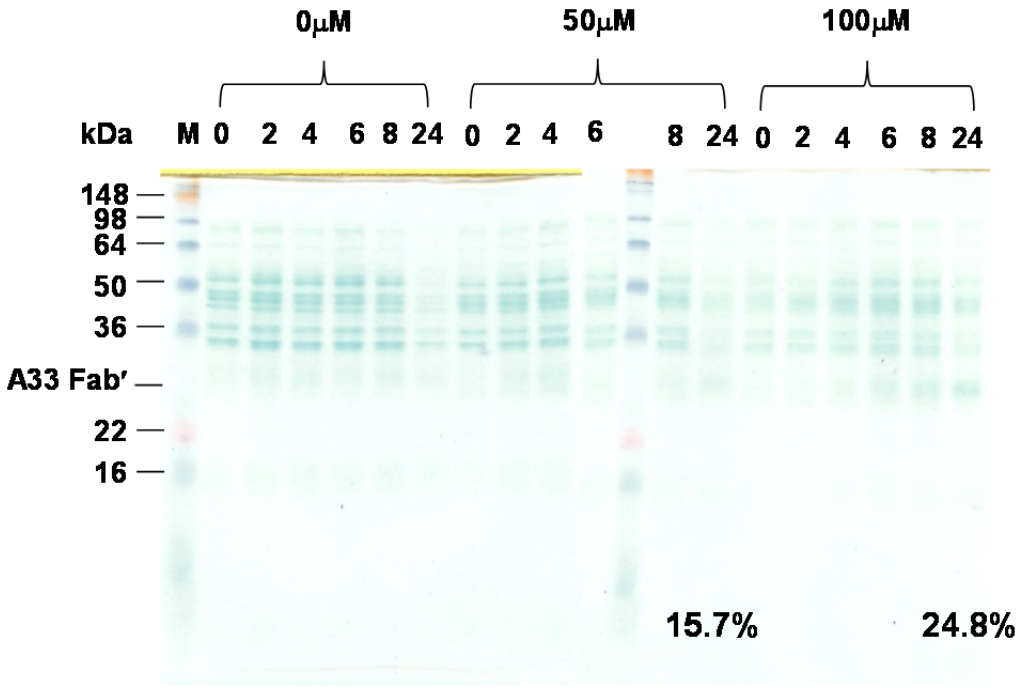

Fig. 4.6 Reducing 14% SDS-PAGE analysis of 1mL cell pellets at different point of induction , after reducing the temperature (30°C to 25°C) at point of induction. The number showed on the bottom of the gel indicated the percentage of Fab′ estimated by ImageJ.

In striking contrast, lowering the temperature to 25°C upon induction resulted in significant increases in percentage of Fab′ content. The yield of A33 Fab′ has risen from: 3.4 to 15.7% for 50 μM IPTG; and 15.4 to 24.8% for 100 μM IPTG compared the results in Fig. 4.4 Fig. 4.6. Although there was a larger (12.3%) increase of Fab′ with 50 μM but applying 100 μM was able to push the Fab′ up to 24.8% of [total protein] (ca. 339.1 mg/L) within the cells, therefore, the potential yield of A33 Fab′ could be around 84.1 mg/L. This significant improvement on the Fab′ production was very promising and encouraging. The result has demonstrated the possibility to achieve our goal (100 mg/L) of producing A33 Fab′ in a 5L scale fermentor, as a quarter of total protein within the cells could be potential product.

4.4.4. Production of humanised A33 Fab′ with temperature shift strategy in 5 litre fermentor

A 5 L scale fed-batch fermentation with *E.coli* W3110 strain harbouring plasmid (pTTOD A33gL4gH2Fab) (Celltech, UK) was carried out in order to increase the overall Fab′ production. Experiment was conducted as described in method section (4.2.4), induction with 0.5 M IPTG was performed when OD_{600} reading reached 80. However, in this batch, the induction was performed at OD_{600nm} ~107.2 then harvesting at 24 h post-induction, final OD reading was 158.

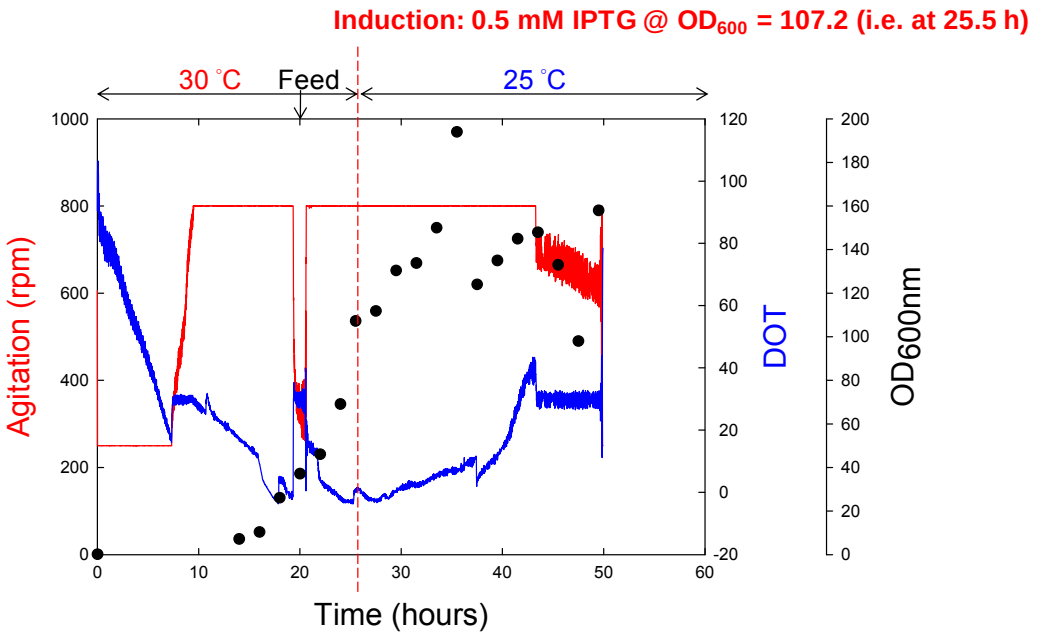

Fig. 4.7 Result of A33 Fab′ fermentation. Harvested at 24 h post-induction, recommended harvesting time will be 24-36 h post-induction (UCB Celltech)

A very typical *E.coli* growth cure in the minimum media has shown in Fig. 4.7. The first 8 h cells grew steadily and slowly which can be indicated by the level of dissolved oxygen (DOT) constantly decrease from 100 to below 30 over the period of time. After the cells have adapted to the environment, because the

increase of biomass, the DOT was below the set point, therefore agitation speed starting to rise. At 16 h after inoculation, the cells were in exponential growing phase; OD reading was rapidly increase also started the glycerol feeding when OD reached 30 to avoid depletion of carbon source. Until the OD reading was over 80, 0.5 M of [IPTG] was added into fermentor for expression A33 Fab′, after the induction, the OD reading was fluctuated between 90~160, this was possibly caused by high cell density aggregation and rapidly settling of cells in the PBS dilution buffer. According to Humphreys *et al.*, (2002), after 24 h post-induction OD_{600} should be ~100, but we harvested at OD~158. This could be a promising result judging from the amount of IPTG we have added but there was no decrease of OD reading. The fermentation protocol was provided by UCB Celltech then modified with improve method (Sevastsyanovich *et al.*, 2009), the result able to generate relative high biomass when compared with original protocol by Humphreys *et al.*, (1996, 1997, 2002) and previous Fab D1.3 fermentations (See Chapter 2).

4.4.5. Extraction of A33 Fab′ from periplasm by heat treatment and osmotic shock

In chapter 3, we have systematically investigated various releasing conditions (i.e. Osmotic shock and 0.1% deoxycolate) regarding the cell physiology and membrane stability to the surrounding environment (i.e. static and vortex, length of incubation, pH) then trying to identify the better conditions for selectively and effectively extracting periplasmic proteins from of *E.coli*. Likewise, there were two release methods being investigated in this section (i.e. osmotic shock and heat treatment). The 1 mL pellets were collected in

three different timing (i.e. pre-induction, 12 h post-induction and 24 h post-induction). Those samples were treated with osmotic shock (OS1&2) and heat treatment, respectively. Supernatants were separated by 14% SDS-PAGE based on the same amount of total protein (5 μg) and left over pellets were resuspended in different volume of Laemmli electrophoresis buffers based on the OD reading accordingly (Fig. 4.8).

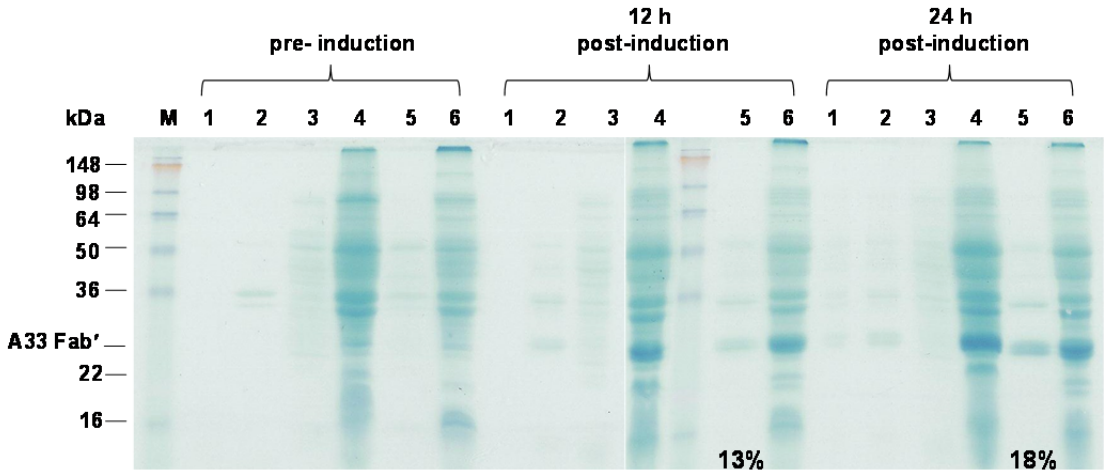

Fig. 4.8 Reducing 14% SDS-PAGE analysis of fractions arising from osmotic shock and heat treatment extractions of cells harvested at various times of pre and post-induction. M: marker, 1: Culture broth, 2: OS1 supernatant, 3: OS2 supernatant, 4: Pellet after osmotic shock, 5: Supernatant from heat treatment, 6: Pellet after heat treatment.

As mentioned above, the protein bands represented A33 Fab′ was slightly above 22 kDa according to the protein marker. Not surprisingly, lane 1 to 6 from the pre-induction samples did not show any clear band around 22 kDa position. At second bracket of sample from 12 h post induction, it was clear A33 Fab′ appeared in land 2 to 6, which means the Fab was in periplasm (OS1), cytoplasm (OS2) and pellet after osmotic shock. Likewise heat treatment fraction in lane 5 and pellet after heat treatment in lane 6 showed clear protein band for the Fab′ but seemed more intense than the samples

from osmotic shock (lane2 and 3). Samples collected 24 h post induction has significantly increased of band intensity compared to the samples in the middle bracket. Further, by loading the same amount of total protein, a stronger protein pattern and A33 Fab′ band was visible in the case of using heat treatment extraction (lane5) in comparison to osmotic shock (lane2). For the same reason, therefore stronger band intensity suggesting higher percentage of A33 Fab′ was produced (ca~18%) in the 24 h post-induction (lane6). Noticeably, two samples from culture broth between 12 and 24 h post induction showed slightly leakage of proteins indicated that cells were probably starting to lyse. However, there was still 5% increase of Fab′ production from 12 to 24 hour post induction in the heat treatment fraction. As the result, the lost in the culture broth was acceptable. Furthermore, this result also confirmed that heat treatment working better than the osmotic shock for the A33 Fab′, because the protein bands were much clear in the lane 5 compared with lane 2 in those two different samples. Although heat treatment has shown better protein release efficiency and selectivity over osmotic shock, but because of the high temperature requirement for the heat treatment, this method may not be suitable as a generic periplasmic protein release method when dealing with other heat sensitive proteins. In the case of releasing A33 by heat treatment, because it is likely to be a thermal stable protein, so the method is well suited for the case (Humphreys *et al.*, 2002; Humphreys, 2007).

4.4.6. Western blotting analysis of the fermentation cell extracts

As mentioned above, western blotting is a power tool to confirm the target protein has been correctly expressed and a great tool to detect protein when the expression was not clear visualised on the SDS-PAGE. Samples from 24 hour post-induction were firstly separated by 14% SDS-PAGE then wet transferring onto PVDF membrane for the western blotting. Lane 1 was loaded cell pellet collected before-induction performed as a negative control. Samples from culture broth, OS1 fraction, OS2 fraction, pellet after osmotic shock, heat treatment fraction and pellet after heat treatment were loaded from lane2 to 7, respectively. The results were shown in Fig. 4.9.

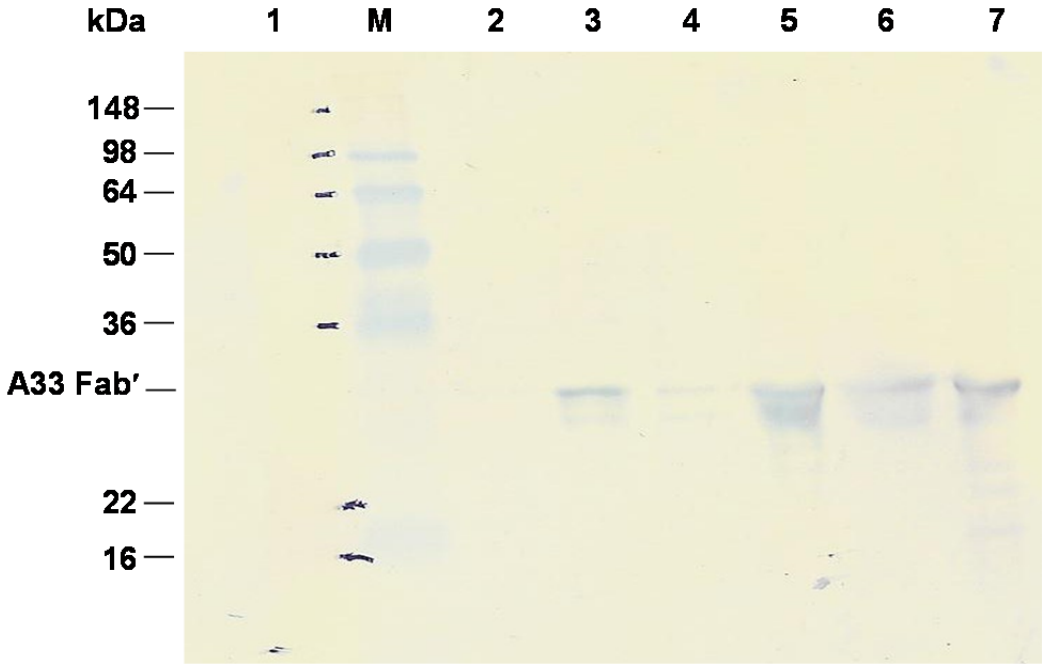

Fig. 4.9 Western blotting analysis shows Fab′ content from the supernatant and pellet after osmotic shock and heat treatment extraction. Lane 1: Pellet before induction, M: Sea-Blue pre-stain protein marker, 2: Culture broth from 24 h post-induction, 3: OS1 supernatant from 24 h post-induction, 4: OS2 supernatant from 24 h post-induction, 5: Pellet after osmotic shock, 6: Sample from heat treatment supernatant, 7: Pellet after heat treatment.

Noticeably, lane 1 (pellet before induction) was the pellet sample took before induction which did not show any single band on the membrane which suggested that there was no leaky express happened in this strain.

In the previous result (Fig. 4.8), sample from culture broth at 24 h pot-induction only showed very minor proteins band across the lane. The same sample was loaded here in lane2 (culture broth) , the band was also extremely indistinct and vague. Clearly, these results have demonstrated the same fact that only very little proteins were leaked into culture broth and most of them were not the A33 Fab′. More importantly, the integrity of cells was still intact even though harvested after 24 h induction, thus no obvious band appearing in the lane2. This also suggested that if cells were able to cultivate for long time then possibly producing more protein or higher concentration of IPTG can be applied to boost expression. Moreover, it showed a great advantage for the following protein purification to avoid multiple locations distributions for the Fab′ accumulation, only in periplasm, which would consequently make the initial feedstock less contaminated and ease the purification process (Venturi *et al.*, 2002; de Marco, 2009; Sockolosky and Szoka, 2012).

Interestingly, the band intensity in lane3 (OS1 supernatant) was stronger than 4 (OS2 supernatant), suggested most Fab′ was allocated in periplasm. However, in lane5 (pellet after osmotic shock) appeared most intensive Fab′ band compared with OS 1 and 2. This showed employing osmotic shock as a mean to disruption cell membrane was not effective to extract the majority of Fab′ from the cell envelope. In striking contrast, Fab′ released by heat

treatment showed in lane6 (heat treatment sample) was much stronger than osmotic shock, even stronger than the sum of two lanes2 and 3, which again matched up with the results showed in Fig. 4.8 that at 24 h post induction, lane5 are far stronger than lane2 and 3. Not surprisingly, lane7 (pellet after heat treatment) was much weaker than lane5 (pellet after osmotic shock). Presumably, equally amount of Fab′ was produced in cells, the more being released; the less remained within the cells. Those results have indicated that heat treatment could a more suitable extraction method than osmotic shock for the A33 Fab′. Meanwhile, as mentioned in the introduction SMAPLs has demonstrated several successful applications in protein release and purification (Knowles *et al.*, 2009; Jamshad *et al.*, 2011). It would be very interesting to compare the SMALPs and heat treatment which are more suitable or effective for periplasmic release and A33 Fab′.

4.4.7. Heat treatment extraction and SMALPs release study on A33 Fab′

Despite the heat treatment extraction has shown very promising results from the above experiments for releasing the protein from periplasm, there are still concerns to use it as a generic protein release method. Exposure proteins under high temperature (60°C) for long period of time (16 h) may cause some proteins change their conformation (Digel *et al.*, 2006) or denature thereby losing its function, such as enzyme activity (Argos *et al.*, 1979). For the SMAPLs can be easily employed in the room temperature to release proteins. The experiments were conducted in two different volume (i.e. 1 mL and 3 mL) of heat treatment buffer, 50 mM Tris buffer and 2.5% SMALPs, the

concentration of SMALPs is based on experiment data provided from colleagues in school of Bioscience (Personal communication with Prof. Tim Dafforn, University of Birmingham, UK). The supernatant from each samples were separated by 14% SDS-PAGE as shown below in Fig. 4.10.

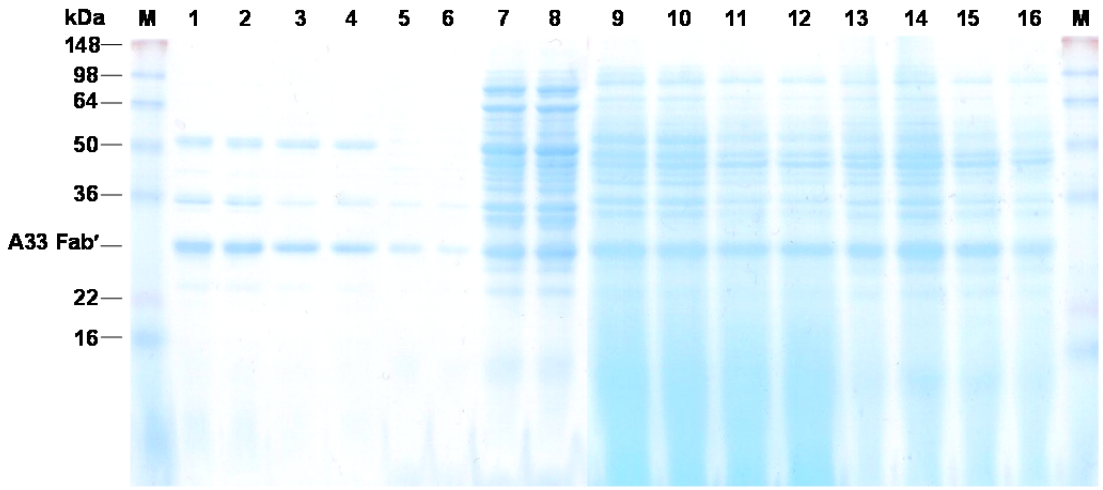

Fig. 4.10 Reducing 14% SDS-PAGE analysis shows 1 mL cell pellets with different methods and volumes for releasing A33 Fab′. Lane1-2: 1mL standard heat extraction; 3-4: 3mL standard heat extraction; 5-6: 1 mL 50 mM Tris RT, O/N; 7-8: 3 mL 50mM Tris RT, O/N; 9-10: 1 mL 2.5% SMALPs, 50 mM Tris 2 h RT; 11-12: 1 mL 2.5% SMALPS, 50 mM Tris O/N RT; 13-14: 3 mL 2.5% SMALPS, 50 mM Tris 2 h RT; 15-16: 3 mL 2.5% SMALPS, 50 mM Tris O/N RT.
*RT means at room temperature incubation. O/N means incubation for overnight.

From Fig. 4.10 illustrated each extract from different release conditions was loaded in duplicate to compare and ensure the results consistency. Since the purpose of this experiment was testing the release efficiency of each buffer and conditions, the loading was based on the ratio of dilution, for example, resuspension the pellet with 1 mL buffer, 5 μL of sample was loaded on the gel, resuspension with 3 mL buffer, 15 μL of sample was loaded, thus neglecting the dilution factor on different volume applied for pellet resuspension. Interestingly, samples loaded on the gel from both volume of heat treatment appeared similar compared between lane1 to 4, only few major

bands including Fab′ appeared on the gel. This suggested regardless the ratio of extraction buffer to the cell pellet; the release behaved similar level of effectiveness and selectivity for the heat treatment. Directly applied 1:1 ratio of 50 mL Tris buffer to the cell pellet was not possible to extract many proteins. More strikingly, increase the ratio three times of the extraction buffer was able to unselectively release proteins from cells. However, the release seemed causing by repeating frozen and thaw damaged the outer membrane damaged plus the excessive buffer used to resuspend the cells thereby causing unselective protein release from the cell envelope. Employing different ratio of SMALPs to the cell pellet and different incubation time length were shown from lane 9 to 16. Lane 9&10, 11&12 were samples tested with 1 mL 2.5% SMALPS in 50mM Tris buffer pH 8 then incubating for 2 h and overnight in room temperature, respectively. This was for examining the effect on the length of time for extraction. The results did not appear any significant difference on the gel, which suggest that SMAPLs was able to release proteins within 2 h incubation, longer incubation time did not enhance the protein release. Arguably Fab′ seemed to be the major band on those lanes, but many other species proteins were also seen on the gel. Furthermore, there was polymer smearing on the bottom part of gel. This could be the problem for the further protein purification to separate polymer and the Fab′. As demonstrated earlier, increase of volume on Tris buffer enhanced the ability for protein release. The results showed in lane 13-16 were obtained by investigating the effect on ratio of extraction buffer to the cell pellet. Triple amount of buffer was used to resuspend the cell pellet was shown in lane 15&16. Comparing to lane 13&14, which used 1mL of SMAPLs buffer to

extract proteins was almost identical. This implied diluting the cell density did not increase the efficiency for protein extraction. Furthermore, using 3mL 50mM Tris buffer in the absence of 2.5% SMAPLs was able to achieve similar level of protein extraction as the presence of SMAPLs. Therefore, it was arguably from the above results could suggest that small amount of 2.5% SMALPs with Tris buffer should be the better condition from the other conditions. This said, when the volume increases, the effect from Tris buffer was greater on protein release over the SMALPs. Nevertheless, the results from Fig. 4.10 have confirmed that the heat treatment for periplasmic release for the A33 Fab′ gave the best result compared with other chemicals and conditions applied.

4.4.8. Study on heat treatment for periplasmic protein

The result above has demonstrated SMAPLs was capable of releasing fair amount of Fab′ from periplasm. However, heat treatment owning the merits In terms of clarity and process complexity obviously was a better method to employ for the A33 Fab′ extraction. Taking collectively, optimisation of heat treatment condition was investigated in this section. From protein extraction point of view, maximising the protein release from periplasm was the goal to achieve. On the other hand, in the view of the process intensity, utilising minimum amount of buffer to release the proteins not only concentration the products in after releasing but also reduced the volume for the subsequent separation process. Therefore, there were two important questions need to be answer here. Firstly, could volume of buffer effect on the composition of release proteins, for example the less buffer applied might have less Fab′

released compared to other proteins. Secondly, the relation between the ratios of buffer to cell pellet, if increase buffer volume to resuspend cell pellet would enhance protein release. In order to distinguish the change on the releasable protein composition, the samples were loaded equal amount of total protein and separated on 14% SDS-gel.

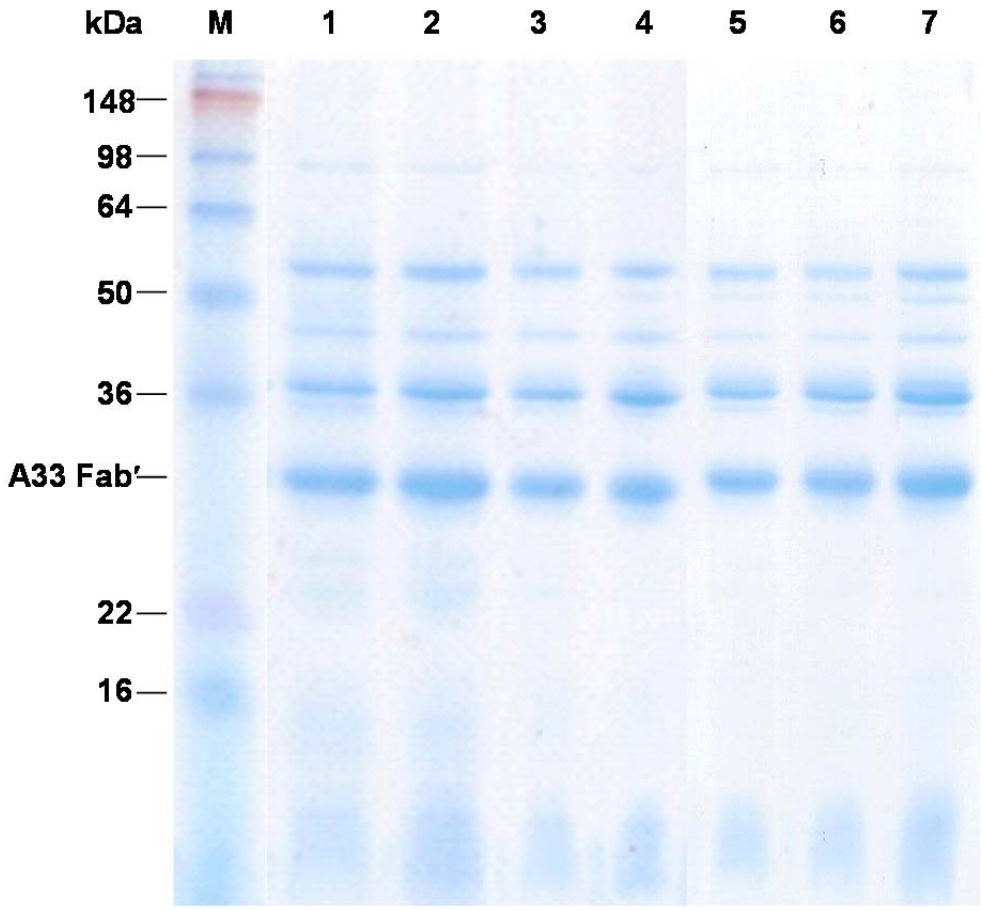

Fig. 4.11 Reducing 14% SDS-PAGE analysis shows the results of heat treatment extraction with various cell density conditions. The percentage decreasing from lane 1 to 7 are 65.8%, 43.9%, 32.9%, 26.3%, 13%, 6.5% and 3.25%, respectively. M represents the protein marker.

In Fig. 4.11 the cell density expression was calculated from the ratio of buffer to the cell pellet. The wet weight of this batch of fermentation at point of harvest was 131.57 g/L. When resuspend with 1 mL cell pellet with equal volume of the heat treatment buffer, the cell density was around 13% (w/v).

Likewise, the cell densities were derived from resuspending 1 mL cell pellet with different volumes of buffer.

Scrutiny of the gel above, every lane was nearly identical to each other despite the samples were treated with different release conditions. Moreover, all the major band of Fab′ appeared to be similar intensity. The result suggested there was no direct relation between cell density and the composition of releasable protein, which means regardless the volume of buffer applied, the percentage of every releasable proteins remaining consistent. More importantly, applying less heat treatment buffer for protein release did not influence on the releasable Fab′, in contrast it might help to concentrate proteins in supernatant. Next result in Fig. 4.12 illustrated amount of total protein released against several cell densities showed above.

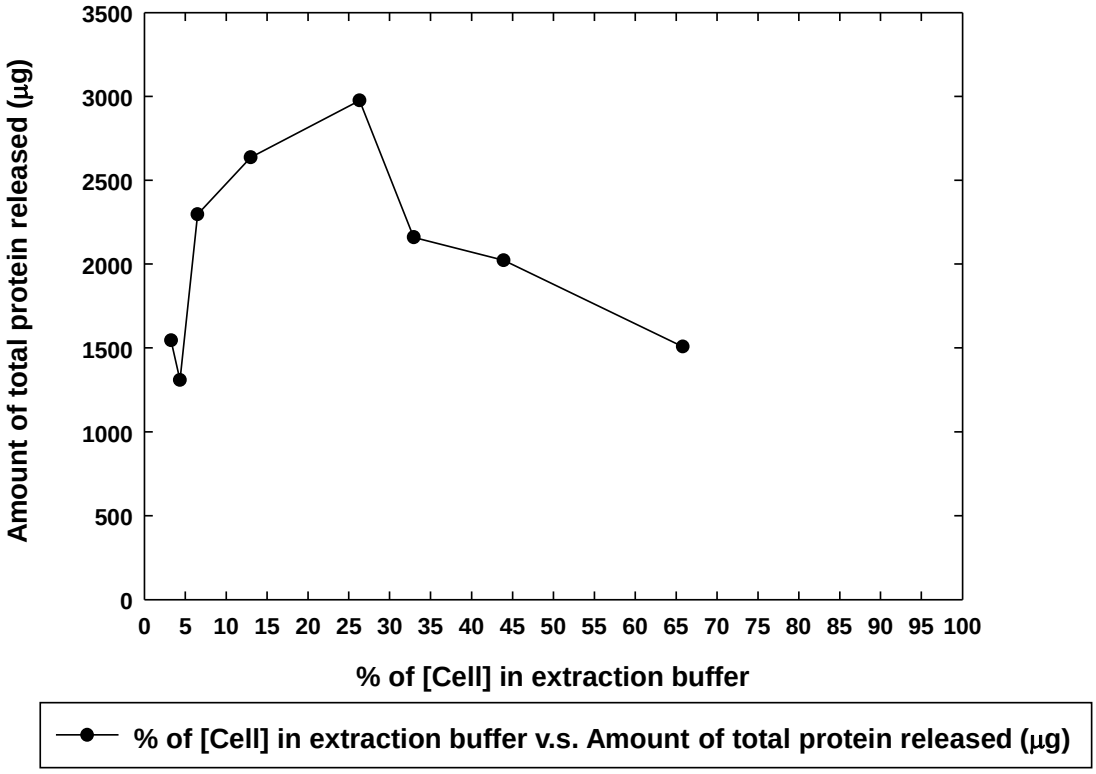

Fig. 4.12 Plots of release efficiency of heat extraction in different cell concentration. Release experiments were conducted of re-suspending 1 mL cell pellet in various volume of extraction buffer.

The overall result showed a hump on the graph. Amount of total protein released starting from 1.5 mg at the lowest cell density, began to rise when the cell density increase. The peak was reached by 27% cell density was applied; nearly 3 mg of total protein was able to release. After that, the effectiveness slumped sharply to just above 2 mg of total protein released and then further dropped to 1.5 mg at the highest cell density was used. The results showed here was able to answer the second question raise above, that cell density had huge impact on the protein release efficiency. Not surprisingly, on the either sides of extreme conditions did not show effective

protein release compared to the other conditions, only half amount of protein was released. Clearly, the optimum condition of heat treatment was using 27% (w/v) cell density for protein extraction, which was half the buffer volume. Several advantages could be taken here. First, as buffer volume was only half from the original volume, therefore protein concentration was doubled when released from periplasm. Second, it was always a desired goal to reduce handling volume for the downstream purification in the large scale, also saved the cost of consumable usages. Third, when the volume was reduced, the process time would be shorted, so the overall and labour cost would be benefited. Another effective release was observed at 13% cell density, which applied the buffer to the original volume of cell pellet for protein extraction. Under this condition also showed strong result, where nearly 2.7 mg of total protein was release, only 11% less from the optimal condition. In the lab scale, buffer volume was not an issue to consider would be a more suitable condition to employ. Because reduced half volume of heat treatment buffer might cause incompletely mixed, especially when the biomass was high, the cell pellet would require more buffer for better resuspension. As the results showed in Fig. 4.12 suggested two potential conditions could be applied when release the Fab′, in large scale, half the extraction buffer not only concentrate the protein in supernatant but also improve the protein release. For the use of lab scale, same volume to the original cell pellet could offer similar protein release efficiency, and also ensure mixing properly because it could be very difficult to resuspend the cell pellet when the biomass is really high. Despite all the facts, this is only a preliminary result for releasing periplasmic A33 Fab′, although the results has suggested the standard protocol might not be the

optimal condition to apply, but for the consistency of the experiments, 13% cell density for protein release was selected for further experiments.

4.5. **Conclusions**

The preliminary results from shake flask experiments in Fig 4.3 and 4.4 revealed the effects on IPTG concentration and cultivation temperature towards the cell growth and the recombinant protein production. We then selected 50 μM and 100 μM IPTG for temperature reduction experiment showed the 15.7% and 24.8% (ca. 54.45 mg/L and 84.1 mg/L of A33 Fab′) of total protein produced within the cell was Fab′. Comparing results between Fig 4.4 and 4.6 showed around 10% increase of Fab′ production in both conditions. Thus, adopting the fermentation protocol provided by UCB Celltech and modified based on the results from the shake flask experiments with improved protocol (Sevastsyanovich *et al.*, 2009), we were able to performed a 5 L scale fed-batch fermentation and reached relatively high biomass in the end (OD_{600nm}~107). More importantly, amount of releasable A33 Fab′ from this batch estimated by Image J suggested around 300 mg/L, which was approximate 12.5% of total protein, was produced. Furthermore, the sample collected at 24 h post-induction contained 5% more Fab than the 12 h post-induction, which suggested proteins showed in culture broth was very minor and the overall Fab′ production was increase along with the cultivation time. Since we were able to produce substantial amount of Fab′ in the periplasm, therefore it was crucial to investigate three current protein extractions method could be more effective and selective. As a generic method, osmotic shock was wildly used for protein release, but obviously can

be seen from Fig 4.8 and Fig 4.9, the heat treatment was able to more effectively and selectively release Fab′. Comparing the results from Fig 4.10, Although SMALPs [poly(styrene-co-maleic acid) lipid particles] has shown few successful application (Knowles *et al.*, 2009; Maeda *et al.*, 2009; Jamshad *et al.*, 2011) but the release performance seemed not as selective as heat treatment for the A33 Fab′. Moreover, in the presence of SMALPs showed strong interference on the SDS gel. To elimilate the effect of polymer dialysis procedure would be required which clearly was a drawback when the SMALPs was empolyed to release periplasmic proteins. Therefore, heat treatment extraction was selected for the further optimisation, a systematically release experiment was carried out with series of different cell density samples. Interestingly, the result from Fig 4.11 suggested that there was no direct relation between cell density and the composition of releasable protein, regardless the volume of buffer applied, the percentage of every releasable proteins remaining consistent. When plotted the total protein released against various cell density conditions, the result was surprised suggesting that 27% (w/v) cell density for protein extraction, which was half the buffer volume to cell pellet released almost 3 mg of total protein. Another effective release was observed at 13% cell density, which applied the buffer to the original volume of cell pellet for protein extraction and also able to release nearly 2.7 mg of total protein, just 10% less than the optimum condition. Because the performance from those two conditions was not hugely different, to ensure the mixing and pellet resuspension, 13% (w/v) cell density was selected for extracting A33 Fab′ in the future experiments.

To conclude, a successful A33 Fab′ fermentation in 5 L fermenter was performed in the following condition. Cultivation temperature was at 30°C and decreased to 25°C upon induction, induction was performed at OD_{600} ~80 with 0.1mM IPTG. Cells were harvested at 24 h post-induction. The optimum condition of heat treatment was using 27% (w/v) cell density for total protein extraction (i.e. ~ 3 g/L), but to ensure mixing performance in large scale, 13% (w/v) cell was recommended for protein release (i.e. 2.7 g/L).

4.6. **References**

Argos, P., Rossmann, M.G., Grau, U.M., Zuber, H., Frank, G., and Tratschin, J.D. (1979). Thermal stability and protein structure. UCLA Forum in Medical Sciences 159–69.

Baneyx, F. (1999). Recombinant protein expression in *Escherichia coli*. Current Opinion in Biotechnology *10*: 411–421.

Burnette, W.N.N. (1981). “Western blotting”: electrophoretic transfer of proteins from sodium dodecyl sulfate--polyacrylamide gels to unmodified nitrocellulose and radiographic detection with antibody and radioiodinated protein A. Analytical Biochemistry *112*: 195–203.

Chapman, A.P. (2002). PEGylated antibodies and antibody fragments for improved therapy: a review. Advanced Drug Delivery Reviews *54*: 531–545.

Digel, I., Maggakis-Kelemen, C., Zerlin, K.F., Linder, P., Kasischke, N., Kayser, P., Porst, D., Temiz Artmann, A., and Artmann, G.M. (2006). Body temperature-related structural transitions of monotremal and human hemoglobin. Biophysical Journal *91*: 3014–21.

Donovan, R.S., Robinson, C.W., and Glick, B.R. (1996). Review: optimizing inducer and culture conditions for expression of foreign proteins under the control of the lac promoter. Journal of Industrial Microbiology *16*: 145–54.

Fountoulakis, M., and Gasser, R. (2003). Proteomic analysis of the cell envelope fraction of *Escherichia coli*. Amino Acids *24*: 19–41.

Hoffmann, F., and Rinas, U. (2004). Stress induced by recombinant protein production in *Escherichia coli*. Advances in Biochemical Engineering/biotechnology *89*: 73–92.

Hu, X., O’Hara, L., White, S., Magner, E., Kane, M., and Wall, J.G. (2007). Optimisation of production of a domoic acid-binding scFv antibody fragment in *Escherichia coli* using molecular chaperones and functional immobilisation on a mesoporous silicate support. Protein Expression and Purification *52*: 194–201.

Humphreys, D.P. (2007). Periplasmic Expression of Antibody Fragments. In The Periplasm, (American Society for Microbiology), pp 361–388.

Humphreys, D.P., Carrington, B., Bowering, L.C., Ganesh, R., Sehdev, M., Smith, B.J., King, L.M., Reeks, D.G., Lawson, A., and Popplewell, A.G. (2002). A plasmid system for optimization of Fab’ production in *Escherichia coli*: importance of balance of heavy chain and light chain synthesis. Protein Expression and Purification *26*: 309–20.

Humphreys, D.P., Chapman, a P., Reeks, D.G., Lang, V., and Stephens, P.E. (1997). Formation of dimeric Fabs in *Escherichia coli*: effect of hinge size and isotype, presence of interchain disulphide bond, Fab' expression levels, tail piece sequences and growth conditions. Journal of Immunological Methods *209*: 193–202.

Humphreys, D.P., Weir, N., Lawson, a, Mountain, a, and Lund, P. a (1996). Co-expression of human protein disulphide isomerase (PDI) can increase the yield of an antibody Fab' fragment expressed in *Escherichia coli*. FEBS Letters *380*: 194–7.

Jamshad, M., Lin, Y.-P., Knowles, T.J., Parslow, R. a, Harris, C., Wheatley, M., Poyner, D.R., Bill, R.M., Thomas, O.R.T., Overduin, M., and Dafforn, T.R. (2011). Surfactant-free purification of membrane proteins with intact native membrane environment. Biochemical Society Transactions *39*: 813–8.

Kilikian, B.V., Suárez, I.D., Liria, C.W., and Gombert, A.K. (2000). Process strategies to improve heterologous protein production in *Escherichia coli* under lactose or IPTG induction. Process Biochemistry *35*: 1019–1025.

Knowles, T.J., Finka, R., Smith, C., Lin, Y.-P., Dafforn, T., and Overduin, M. (2009). Membrane proteins solubilized intact in lipid containing nanoparticles bounded by styrene maleic acid copolymer. Journal of the American Chemical Society *131*: 7484–5.

Kosinski, M., Rinas, U., and Bailey, J. (1992). Isopropyl-β-d-thiogalactopyranoside influences the metabolism of *Escherichia coli*. Applied Microbiology and Biotechnology *36*:

Lee, S.W., and Edlin, G. (1985). Expression of tetracycline resistance in pBR322 derivatives reduces the reproductive fitness of plasmid-containing *Escherichia coli*. Gene *39*: 173–80.

Maeda, H., Bharate, G.Y., and Daruwalla, J. (2009). Polymeric drugs for efficient tumor-targeted drug delivery based on EPR-effect. European Journal of Pharmaceutics and Biopharmaceutics : Official Journal of Arbeitsgemeinschaft Für Pharmazeutische Verfahrenstechnik e.V *71*: 409–19.

Marco, A. de (2009). Strategies for successful recombinant expression of disulfide bond-dependent proteins in *Escherichia coli*. Microbial Cell Factories *8*: 26.

Miao, F., and Kompala, D.S. (1992). Overexpression of cloned genes using recombinant *Escherichia coli* regulated by a T7 promoter: I. Batch cultures and kinetic modeling. Biotechnology and Bioengineering *40*: 787–96.

Mücke, M., Ostendorp, R., and Leonhartsberger, S. (2009). E. coli Secretion Technologies Enable Production of High Yields of Active Human Antibody Fragments. BioProcess Technical.

Novagen (1999). pET System Manual.

Pinsach, J., Mas, C. de, López-Santín, J., Striedner, G., and Bayer, K. (2008). Influence of process temperature on recombinant enzyme activity in *Escherichia coli* fed-batch cultures. Enzyme and Microbial Technology *43*: 507–512.

Ramírez, D.M., and Bentley, W.E. (1995). Fed-batch feeding and induction policies that improve foreign protein synthesis and stability by avoiding stress responses. Biotechnology and Bioengineering *47*: 596–608.

Ratledge, C., and Kristiansen, B. (2006). Basic Biotechnology (Cambridge University Press).

Sevastsyanovich, Y., Alfasi, S., Overton, T., Hall, R., Jones, J., Hewitt, C., and Cole, J. (2009). Exploitation of GFP fusion proteins and stress avoidance as a generic strategy for the production of high-quality recombinant proteins. FEMS Microbiology Letters *299*: 86–94.

Simmons, L.C., Reilly, D., Klimowski, L., Raju, T.S., Meng, G., Sims, P., Hong, K., Shields, R.L., Damico, L.A., Rancatore, P., Yansura, D.G., and Shantha Raju, T. (2002). Expression of full-length immunoglobulins in *Escherichia coli*: rapid and efficient production of aglycosylated antibodies. Journal of Immunological Methods *263*: 133–147.

Sockolosky, J.T., and Szoka, F.C. (2012). Periplasmic production via the pET expression system of soluble, bioactive human growth hormone. Protein Expression and Purification *87*: 129–135.

Venturi, M., Seifert, C., and Hunte, C. (2002). High level production of functional antibody Fab fragments in an oxidizing bacterial cytoplasm. Journal of Molecular Biology *315*: 1–8.

Vera, A. (2007). The conformational quality of insoluble recombinant proteins is enhanced at low growth temperatures. Biotechnology And *96*: 1101–1106.

Weickert, M.J., Doherty, D.H., Best, E.A., and Olins, P.O. (1996). Optimization of heterologous protein production in *Escherichia coli*. Current Opinion in Biotechnology *7*: 494–499.

Weir, A.N.C.A., and Bailey, N.A.N. (1995). Process for obtaining antibodies utilizing heat treatment (US).

5. Continuous protein purification using functionalised magnetic nanoparticles in aqueous micellar two-phase systems

5.1. Abstract

A novel technique for technical-scale continuous purification of proteins is presented. It is based on the combined use of functionalised magnetic nano-particles and an Aqueous Micellar Two-Phase System featuring the non-ionic surfactant, Eumulgin ES, which undergoes temperature induced phase separation at ~25°C. In the first step, conducted below the transition temperature (i.e. 15°C), the magnetic sorbent particles are added into the single dispersed phase and bind the protein of interest. Next, on raising the temperature to 30°C the protein-laden magnetic particles partition strongly into the micelle-rich top phase of the micellar two-phase system that's formed. The magnetically susceptible top phase is then continuously separated from the micelle-poor phase in a flowthrough tailor-made magnetic extractor featuring a permanent magnet providing an upwardly acting magnetic force. This separation device was shown to be effective for continuous separation of a wide range of differently sized magnetic particle sorbents (i.e. from 2 μm diameter to as small as 25 nm) from a 10% (w/w) Eumulgin ES system; high separation efficiencies were recorded for the phase-forming surfactant (87 to >98%), and all magnetic sorbent particles tested (95 – 99.9%). Finally, protein purification by continuous magnetic extraction was demonstrated at 15 L scale for the recovery of an antibody fragment, A33 Fab´, from a crude extract of *E. coli* periplasm. Nearly 70% of the A33 Fab´ initially present in the extract at 15.6% of the total protein content was recovered in a 2 – fold concentrated and highly purified (>98%) state. Further, the amounts of

magnetic sorbent and phase-forming surfactant lost in the process were very small; thus recycling of both components into subsequent rounds of continuous magnetic extraction is highly feasible.

5.2. **Introduction**

Preparative chromatography, a core technology within the biopharmaceutical sector for several decades, plays critical roles in the downstream processing of modern biopharmaceuticals. However, against increasing pressures (rocketing product titers, increasing size and complexity of emerging bio-products to name but a few), it is increasingly being viewed as a serious bottleneck in manufacturing (Low *et al.*, 2007; Leonardo *et al.*, 2008). Against this backdrop, the modification/improvement of existing traditional fixed column chromatography systems (Müller *et al.*, 2013), or their replacement with integrated and/or continuous separation processes represent increasingly important challenges to solve. Aqueous two-phase systems (ATPS) have long been regarded as possible alternatives ever since Albertsson (1956) classical demonstration of selective partitioning of (bio)molecules between two aqueous phases of a mixture of polymers and/or salts. Aqueous Micellar Two-Phase Systems (AMTPS) introduced by Bordier (1981) some 25 years later differ considerably from classical ATPS. AMTPS feature non-ionic surfactants which undergo temperature-induced phase separation resulting in two phases, i.e. one 'micelle-rich' (or 'coacervate-rich') and the other 'micelle-poor' (Tani *et al.*, 1998). Numerous applications and combinations of phase-forming polymers have been proposed since the early 1980s for the selective enrichment of a protein in one of the aqueous phases (also described as aqueous two-phase extraction, ATPE, or cloud point extraction, CPE) (Tani *et al.*, 1998; Hatti-Kaul, 2001). A striking advantage of ATPE is the ease with which its operation can be up-scaled and made continuous, and as consequence several process schemes demonstrating the feasibility of continuous bioprocessing exploiting ATPS (Sarubbo *et al.*, 2003; Vázquez-Villegas *et al.*, 2011; Rosa *et al.*, 2012) and AMTPS (Trakultamupatam *et al.*, 2004; Ingram *et al.*,

2012) have been published within the last decade. The high cost and loss of phase-forming components in the target protein-depleted phase represent a significant economic hurdle to overcome, but the main reasons for ATPE's perceived lack of viability are that the physical principles underlying the partitioning behavior of a given target protein between the phases remain unclear; and that very considerable experimental effort is required to identify an economically attractive system (Oelmeier *et al.*, 2011). Affinity-enhanced ATPS were introduced (Kopperschläger and Birkenmeier, 1990) in order to circumvent the above issues. In affinity ATPS the phase-forming polymer is either chemically modified, or alternatively ligands are 'introduced', by one of a variety of ways, into the two-phase system to enhance the partitioning of a molecule of interest into one of the two phases (Azevedo *et al.*, 2009). The introduction of ligands into ATPS by adding functionalised magnetic particles constitutes a particularly attractive class of affinity-enhanced ATPS (Suzuki *et al.*, 1995; Franzreb *et al.*, 2006; Gai *et al.*, 2011). The combination of ATPS with magnetic particles can dramatically enhance the rate of phase separation following application of an external magnetic field *cf.* traditional affinity ATPS, provided that the particles partition strongly into the dispersed phase (Wikstrom *et al.*, 1987; Flygare *et al.*, 1990; Larsson, 1994).

Previously, in our laboratories we introduced the new concept of 'Magnetic Extraction Phases (MEPs)' (Becker *et al.*, 2009), illustrated by the successful combination of magnetic cation exchange micro-sorbents with a Triton X-114 based AMTPS, to separate lysozyme from ovalbumin. Here, sorption of the target molecule, lysozyme, was performed at a temperature in the single-phase regime (T_S). Phase separation was subsequently induced by raising the temperature (T_T, denoting two-phase regime). The protein-loaded particles accumulated in the micelle-rich phase of the resulting AMTPS and the micelle-poor phase was removed. In the following step, an

AMTPS was set up using an appropriate elution buffer and the micelle-rich phase that was obtained post sorption. Previously bound protein species were desorbed from the particles and partitioned variously within the AMTPS according to their individual partition coefficients (K), whilst all of the magnetic sorbent particles moved into the micelle-rich phase. More recently, we extended the MEP concept to nano-scaled magnetic sorbents and an AMTPS based on the non-ionic surfactant, Eumulgin ES (Fischer and Franzreb, 2012). The 'Eumuglin ES AMTPS' represents a significant improvement over 'Triton X-114 AMTPS'. For instance, it simultaneously reduced surfactant costs, afforded the use of a moderate phase separation temperature, and importantly, yielded extreme differences in the partitioning coefficients of the target protein and the magnetic sorbent particles. As a direct consequence of extreme K-values, on elution the target protein partitioned exclusively to the micelle-poor phase, whereas the magnetic sorbents accumulated entirely in the micelle-rich phase. The MEP experiments described above using the new improved combination (Eumuglin ES AMTPS plus magnetic nano-particle sorbents) were performed at laboratory scale. In this study, we detail the systematic transfer of lab-scale manual MEP operation to a technical-scale 'Continuous Magnetic Extraction' (CME) process. We demonstrate continuous separation of cation exchange functionalised magnetic nano-particles from the micelle-poor phase at flow rates of several liters per hour; and subsequently apply CME for the continuous capture and purification of an antibody fragment from a crude *E. coli* cell extract.

5.3. **Materials and Methods**

5.3.1. Materials

Four different functionalised magnetic particles were employed in this study. 'Poly(NIPA-*co*-AAc)' particles (200 nm mean diameter by dynamic light scattering), received as a gift from Dr. Rodica Turcu (National Institute for Research and Development of Isotopic and Molecular Technologies, NIIMT, Cluj-Napoca, Romania), featured magnetite cores embedded in a matrix of poly(*N*-isopropylacrylamide-*co*-acrylic acid). 'MagPrep Silica 25' and 'MagPrep SO_3 100' particles were kindly donated by Dr. Johannes Bauer (Merck KGaA, Darmstadt, Germany). Both particles comprised magnetite crystals coated with a thin layer of silica, however, the surface of the latter was further functionalised with sulfonate (SO_3^-) moieties analogous to those commonly employed for strong cation exchange (CEX) chromatography media. Scanning electron microscopy revealed single particles of narrow size distribution, measuring 25 nm and 100 nm across for the base silica coated and sulfonate derivatised particles respectively. Chemagen M-PVA-DEAP particles were supplied by PerkinElmer chemagen Technologie GmbH (Baesweiler, Germany). This material is a spherical beaded 'polyvinyl alcohol (PVA) – magnetite' composite of *ca.* 2 μm, functionalised with diethylaminopropyl (DEAP) groups. The strong CEX beaded chromatography medium, Fractogel® EMD SO_3 (M) was a further donation from Dr. Johannes Bauer (Merck KGaA, Darmstadt, Germany), and the HiTrap rProtein G column was from GE Healthcare (Uppsala, Sweden). *E. coli* strain W3110 expressing the A33 Fab´ (Humphreys *et al.*, 1996) and protocols for its cultivation were acquired from UCB Celltech (Slough, UK) under a Material Transfer Agreement. The non-ionic surfactant, Eumulgin ES (PPG-5-Laureth-5, CAS-No.: 68439-51-0), was purchased

from Cognis (Düsseldorf, Germany). The chemicals, sodium tetraphenylborate (ACS reagent, ≥99.5%), barium chloride (99.9% trace metal basis), Tris(hydroxymethyl)aminomethane (ACS reagent, ≥99.8%), bicene (BioXtra, ≥99% by titration), glycine (for electrophoresis, ≥99%), acetone (≥99.8%), methanol (≥99.9%), glacial acetic acid (ACS reagent, ≥99.7%), were all obtained from Sigma-Aldrich (St. Louis, MO, USA). Phosphate buffered saline (Dulbecco 'A' tablets) was purchased from Oxoid Limited (Basingstoke, UK), disodium hydrogen phosphate and sodium chloride were supplied by Carl Roth (Karlsruhe, Germany) or Sigma-Aldrich, and citric acid monohydrate and Coomassie Brilliant Blue R250 (C.I. 42660) were from Merck Millipore (Darmstadt, Germany). Pre-cast 15% mini-PROTEAN® TGX™ gels, Precision Plus Protein™ All Blue Standards and Laemmli sample buffer were supplied by Bio-Rad Laboratories Inc. (Hercules, CA, USA). UltraPure Protogel was from National Diagnostics (Hessle, Yorks, UK) and See® Blue Plus 2 Prestained Standard, Simply Blue™ SafeStain and Quant-iT™ PicoGreen® dsDNA kit were all acquired from Invitrogen Life Technologies (Carlsbad, CA, USA). The bicinchoninic acid (BCA) protein assay kit and bovine serum albumin (BSA; fraction V powder, ≥96% pure by electrophoresis) were both obtained from Sigma-Aldrich. All other chemicals not stated above were from Sigma-Aldrich or Merck Millipore. The water used in all experiments was deionised and purified using a Millipore Milli-Q Ultrapure system.

5.3.2. Determination of AMTPS phase diagrams

The location of the curve defining the two-phase and single-phase regimes within a T-x diagram (where x is the mass fraction of the surfactant in the mixture) was determined as follows. Different fractions of surfactant and the corresponding buffers

were weighed into 15 mL centrifuge tubes. The centrifuge tubes were tempered in a temperature-controlled water bath (Model RC 20 S, Lauda Brinkmann, Deran, NJ, USA), and incubated for a minimum of 12 h until complete phase separation had been achieved. After this period the top and bottom phases of the resulting two-phase system were quickly separated and retained for subsequent analysis of the surfactant concentrations in each phase (see 5.3.9 Analysis).

5.3.3. Magnetic extractor for CME

The tailor-made magnetic extractor constructed for the CME studies described in this work (Fig 5.1a) features a separation chamber, housed within a permanent magnet yoke (627 mm length × 235 mm width × 306 mm height) fabricated by Steinert Elektromagnetbau GmbH (Cologne, Germany). The specially designed magnet and pole shoe arrangement results in a vertical magnetic field component, which steadily increases towards the upper side of the separator chamber (Fig 5.1b). The above components are themselves accommodated in an isolated, temperature regulated polystyrene case. The inner dimensions of the separation chamber are 500 mm (length) × 120 mm (width) × 50 mm (height), and a 38 mm high fixed weir is installed within it to give a total liquid volume within the separator chamber of 2.28 L (500 mm × 120 mm × 38 mm).

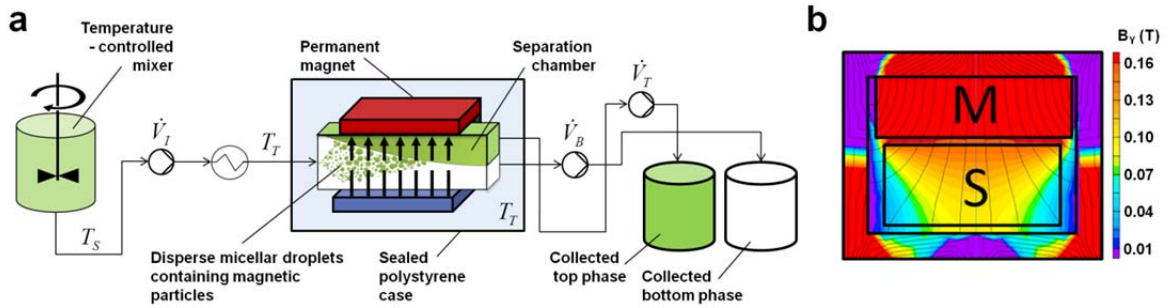

Fig. 5.1 Schematic illustrations of **(a)** the CME process and component parts (see text for details) and **(b)** Finite element simulation of the magnetic field generated by the CME system's permanent magnet. The magnet consists of the magnetic ferrite material (M) and a surrounding pole shoe. A settler can be installed in the space (S), where the vertical flux density, B_Y (T) steadily increases towards the upper side, thereby imposing a lifting force on any magnetic particles within 'S'.

5.3.4. Phase separation experiments

Phase separation velocities within the magnetic extractor were determined for operation with and without magnetic particles. For these studies, an AMTPS composed of 10% (w/w) Eumulgin ES and 90% (w/w) 50 mM sodium citrate, pH 3, poly(NIPA-*co*-AAc) particles and a temperature of T_T = 30°C were employed. The coacervate ratio, C_R, (defined in the following section, 2.5) was kept constant at 0.2, and the feed rate ($\dot{V}_I$) was varied from 0.5 to 25 L/h. The system was run at the corresponding flow rate until the volume in the separation chamber had been exchanged at least twice. Samples were taken from the top and bottom outlet of the magnetic separator and analysed for Eumulgin ES content (see 5.3.9 Analysis). All experiments were first performed in the absence of the magnetic particles, and thereafter with poly(NIPA-*co*-AAc) using the same set-up and a magnetic particle concentration of 2 g/L. Long-term continuous operation of the magnetic extractor was investigated in 'loop mode'. In this configuration, the exiting top and bottom phases are re-injected into the tempered stirred tank, and continuous operation of the magnetic extractor for several hours without using excessive amounts of material, is possible. The operational parameters employed for loop mode operation were as

follows: the initial magnetic particle concentration in the stirred tank was 2 g/L, the total volume of AMTPS was 9 L, the flow rate was 9 L/h, and T_S and C_R were set to 30°C and 0.33 respectively. Samples of the initial feed, and the top and bottom phases withdrawn at various times during operation, were analysed for magnetic particle and surfactant contents (see 5.3.9 Analysis).

5.3.5. Equations describing CME performance

The phase separation curve for the above AMTPS was obtained by plotting the temperature against the surfactant concentrations determined in the phases after complete phase separation.

The volume fractions of the top (V_T) and bottom (V_B) phases can be calculated from the surfactant concentrations according to Equation 5.1 the 'lever rule' (McCabe et al., 2005; Kamei et al., 2002):

$$\frac{V_T}{V_B} = \frac{w_{S,0} - w_{S,B}}{w_{S,T} - w_{S,0}} = R$$

Equation 5.1

Here, $w_{S,0}$, $w_{S,B}$ and $w_{S,T}$ are the surfactant mass fractions of the phases before and after phase separation, and R is denoted the 'phase-volume ratio'. During continuous operation of the magnetic extractor, the phase-volume ratio between the withdrawn top and bottom phases can be expressed as the pump ratio, P, according to Equation 5.2:

$$P = \frac{\dot{V}_T}{\dot{V}_B}$$

Equation 5.2

As shown in Eqn 5.2, *P* is controlled by the feeding rate, $\dot{V}_I$, and the discharge rate of the bottom phase, $\dot{V}_B$. The amount of liquid removed by the top effluent is determined by the difference in flow rates between the inlet and the bottom effluent, and the ratio of the flow rate leaving the top effluent and the inlet flow rate therefore is defined as coacervate ratio, C_R, (Eqn 5.3) with $\dot{V}_T$ being the flow rate of the top phase discharge:

$$C_R = \frac{\dot{V}_T}{\dot{V}_I} = \frac{\dot{V}_I - \dot{V}_B}{\dot{V}_I} = \frac{P}{P+1}$$

Equation 5.3

Theoretically, the ideal operation point of the magnetic extractor should occur when *P* = *R*. However, in order to prevent the loss of target component, particles, and surfactant, the CME was operated in a manner that emphasised complete removal of the top phase rather than preventing contamination of the top phase with traces of bottom phase. The theoretical minimum C_R required ($C_{R,min}$) to achieve complete removal of the top phase during CME operation was calculated according to Equation 5.4:

$$C_{R,\min} \geq \frac{R}{R+1}$$

Equation 5.4

The C_R value employed experimentally was derived from the theoretical minimum value obtained, but was adjusted to include a safety factor of 5 – 10%.

The rates of removal of magnetic particles and surfactant from the initial feed during CME are defined in terms of individual separation efficiencies for the magnetic

particles (S_P) and phase-forming surfactant (S_S) according to Equation 5.5 and 5.6; where the particle and surfactant concentrations are respectively: $c_{P,I}$ and $c_{S,I}$ in the initial streams; and $c_{P,B}$ and $c_{S,B}$ in the discharged bottom phases.

$$S_P = (1 - \frac{\dot{V}_B \cdot c_{P,B}}{\dot{V}_I \cdot c_{P,I}}) \cdot 100$$

Equation 5.5

$$S_S = (1 - \frac{\dot{V}_B \cdot c_{S,B}}{\dot{V}_I \cdot c_{S,I}}) \cdot 100$$

Equation 5.6

5.3.6. Preparation of crude E. coli extract

Pilot-scale demonstration of CME's utility for recovery of a model bioproduct from a realistic biological feedstock (section 5.3.7) and parallel lab-scale chromatographic purification experiments (section 5.3.8) were conducted using extracts prepared from fed batch fermented *E. coli* W3110 cells expressing a recombinant antibody fragment, A33 Fab´ (Humphreys *et al.*, 1996) targeted to the periplasm. Fed batch fermentative production of A33 Fab´ containing cells was performed in an Electrolab FerMac 300 series reactor (initial volume = 2 L; final volume = 2.28 L) using proprietary methods originating from UCB Celltech (Slough, UK) and modified in house.

At the end of cultivation ($OD_{600\ nm}$ = 188) the cells (378 g wet weight) were harvested by centrifugation (11,000 g_{av}, 0.5 h, 4°C) in the JA-10 rotor of Beckman Model J2-21 centrifuge (Beckman Coulter, Inc., Brea, CA, USA), before resuspending with 2.28 L of 0.1 M Tris-HCl buffer, pH 7.4, supplemented with 10 mM EDTA and incubating at 60°C in a water bath. After 16 h the heat permeabilised cells were removed by low speed centrifugation (3,255 g_{av}, 0.5 h, 4°C) in a Jouan C422 bench top centrifuge (SelectScience Ltd., Bath, UK), to yield a crude extract containing periplasmic

species (Katsui *et al.*, 1982; Weir and Bailey, 1995). For CME experiments (section 5.3.7) the resulting crude periplasmic extract (conductivity = 21 mS/cm) was simply diluted 10 fold with 20 mM sodium phosphate buffer, pH 5.6 (yielding a feed with conductivity of ~4.3 mS/cm). For chromatographic experiments (section 5.3.8) the crude periplasmic extract was not diluted, but instead received extensive conditioning to remove troublesome insoluble and fouling materials (i.e. outer membrane fragments, lipopolysaccharide and nucleic acids) issued into the extract from the thermally-treated cells, and adjust the pH and/or conductivity for binding.

5.3.7. Continuous magnetic extraction of A33 Fab´ from E. coli extract

An AMPTS consisting of 10 – fold diluted crude E. coli periplasmic extract, 10% (w/w) Emulugin ES, 20 mM sodium phosphate buffer, pH 5.6, and 1.38 g/L MagPrep SO_3 particles was set up in the following way. Emulugin ES (1.47 kg) was first mixed with 11.46 L of 25 mM sodium phosphate buffer in a 50 L double-walled (jacketed) glass stirred tank reactor (STR). Three hundred milliliter of a 68 g/L suspension of MagPrep SO_3 particles previously equilibrated in 22 mM sodium phosphate buffer, pH 5.6, was then added to the vessel. Finally, after 600 s of mixing, the binding step was initiated by pouring a 1.47 L portion of crude periplasmic extract into the STR. In all STR operations the temperature was maintained at T_S = 15°C, and constant stirring at 140 rpm was provided by a PTFE coated 3-blade impeller (60 mm width × 25 mm height; = 45°) driven by an overhead mixer (IKA Eurostar digital, IKA-Werke GmbH, Staufen, Germany) After 900 s of binding in the STR, the resulting magnetic particle doped two-phase system was separated by magnetic extraction (T_T = 30°C, C_R = 0.2, $\dot{V}_I$ = 5 L/h), and the exiting top and bottom phase streams were collected separately. For

the washing phase, the collected top phase was transferred back into the STR vessel, were it was mixed with 2 volumes of wash buffer (20 mM sodium phosphate, pH 5.6) for 900 s, before re-processing through the magnetic extractor and collecting the separately discharged top and bottom phase streams. Finally, in the elution step the top phase leaving the magnetic extractor unit was again transferred into the stirred tank, and this time mixed with 2 volumes of wash buffer supplemented with 0.75 M NaCl (so that the final NaCl concentration during elution was 0.5 M). After 900 s of mixing at 15°C, the STR contents were subjected to a last round of CME at 30°C, and the two discharged phases were collected.

During and after each step in the CME process, the top and bottom phases were sampled and these were analysed for magnetic particle, Eumulgin ES, DNA, total protein and A33 Fab´ contents (section 5.3.9). At the end of each separation when the top phase discharge ran dry the bottom phase was removed until it started to cloud, at which point the bottom valve was closed and the remaining liquor was added into the top phase collection tank. Prior to conducting the next CME step, the separation chamber was flushed with the sodium phosphate buffer solution to displace any residual particles from the unit back into the STR vessel.

5.3.8. Chromatography

All chromatography was done at room temperature using conditioned heat-treated *E. coli* derived liquors (section 5.3.6) and 1 mL packed beds (diameter ~7 mm, bed height ~25 mm) in plastic columns connected to an Äkta Explorer 100 Air chromatography workstation (GE Healthcare, Uppsala, Sweden). The mobile phase compositions recommended by Humphreys *et al.* (2002) and Pabst *et al.* (2009) were employed for Protein G affinity and CEX chromatography respectively, and for all

chromatographic stages the mobile phase velocity was 60 mL/h (~155 cm/h). Prior to application on a HiTrap rProtein G chromatography column pre-equilibrated with phosphate buffered saline (PBS), the extract was adjusted to pH 6.6 with 1 M acetic acid, and then clarified by centrifugation at 9,391 g_{max} and 4°C for 0.75 h in Sigma 3K30 centrifuge (SciQuip Ltd, Merrington, UK) fitted with type 12150 rotor, followed by filtration through a 0.22 μm Millex® GP filter unit (Merck Millipore, Nottingham, UK). After loading 30 mL of extract the column was sequentially washed with 5 column volumes (CVs) of PBS and then eluted using 10 CVs of 0.1 M glycine-HCl buffer, pH 2.7. The pH of eluate fractions was immediately adjusted to neutrality by addition of 2.5 M Tris base, before storing at 4°C for subsequent analysis by SDS-PAGE and BCA assay (5.3.9 Analysis).

The *E. coli* extract feedstock employed for CEX chromatography was prepared by clarification (9,391 g_{max}, 0.75 h, 4°C; 0.22 μm filtered) followed by buffer exchange into 20 mM sodium acetate, pH 5.6. A commercial centrifugal filter system (Amicon Ultra 15 - NMWT 10 kDa, Merck Millipore, Nottingham, UK) in a Jouan C422 bench top centrifuge (3,255 g_{av}, 0.5 h, 4°C) was employed for the buffer exchange step as per the manufacturer's instructions. Thirty milliliters of the resulting extract (~3 mS/cm) was loaded onto a packed bed of the Fractogel® EMD SO_3 (M) matrix previously equilibrated with 20 mM sodium acetate, pH 5.6. After washing with 5 CVs of the same buffer, the column was developed with linear gradient of increasing salt (0 to 1 M NaCl) over 15 CVs. Fractions collected during chromatography were retained for analysis of protein composition, A33 Fab´ and protein contents (see 5.2.9 Analysis).

5.3.9. Analysis

Magnetic field simulations were performed using QuickField 5.7 finite element simulation software (Tera Analysis, Svendborg, Denmark). The magnetic characteristics of the ferrite material were supplied by the manufacturer of the magnet (Steinert Elektomagnetbau GmbH, Cologne, Germany).

Eumulgin ES concentrations were determined using a potentiometric end-point method developed for assay of polyoxyethylated non-ionic surfactants (Fischer and Franzreb, 2011), relying on the formation of a pseudo cationic complex of the polyoxyether moiety with barium ions followed by precipitation in the presence of tetraphenyl boronate. Surfactant concentrations were obtained by comparing recorded end-point volumes with those obtained from a standard calibration curve prepared using solutions of known Eumulgin ES concentration.

The magnetic particle content in samples was determined gravimetrically as follows. Magnetic particles in samples were retrieved from solution with the aid of a powerful permanent bar magnet. The supernatants were carefully removed and the particles were washed sequentially once with 15 mL of methanol and twice with 15 mL of water. In between each wash, the ‘particle/solution’ mixtures were subjected to magnetic separation and the supernatants were carefully discarded. The magnetic particles were then resuspended with 1 mL of water, transferred to pre-weighed glass HPLC vials and dried in an oven at 60°C for at least 16 h. After cooling to room temperature in a dessicator jar, the vials were re-weighed and the amount of support particles in each sample was calculated from the change in weight of the vial.

Protein content in samples was determined using a micro BCA assay kit (Pierce, Rockford, IL, US) adapted for use with a Cobas Mira Plus automatic robotic station

(Roche Diagnostics, Switzerland). To eliminate the influence of Eumulgin ES on the BCA assay and SDS-PAGE, it was removed from samples in a prior protein precipitation step. Ice cold 100% (w/v) trichloroacetic acid was added to samples (and BSA protein standards) to a final concentration of 15% (w/v), and mixed on a vortex mixer before incubating on ice for 0.5 h. The resulting protein precipitates were recovered by centrifuging in a microfuge, and then decanting the supernatants, washing the pellets twice with ice cold acetone and finally drying in a centrifugal vacuum concentrator (5301 Vacufuge, Eppendorf, Hamburg, Germany).

The protein compositions of fractions were analysed by reducing SDS-PAGE (Laemmli, 1970) in either 14% (w/v) polyacrylamide slab gels cast in house[3] or 15 (w/v) pre-cast polyacrylamide gels in a Mini-Protean® Tetracell electrophoresis system (Bio-Rad Laboratories, Hercules, CA, USA). After electrophoresis, 15% (w/v) polyacrylamide gels were stained with 0.1% (w/v) Coomassie Brilliant Blue R250, dissolved in 40% (v/v) ethanol and 10% (v/v) acetic acid) for 1 h at room temperature, and were subsequently destained at the same temperature in a solution composed of 7.5% (v/v) acetic acid and 10% (v/v) ethanol.

The method of casting and running 14% (w/v) SDS-PAGE was the same as described in the Chapter 4 section 4.3.7.2.

The A33 Fab´ content was determined by densitometric analysis of scanned TIFF images of appropriately loaded Coomassie Blue stained gels following electrophoresis. The images were captured with an HP ScanJet C7716A flat bed scanner (Hewlett-Packard Company, Palo Alto, CA, USA) at a resolution of 2400 dpi, and analysed using ImageJ software (Schneider *et al.*, 2012). Samples and

[3] For a detailed description of the methods employed for preparation, electrophoresis, and staining the reader is referred to Chapter 4 (section 4.3.7.2.).

rProteinG affinity chromatography purified A33 Fab´ standards were loaded on the same gels. A linear correlation between A33 Fab´ applied and band intensity was found in the range 0.1 to 1 μg A33 Fab´; hence, the volumes of samples applied to gels for 'densitometry' were adjusted to fall within this range.

DNA contents were determined using a commercial fluorescence based assay (Quant-iT™ PicoGreen® dsDNA kit) in 96 – well plate format with an Ascent Fluoroskan Fluorometer (Thermo Labsystems, Waltham, MA, USA) employing excitation and emission wavelengths of 480 nm and 535 nm respectively.

5.4. **Results and discussion**

5.4.1. Apparatus for CME

CME employs a novel magnetic extractor set-up, the principle of which is illustrated in Fig 5.1a. At the set-up's core is a temperature-controlled magnetic field enhanced mixer-settler. In the mixer, sorption of the target molecule to the magnetic sorbent occurs at a temperature, T_S, at which the fluid forms a single phase. In the following continuous settler, the AMTPS is heated up to a temperature, T_T, at which point the fluid forms two phases. For phase separation, the fluid is pumped into a separation chamber surrounded by a specially designed permanent magnet (Fig 5.1a and 5.1b), which is itself located within the interior of a sealed polystyrene case containing a temperature-controlled heater that functions to maintain the temperature at T_T. Micellar droplets doped with magnetic nano- or micro-particles form as fluid passes through the reactor. The external magnetic field generated by the permanent magnet simultaneously enhances: (i) the migration velocity of these micellar droplets; (ii) initial droplet coalescence; and (iii) coalescence at the inter-phase of the two-phase

system. Finally, a particle-free micelle-depleted bottom phase is discharged from the lower effluent of the separation chamber, while a micelle and particle-enriched phase is withdrawn from the upper effluent.

5.4.2. Physico-chemical and hydrodynamic characterisation

Fig. 5.2 illustrates the phase diagram for 10% (w/w) Eumulgin ES-based AMTPS concocted with various solutions. The similarity of the plots is striking. The influence of pH (between 3 and 8.8) on Eumulgin ES AMTPS phase transition appears negligible over the studied range of temperature (25 – 40°C). Further, the impact of proteins and other suspended species within the extract on Eumulgin ES AMTPS phase transition also appears to be small. In view of the transition point from the single-phase to the two-phase regime of *ca.* 26°C the application of CME with the present Eumulgin ES based AMTPS for thermo-labile proteins may appear challenging. It should be noted however, that doping the AMPTPS with additional components (e.g. various salts) can drastically reduce the phase transition temperature (Tani *et al.*, 1998); thereby creating a much 'friendlier' environment for more temperature-sensitive proteins.

Important process parameters, R and $C_{R,min}$ can be derived from the phase diagrams (Fig 5.2) and Table 5.1 shows the calculated values for an 10% (w/w) Eumulgin ES based AMTPS in 50 mM sodium citrate buffer pH 3. For complete top phase removal at 30°C a minimum C_R of 0.19 is required.

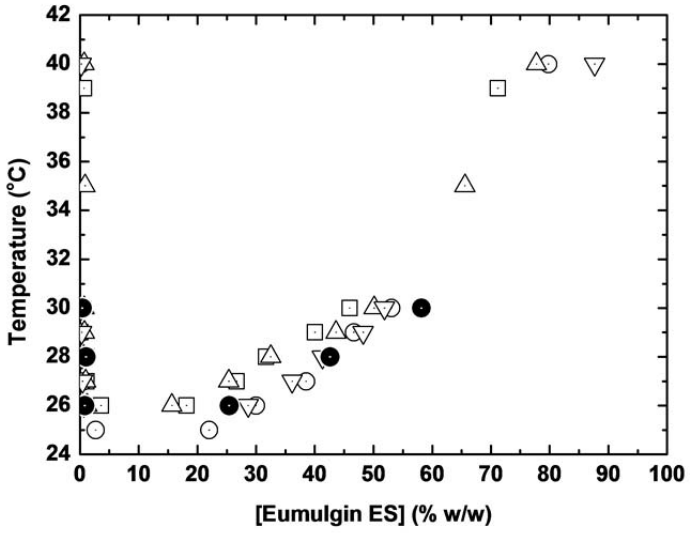

Fig. 5.2 Phase diagrams (co-existence curves) for 10% (w/w) Eumulgin ES-based AMTPS in water (□), 50 mM sodium phosphate buffer pH 7.0 (○), 50 mM sodium citrate buffer, pH 3 (△), 50 mM bicene buffer, pH 8.8 (▽), *E. coli* extract diluted with 20 mM sodium phosphate buffer pH 5.6 (●).

Table 5.1 Volume ratio (*R*) and minimum coacervate ratio ($C_{R,min}$) for a 10% (w/w) Eumulgin ES-based AMTPS in 50 mM sodium citrate buffer, pH 3. The values were calculated using Equations 5.1 and5.4.

Temperature (°C)	Volume ratio, *R* (-)	Minimum coacervate ratio, $C_{R,min}$
29	0.27	0.22
30	0.23	0.19
35	0.16	0.14
40	0.14	0.12

The phase separation efficiency of the Eumulgin ES-based AMTPS during operation of the CME process was initially monitored in the absence of magnetic particles, by analyzing the surfactant's distribution within the top and bottom-phase effluents as a function of feed flow rate. In these runs the Eumulgin ES concentration of the feed was 9.6% (w/w), and the phase separation temperature and C_R were set to 30°C and 0.2, respectively. Fig. 5.3 shows the results obtained. When operated flow rates exceeding 15 L/h no phase separation is observed; both streams exit the separator

with Eumulgin ES concentrations practically equal to that of the feed. But as the flow rate is reduced from 15 L/h, phase separation starts to occur. For example, an approximate halving in flow rate results in top and bottom phase concentrations of ~21% (w/w) and ~4% (w/w) respectively. At steady state the maximum top phase and minimum bottom surfactant concentrations achievable, of ~32% and ~0.7% respectively, are reached at flow rates of ≤ 2 L/h.

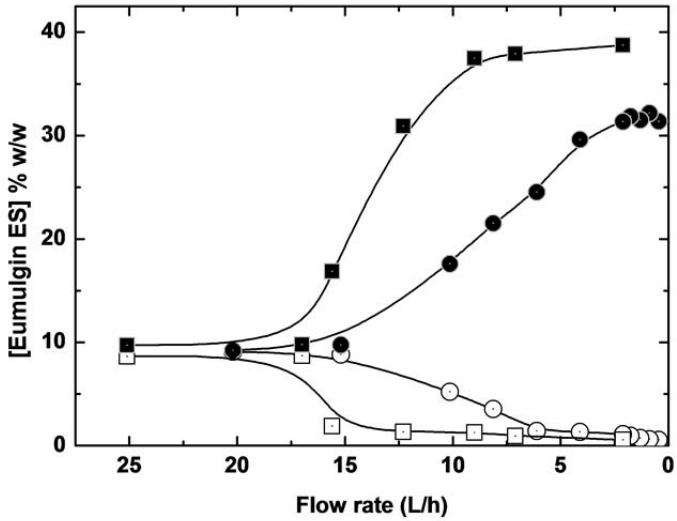

Fig. 5.3 Eumulgin ES phase separation in the magnetic extractor during continuous operation at different flow rates in the absence (○,●) and the presence (□,■) of 2 g/L poly(NIPA-*co*-AAc) magnetic particles. The bottom and top phase concentrations are indicated by open symbols and filled black symbols respectively.

The benefits of incorporating magnetic particles in the Eumulgin ES AMTPS are strikingly illustrated (Fig 5.3). In this case phase separation is evident even at a flow rate of 17 L/h, and maximum phase separation is attained at *ca.* 9 L/h (surfactant concentrations in the top and bottom phase of 38% and 0.7% respectively). The 'seeding' of magnetic particles partitioning exclusively to the dispersed micellar droplets of the nascent two-phase system makes the droplets strongly susceptible to manipulation from an externally applied magnetic field. In the present system the

magnetic force acts upwards to enhance the lift or flotation velocity of the 'magnetic droplets' (Fig 5.1b). A further gain from the inclusion of magnetic particles is the increased rate of droplet coalescence observed; a direct consequence of which is that the maximum surfactant concentration in the micelle-rich top phase rises from 32% to 38% (see Fig 5.3). However, in both continuous AMTPS extraction processes (i.e. traditional and magnetic particle doped), the maximum Eumulgin ES concentration in the top phase, at a phase separation temperature of 30°C, was much lower than that obtained from the phase diagram (i.e. ~50%; Fig 5.2). These differences for continuous extraction most likely reflect incomplete phase separation. In batch mode 'Eumulgin ES AMTPS' experiments, complete phase separation generally occurs within 16 – 20 h. In the magnetic extractor by contrast, the maximum residence times are just 55 minutes when operated with magnetic particles, and 5 h in their absence.

Complete closing of the mass balance for the surfactant exiting the extractor against that entering it was not possible, especially at low flow rates in the absence of magnetic particles where the lowest mass balance recorded was 67%. The most likely reason for this is that the micelle-rich top phase accumulates in the reactor in front of the weir. Much better closure of the surfactant mass balance was achieved when the magnetic particles are introduced into the AMTPS; presumably because the applied magnetic field helps to 'lift' the magnetic particle-doped surfactant-rich phase over the weir. Nevertheless, *ca.* 8% of the surfactant entering the CME remained unaccounted for. An investigation into the long-term stability of CME's phase separation performance over several hours (i.e. loop mode operation) was therefore performed, and the Eumulgin ES and the particle concentrations in the feed and exiting top and bottom phases were monitored throughout.

Fig. 5.4a shows how particle concentrations within the injected feed and the top and bottom phases vary during 2.7 h of continuous operation. The magnetic particles are continuously separated from the feed; the particles are concentrated *ca.* 3.5 fold (relative to the initial feed) to a value of ~7 g/L within the micelle-rich top phase of the system and the clarified bottom phase is discharged with a very low constant particle concentration of just 0.02 g/L (i.e. equivalent to 1% of the feed value). Also striking is that the injected particle concentration remained at the initial feed value of 2 g/L throughout operation.

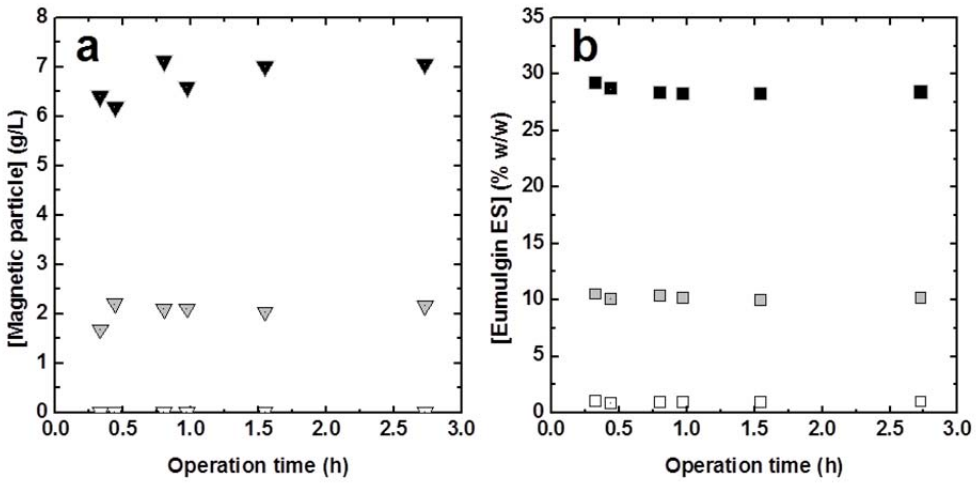

Fig. 5.4 Continuous separation of **(a)** magnetic particles and **(b)** phase-forming surfactant in the magnetic extractor at a flow rate of 9 L/h. The feed contained initial particle and surfactant concentrations of 2 g/L and 10% (w/w) respectively. Key: Initial feed (filled gray symbols), bottom phase (open symbols) and top phase (filled black symbols).

Given that the effluents leaving the magnetic extracted are recycled back into the stirred feed tank, during long-term experiments any tendency for particles to build up within the separation chamber would result in a reduced particle concentration in the effluent, and consequently therefore, dilution of the recycled feed. Clearly, particles are not held back and accumulated within the reactor, but are instead continuously discharged from it. Matching continuous operation data illustrating variance of the

phase-forming surfactant concentrations within the feed, top and bottom phases is presented in Fig. 5.4b. Here again, the Eumulgin ES concentrations of the initial feed and both exiting leaving streams remain constant over the whole 2.7 h of operation. The initial feed concentration of 10% (w/w) Eumulgin ES is steadily separated so that the concentrations of surfactant in the discharged bottom and top phases are respectively 0.9% and 29% (w/w). As the C_R value (Equ 5.3) employed in these long-term recycle studies was 0.33, the surfactant mass balance closed to practically 100%.

In addition to the 200 nm sized poly(NIPA-*co*-AAc) magnetic sorbent particles described thus far, we have tested various other magnetic particle materials in the CME set-up. An illustration of this is shown in Table 5.2 which presents the particle separation efficiencies obtained in experiments conducted with four different magnetic particles seeded into Eumulgin ES based AMTPS at a concentration of 2 g/L. Separation of the two largest functionalised magnetic particles, i.e. the 200 nm cation exchanger (poly(NIPA-*co*-AAc)) and 2 μm anion exchange sorbent (M-PVA-DEAP), was achieved at a flow rate of 9 L/h with >99% efficiencies. For the smaller 'MagPrep' materials (25 and 50 nm), maintenance of high particle separation efficiency (>95%) required reduction in the operating flow rate to 5 L/h. This aside, the data confirm CME as a versatile process being able to function with a wide range of different magnetic particle sizes (25 – 2000 nm) and surface chemistries.

5.4.3. Continuous magnetic extraction of an antibody fragment from an E. coli extract

To demonstrate 'proof-of-concept', i.e. the feasibility of continuous magnetic extraction of proteins at liter scale, the technique was applied for the recovery of an

industrially relevant antibody fragment (A33 Fab´) from a crude *E. coli* periplasmic extract. The extract was prepared by incubating freshly grown *E. coli* cells containing A33 Fab´ in a buffer held at 60°C for 16 h to release the periplasmic contents. The fundamental basis for this periplasmic release method was first reported >30 years ago by Katsui and co-workers (1982) who observed 'blebbing' and vesiculation of the outer membrane (exclusively), which increased the latter's permeability and led to selective release of periplasmic contents. While inappropriate for thermolabile products, extended thermally mediated release treatments appear well suited to antibody products, because removal of partially degraded and/or incorrectly folded antibodies from soluble correctly folded ones is facilitated (Weir and Bailey, 1995).

A 10% (w/w) Eumulgin ES AMPTS seeded with MagPrepSO_3 particles (1.4 g/L) was used and the feed flow rate was set to 5 L/h to guarantee complete particle separation (Table 5.2). Additional process parameters for CME were identified from a phase diagram constructed using 10% (w/w) Emulgin ES and the A33 Fab´ containing *E. coli* extract diluted 10 – fold with 20 mM sodium phosphate buffer, pH 5.6. As noted earlier (Fig 5.2) the similarity of the resulting diagram to those obtained in water and buffered systems confirmed that the impact of proteins and other suspended species within the extract on Eumulgin ES AMTPS phase transitions was negligible.

After 600 s of adsorption in the STR at T_S = 15°C the temperature of the feed was raised to 30°C (T_T) by means of a heat exchanger while being pumped into the separation chamber. At this temperature the single dispersed phase split into two constituent phases. Protein-laden magnetic CEX particles became enriched in the micelle-rich top phase leaving the separation chamber, while unbound host cell

proteins and other non-binding species present in the extract exited in the micelle-poor bottom phase. In the subsequent washing step, the micelle-rich top phase containing ‘protein-loaded’ magnetic particles was mixed with two volumes of 20 mM sodium phosphate buffer, pH 5.6, for 900 s and then separated again by magnetic extraction, to remove entrained *E. coli* derived contaminants carried over in the top phase from the initial adsorption step. Finally, recovery of A33 Fab´ from the $MagPrepSO_3$ rich top phase was achieved by mixing with two volumes of binding buffer supplemented with 0.75 M NaCl (bringing the NaCl concentration to 0.5 M), and once again subjecting to magnetic extraction. In this step, the micelle-poor bottom phase now contained the eluted target species, and the ‘eluted’ magnetic sorbent particles and the majority of the surfactant were discharged in the top phase.

Table 5.2 Magnetic particle tested in the CME set-up and achieved separation efficiencies

Magnetic support (Manufacturer)	Description of particle materials	Mean size (nm)	Flow rate (L/h)	Separation efficiency (%)
MagPrep Silica 25 (Merck KGaA)	Magnetite crystals coated with a thin layer of silica	25	5	>95
MagPrep SO_3^- 100 (Merck KGaA)	Magnetite crystals coated with a thin layer of silica and then functionalised with sulfonate moieties	100	5	>99
Poly(NIPA-co-AAc) (NIIMPT, Romania)	Magnetite embedded within a poly(*N*-isopropylacrylamide-*co*-acrylic acid) matrix	200	9	>99
M-PVA-DEAP (PerkinElmer chemagen Technologie GmbH)	Spherical beaded polyvinyl alcohol – magnetite composite particle functionalised with diethylaminopropyl groups	2000	9	>99

The compositions of the initial feed and the bottom discharged phases arising from each step in the CME purification process are presented in Table 5.3. During CME processing the total volumes issuing from the each consecutive step fell progressively from an initial 14.7 L to a final <5.1 L. The trace levels of magnetic particles in all exiting bottom phases (1 – 17 mg/L) provide striking evidence for virtually exclusive partitioning of magnetic particles into the top phase. The concentrations of Eumulgin ES, DNA, protein and Fab´ carried over into the final eluate were 0.34% (w/w), 0.34 mg/L, 147 μg/L and 145 μg/L respectively, representing mass recoveries in this fraction of just 1.1 and 1.2% for DNA and Emulgin ES, 10.6% for protein and 66.7% for the target species, A33 Fab´. Mass balances of all relevant species (A33 Fab´, total protein, DNA, particles, surfactant) were calculated by adding together the masses of each component in all exiting bottom phases and the discharged eluate top phase and comparing the summated values with the initial masses supplied in the feed (Table 5.3). The low mass balances observed for total protein and DNA likely stem, at least in part, from incomplete desorption of both biopolymer types from the magnetic carrier particles. Support for this contention comes from reducing SDS-PAGE analysis of supernatants obtained after boiling supports in sample buffer, which confirmed the presence of several characteristic *E. coli* outer membrane proteins (Schnaitman, 1974; Osborn and Wu, 1980; Schäfer *et al.*, 1999), but no A33 Fab´. By contrast, the total A33 Fab´ mass accounted for was significantly over-emphasised; most likely arising from exaggerated assay of the Fab´ contents of the bottom phase unbound and wash fractions and top phase elution fraction by scanning densitometry. The presence of residual Fab´ in the bottom phase post adsorption (Table 5.3) confirms that not all of the Fab´ had been removed from the extract. This loss in target yield is not due to magnetic extraction process *per se*, but instead to the use of insufficient quantities of

particles in the process. In addition to increasing the total magnetic sorbent particle concentration in the system, employing a higher capacity sorbent particle would guarantee improved binding performance. Visual evidence for the successful purification of A33 Fab´ by CME is provided in Fig 5.5. Potential improvements aside, comparison of lanes 2 (starting feed) and 4 (the final eluate) clearly demonstrates that, even in its unoptimised state, CME can deliver a high level of target purification.

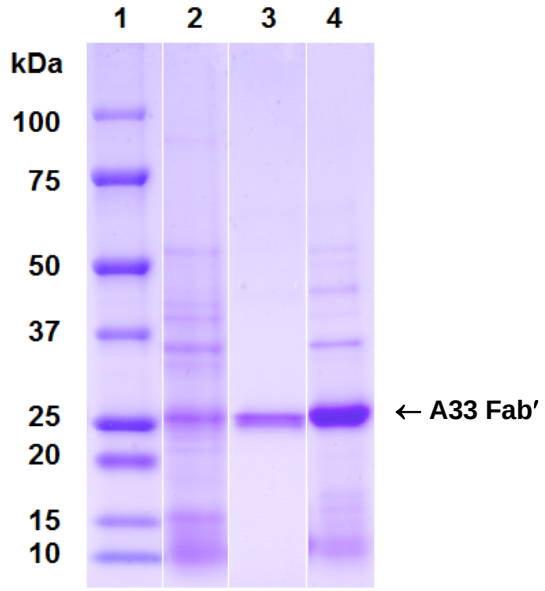

Fig. 5.5 Reducing SDS-PAGE analysis (15% polyacrylamide gel) of fractions from CME based purification of A33 Fab´ from a crude E. coli periplasmic extract. Key: lane 1 – Molecular weight markers; lane 2 –; crude periplasmic extract lane 3 –rProtein G purified A33 Fab´; lane 4 – bottom phase eluate.

In the present example, comparison of the compositions of the feed and exiting elution fraction shows magnetic particle and Eumulgin ES removals of >99.9% and >98% respectively, combined with depletion of >95% of the total host cell protein and >98% of DNA, leading to a final A33 Fab´ purity of >98% and yield of 67%. Further, the A33 Fab´ binding capacity of the MagPrep SO_3 sorbent in the process was >36 mg/g.

5.4.4. Benchmarking

The initial feedstocks for CME and chromatography received very different pretreatments. During preparation of the AMTPS for CME the heat treated *E. coli* extract was effectively diluted 10 fold with sodium phosphate buffer, pH 5.6, but received no further clarification (see sections 5.3.6 & 5.3.7). Thus, the feedstock though essentially cell free still contained fine suspended solids (especially fine cell envelope debris) and other troublesome species (e.g. nucleic acid polymers) that had issued from the cells during heat treatment. Extracts for rProtein G and CEX chromatography were not diluted, but instead received extensive pretreatment to remove potential column fouling materials, and adjust the pH and/or conductivity for binding (see 5.2.8).

Table 5.3 Summary of the volumes and concentrations of the bottom phases resulting from conducting the sorption, wash and elution steps in the CME.

Process step	Volume (L)	Magnetic support (g/L)	Eumulgin ES (% w/w)	DNA (mg/L)	Total protein (g/L)	A33 Fab´ (g/L)
Initial Solution	14.723	1.380	10.00	10.43	0.480	0.075
Post-sorption	11.39	0.006	2.83	7.08	0.178	0.029
Washing	7.773	0.017	1.67	3.82	0.072	0.021
Eluate	5.082	0.001	0.34	0.34	0.147	0.145
Mass balance(%)[a]	-	*115*	*67*	*74*	*52*	*140*

[a] The sum of the mass flow of all bottom phases and the eluate top phase was compared to the initial mass flow in the feed.

The initial A33 Fab´ purity increased from 15.6% to nearly 20% (Table 5.4, Fig 5.6) in the common high speed centrifugation step (~9,400 g_{max} for 0.75 h) as >20% of total protein was removed (specifically outer membrane species) without loss in Fab´, regardless of whether the extract had received prior pH adjustment (for Protein G affinity only). The subsequent 0.22 micron filtration step immediately prior to Protein G affinity chromatography saw small l losses in both total protein and Fab´, but the Fab´ purity (19.8%) was not impaired.

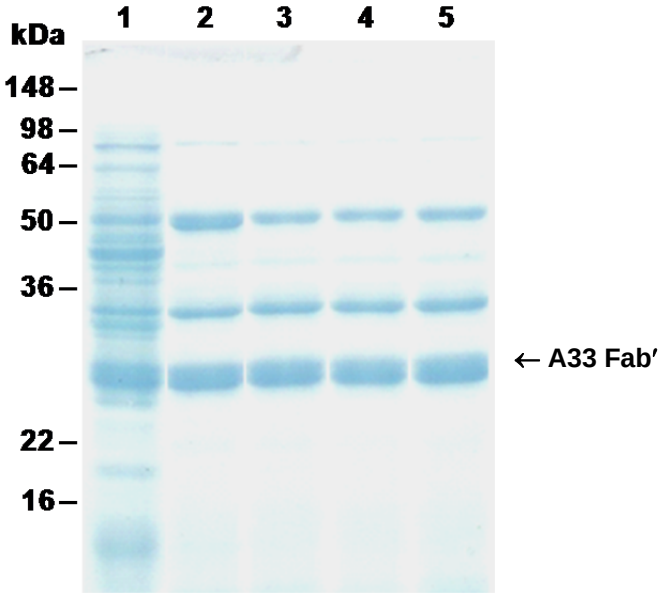

Fig. 5.6 Reducing SDS-PAGE analysis (14% polyacrylamide gel) of *E. coli* periplasmic extracts during conditioning steps prior to chromatography. Key: lane 1 – *E. coli* cells prior to heat treatment; lane 2 – crude periplasmic extract (supernatant recovered after heat treatment and low speed centrifugation – 3,255 g_{av}, 0.5 h, 4°C); lane 3 – periplasmic extract after high speed centrifugation (9,391 g_{max}, 0.75 h, 4°C); lane 4 – periplasmic extract after adjusting pH to 6.4 and high speed centrifugation (9,391 g_{max}, 0.75 h, 4°C); lane 5 – after 0.22 μm filtered pH adjusted and centrifuged periplasmic extract.

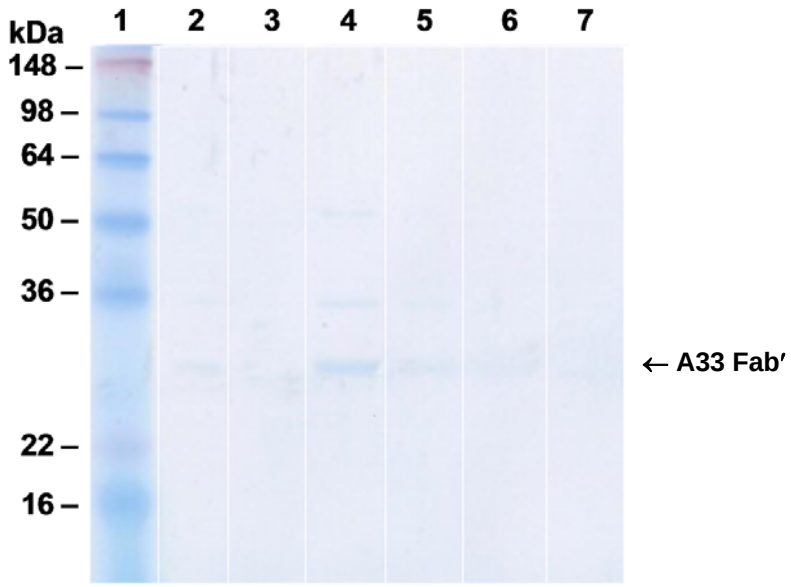

Fig. 5.7 Reducing SDS-PAGE analysis (14% polyacrylamide gel) of flowthrough fractions collected during the buffer exchange steps prior to cation exchange chromatography. Key: lane 1 – Molecular weight markers; lanes 2 – Flow through fraction of heat extraction sample; land 3 - 7. Flow through fraction of 5 sequential buffer exchange steps by adding 20 mL of 20 mM phosphate buffer at pH 7.

Because of the high ionic strength of the periplasmic extract, a diafiltration step was necessary prior to CEX chromatography on Fractogel EMD SO_3. A centrifugal buffer exchange step was employed for this, and substantial and indiscriminate step losses of ~45% of the total protein and A33 Fab´ were experienced (Table 5.4, Fig 5.7). Collectively, the numerous conditioning steps necessary to prepare the extracts for chromatography, while improving initial Fab´ purity (from 15.6 to 20%), resulted in overall losses of A33 Fab´ yield of ~10% prior to Protein G affinity and >50% before CEX chromatography (Table 5.4).

The benchmarking was done at much reduced scale *cf.* CME, using 30 mL volumes of conditioned extracts applied to 1 mL beds of rProtein G Sepharose HP and EMD Fractogel EMD SO_3 (Fig 5.8 & 5.9, Table 5.5 & 5.6).

The rProtein G Sepharose column was challenged with extract containing 103 mg of total protein, of which 20.4 mg was A33 Fab´. More than 80% of total protein and

>56% of the Fab´ applied passed through the column in the flowthrough fraction, and a further 15% of total protein and >23% of the Fab´ eluted during washing prior to elution (Fig 5.6 and Table 5.5). Bound A33 Fab´ was desorbed from the column using a pH step gradient (Fig 5.8a). Approximately 4 mg of the Fab´ was recovered in 3.3 CVs in a highly purified state, i.e. 100% by scanning densitometry (Fig 5.8b); corresponding to an overall target recovery of just 20% (Table 5.6), and binding capacity of 4.1 mg Fab´ per mL of sorbent. For CEX chromatography, owing to heavy losses incurred in preparing the extract for CEX (Table 5.4), the diafiltrated periplasmic extract (30 mL) loaded on to the column contained a reduced challenge of ~56 mg of total protein and 11.3 mg A33 Fab´ (Table 5.7, Fig 5.9). Seventy percent of the total protein was accounted for in the flow-through fraction, but only 2.3% of the Fab´ was lost. Evidently the capacity of the Fractogel EMD SO_3 matrix for A33 Fab´ from conditioned periplasmic extract under the binding conditions employed (pH 5.6, conductivity= 3 mS/cm) was not challenged in this study

Table 5.4 Impact of feedstock conditioning on extract composition and Fab´ yield prior to chromatography. See text for details.

Sequential conditioning step	Volume (L)	Fab´ (mg)	Protein (mg)	Fab´ purity (%)	Protein yield (%)	Fab´ yield (%)	PF[a]
None	0.2	150	960	15.6	100	100	1.0
pH adjustment (Protein G only)	0.2	-	-	-	-	-	-
Centrifugation (+/- prior pH adjustment)	0.2	150	761	19.7	79.3	100	1.26
0.22 μm filtration	0.2	136	686	19.8	71.5	90.7	1.27
Buffer exchange(CEX only)	0.2	74.5	371	20.1	38.6	49.7	1.29

[a]PF = purification factor

After washing, the column was developed with a linear salt gradient (Fig 5.9a). Ninety-seven percent (11.0 mg) of the Fab´ was detected in the elution peak (Fig. 5.9b), which was eluted in 5 CVs between 0.2 and 0.5 M added NaCl. The purity of the pooled peak (7 CVs) (all fractions containing Fab´, Fig. 5.9 a lane 9-15) was purity of 95.4% (Table 5.6).

The lack of need for expensive, extensive and 'yield compromising' feedstock conditioning steps prior to sorption represents a key advantage of direct capture techniques, such as CME. How CME based purification compares with Protein G affinity and CEX chromatography in packed bed columns is shown in Table 5.7. Though direct comparisons of CME with chromatography are made difficult by the different levels of feedstock conditioning received in each case, it is nevertheless clear that the CME process compares very favorably with Protein G affinity and CEX chromatography in terms of Fab´ purity and yield. Moreover, the advantages of CME over chromatography are further enhanced when the losses in Fab´ yield during extract conditioning (Table 5.4) are taken into account. The same sulfonate ligand was used for CEX chromatography and CME. It is interesting to note, therefore, that despite CME's lack of multiple stages, the technique delivered comparable or even higher purity (98% *cf.* 95.4%; Table 5.7). Possible differences in surface properties of the MagPrepSO_3 and Fractogel EMD SO_3 sorbents aside, a further potential explanation for the higher purity observed in the CME process is the virtually complete exclusion of freely dissolved proteins from the micelle-rich phase. The use of anionic sulfonate ligands in both processes dictates that measures to reduce the ionic strength of the periplasmic feedstock are mandatory. Here, for traditional fixed-bed CEX chromatography diafiltration, was employed (seriously impairing Fab´ yield; Table 5.4), but for the CME process this time-consuming step was rejected in favor of

simple dilution, given that the extraction set-up could easily handle large volumes of partially clarified feed.

Table 5.5 Purification table for the recovery of A33 Fab´ from a conditioned *E. coli* extract (see Table 5.5) by affinity chromatography on rProtein G Sepharose HP.

Step	Fab (mg)	Total protein (mg)	Fab yield (%)	Total protein yield (%)	Fab purity (%)	Purification factor
Load	20.4	102.9	100	100	19.8	1.0
FT	11.5	83.0	56.4	80.7	13.9	0.70
Wash	4.8	15.8	23.5	15.35	30.4	1.53
Elution	4.1	4.1	20.1	4.0	100	5.05

Table 5.6 Purification table for the recovery of A33 Fab´ from a conditioned periplasmic extract (see Table 5.6) by cation exchange chromatography on Fractogel EMD SO_3.

Step	Fab (mg)	Total protein (mg)	Fab yield (%)	Total protein yield (%)	Fab purity (%)	Purification factor
Load	11.3	55.7	100	100	20.1	1.0
FT	0.26	38.7	2.3	69.5	3.31	0.165
Wash	0.04	5.4	0.35	9.8	3.57	0.178
Elution	11.0	11.5	97	20.7	95.4	4.75

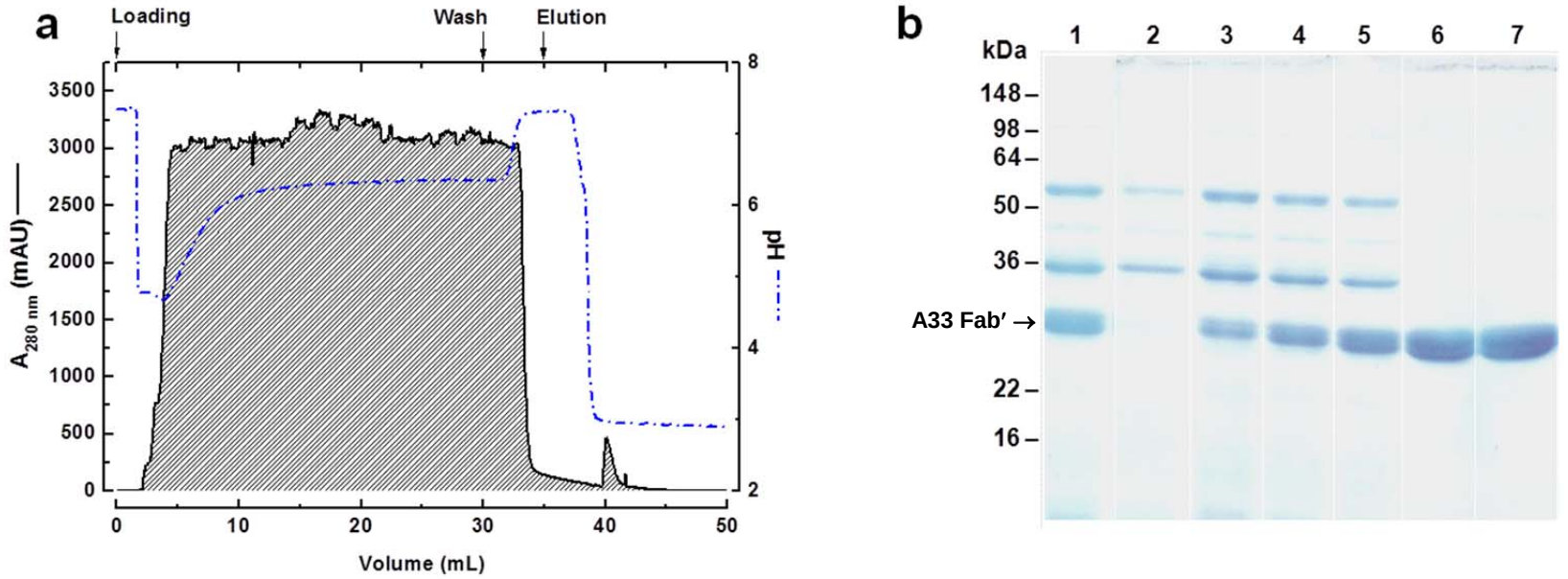

Fig. 5.8 Chromatogram **(a)** and **(b)** corresponding reducing SDS-PAGE analysis (14% polyacrylamide gel) for the recovery of A33 Fab´ from conditioned periplasmic extract by affinity chromatography on rProtein G Sepharose HP (Table 5.7). Key: lane 1 – Feed (conditioned extract); lanes 2 - 4 – loading flowthrough; lane 5 – wash; lanes 6 & 7 – elution peak.

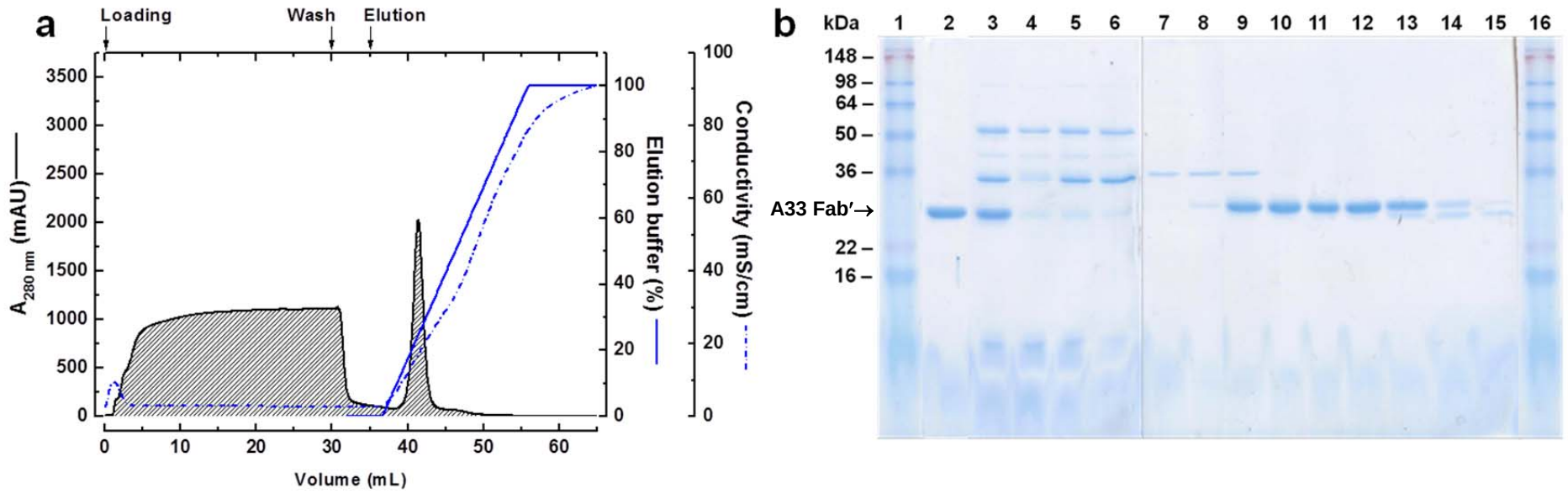

Fig. 5.9 Chromatogram **(a)** and **(b)** corresponding reducing SDS-PAGE analysis (14% polyacrylamide gel) for the recovery of A33 Fab´ from conditioned periplasmic extract by cation exchange chromatography on Fractogel EMD SO_3 (Table 5.6). Key: lanes 1 & 16 – molecular weight markers; lane 2 – rProtein G Sepharose HP purified A33 Fab´; lane 3 – feed (conditioned extract); lanes 4 & 5 – loading flowthrough; lane 6 – wash; lanes 7 to 15 – elution peak.
Lane 7-8 was eluted 2 CV before the peak was detected, lane 9-15 was eluted at the peak and after.

Table 5.7 Comparison of CME with conventional adsorption chromatography for the recovery of A33 Fab´ from *E. coli* extracts. See text for details.

Method (*adsorbent*)	Feedstock					Eluate		
	Conditioning history (pH, Σ)	Volume (L)	Fab´ (mg)	Protein (mg)	Initial Fab´ purity (%)	Final Fab´ purity (%)	Fab´ step yield (%)	Step PF[a]
CME (*MagPrepSO_3^- 100*)	10× diluted with buffer (pH 5.6, = 4.3 mS/cm)	14.72	1,104	7,067	15.6	98	67	6.3
Affinity chromatography (*rProtein G Sepharose HP*)	pH adjusted, centrifuged & 0.22 μm filtered (pH 6.6, = 17 mS/cm)	0.03	20.4	102.9	19.8	100	20	5.1
CEX chromatography (*Fractogel EMD SO_3^-)*	Centrifuged, 0.22 μm filtered, buffer exchanged (pH 5.6; = 2.9 mS/cm)	0.03	11.2	55.7	20.1	95	97	4.7

[a]PF = purification factor

The high salt concentration of the original crude periplasmic extract (= 21 mS/cm) presented no problems to Protein G affinity chromatography, but the presence of suspended solids and fouling materials necessitated subjecting the extract to extensive clarification beforehand, which compromised Fab' yield (Table 5.4); the low capacity (4 mg/mL) and expense of the rProtein G derivatised chromatography matrix are further detractions.

5.4.5. Review of the Recyclability of the CME Components – Surfactants and Magnetic Sorbent Particles

Reuse of the phase-forming component of an AMTPS is one striking advantage of AMTPS, over conventional ATPS. This is because it is only the micelle-depleted phase that is removed or discharged during all steps, i.e. sorption, washing and elution. In the case of CME, the micelle-rich top phase contains magnetic particle sorbents; which at end of the elution step can be re-cycled back into the next sorption stage, and so on. In order to calculate the theoretical amount of the recyclable phase-forming component, Eumulgin ES, samples of micelle-depleted bottom phases from the binding, washing and elution steps were removed during the continuous operation of the CME device for off-line analysis of surfactant, concentration. Table 5.8 compares the surfactant concentrations measured under continuous mode with those immediately after finishing the individual processing steps and discharging the separator contents into the collection tank.

Table 5.8 Comparison of surfactant concentrations in the bottom phase during CME operation and after discharging the separator.

Process step	[Eumulgin ES] (%w/w)	
	During operation	After discharging the separator
Binding	0.9	2.8
Washing	1.0	1.7
Elution	0.2	0.34

For all processing steps the Eumulgin ES concentrations are significantly higher (1.7 – 3.1 fold) after finishing each process step and discharging the separator, and are related to the ratio of volumes of the CME separation chamber (2.8 L) to that of the fluids processed through it (6.8 – 14.7 L). After complete processing of the feedstock, the CME separation chamber must be drained. During this operation, incomplete phase separation results in higher losses of surfactant *cf.* continuous mode. The problem of incomplete phase separation during drainage could be reduced by using an adjustable weir, which follows the phase boundary during the process. An adjustable weir could additionally aid optimisation of the CME set-up for different C_R values. However, for large feed volumes or truly continuous operation, the impact of surfactant that is lost during this drainage would be insignificant; thus values indicated in the left hand column ('During operation') of Table 5.8 are more pertinent to CME.

The amount of recyclable surfactant, i.e. that which can be recycled from the top phase arising from the elution step into a subsequent sorption cycle, was calculated (from the loss of surfactant in the bottom phases during the continuous operation of the magnetic extraction) to be 87%. Further, the total particle loss after binding, washing and elution amounted to only ~1% of the initial amount used, leaving the

remaining 99% available for use in a subsequent cycle of CME. In summary, effective reuse of both the phase-forming surfactant and magnetic sorbent particles is clearly achievable in CME based processes.

5.5. **Conclusions**

Continuous Magnetic Extraction (CME) has been introduced as a promising and potentially low cost continuous bioseparation process. It is based on the concerted use of functionalised magnetic sorbent particles together with AMTPS. Magnetic sorbents which partition exclusively to the micelle-rich phase of an AMTPS are separated in a novel pilot-scale extractor comprising a mixer and a magnetic field-enhanced flow-through phase separator. We have demonstrated that this CME device can be operated at flow rates of several liters per hour, at close to ambient temperatures (15 – 30°C), with particle separation efficiencies of >99%. Further, the phase-forming non-ionic surfactant employed in this work, Eumulgin ES, was continuously split into micelle-rich and micelle-depleted phases with a separation efficiency of >98%.

Subsequently, CME was successively applied for the direct capture of the antibody fragment A33 Fab´ from a crude *E. coli* periplasmic extract, employing CEX functionalised magnetic nano-particle sorbents. Nearly 70% of the A33 Fab´ initially present was recovered in the magnetic particle-free bottom phase eluate in 2 – fold concentrated form with a purity of >98%, corresponding to a purification factor of 6.3. The corresponding top phase eluate stream contained the magnetic sorbent particles and most of the phase-forming surfactant. In CME magnetic nano-particle sorbents were recovered with a recycling efficiency of >99% over three consecutively operated extractions, during which 13% of the phase-forming surfactant was lost. The

remaining 87% of phase-forming surfactant was collected together with the magnetic sorbents particles after the final elution step. Clearly therefore, recycling both the magnetic sorbents and the phase-surfactant particle into subsequent rounds of CME is highly feasible. Taken collectively, the results of this study identify CME as a viable means of performing continuous purification of target macromolecules from complex biological feedstocks at relatively low cost.

5.6. **References**

Albertsson, P.-Å. (1956). Chromatography and Partition of Cells and Cell Fragments. Nature *177*: 771–774.

Azevedo, a. M., Rosa, P.A.J., Ferreira, I.F., Pisco, A.M.M.O., Vries, J. de, Korporaal, R., Visser, T.J., and Aires-Barros, M.R. (2009). Affinity-enhanced purification of human antibodies by aqueous two-phase extraction. Separation and Purification Technology *65*: 31–39.

Becker, J.S., Thomas, O.R.T., and Franzreb, M. (2009). Protein separation with magnetic adsorbents in micellar aqueous two-phase systems. Separation and Purification Technology *65*: 46–53.

Bordier, C. (1981). Phase separation of integral membrane proteins in Triton X-114 solution. The Journal of Biological Chemistry *256*: 1604–7.

Fischer, I., and Franzreb, M. (2011). Direct determination of the composition of aqueous micellar two-phase systems (AMTPS) using potentiometric titration—A rapid tool for detergent-based bioseparation. Colloids and Surfaces A: Physicochemical and Engineering Aspects *377*: 97–102.

Fischer, I., and Franzreb, M. (2012). Nanoparticle Mediated Protein Separation in Aqueous Micellar Two-Phase Systems. Solvent Extraction and Ion Exchange *30*: 1–16.

Flygare, S., Wikström, P., Johansson, G., and Larsson, P.O. (1990). Magnetic aqueous two-phase separation in preparative applications. Enzyme and Microbial Technology *12*: 95–103.

Franzreb, M., Siemann-Herzberg, M., Hobley, T.J., and Thomas, O.R.T. (2006). Protein purification using magnetic adsorbent particles. Applied Microbiology and Biotechnology *70*: 505–16.

Gai, Q., Qu, F., Zhang, T., and Zhang, Y. (2011). Integration of carboxyl modified magnetic particles and aqueous two-phase extraction for selective separation of proteins. Talanta *85*: 304–9.

Hatti-Kaul, R. (2001). Aqueous two-phase systems. A general overview. Molecular Biotechnology *19*: 269–77.

Humphreys, D.P., Carrington, B., Bowering, L.C., Ganesh, R., Sehdev, M., Smith, B.J., King, L.M., Reeks, D.G., Lawson, A., and Popplewell, A.G. (2002). A plasmid system for optimization of Fab' production in *Escherichia coli*: importance of balance of heavy chain and light chain synthesis. Protein Expression and Purification *26*: 309–20.

Humphreys, D.P., Weir, N., Lawson, a, Mountain, a, and Lund, P. a (1996). Co-expression of human protein disulphide isomerase (PDI) can increase the yield of an antibody Fab' fragment expressed in *Escherichia coli*. FEBS Letters *380*: 194–7.

Ingram, T., Storm, S., Glembin, P., Bendt, S., Huber, D., Mehling, T., and Smirnova, I. (2012). Aqueous Surfactant Two-Phase Systems for the Continuous Countercurrent Cloud Point Extraction. Chemie Ingenieur Technik n/a–n/a.

Katsui, N., Tsuchido, T., Hiramatsu, R., Fujikawa, S., Takano, M., and Shibasaki, I. (1982). Heat-induced blebbing and vesiculation of the outer membrane of *Escherichia coli*. Journal of Bacteriology *151*: 1523–31.

Kopperschläger, G., and Birkenmeier, G. (1990). Affinity partitioning and extraction of proteins. Bioseparation *1*: 235–54.

Laemmli, U.K. (1970). Cleavage of Structural Proteins during the Assembly of the Head of Bacteriophage T4. Nature *227*: 680–685.

Larsson, P.-O. (1994). Aqueous Two-Phase Systems-Magnetically enhanced phase separation. Methods in Enzymology *228*: 112–117.

Leonardo, G., Ventani, M., and Uwe, G. (2008). Antibody Purification Using Membrane Adsorbers. BIOPHARM INTERNATIONAL *21*: 48.

Low, D., O'Leary, R., and Pujar, N.S. (2007). Future of antibody purification. Journal of Chromatography. B, Analytical Technologies in the Biomedical and Life Sciences *848*: 48–63.

Müller, T.K.H., Cao, P., Ewert, S., Wohlgemuth, J., Liu, H., Willett, T.C., Theodosiou, E., Thomas, O.R.T., and Franzreb, M. (2013). Integrated system for temperature-controlled fast protein liquid chromatography comprising improved copolymer modified beaded agarose adsorbents and a travelling cooling zone reactor arrangement. Journal of Chromatography. A *1285*: 97–109.

Oelmeier, S.A., Dismer, F., and Hubbuch, J. (2011). Application of an aqueous two-phase systems high-throughput screening method to evaluate mAb HCP separation. Biotechnology and Bioengineering *108*: 69–81.

Osborn, M.J., and Wu, H.C. (1980). Proteins of the outer membrane of gram-negative bacteria. Annual Review of Microbiology *34*: 369–422.

Pabst, T.M., Suda, E.J., Thomas, K.E., Mensah, P., Ramasubramanyan, N., Gustafson, M.E., and Hunter, A.K. (2009). Binding and elution behavior of proteins on strong cation exchangers. Journal of Chromatography. A *1216*: 7950–6.

Rosa, P. A J., Azevedo, a M., Sommerfeld, S., Bäcker, W., and Aires-Barros, M.R. (2012). Continuous aqueous two-phase extraction of human antibodies using a packed column. Journal of Chromatography. B, Analytical Technologies in the Biomedical and Life Sciences *880*: 148–56.

Sarubbo, L.A., Oliveira, L. A, Porto, A.L.F., Lima-Filho, J.L., Campos-takaki, G.M., and Tambourgi, E.B. (2003). Performance of a perforated rotating disc contactor in the continuous extraction of a protein using the PEG–cashew-nut tree gum aqueous two-phase system. Biochemical Engineering Journal *16*: 221–227.

Schäfer, U., Beck, K., and Müller, M. (1999). Skp, a molecular chaperone of gram-negative bacteria, is required for the formation of soluble periplasmic intermediates of outer membrane proteins. The Journal of Biological Chemistry *274*: 24567–74.

Schnaitman, C.A. (1974). Outer membrane proteins of *Escherichia coli*. 3. Evidence that the major protein of *Escherichia coli* O111 outer membrane consists of four distinct polypeptide species. Journal of Bacteriology *118*: 442–53.

Schneider, C.A., Rasband, W.S., and Eliceiri, K.W. (2012). NIH Image to ImageJ: 25 years of image analysis. Nature Methods *9*: 671–675.

Suzuki, M., Kamihira, M., Shiraishi, T., Takeuchi, H., and Kobayashi, T. (1995). Affinity partitioning of protein a using a magnetic aqueous two-phase system. Journal of Fermentation and Bioengineering *80*: 78–84.

Tani, H., Kamidate, T., and Watanabe, H. (1998). Aqueous Micellar Two-Phase Systems for Protein Separation. Analytical Sciences *14*: 875–888.

Trakultamupatam, P., Scamehorn, J.F., and Osuwan, S. (2004). Scaling Up Cloud Point Extraction of Aromatic Contaminants from Wastewater in a Continuous Rotating Disk Contactor. I. Effect of Disk Rotation Speed and Wastewater to Surfactant Ratio. Separation Science and Technology *39*: 479–499.

Vázquez-Villegas, P., Aguilar, O., and Rito-Palomares, M. (2011). Study of biomolecules partition coefficients on a novel continuous separator using polymer-salt aqueous two-phase systems. Separation and Purification Technology *78*: 69–75.

Weir, A.N.C.A., and Bailey, N.A.N. (1995). Process for obtaining antibodies utilizing heat treatment (US patant 5665866) (Filing date: 14th March 1995).

Wikstrom, P., Flygare, S., Grondalen, A., Larsson, P.O.O., Wikström, P., and Gröndalen, a (1987). Magnetic aqueous two-phase separation: a new technique to increase rate of phase-separation, using dextran-ferrofluid or larger iron oxide particles. Analytical Biochemistry *167*: 331–9.

6. Fabrication and characterisation of thermoresponsive polymer fimbriated immobilised metal affinity adsorbents

6.1. Abstract

The preparation and characterisation of immobilised metal affinity magnetic adsorbents possessing thermoresponsive behaviour is described. Cerium (IV) initiated 'graft from' polymerisation techniques were employed to the convert nonporous magnetite – poly(vinyl alcohol) composite particle, M-PVA, into a trio of adsorbents fimbriated with: (i) (poly(N-isopropylacrylamide), pNIPAAm; (ii) poly(N-vinylimidazole), pVI; and (iii) both polymers, [pNIPAAm + pVI]. Qualitative FTIR was used to corroborate the presence of the different grafted polymers in the surfaces of 'finished' supports (and intermediate in their manufacture in the case of the mixed polymer brush modifed adsorbent) and quantitative ATR – FTIR (employed on pre- and post- polymerisation reaction supernatants) confirmed that equal amounts of monomers had been grafted into all three supports (i.e. 8.75 – 9.35 mmol/g M-PVA), and further that the mixed polymer brush modified material [pNIPAAm + pVI] contained roughly equal amounts of N-isopropylacrylamide (4.35 mmol/g M-PVA) and N-vinylimidazole (4.4 mmol/g M-PVA). In binding studies with a recombinant heat stable hexahistidine tagged Green Fluorescent Protein (His6-GFP) rapid binding was observed for all three Cu^{2+} charged polymer modified supports, and the binding capacities were shown to be strongly influenced by pVI content and adsorption temperature, whereas nonspecific binding correlated

with pNIPAAm. The weaker binding at higher temperature was successively exploited for temperature mediated elution under binding conditions. The highest initial capacity for His6-GFP (40 mg/g) and best desorption performance (>90% recovery) was observed for M-PVA modified with Cu^{2+}-poly(N-vinylimidazole). By contrast, little or no protein elution was observed for Cu^{2+} charged Chelating Sepharose Fast Flow (fixed or immobile Cu^{2+}-IDA ligands) during temperature switching. The observed differences in thermally mediated elution behaviour of the Cu^{2+} coordinating polymer brush modified M-PVA and Chelating Sepharose Fast Flow media are explained by the effects of temperature on the mobility of polymer bound Cu^{2+} ligands cf. fixed immobile Cu^{2+} ligands, and conclusions on the use of polymers displaying normal and inverse temperature solubility behaviour in immobilised metal affinity adsorption are reached.

6.2. **Introduction**

High-cost processes consuming excessive amounts of buffers and generating disproportionate levels of waste are serious drawbacks of adsorption-desorption based methods employed by the Biopharmaceutical sector (Przybycien *et al.,* 2004; Jagschies, 2008; Maharjan *et al.,* 2008). Effective solutions to these problems have not yet been forthcoming, but would clearly make for much leaner, greener and more sustainable manufacturing of these valuable bio-commodities (Maharjan *et al.,* 2008).

In the above context, an important objective within the European Framework 7 'MagPro^{2}Life' project is to design, demonstrate and iteratively refine an entirely new separation concept that relies on discrete local changes in temperature, rather than chemical means, to control adsorption-desorption equilibria. This new approach owes much of inspiration to recent advances dealing with the use of smart or intelligent polymers to creating novel materials with 'self-adaptive' surfaces (Luzinov *et al.,* 2004; Kizhakkedathu *et al.,* 2004; Kanazawa and Okano, 2011).

Temperature-sensitive polymers exhibit a critical solution temperature (CST) behaviour, where phase separation is induced by surpassing a certain temperature. Two categories of thermo-responsive behaviour are known. Polymers are either: water-soluble at high temperature, and insoluble at low temperature (at the so-called upper critical solution temperature, UCST); or water-soluble at low temperature, and insoluble at high temperature. Temperature-sensitive polymers falling into the second category (referred to as 'smart thermoresponsive polymers') are generally more useful, especially

for applications involving biological entities that prohibit high temperature operation (Taylor and Ceranowski, 1975; Galaev and Mattiasson, 1999), as they exhibit inverse temperature solubility behaviour (Fig. 6.1) at a critical temperature known as the lower critical solution temperature, LCST (Taylor and Ceranowski, 1975; Galaev and Mattiasson, 1999).

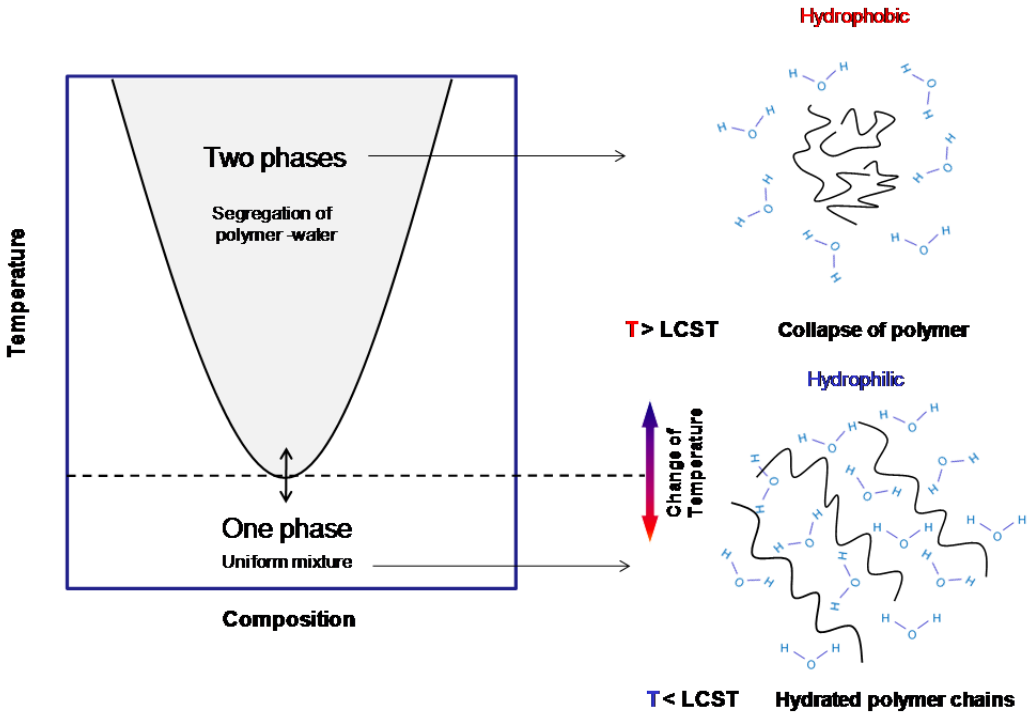

Fig. 6.1 Schematics drawings illustrating the phase behaviour of a polymer-solvent system with LCST (left) and the inverse temperature solubility behaviour (right) of thermoresponsive polymers at the LCST, i.e. hydrated polymer below the LCST and entropic loss of water and chain collapse above LCST. Courtesy of K. Zourna.

Below the LCST, the hydrophilic and completely miscible with water polymer develops a highly swollen coiled chain conformation (Fig. 6.1, bottom right). When the temperature increases above the LCST, the polymer is hydrophobic (Fig. 6.1, top right) and becomes incompatible with water, i.e. the polymer–water homogeneous mixture encounters phase separation (Fig. 6.1, left), where the polymer becomes globular and separates from the water-enriched

phase (Luzinov *et al.,* 2004; Zourna, 2009)]. Thus, a sudden shift in temperature away from the LCST point, can cause reversible and dramatic changes in the state of the polymer from hydrophilic to hydrophobic and back.

Poly(*N*-isopropylacrylamide), hereafter referred to by the abbreviation pNIPAAm, is perhaps the best studied smart thermoresponsive polymer. Its phase transition from a hydrophilic to a hydrophobic structure occurs suddenly at the LCST, which experimentally lies between *ca.* 30 and 35 ºC, depending on the exact microstructure of the macromolecule (Kubota *et al.,* 1990)). pNIPAAm (Fig. 2) is composed of amide groups that are hydrophilic and isopropyl groups that are hydrophobic (Kubota *et al.,* 1990; Schild, 1992)).

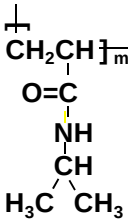

Fig. 6.2 Chemical structure of the poly N-isopropyl acrylamide (pNIPAAm) repeat unit.

Below the LCST, the water molecules cover the hydrophobic groups and the hydrogen bonds between the amide groups and water stabilise the solution, whereas above the LCST the hydrogen bonds become so weak that the attractions between the hydrophobic groups become bigger (de-mixing of polymer chains). As the water molecules destabilise around the isopropyl group, there is no available energy for mixing as the heat absorbed by the system is lower than the change in enthalpy and ultimately the chains de-mix (Kubota *et al.,* 1990: Schild, 1992; Zourna, 2009).

A handful of publications have demonstrated that the modification of solid substrates with pNIPAAm can impart considerable control over bacterial fouling and cell release (Okano *et al.,* 1993, 1995, Kikuchi *et al.,* 1998; Ista *et al.,* 1999; Takezawa *et al.,* 1990; Liu, 2009). The accumulation of microorganisms at solid-liquid interfaces, results in the formation of biofilms, which can pose hygiene and safety concerns and which can be extremely difficult to prevent and/or remove. In this context, modification of materials with pNIPAAm has been investigated to create switchable substrates for:

(i) temperature-controlled cell harvesting (Kikuchi *et al.,* 1998)];

(ii) recovery of cells from tissue culture substrata without the need for enzymes (Okano et al., 1993, 1995; Takezawa *et al.,* 1990); and

(iii) most recently in our laboratories for reducing cell sorption and enhancing cell release from magnetic adsorbent particles under binding conditions, i.e. without changing the buffer composition (Liu, 2009).

Collectively, these studies demonstrate that:

(i) the solvated for pNIPAAm is not intrinsically fouling resistant;

(ii) cell release can occur in both directions (i.e. cooling or heating) across pNIPAAm's LCST with the same cell type; and

(iii) phase transition is perhaps the most important factor in removal of microorganisms.

A large body of work on the use of pNIPAAm to modify chromatography media has appeared since the first reports appeared in the early 1990s

(Gewehr *et al.,* 1992; Hosoya *et al.,* 1994, 1995). Most work thus far has concentrated on exploiting the principle of extension and collapse of polymer chains for: (i) thermoresponsive size exclusion similar to 'chemical valves' (Gewehr *et al.,* 1992; Hosoya *et al.,* 1994; Adrados *et al.,* 2001)); (ii) modulating hydrophobicity in HPLC (Hosoya *et al.,* 1995; Adrados *et al.,* 2001; Yaksuiji *et al.,* 1994; Ayano *et al.,* 2006a; Kanazawa *et al.,* 1996, 1997, 1998); (iii) balancing electrostatic and hydrophobic interactions in ion exchange by employing thermoresponsive and electrostatic components in the same polymer (Kobayashi *et al.,* 2002, 2003; Sakamoto *et al.,* 2004; Ayano *et al.,* 2006b; Maharjan *et al.,* 2009; Nagase *et al.,* 2010; Müller *et al.,* 2013) or surface (Liu, 2009); and (iv) 'in pseudoaffinity chromatography (Maharjan *et al.,* 2008; Yoshizako *et al.,* 2002).

To date however, most work on pNIPAAm in chromatography concerns the modification of small pored inorganic (glass, silica) or hydrophobic (polystyrene based) resins chromatography supports intended for use in analytical HPLC separations of small molecules (especially mixtures of steroids). In stark contrast, the use of pNIPAAm for modifying macroporous hydrogel chromatography materials appropriate for bioprocess scale separations of macromolecular targets (globular proteins, nucleic acids, viruses) has received very little attention thus far. This is surprising given that the use of temperature responsive chromatography materials offers cost-effective environmentally friendly solutions to the isolation of commercially valuable biocomponents from biopharma, bioindustry, agricultural, food and other complex process streams (Maharjan *et al.,* 2008, 2009; Liu, 2009; Nagase *et al.,* 2010; Müller *et al.,* 2013).

In the work detailed here, Ce(IV) initiated 'graft from' polymerisation techniques developed for the fabrication of tentacular chromatography matrices (Müller, 1986, 1990; Janzen *et al*., 1990; Brooks and Müller, 1996; Hritcu *et al.,* 1999; Brooks *et al.,* 2000) were employed to convert non-porous magnetic supports into thermoresponsive magnetic immobilised metal affinity adsorbents by growing 'mobile' temperature sensitive Cu^{2+} coordinating polymer brush layers *in situ*. Three different polymer brush modified supports were made, i.e. one featuring the temperature-sensitive smart polymer, poly(*N*-isopropylacrylamide), another of the metal chelating polymer, poly(*N*-vinylimidazole), and the third comprising a mixed brush arrangement composed of equal numbers of adjacent poly(*N*-isopropylacrylamide) and poly(*N*-vinylimidazole) chains. Following characterisation by FT-IR, the finished supports were charged with Cu^{2+} ions and then subjected to a battery of protein binding and desorption tests aimed at evaluating the feasibility of thermally mediated target protein elution under binding conditions. Comprehensive control studies were also conducted using a Cu^{2+} charged commercial immobilised metal affinity chromatography matrix featuring 'fixed' (i.e. immobile) ligands.

6.3. **Materials and Methods**

6.3.1. Materials

M-PVA 012 (Lot no. R2-0109027), the spherical beaded 'magnetite – polyvinyl alcohol (Mr 130,000; acetyl content: 10.0-11.6 %; degree of hydrolysis: 86.8-88.7 %)' composite base matrix used in this study, was a gift from Chemagen Biopolymer-Technologie AG (Baesweiler, Germany). Brown's (2009) detailed magnetic and physical characterisation of this support particle confirmed it as superparamagnetic, roughly spherical, relatively monodisperse (D_{50} = 1.9 μm, $D_{20\text{-}80}$ of 1.5–2.6 μm), possessing high saturation magnetisation (42 Am^2 g^{-1}) and a highly textured surface (~55 m^2/g). Chelating Sepharose Fast Flow was purchased from GE Healthcare (Uppsala, Sweden), and the free polymers, poly(*N*-isopropylacrylamide) (M_w 19,000 – 30,000) and poly(*N*-vinylimidazole) (M_n 8,300, M_w/M_n = 3.4) were obtained from Sigma-Aldrich Company Ltd. (Gillingham, UK) and Polymer Source Inc. (Montreal, Canada) respectively. Haemoglobin from bovine blood (lyophilised powder) was acquired from Sigma-Aldrich Company Ltd. (Gillingham, UK) and used without further purification. Purified recombinant *N*-terminal hexa-histidine tagged *Aequorea victoria* Green Fluorescent Protein (His_6-GFP) was kindly supplied by J. Becker (KIT, Leopoldshafen, Germany). Bovine serum albumin (BSA) standards were obtained from Pierce Chemical Company (Rockford, IL, USA). The chemicals employed for modification of M-PVA and in subsequent binding and desorption studies – acetone (≥99.8%), methanol (≥99.9%), *1*-vinylimidazole (≥99%, VI), *N*-isopropylacrylamide (97%, NIPAAm); ammonium cerium (IV) nitrate (99.99%), sodium sulphate (ACS reagent, anhydrous

powder, ≥99.0%), 4-ethoxyphenol (99%), glacial acetic acid (ACS reagent, ≥99.7%), sodium acetate (ACS reagent, ≥99.0%), sodium dihydrogen phosphate (≥99%), disodium hydrogen phosphate (≥99.0%), imidazole (≥99.9%), copper (II) chloride (anhydrous, ≥99.995% trace metals basis), sodium chloride (≥99.5%), sodium hydroxide (pellets, anhydrous, >98%) and potassium bromide (≥99%, FT-IR grade) – were all from the Sigma-Aldrich Company Ltd (Poole, Dorset, UK), and bottled oxygen-free nitrogen gas was supplied by British Oxygen Co Ltd (Windlesham, Surrey, UK). All other chemicals not stated above were from Sigma-Aldrich or Merck Chemicals Ltd. Milli-Q water was used in all experiments.

6.3.2. Support handling

Side-pull magnetic racks (Chemagic Stands 50k Type A and 2x12, Chemagen Biopolymer-Technologie AG, Baesweiler, Germany) employing neodymium-iron-boron permanent magnets were employed for recovering magnetic M-PVA supports from suspension during their modification and subsequent use. Depending on experimental requirements Chelating Sepharose Fast Flow adsorbents were separated from the small volumes of bulk phases either by allowing sufficient time to settle (0.5 h) under gravity or alternatively within 10 s using a 6,500 *g* centrifugal pulse administered in a microcentrifuge.

6.3.3. Preparation of polymer grafted M-PVA supports by Cerium (IV) 'graft from' initiated reactions

The procedures used in this work for the generation of homopolymer and mixed polymer grafted M-PVA particles by Ce(IV) initiated 'graft from' free-radical polymerisation are based on methods previously developed in our laboratories (Brown, 2009, Brown *et al.,* 2013; Willett, 2009; Zourna, 2009). The detailed protocols employed are presented immediately below and are schematically represented in Figures 6.3 and 6.4, and the key grafting parameters are summarised in Table 6.1.

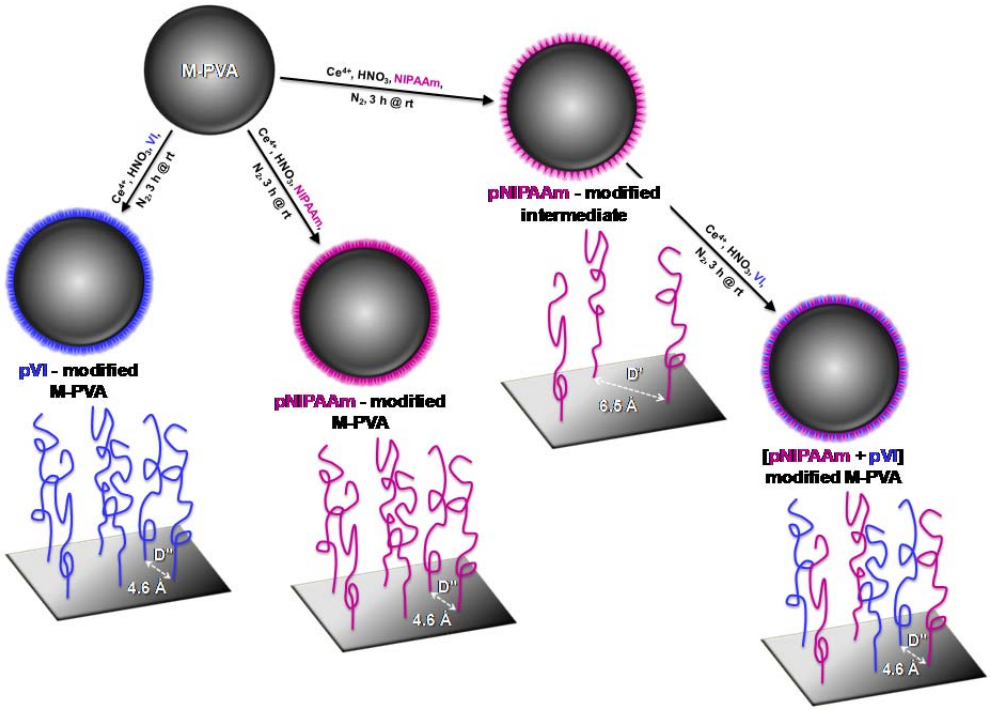

Fig. 6.3 General scheme illustrating the preparation routes and idealised appearance (equal polymer chain lengths and graft density; see Table 6.1) of the pVI, pNIPAAm and [pNIPAAm + pVI] modified M-PVA supports made in this work. The calculated intergraft spacing (cited in Table 6.1) for the pNIPAAm intermediate (D' = 6.5 Å) in the two step procedure grafting procedure and of all three 'finished' supports (D" = 4.6 Å) are indicated.

a **b**

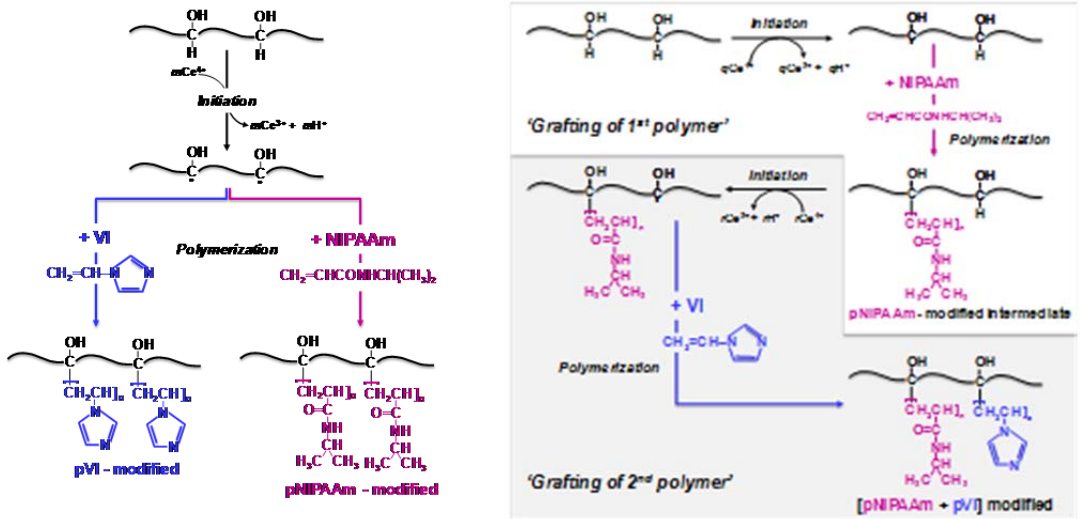

Fig. 6.4 Schemes illustrating the basic chemistry involved in single (a) and sequential two-step (b) cerium (IV) initiated 'graft from' polymerisation of vinyl monomers (VI and NIPAAm in this work) into the polyvinyl alcohol (PVA) matrix of M-PVA supports.

Table 6.1 Summary of key grafting parameters and characterisation data for the polymer fimbriated M-PVA supports made and used in this study.

Key grafting parameters					Support characterisation									
Support fimbriated with	Grafting in:	Monomer presented (mmol monomer /g M-PVA)	Initiator (mmol Ce^{4+} /g M-PVA)	$DP_{100\%}$ (units)[a]	Monomer consumed (%)[b]	DP_{obs} (units)	Inter-graft spacing (Å)[c]		Monomer installed (mmol/g M-PVA)	Grafted polymer content (g/g M-PVA)			Finished support	
							D'	D"		pNIPAAm	pVI	Total	Grafted polymer content (% w/w)	Polymer brush description
pNIPAAm	1 step	NIPAAm (110)	0.44	250	8.5	22	na	4.6	9.35	1.07	na	1.07	51.7	$p(NIPAAm)_{22}$ – 4.6 Å
pVI	1 step	VI (44)	0.44	100	21	21	na	4.6	9.24	na	0.87	0.87	46.5	$p(VI)_{21}$ – 4.6 Å
pNIPAAm followed by pVI	2 steps	1: NIPAAm (55) 2: VI (4.4)	0.22 0.22	250 20	7.9 100	20 20	6.5 na	na 4.6	4.35 4.40	0.49	na 0.41	0.47 0.90	na 47.4	$[p(NIPAAm)_{20}$ + $p(VI)_{20}]$ – 4.6 Å

Key: [a]$DP_{100\%}$ is the degree of polymerisation expected for 100% monomer consumption; [b]Determined by FT-IR; [c]Calculated inter-graft spacings of assuming reaction of every Ce^{4+} results a grafted polymer chain. D' and D" respectively denote the intermediate and final spacings achieved (depicted in Fig. 6.1); na = not applicable.

6.3.3.1. M-PVA base matrix conditioning for polymer grafting

Prior to polymer grafting, 0.5 g quantities of M-PVA particles were transferred to fresh 50 mL polypropylene falcon tubes (Fisher Scientific UK Ltd, Loughborough, UK) and then washed exhaustively at room temperature by sequential cycles of resuspension, mixing and magnetic separation with 30 mL aliquots of the following solutions: water; 50% (v/v) acetone in water; 100% acetone; 50% (v/v) acetone in methanol; 100% methanol; 50% (v/v) methanol in water; twice with water; 1 M NaCl; and finally twice with degassed nitrogen purged water, before resuspending in a final volume of 15 mL. During each wash step, the particle mixtures were mixed for 30 s using a Fisherbrand WhirliMixer™ (Fisher Scientific UK Ltd., Loughborough, UK), before separating magnetically and carefully discarding the wash supernatants.

Immediately prior to polymerisation separate aqueous stock suspensions of washed M-PVA particles (33.33 mg/mL), 1-vinylimidazole (VI, 1.47 M), *N*-isopropylacrylamide (NIPAAm, 3.67 M) and 147 mM ammonium cerium (IV) nitrate in 2 M nitric acid were sparged with steady streams of nitrogen for 0.5 h, while housed in a zipper-locked inflatable glove box (AtmosBag, Sigma-Aldrich, UK).

6.3.3.2. Preparation of linear homopolymer brush modified M-PVA particles by Cerium (IV) initiated polymerisation

For the preparation of M-PVA supports grafted with pVI and pNIPAAm homopolymer brushes 3 mL aliquots of the nitrogen purged VI (4.4 mmol) or

NIPAAm (11.0 mmol) solutions were mixed with 3 mL of nitrogen purged M-PVA particles (100 mg). The tubes were immediately sealed and then placed on a Vibrax shaker (IKA®-Werke GmbH, Staufen, Germany) for 300 s operating at 2000 rpm. After this period the tubes were transferred back to the nitrogen environment of the glove box, and the 'graft from' polymerisation reactions were initiated by addition of 300 μL portions of ammonium cerium nitrate /nitric acid solution (containing 44 μmol Ce^{4+}) to each tube, before re-sealing, and returning to the Vibrax shaker. After 3 h of reaction at room temperature the supernatants were removed with the aid of a magnetic rack and the polymer grafted supports were subsequently washed on a vortex mixer for 60 s each with 10 mL portions of the following solvents: 0.2 M Na_2SO_3 in 10% v/v acetic acid (stop solution); water (2x); 1 M NaCl (2x); water (2x) before storing water at 4°C until required.

The monomers VI and NIPAAm were employed at 44 and 110 mmol per gram of M-PVA and the initiator, Ce^{4+} was used at 0.44 mmol per g M-PVA (corresponding to an inter-chain spacing, D" of 4.6 Å; Table 6.1) so that the molar ratios of VI: Ce^{4+} and NIPAAm: Ce^{4+} entering the reactions were 100:1 and 275:1 respectively. Based on Zourna's (2009) findings the 2.5 fold higher monomer: initiator ratio employed in reactions with NIPAAm *cf.* those with VI is necessary, given her observation of much lower efficiencies of NIPAAm consumption in aqueous Cerium (IV) initiated reactions *cf.* those towards VI and especially acrylic acid monomers.

6.3.3.3. Preparation of linear mixed functionality polymer brush modified M-PVA particles by sequential Cerium (IV) initiated polymerisation

Creation of mixed [pNIPAAM + pVI] grafted surfaces on M-PVA was performed in two overall steps. In the first of these, pNIPAAM was grafted onto the unmodified M-PVA surface using half the amounts of NIPAAm monomer and ammonium cerium nitrate employed for pNIPAAm homopolymer modification of M-PVA, i.e. 55 mmol NIPAAm and 0.22 mmol Ce^{4+} per gram of M-PVA, generating M-PVA supports lightly fimbriated with pNIPAAM (D' = 6.5 Å; Table 6.1). This was followed by a second step, in which pVI was grafted (in between the tethered pNIPAAm chains on M-PVA's surface leading to supports with mixed polymer brush surfaces comprising adjacent pNIPAAm and pVI chains spaced 4.6 Å apart (Table 6.1). The amounts of VI and Ce^{4+} employed in the second step were 4.4 and 0.22 mmol/g M-PVA respectively.

In the first step nitrogen purged NIPAAm stock solution (1.5 mL, 5.5 mmol) and nitrogen purged water (1.65 mL) were added to 3 mL of nitrogen purged M-PVA particle suspension contained in a fresh falcon tube. The tube was immediately sealed and placed on a Vibrax shaker (IKA1-Werke GmbH, Staufen, Germany) for 300 s operating at 2000 rpm. After this time the tubes were transferred back to the nitrogen environment of the glove box where 150 μL of ammonium cerium (IV) nitrate (22 μmol) was added, and the tube was then re-sealed and returned to the Vibrax shaker for a further 3 h. The supernatant was then removed with the aid of a magnetic rack and the particles were re-suspended in 10 mL of 14.5 mM 4-ethoxyphenol solution

and vortexed for 600 s to quench the reaction. The resulting pNIPAAm-fimbriated M-PVA supports were then washed sequentially with 10 mL portions of 0.2 M Na_2SO_3 in 10% (v/v) acetic acid; water (2×); 1 M NaCl (2×); and water (2×) and resuspended with nitrogen purged water to a volume of 3 mL.

For the second step in the synthesis of [pNIPAAm + pVI] modified M-PVA, only half of the pNIPAAm-fimbriated support suspension was employed and the remainder was retained for FT-IR analysis.

After sparging the pNIPAAm-fimbriated intermediate slurry (1.5 mL, equivalent to 50 mg of original M-PVA particle) with a steady stream of nitrogen for 600 s, nitrogen purged VI solution (150 μL, 0.22 mmol) and water (1.425 mL) was added, the tube was resealed and the contents were mixed on a Vibrax shaker at 2000 rpm. After 300 s of incubation the tube was returned nitrogen filled and 75 μL of 2 M nitric acid containing 11 μmol ammonium cerium (IV) nitrate was before, resealing the tube and shaking (2000 rpm) at room temperature for 3 h. At the end of this period [pNIPAAm+ pVI] fimbriated particles were magnetically retrieved from the spent reaction liquor, re-suspended in 5 mL of 14.5 mM, 4-ethoxyphenol solution and mixed for 600 s on a Vibrax shaker. Finally, after washing as previously described(with 0.2 M Na_2SO_3 in 10% (v/v) acetic acid, twice with water, twice with 1 M NaCl, and finally twice with water) the finished [pNIPAAm + pVI] fimbriated M-PVA supports were stored in 3 mL of water at 4°C until required.

6.3.4. Further purification of hexahistine-tagged Green Fluorescent Protein (His_6-GFP)

The recombinant His_6-GFP received (~3 mg/mL) and used in this work had been intracellulary expressed and cultivated in *E. coli* BW3110 (harbouring pJOE 4056.2) and subsequently purified (>95% by SDS-PAGE) from a centrifugally clarified cell homogenate by immobilised metal affinity adsorption on Cu^{2+}-IDA (iminodiacetic acid) linked supports. Before use portions were mixed five-fold with 20 mM sodium phosphate buffer pH 6.8 supplemented with 200 mM NaCl and applied to individual centrifugal filter units (Amicon Ultra-15, MWCO 10 kDa; Millipore U.K. Ltd, Watford, UK), before centrifuging at 4000 rpm and 6°C in a Jouan C 4 22 centrifuge (Jouan, Nantes, France) for 0.5 h. The pale blue Cu^{2+} containing permeate was discarded, fresh 20 mM sodium phosphate, pH 6.8 + 200 mM NaCl was added to each filter unit, and following mixing these were recentrifuged. After a total of five such treatments the retained purified His_6-GFP (0.6 mg/mL in 20 mM sodium phosphate, pH 6.8, 200 mM NaCl) was recovered from all of the filter units, pooled and stored at 4°C until required.

6.3.5. Adsorption–desorption experiments with Cu^{2+} – Chelating Sepharose Fast Flow

Chelating Sepharose Fast Flow was washed exhaustively with water on sintered glass filter funnel under vacuum, before transferring to a fresh 50 mL plastic falcon tube and resuspending in 0.2 M $CuCl_2$. After mixing for 0.5 h at 2000 rpm on an orbital shaker the support slurry was poured back into the sintered glass filter funnel and washed copiously with the water, then 20 mM

sodium acetate buffer pH 4.0 containing 0.5 M NaCl; and finally the binding buffer, 20 mM sodium phosphate, pH 6.8 supplemented with 0.2 M NaCl.

For batch binding tests, pure solutions haemoglobin and His_6-GFP solutions of defined concentrations (c_0 = 25 μg/mL to 1.1 mg/mL) were prepared in binding buffer. Aliquots (5 mL) of these protein solutions were added to 0.1 mL volumes of settled Cu^{2+}-charged Chelating Sepharose Fast Flow contained in Eppendorf tubes before mixing at various temperatures between 19 and 42 ºC, for 1 h with shaking (1250 rpm, Thermomixer Comfort shaker, Eppendorf, Hamburg, Germany). After an additional 0.5 h at the selected incubation temperature without shaking, the supernatants were carefully removed and analysed for residual protein content (see 6.3.9 Analysis). Protein bound to the supports was determined from the difference in protein concentrations of the initial binding solution (c_0) and the supernatant after binding (c*), and where appropriate the data was fitted to the Langmuir equation (Eq. 6.1) using the χ^2 minimisation procedure of SigmaPlot software version 11.0 (Systat Software Inc, CA, USA):

$$q^* = (q_{max} * c^*)/(K_d + c^*)$$

Equation 6.1

where q* and c* represent the equilibrium concentrations of the adsorbed and liquid-phase protein respectively; q_{max} is the support's maximum protein binding capacity; and K_d is the dissociation constant.

Two types of desorption study were performed, i.e. chemically and thermally mediated, and for both, between buffer changes, the supports were rapidly

recovered from suspension by pulsed (10 s) centrifugation (6,500 *g*) in a microcentrifuge.

The effect of adsorption temperature on subsequent chemically mediated recovery of haemoglobin and His_6-GFP was examined in the following way. After 1 h of binding at various temperatures under mixing (1250 rpm) the supports were allowed to settle (0.5 h) at the same temperature, and the supernatants were removed and retained for analysis of residual protein content. The supports (0.1 mL) were then washed sequentially, at either room temperature or the binding temperature, with changes (each of 600 s duration) of the binding buffer (4 × 1 mL) and then 0.2 M imidazole (5 × 1 mL), before finally stripping any residually bound protein off the supports in a wash with 1 mL of 0.5 M NaOH.

Attempts to dislodge bound protein under binding conditions by cycling the temperature between 22 and 42°C were conducted in the following way. Following an initial protein binding step conducted at 22°C as described above, the settled supports (0.1 mL) were recovered and incubated for 600 s contact at 1250 rpm with 1 mL aliquots of: (i) binding buffer at 22° (2×), before (ii) initiating the temperature switching regime (i.e. → 42°C → 22°C → 42°C → 22°C) using fresh binding buffer at each temperature; followed by (iii) three changes of binding buffer supplemented with 0.2 M imidazole (22°C); and finally (iv) stripped with 1 M NaOH (22°C).

6.3.6. Protein binding and elution studies with polymer fimbriated M-PVA particles

After washing once with water polymer brush modified M-PVA supports were resuspended with 0.2 M $CuCl_2$ at a particle concentration of 2 mg/mL and incubated for 900 s at 2000 rpm on a Vibrax shaker. Following magnetic retrieval the supports were subsequently incubated in a similar manner (900 s, 2000 rpm) with water and then two changes of binding buffer (20 mM sodium phosphate buffer, pH 6.8 + 0.2 M NaCl).

For equilibrium binding studies, 1.33 mL aliquots of pure His_6-GFP solutions of defined concentrations (c_0 = 12 μg/mL – 0.60 mg/mL in binding buffer) were mixed at 22°C or 42°C with 1 mg portions of the different supports in Thermomixer Comfort (Eppendorf, Hamburg, Germany) shakers operated at 1250 rpm. After 1 h of incubation the supports were magnetically separated from the bulk phase, the supernatants were assayed for residual protein content (6.2.9 Analysis) and support bound protein (q*) was computed from the difference in bulk phase protein concentrations before (c_0) and after binding (c*), and the resulting ‘q* vs. c* plots were fitted to the Langmuir model (Eq. 6.1).

The kinetics of binding were examined at 22°C using 3 mg quantities of the different polymer brush modified supports mixed with 1 mL of 300 mg/L His_6-GFP (i.e. binding challenge of 100 mg His6-GFP/g support) on a Vibrax shaker at 2000 rpm. After various times (~15 s to 1 h) the supports were rapidly separated from solution, and the amounts of bound protein at each were determined from the drop protein concentration. For the 15 s time points

supports were rapidly mixed with His_6-GFP on a Whirlimixer (<5 s), and then immediately separated by in a microcentrifuge (at 6500 *g* for 10 s).

Thermally mediated elution studies were performed in the following way. Supports (3 mg) were incubated with 1 mL of 0.3 mg/mL His6-GFP for 1 h at 22°C on a Vibrax shaker (2000 rpm). Each of the support samples was then subjected to a total of 9 washes with binding buffer. For each support type four different contact times (30, 180, 600 and 1800 s) were investigated and these times were kept constant for all 9 washes. The first wash was performed at the binding temperature (22°C), but thereafter 8 temperature transitions were made with 1 mL aliquots of fresh binding buffer (washes 2 – 9), i.e. →42°C → 22°C → 42°C → 22°C → 42°C → 22°C → 42°C → 22°C, maintaining the same elution time for all washes in the series. Two thermomixers set at 22 and 42 °C were employed for these experiments, both operating at 1250 rpm.

6.3.7. Temperature measurements

Prior to carrying out thermally mediated elution studies (6.3.6) time dependent temperature measurements were performed on 0.5, 1 and 2 mL samples of binding buffer in 2 mL screw-capped Eppendorf vials switched from between the two thermomixers. Temperature measurements were conducted in both directions, i.e. from 22 to 42°C and from 42 to 22°C samples using an electronic handheld two channel thermometer (RS 206-3750, RS Components Ltd., Corby, UK.).

6.3.8. Temperature induced phase transition measurements on additive doped pNIPAAm solutions

The influence of additives (sodium phosphate, NaCl, and $CuCl_2$) on the phase transition behaviour of pNIPAAm in water was studied in a similar manner to that we've reported recently (Müller *et al.,* 2013). The optical transmittance at 500 nm of a series of solutions containing 0.5 g/L pNIPAAm (equivalent to a NIPAAm monomer concentration of 4.4 mM) variously doped with additives (used singly and in combination), i.e. 20 mM sodium phosphate buffer pH 6.8 containing 0.2 M NaCl, $CuCl_2$ (2.2 or 4.4 mM), pVI (VI concentration = 4.4 mM) were measured at various temperatures in a Cecil CE7500 UV/visible dual beam spectrophotometer (Cecil Instruments Ltd, Cambridge, UK) equipped with a water thermostatted cuvette holder. Control measurements with the 'pNIPAAm free' solutions of the additives, were also conducted.

6.3.9. Analysis

Complete consumption of bulk phase 'orange' Ce^{4+} ions by M-PVA supports during Ce(IV) initiated 'graft from' polymerisation reactions was confirmed by measuring the optical densities of pre and post reaction supernatants at 353 nm using a UVICON 922 spectrophotometer (Kontron Instruments, Bletchley, UK).

Fourier Transform Infrared (FT-IR) spectroscopy analysis was employed for both qualitative and quantitative analysis of polymer grafting onto M-PVA. Qualitative FT-IR methods were used to detect the chemical changes that occur on M-PVA during the grafting of homo and mixed polymer brush

surfaces. Quantitative FT-IR methods were used to quantify the presence of pNIPAAM and pVI on M-PVA supports, via measurement of NIPAAM and VI monomer consumption during polymer grafting.

Solid samples, used for qualitative FT-IR, were prepared by drying aliquots of particle suspension on watchglasses in an oven (60°C, 20 h) and grinding the dried particles (~3 mg) with 300 mg potassium bromide in an agate mortar to create a very fine homogenous powder. This powder was pressed in a 13 mm die at 15 tonnes with an Atlas manual hydraulic press (Model GS15011, Specac Ltd, Orpington, Kent, UK) to give tablets suitable for FT-IR analysis. FT-IR spectra of these sample tablets were recorded using a Nicolet 380 FT-IR (Nicolet 380, Thermo Fischer Scientific, Waltham, MA, USA) in direct beam mode. The spectra were scanned 64 times at a resolution of 2 cm^{-1} before averaging.

Quantitative FT-IR was performed from spectra of liquid reaction mixture samples (150 μL), measured using Attenuated Total Reflectance (ATR) mode FT-IR. 10mL of each sample solution was placed on the Smart 53 Orbit diamond accessory of the Nicolet 380 FT-IR and scanned 64 times at 2 cm^{-1} resolution in ATR mode. Background spectra were taken every 0.5 h during the course of sample measurements by taking a measurement with no sample on the Smart 53 Orbit. These background spectra provide a reference to allow the Nicolet 380 to correctly scale the absorption intensity of sample spectra. The concentrations of monomers after reactions were determined from the areas of characteristic peaks in their ATR FT-IR spectra. For NIPAAm the peak area from 1625 to 1500 cm^{-1} (corresponding to N-H

bending in the amide group at ~1550 cm^{-1}) was used (Müller *et al.,* 2013). The amount of VI present in liquid samples was calculated from the peak at 1490 cm^{-1} (between 1535 and 1450 cm^{-1}) which is typical of C-C stretching in the imidazole ring of VI (Luo *et al.,* 1999; Zhang *et al.,* 2000). The concentrations of unreacted NIPAAm and VI were estimated by reference to standard curves of peak area vs. concentration with high accuracy for both monomers (R^2 values of >0.992 for NIPAAm and >0.995 for VI; Zourna, 2009).

Gravimetric analysis was routinely performed on solid supports at all stages during their modification and use. Small volumes (typically 0.2 – 1 mL) of homogeneously dispersed particle suspensions were pipetted into fresh labelled pre-weighed glass HPLC vials which were then dried to constant weight in a 60°C oven. After 16 – 20 h at 60°C the vials were cooled to room temperature in a dessiccator jar and weighed accurately on Mettler AT261 analytical balance (Delta range, Leicester, UK). The weight of the sample was calculated from the difference in weight of the vial before and after sample addition.

Protein contents in samples arising from batch binding and desorption studies were routinely determined by the Bradford (1976) assay employing ‘Coomassie Plus the Better Bradford™ Reagent' (Pierce, Rockford, IL, USA) and were expressed in BSA equivalents. All optical density readings were performed at a wavelength of 595 nm in a UVICON 922 dual beam spectrophotometer (Kontron Instruments, Bletchley, UK) in disposable high optical quality acrylic cuvettes (Sarstedt AG + Co, Nümbrecht, Germany).

6.4. **Results and Discussion**

6.4.1. Characterisation of the effects of temperature on target protein adsorption to and desorption from 'immobile' Cu^{2+}-IDA ligands

Earlier seminal studies (Hemdan and Porath, 1985; Hutchens and Yip, 1991; Finette *et al.,* 1997) have shown the effects of temperature on the binding of proteins to immobilised Cu^{2+} supports to be very complex in nature[4]. For example, Hutchens and Yip (1991) observed that change from 0 to 37°C exerted little to no effect on the maximum binding capacities to hen egg white lysozyme and ribonuclease A. However, the variance of interaction affinity with temperature of the same two protein species was markedly difference; binding affinity for lysozyme dropped significantly with increase in temperature, but that for ribonuclease remained essentially unchanged. Therefore, it is curcial to carefully selecte model proteins, whose binding behaviour should not be affected significantly by temperature changes, hence the modules proteins could be used for evaluting temperature effect on binding matrices.

A prerequisite for the creation of supports featuring surfaces co-grafted with immobilised metal affinity ligands and thermoresponsive polymer chains was to first study the effects of temperature on the binding and desorption behaviour of selected model protein probes on immobilised metal affinity supports in the absence of grafted thermoresponsive polymer chains. A

[4] Best explained by appreciation of differences in solvent-accessibilities, surface distribution of histidine residues, pK_a values of the individual histidyl side chains and architectural and chemical features of the protein surface structure in the immediate environment of the surface-exposed histidines (Hutchens and Yip, 1991).

commercial macroporous immobilised metal affinity chromatography support, (Chelating Sepharose Fast Flow) and two coloured [5] proteins previously employed in our laboratories for the characterisation of immobilised metal affinity supports (the red haem protein, bovine haemoglobin with its 20 surface exposed histidine residues and a hexahistidine tagged Green Fluorescent Protein (His_6-GFP) were selected for this purpose. Haemoglobin is a soft tetrameric protein of roughly 60 kDa size, which likely undergoes considerable deformation, size change and partial unfolding when it docks on Cu^{2+} functionalised surfaces (Gekko and Hasegawa, 1986; O'Brien *et al.*, 1997). Further, haemoglobin is acutely thermal sensitive protein, its conformation altering significantly with increasing temperature (Clementi *et al.*, 1994) in particular abrupt conformational changes occur just 2 – 3ºC above body temperature (Digel *et al.*, 2006). Compared to haemoglobin, the light emitting protein GFP from the jellyfish *Aequorea aequorea* is a comparatively small (27 kDa) and robust β-barrelled protein (Li *et al.*, 2001; Scheyhing *et al.*, 2002) resistant to harsh conditions including extreme temperatures, chaotropic salts, proteases, and organic solvents. According to Scheying and co-workers (2002) GFP is supremely stable up to 65°C, and undergoes only small conformational changes between 15 and 65°C.

Target adsorption was studied over the operating temperature range employed previously for the successful demonstration of thermally mediated elution from thermo-IEX chromatography materials (Li, 2009; Müller *et al.*, 2013) i.e. 20 – 42°C. Supports laden with adsorbed protein were

[5] Colour was not exploited for quantitative assay, but was instead employed to rapidly confirm target binding (disappearance from solution) and desorption (appearance in solution) in advance of quantitative determination by Bradford (1976) assay.

subsequently incubated at either room temperature of the adsorption temperatures using binding buffer and/or 0.2 M imidazole, before stripping with 0.5 M NaOH. Adsorption isotherms conducted at the low and high ends of the operating regime, and plots of equilibrium binding capacity vs. temperature determined in the linear and non-linear regions of the binding isotherms are shown in Figures 6.5 and 6.6 respectively. The fitted Langmuir parameters describing the binding data for His_6-GFP (Fig. 6.5a) and bovine haemoglobin (Fig. 6.5b) on Cu^{2+} – Chelating Sepharose Fast Flow at 22 and 42°C are shown in Table 6.2.

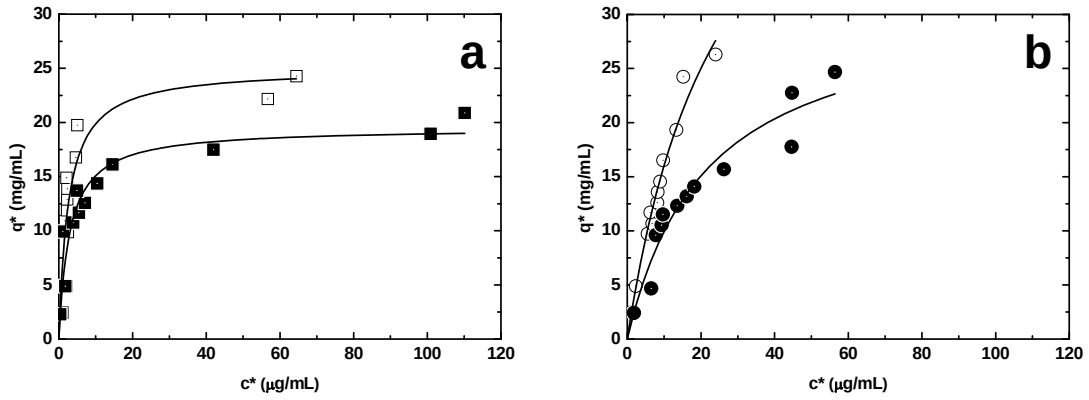

Fig. 6.5 Langmuir adsorption isotherms for the binding of **(a)** His_6-GFP and **(b)** bovine haemoglobin to Cu^{2+} – Chelating Sepharose Fast Flow at 22°C (white symbols) and 42°C (black symbols).

Scrutiny of Figs 6.5a and 6.5b reveals that the binding of both target proteins to Cu^{2+}-IDA Sepharose Fast Flow deteriorates when the temperature is raised from 22°C to 42°C. The effects are more noticeable for the weaker binding, softer and less thermally stable haemoglobin molecule (Fig. 6.5b). Here, partial unfolding on adsorption exacerbated at the higher temperature, leads to multi-layer protein binding, evidenced by capacities 5 times greater than

those observed for His_6-GFP (Fig. 6.6, i.e. >120 mg/mL *cf.* <25 mg/mL). By contrast, the adsorption of His_6-GFP is less affected by the 20°C rise (Figs 6.5a and 6.6), for example, the q_{max} falls ~25% (from 25 to 19.5 mg/mL) and the K_d rose slightly from 2.6 to ~2.9 mg/mL resulting in reduction in the tightness of binding (i.e. the initial slope of the isotherm, q_{max}/K_d) from 9.7 to 6.7 mL/mL matrix (Table 6.2). The most significant differences between the binding behaviour of the haemoglobin *cf.* His_6-GFP to Cu^{2+} – Chelating Sepharose fast Flow are the weaker binding strength, but much higher binding capacity, and more marked deterioration in binding performance with temperature increase from 22 to 42°C. The isotherm results suggested that both model proteins (i.e. single layer binding region) are suitable candidates to evaluate the adsorption and desorption performance on Cu^{2+} – Chelating Sepharose Fast Flow and thermal responsive polymer surface modified magnetic pariticles during temperature changes (from 22 to 42°C).

Table 6.2 Langmuir parameters[a] describing the adsorption of bovine haemoglobin and His_6-GFP to Cu^{2+} – Chelating Sepharose Fast Flow at 22 and 42°C.

Protein	Temperature (˚C)	q_{max} (mg/mL)	K_d (mg/mL)	Initial slope, Q_{max}/K_d (mL/mL)
Bovine haemoglobin	22	56.85	25.45	2.23
	42	31.27	21.47	1.46
His_6-GFP	22	25.00	2.58	9.69
	42	19.50	2.92	6.68

Key: [a]Figures 6.5a and 6.5b adsorption data were fitted to the Langmuir model (Eqn. 6.1).

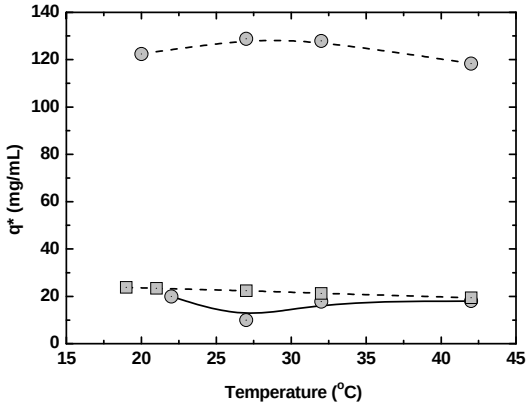

Fig. 6.6 'Q* vs. temperature' plots for His_6-GFP in the non-linear high occupancy binding region (--■--) and haemoglobin in both linear single layer binding (–●–) and non-linear multiple layer (--●--) binding regions.

Figure 6.7 shows the impact that adsorption temperature/history has on ease of target recovery from supports under two sets of conditions, namely desorption at the temperature used for adsorption, and desorption at room temperature. It is important to recognise that reducing the temperature under binding conditions is clearly not an effective means for recovering either target protein from a support surface featuring 'immobile' i.e. Cu^{2+}-IDA ligands (examine the areas shaded light grey of Figs 6.7a and 6.7c). In fact, the best recoveries under binding conditions were obtained from supports that had not been exposed to a temperature change, and moreover the optimum temperatures for haemoglobin (Fig. 6.7b) and His_6-GFP (Fig. 6.7d) recovery

appeared protein dependent, i.e. 27°C for haemoglobin (24% desorbed) and 42°C for His_6-GFP (17% desorbed).

Very different patterns of behaviour were noted for imidazole induced elution (shown by diagonal lines on white) of haemoglobin and His_6-GFP. For Cu^{2+}-IDA supports heavily saturated with multi-layers of haemoglobin (binding challenge = 150 mg/mL adsorbent; Fig. 6.7a) imidazole mediated elution at 22°C desorbed ~10% of haemoglobin bound at 22 and 42°C, and just half this amount at the intermediate temperatures (27 and 32°C) (Fig. 6.7a). Interestingly, much better haemoglobin recoveries were observed from supports that had been challenged with 5 – fold less haemoglobin per mL of adsorbent. Here, a distinct optimum haemoglobin recovery (of ~43%) was observed when both binding and elution were performed at 27°C. An altogether different response was displayed for His_6-GFP regardless of whether desorption was performed at room temperature (Fig. 6.7c) or the adsorption temperature (Fig. 6.7d), i.e. increasing the adsorption temperature made subsequent elution with imidazole progressively more effective (rising from *ca.* 48 at 19°C to 63 – 70% at 42°C recovery).

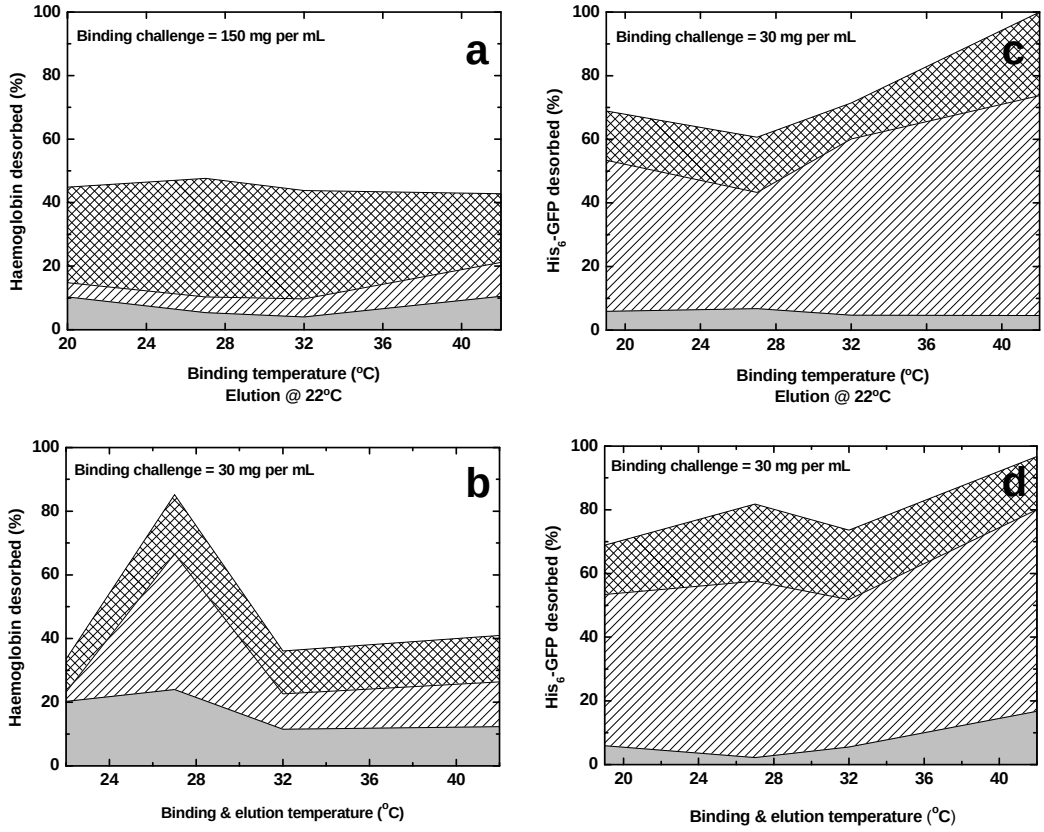

Fig. 6.7 Impact of adsorption temperature on subsequent recovery of **(a & c)** haemoglobin and **(c & d)** His_6-GFP from Cu^{2+} charged Chelating Sepharose Fast Flow. Protein saturated supports (non-linear binding range after being challenged with protein at 30 or 150 mg/mL of adsorbent) were treated at room temperature (a & c) or adsorption temperature b & d). Each support was exposed sequentially to a total of 10 washes, i.e. 4 washes of binding buffer only (light grey), followed by 5 washes with 0.2 M imidazole (diagonal lines on white) and finally a single NaOH stripping treatment (cross-hatching on white).

Further evidence that changing the bulk phase temperature under binding conditions cannot be employed for recovering target proteins from 'immobile' Cu^{2+}-IDA ligand bearing surfaces is illustrated in Figure 6.8. In these experiments repeated temperature switching was employed over 4 of the 10 desorption cycles by increasing the wash temperature to 42°C during washes 3 and 5. It is noticeable that the highest release of both His_6-GFP (Fig. 6.8a) and haemoglobin (Fig. 6.8b) during thermal switching occurred during these hot washes. The very tight binding of His_6-GFP to Cu^{2+} at 20°C in binding

buffer noted earlier (Fig. 6.5a, Table 6.2) was reflected in calculated partition coefficients[6], α, very close to unity (i.e. α = 0.996 for 'cold' washes 4 & 6), and raising the temperature to 42°C exerted hardly any relaxation in binding affinity (α = 0.985 for 'hot' washes 3 and 5). A similar pattern with respect to variation in α during temperature switching under binding conditions was observed for weaker binding haemoglobin (i.e. mean α values of 0.980 for the 'cold' and 0.972 for the 'hot' washes).

[6] Numerically, the partition or distribution coefficient, α, equals the amount of adsorbed target species divided by total target species in the system (i.e. the sum of the adsorbed and free target).

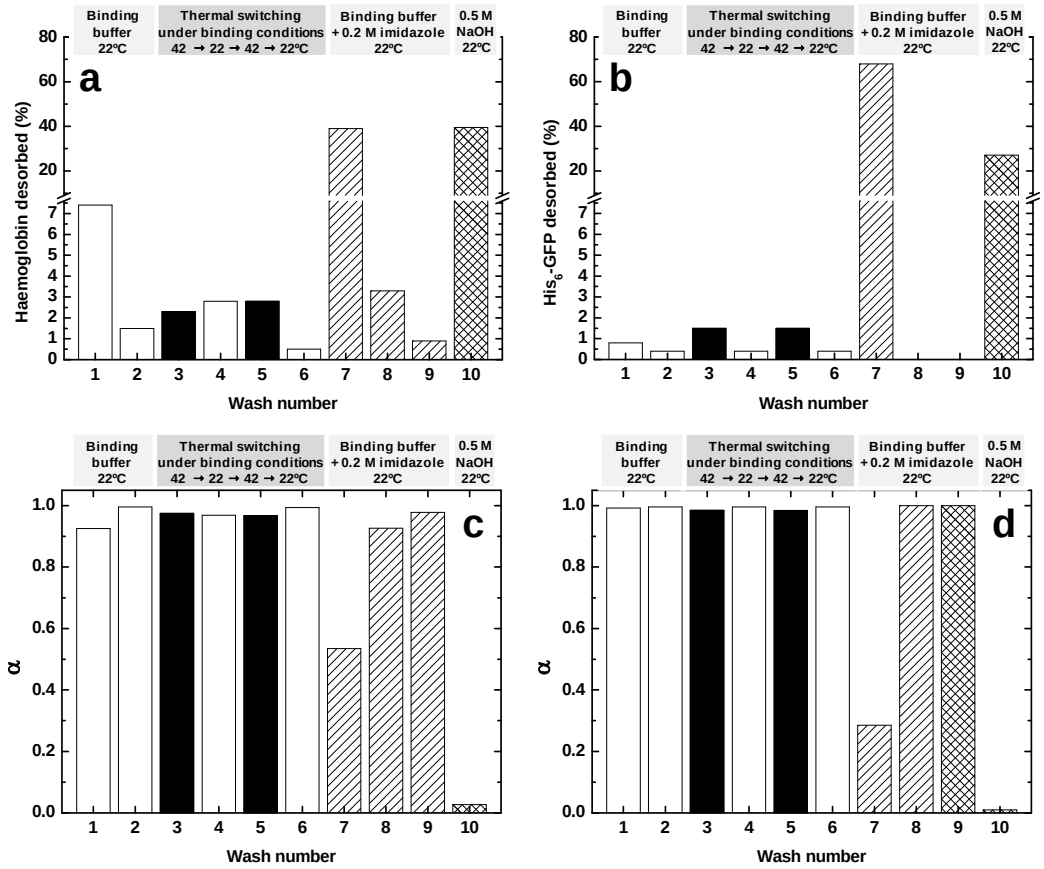

Fig. 6.8 Recovery of bovine haemoglobin **(a)** and His_6-GFP **(b)** from Cu^{2+} charged Chelating Sepharose Fast Flow by temperature switching under binding conditions, and corresponding partition coefficients (α) exhibited by the supports for haemoglobin **(c)** and His_6-GFP **(d)** at each step. Supports loaded with haemoglobin to a capacity of 21.5 mg/mL (linear region of isotherm in Fig. 6.5b) and His_6-GFP to a capacity of 26.2 mg/mL were exposed to 10 sequential wash treatments. In between each wash the supports were recovered by settling under gravity, the supernatants were removed for analysis of desorbed protein content, and the supports were then resuspended in the next wash solution in the series. Key: the base colour of the bars reflects the temperature employed in each case, i.e. 'white' for 20°C and 'black' for 42°C; elution with imidazole and stripping with sodium hydroxide are indicated by 'diagonal lines' and 'cross-hatching' respectively.

Full recovery, following thermal switching, of the either residually bound target protein from Cu^{2+}- Chelating Sepharose Fast Flow could not be achieved by competitive elution with 0.2 M imidazole at 20°C. A single imidazole mediated elution (wash 7) dislodged 68% of the originally bound His_6-GFP (Fig. 6.8b), but only 39% of the bound haemoglobin (Fig. 6.8a), reflecting operational α values of 0.285 for His_6-GFP (Fig. 6.8d) and 0.535 for haemoglobin (Fig. 6.8c).

Subsequent imidazole treatments (washes 8 & 9) recovered small additional amounts of haemoglobin, but failed to desorb any further His_6-GFP.

Substantial 'irreversible' binding to Cu^{2+} – Chelating Sepharose Fast Flow was experienced in these experiments for both target proteins, but was worse for softer more labile haemoglobin *cf.* His_6-GFP (reflected during stripping with 0.5 M NaOH; Fig. 6.8, wash 10). Achieving effective desorption of target proteins carrying high numbers of surface accessible histidine residues from immobilised metal affinity supports coordinating Cu^{2+} ions is tricky, and is made all the more difficult when the target protein is soft (Gekko and Hasegawa, 1990, Kondo *et al.,* 1993) and liable to unfold on binding, as is likely the case for bovine haemoglobin (O'Brien et al., 1997).

6.4.2. Manufacture and characterisation of homopolymer and mixed polymer brush fimbriated M-PVA supports

In this work, Cerium (IV) initiated graft from polymerisation procedures advanced previously in our laboratories (Brown, 2009; Brown et al., 2013; Willett, 2009; Zourna, 2009) were employed to convert an underivatised beaded magnetic support into three different adsorbent materials (Figs 6.3, 6.4 and Table 6.1), i.e.: two featuring tethered linear homopolymer brushes, one of pNIPAAm and the other of pVI; and a third bearing roughly equal numbers of both linear polymers grafted into the same surface in two sequential steps.

Mino and Kaizerman (1958) were the first to propose the use of cerium (IV) as an initiator for the generation of graft copolymers following their demonstration that nitrate and sulphate salts of Ce(IV) are highly effective redox systems when employed in the presence of organic reductants, e.g. alcohols, thiols, glycols, aldehydes and amines. Odian and Kho (1970) subsequently described the chemistry involved when Ce(IV) is employed with poly(vinyl alcohol), pVA, as substrate[7]. Chain growth radical polymerisation from pVA is initiated by removing hydrogen atoms from its backbone. The abstracted hydrogen atoms are subsequently oxidised to hydrogen ions in a reversible redox reaction between pVA and Ce^{4+} ions, during which the latter are reduced to Ce^{3+} and free radicals are generated along the now 'activated' polymer backbone. These immobilised radicals react rapidly with the vinyl functions of the 'free solution' monomers so that initiation of polymerisation occurs only at the surface of the polymer (Mino and Kaizerman, 1958; Müller, 1986, 1990), and polymer chains grow out from the substratum. The main advantage of Ce(IV) initiated polymer grafting is that the polymer chain length and inter-chain spacing can be controlled by tailored the amounts of monomer and catalytic Ce^{4+} initially present in the reaction.

The left hand side of Table 6.1 summarises the key parameters used in the synthesis of the homopolymer and mixed polymer brush modified supports manufactured and used in this work. The pNIPAAm and pVI fimbriated M-PVA materials were made in single Ce(IV) initiated 'graft from' procedures using

[7] According to Odian and Kho (1970) the efficiency of cerium (IV) graft polymerisation appears to be related to the propensity of Ce^{4+} ions to form 'complexes' with appropriate polymers, but the exact nature of its interaction with pVA is not understood. Odian and Kho (1970) and Pitfield (1992) indicate that the Ce^{4+} ion's size enable it to accommodate it within 'pockets' formed between adjacent or proximal secondary hydroxyls along pVA's backbone, whereas larger species (e.g. Ce^{3+}) cannot.

conditions Brown (2009) identified as optimal for the preparation of poly(acrylic acid) (pAAc) fimbriated M-PVA cation exchange adsorbents with extraordinarily high binding capacities for basic target proteins, i.e. q_{max} values up to 832 mg/g.

FT-IR methods were employed extensively in this work both qualitatively, i.e. for the physico-chemical characterisation of the support starting material, intermediates during conversion, and the final polymer brush modified materials themselves (Figs 6.9 – 6.11), and quantitatively on the pre- and post- polymerisation reaction supernatants for estimation of monomer consumption, and from this the amounts of the various polymers grafted on the different supports. For sake of clarity FT-IR spectra for the underivatised M-PVA starting material are shown in all three figures (i.e. Figs 6.9 – 6.11) to ease identification of new peaks corresponding to grafted species, and all spectra are normalised for peak height at 1130 cm^{-1}, given that this region is characteristic of C-O stretching in polyvinyl alcohol (PVA) (Tretinnikov et al., 2013).

Fig. 6.9 FT-IR spectra of M-PVA supports before and after Ce(IV) initiated 'graft from' polymerisation with NIPAAm.

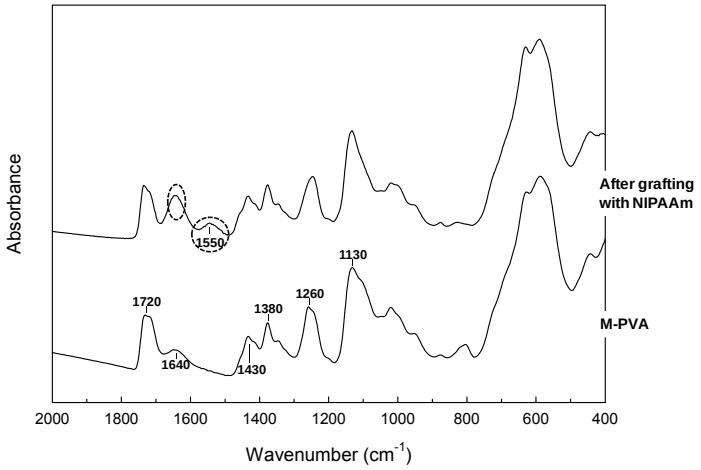

Fig. 6.10 FT-IR spectra of M-PVA supports before and after Ce(IV) initiated 'graft from' polymerisation with NIPAAm.

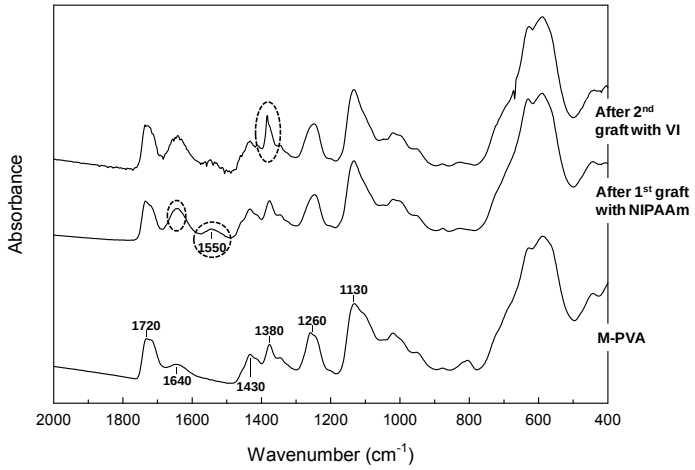

Fig. 6.11 FT-IR spectra of M-PVA supports before and after Ce(IV) initiated 'graft' from polymerisation with VI.

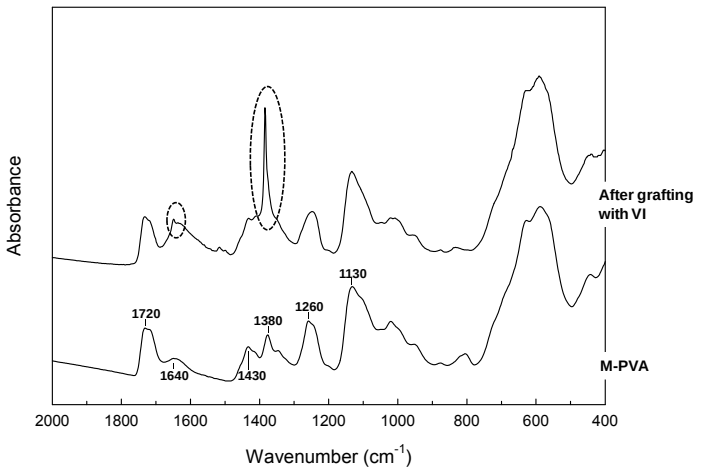

The FT-IR spectrum of unmodified M-PVA shows the expected peaks associated with the pVA backbone, namely CH_2 scissoring and bending at the 1430 cm^{-1}, and alcohol C-O stretches at 1070-1160 cm^{-1}. The prominent peak at 1720 cm^{-1} likely corresponds to carbonyl C=O stretch and is indicative of

the presence of residual acetate groups left over following incomplete hydrolysis of poly(vinyl acetate) pVAc to pVA. Additional peaks at 1380 cm^{-1} (CH_3 bend), and 1260 cm^{-1} (C-C(O)-C stretch) also confirm the presence of acetate groups in M-PVA.

Successful grafting of pNIPAAm into the M-PVA surface was confirmed following Ce(IV) initiated graft polymerisation using NIPAAm for both the 'finished' pNIPAAm modified M-PVA (Fig. 6.9) and 'intermediate' during synthesis of the mixed [pNIPAAm + pVI] modified (Fig. 6.10) by the appearance of a new peak at 1550 cm^{-1}, corresponding to N-H bending in the amide groups of pNIPAAm. An increase in peak height at 1640 cm^{-1} was also seen in both cases (Figs 6.9 & 6.10), corresponding to amide C=O stretching in pNIPAAm.

Two new peaks appeared following Ce(IV) initiated fimbriation of M-PVA with VI (Fig. 6.11) indicating that grafting of pVI into the M-PVA surface had been successful. One of these at 1640 cm^{-1} corresponds to aromatic C-C stretching on the imidazole ring, and the other at 1380 cm^{-1} is consistent with in-plane aromatic C-H wagging. Moreover, the same sharp aromatic C-H wagging peak at 1380 cm^{-1} was also noted, though reduced in magnitude, following the second stage grafting of pVI into the surface of the pNIPAAm fimbriated intermediate (Fig. 6.10), but growth in the signal at 1640 cm^{-1} could not be discerned, most likely owing to masking contributions from the amide C=O of pNIPAAm grafted in the previous step. However, the actural physical length of pVI and pNIPAAm chains is under further investigation.

In the present study the treatment of M-PVA (SA = 55 m^2/g) with an overall ammonium cerium (IV) nitrate initiator concentration of 0.44 mmol/g M-PVA (Table 6.1) resulted in a calculated inter-graft spacing (D") in the all three finished supports of 4.6 Å. The inter-graft spacing of the pNIPAAm intermediate (D') formed during manufacture of the mixed polymer fimbriated support after the first grafting reaction with 0.22 mmol Ce^{4+}/g in the presence of NIPAAm was calculated as 6.5 Å (Table 6.1). These values rest on the assumption that all of Ce^{4+} ions supplied will initiate the outgrowth of grafted polymer chains from the nonporous surface of M-PVA.[8]

The amounts of the NIPAAm and VI monomers supplied in reactions (110 mmol NIPAAm/g M-PVA and 44 mmol VI/g M-PVA corresponding to $DP_{100\%}$ of 250 and 100 respectively; see Table 6.1) were adjusted (based on calibration experiments performed by Zourna, 2009) so that the observed degree of polymerisation (DP_{obs}) of the grafted chains of the polymer brush layers and total amounts of grafted polymer were roughly the same (i.e. DP_{obs} = 20 – 22; 8.75 – 9.35 mmol monomer installed/g M-PVA; grafted polymer contents of 46.5 – 51.7% w/w in the 'finished' supports; Table 6.1).

It should be noted that much higher amounts of NIPAAm monomer were supplied in the Ce(IV) reactions *cf.* VI. The reason for this is that different monomers are consumed at different rates in Ce(IV) initiated graft from reactions performed in aqueous solution. For example, complete monomer consumption was observed in reactions with acrylic acid (AAc) (Brown, 2009)

[8] Brown and Zourna have confirmed that complete disappearance of Ce^{4+} from the reaction liquor occurs within the first 15 minutes. Note, rapid Ce^{4+} disappearance from solution likely reflects pVA's affinity for this species (see previous footnote), but it does not necessarily follow that all Ce^{4+} trapped by the pVA are reduced to Ce^{3+} thereby generating free radicals.

and VI (Zourna, 2009) when supplied at monomer to Ce^{4+} ratios of 20:1, but fell sharply as the ratio was increased (i.e. 59% for AAc at a monomer/Ce^{4+} ratio of 100:1 falling to 25% at 400:1; *cf.* 31-38% for VI at monomer Ce ratio of 100:1). In contrast, monomer consumption for NIPAAm in Ce(IV) initiated grafting reactions was poor (8-12%) at all monomers/Ce^{4+} ratios (20, 100 and 250 to 1) investigated by Zourna (2009). For this reason meeting the target DP_{obs} for pNIPAAm of *ca.* 20 in this study for both the pNIPAAm fimbriated and mixed polymer brush modified M-PVA supports required the use of a monomer/Ce^{4+} ratio of 250:1 in NIPAAm grafting reactions (Table 6.1).

6.4.3. Equilibrium protein adsorption behaviour of Cu^{2+} charged 'homo' and 'mixed polymer brush modified M-PVA supports

The experiments described here are for three polymer modified M-PVA supports with a common final inter-chain spacing of 4.6 Å and polymer chain length of 20 – 22. Hereafter, these support materials will be referred to by the idealised descriptions of their polymer brush layers given in Table 6.1, i.e.: $p(VI)_{21}$ – 4.6 Å; $p(NIPAAm)_{22}$ – 4.6 Å; and [$p(NIPAAm)_{20}$ + $p(VI)_{20}$] – 4.6 Å. The right hand side of Figure 6.11 shows equilibrium adsorption isotherms for His_6-GFP on the polymer brush M-PVA supports after charging with immobilised Cu^{2+} ions. The isotherms were determined at near neutrality at which pH surface accessible histidines are uncoordinated and free to coordinate bound metal ions (Todd *et al.,* 1994; O'Brien *et al.,* 1997), and were well fitted to the Langmuir model (parameters cited in Table 6.3).

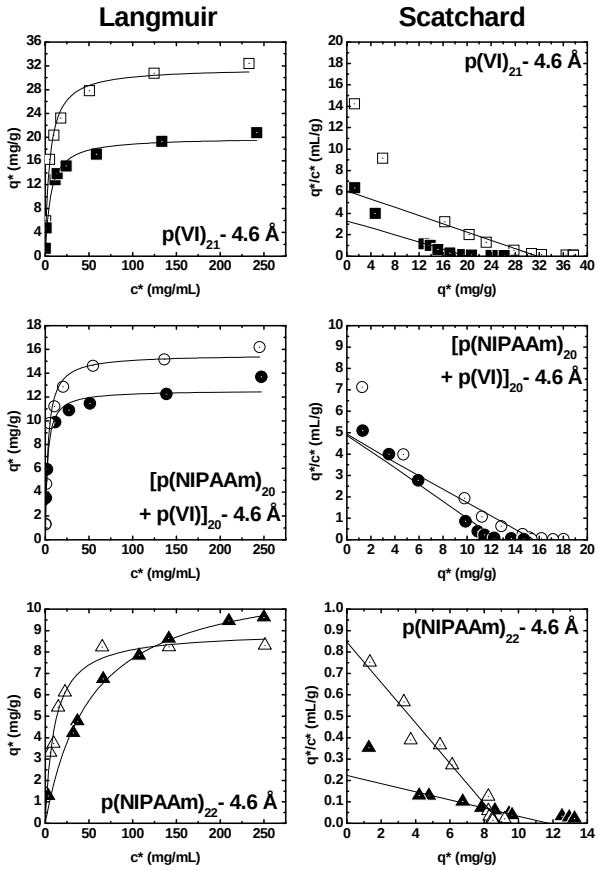

Fig. 6.12 Equilibrium binding isotherms (right) and Scatchard (1949) plots (left) for the binding of His_6-GFP to Cu^{2+} charged 'homo' and 'mixed' polymer brush modified M-PVA supports at 22°C (open symbols) and 42°C (filled symbols). The solid lines through the data sets in both types of plots represent the Langmuir curves fitted to the q* vs. c* data points with the parameter values presented in Table 6.3. The *x*- and *y*- axes intercepts on the Scatchard plots thus respectively represent the q_{max} and initial slope (q_{max}/K_d) cited in Table 6.3.

However, Scatchard (1949) plots (left hand side of Fig. 6.12) for the pVIcontaining brush supports (especially $p(VI)_{21}$ – 4.6 Å) showed slight upward curvature indicative of more complex binding behaviour consistent with at least two different types of binding affinity. As noted earlier (Fig. 6.5) for protein sorption to Cu^{2+}-IDA Sepharose Fast Flow better target binding performance at 22°C *cf.* 42°C was also noted for the Cu^{2+} charged polymer fimbriated M-PVA supports (Fig. 6.12, right). However, the degree of separation of the low and high temperature plots was generally greater (Fig. 6.12, right). For example, in the case of Cu^{2+} – $p(VI)_{21}$ – 4.6 Å dropping the

adsorption temperature from 42 to 22°C degree resulted in a 38% fall in q_{max}, a 17% rise in the K_d and near halving in the tightness of binding (Table 6.3).

Table 6.3 Langmuir parameters[a] describing the adsorption of His_6-GFP to Cu^{2+} charged 'homo' and 'mixed' polymer brush modified M-PVA supports.

M-PVA support	Temperature (˚C)	q_{max} (mg/g)	K_d (mg/mL)	Initial slope, q_{max}/K_d (mL/g)
$p(VI)_{21}$ – 4.6 Å	22	31.66	5.18	6.11
	42	19.96	6.10	3.27
[$p(NIPAAm)_{20}$ + $p(VI)_{20}$] – 4.6 Å	22	15.56	3.15	4.94
	42	12.56	2.58	4.87
$p(NIPAAm)_{22}$ – 4.6 Å	22	8.97	10.58	0.85
	42	11.74	52.47	0.22

[a]Figure 6.11 adsorption data were fitted to the Langmuir model (Eqn 6.1).

Quite different effects on individual Langmuir binding parameters were seen for the Cu^{2+} – $p(NIPAAm)_{22}$ – 4.6 Å, but the overall impact of raising the sorption temperature from 22 to 42°C was the same. Here, though q_{max} rose from 9 to 11.7 mg/g, the K_d rose 5 – fold, leading to a 3.9 – fold reduction in q_{max}/K_d (Table 6.3). The support least affected by temperature was the mixed polymer brush M-PVA, Cu^{2+} – [$p(NIPAAm)_{20}$ + $p(VI)_{20}$] – 4.6 Å. The maximum His_6-GFP binding capacities of this hybrid support material lay midway between those exhibited by the two homopolymer fimbriated supports (Table 6.3). The ~20% drop in q_{max} (from 15.6 to 12.6 mg/g) with increase in temperature was offset by an equivalent drop in K_d (Table 6.3).

In accordance with previous reports comparing the binding strength of vinyl imidazole with iminodiacetic acid (Galaev *et al.,* 1997; Kumar *et al.,* 1998a, 1998b, 1999) comparison of the dissociation constants in this work for the binding of His_6-GFP indicate a weaker interaction with Cu^{2+} ions immobilised on the $p(VI)_{21}$ brush modified M-PVA support (Table 6.3, K_d values of 5.2 and

6.1 mg/mL) *cf.* to the tridentate metal chelating iminodiacetic acid (IDA) of Chelating Sepharose Fast Flow (Table 6.2, K_d values of 2.6 and 2.9 mg/mL).

6.4.4. Characterisation of protein binding kinetics of mobile' Cu^{2+} bearing polymer brush layers grafted on M-PVA

The binding of His_6-GFP to the three Cu^{2+} charged polymer brush modified M-PVA supports at 22°C are displayed in Fig. 6.13. It shows that: (i) the kinetics of equilibrium protein binding are exceptionally fast approaching their maximum capacities within 10 – 15 s in all cases[9]; (ii) the capacities follow the order $p(VI)_{21}$ > [$p(NIPAAm)_{20}$ + $p(VI)_{20}$] > $p(NIPAAm)_{22}$; (iii) the contribution of non-Cu^{2+} based binding (Fig. 6.13 legend) rises with increasing pNIPAAm content in the brush, i.e. from 37% for '0% pNIPAAm' ($p(VI)_{21}$ – 4.6 Å) through 43% for '50% pNIPAAm' ([$p(NIPAAm)_{20}$ + $p(VI)_{20}$] – 4.6 Å), to 67% for the '100% pure pNIPAAm' brush modified support ($p(NIPAAm)_{22}$ – 4.6 Å). Contrary to the ideal situation, i.e. where the thermoresponsive polymer shouldn't bind Cu^{2+} or target protein, it appears that pNIPAAm binds both species. Coordination of Cu^{2+} most likely involves its amide nitrogen (Fig. 6.2).

[9] This observation is not surprising in light of the M-PVA's small size (*ca.* 2 μm) and nonporous nature. Indeed, Hoffmann (2002) has previously determined half-times of order of 10 s for the adsorption of different protein species from various feedstocks to the magnetic chelator adsorbents of similar size.

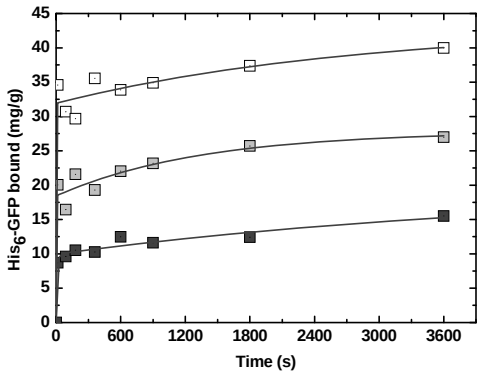

Fig. 6.13 Kinetics of binding at 22°C to Cu^{2+} charged 'homo' and 'mixed' polymer brush modified magnetic M-PVA supports. Key: $p(VI)_{21}$ – 4.6 Å (□); [$p(NIPAAm)_{20}$ + $p(VI)_{20}$] 4.6 Å (■); and $p(NIPAAm)_{22}$ – 4.6 Å (■). In the absence of immobilised Cu^{2+} the His_6-GFP binding capacities (after 1 h) were 13.8, 9.8 and 8.2 mg/g for $p(VI)_{21}$, [$p(NIPAAm)_{20}$ + $p(VI)_{20}$] and $p(NIPAAm)_{22}$ respectively

6.4.5. Influence of additives on the temperature induced phase transition of ungrafted pNIPAAm in solution

The LCST[10] of the pNIPAAm homopolymer in water is widely reported as *ca.* 32°C (Heskins and Guillet, 1968; Taylor and Cerankowski, 1975; Schild, 1992; Maharjan *et al.,* 2008), but is known to be shifted in response to variation in pH (Pei *et al.,* 2004; Maharjan *et al.,* 2008) and the presence of salts (Schild and Tirrell, 1991; Park and Hoffman, 1993; Du *et al.,* 2010; Zhang *et al.,* 2007).

[10] LCST is defined as the temperature at which 50% optical transmittance occurs (Kanazawa *et al.,* 1997).

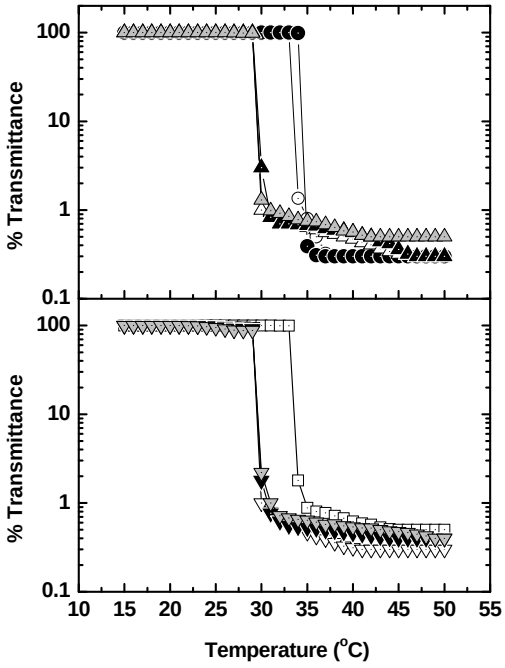

Fig. 6.14 Comparison of temperature-dependent optical transmittance (500 nm) profiles of 4.4 mM solutions of ungrafted free pNIPAAm and pNIPAAm admixed 50:50 with pVI. Top panel – pNIPAAm in water (○), water + 4.4 mM Cu^{2+} (●), in buffer (△), in buffer + 4.4 mM Cu^{2+} (▲), in buffer + 2.2 mM Cu^{2+} (▲).Bottom panel – pNIPAAm + pVI in water (□), in buffer (■), in buffer + 4.4 mM Cu^{2+} (▼), in buffer + 2.2 mM Cu^{2+} (▼).

Figure. 6.14 shows that in the present study the presence of equal numbers of free pVI chains in solution exerted no apparent effect on the temperature dependent 'hydrophilic coil – hydrophobic globule' transition of ungrafted free pNIPAAm. The 'transmittance – temperature' profiles for solutions of pVI in water or buffer, with or without added $CuCl_2$, were optically transparent across the entire temperature range examined (data not shown); consistent with the expected behavior of a polymer exhibiting normal temperature solubility behavior. Conversely the addition of 4 mM $CuCl_2$ to pNIPAAm in water increased the LCST by plus 1°C raising it from 33 to 34°C, while changing the bulk suspending phase from water to buffer (20 mM sodium phosphate pH 6.8 containing 0.2 M NaCl) with or without added $CuCl_2$ shifted by a common minus 4°C (i.e. from 33 to 29°C). The above findings are entirely consistent

with present scientific understanding. The presence of salt in the bulk phase typically lowers the LCST, and this LCST follows the so-called 'Hofmeister series'. According to Du and co-workers (2010) direct interactions between the salt cations and pNIPAAm play a critical role in shifting the LCST as they exhibit much stronger affinity for the polymer *cf.* the anions.

The chain collapse behaviour of pNIPAAm chains tethered to a surface and effective LCST is frequently reported as quite different to that of free pNIPAAm in solution (Zhulina *et al.,* 1991; Zhu and Napper, 1994; Zhu and Napper, 1997; Hu *et al*., 2002; Balamurugan *et al*., 2003; Kizhakkedathu *et al.*, 2004; Wu *et al*., 2008; Toomey and Tirrell (2008); Müller *et al.,* 2013). The phase behaviour is known to be influenced by the method employed, grafting density, extent of cross-linking, architecture and molecular weight of the tethered pNIPAAm chains (Baulin and Halperin, 2003; Yim *et al*., 2004; Plunkett *et al*., 2006; Müller *et al.,* 2013). However, in the present case for linear pNIPAAm chains grown out of the surface of M-PVA supports by Ce(IV) initiated 'graft from' polymerisation Zourna (2009) has shown that lower transition temperature for pNIPAAm chains tethered to M-PVA surfaces (32 – 34°C) is the same as that of the free polymer (33°C in water; see Fig. 6.14).

6.4.6. Characterisation of the effects of temperature on target protein desorption from 'mobile' Cu^{2+} bearing polymer brush layers grafted on M-PVA

In stark contrast to the very poor to non-existent thermally mediated elution from 'immobile' Cu^{2+}-IDA ligands observed for the commercial immobilised metal affinity matrix, Cu^{2+} – Chelating Sepharose Fast Flow, temperature

switching proved much more effective with 'mobile' Cu^{2+} bearing polymer brush modified M-PVA supports. Following binding at room temperature, the supports were washed 9 times in succession and in the process 8 temperature switches were made using the two thermomixer set up (one set at 42°C, the other at 22°C) described in 6.3.7.

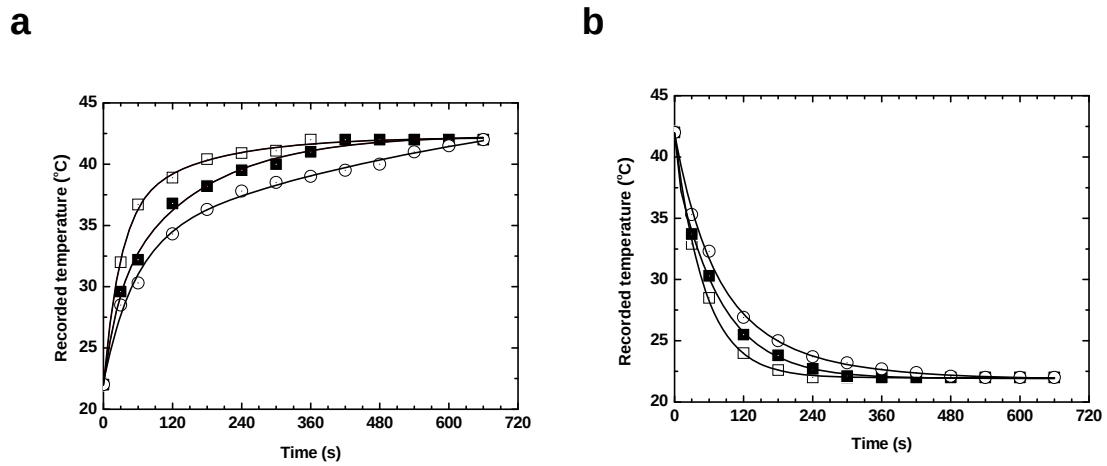

Fig. 6.15 Kinetics of: **(a)** heating of 22°C samples in a thermomixer set at 42°C; and **(b)** cooling of 42°C samples in a thermomixer set at 22°C. Samples of binding buffer (20 mM sodium phoshate, pH 6.8 containing 0.2 M NaCl) of 0.5 mL (□), 1 mL (■) and 2 mL (○) volumes contained in 2 mL screw-capped Eppendorf tubes were incubated with shaking at 1250 rpm. Tubes were removed after various times and their temperatures were immediately recorded using an electronic handheld two channel thermometer. The solid lines through the data points represent the fitting of second order exponential decay curves with R^2 values between 0.996 and 0.9996.

Control experiments with buffer samples of various volumes (0.5 – 2 mL) were conducted to ascertain how quickly temperature changes were effected using the two thermomixers (Fig. 6.15). It is clear that for both heating (Fig. 6.15a) and cooling (Fig. 6.15b) operations the temperature range 29 – 35°C where pNIPAAm undergoes the most of its phase transition (Fig. 6.14) is reached extremely rapidly, i.e. within the first 30 s. This rapid crossing of the LCST explains why the observed kinetics of His_6-GFP desorption from Cu^{2+} –

charged polymer fimbriated non-porous M-PVA supports can be as fast as they appear in Fig. 6.16.

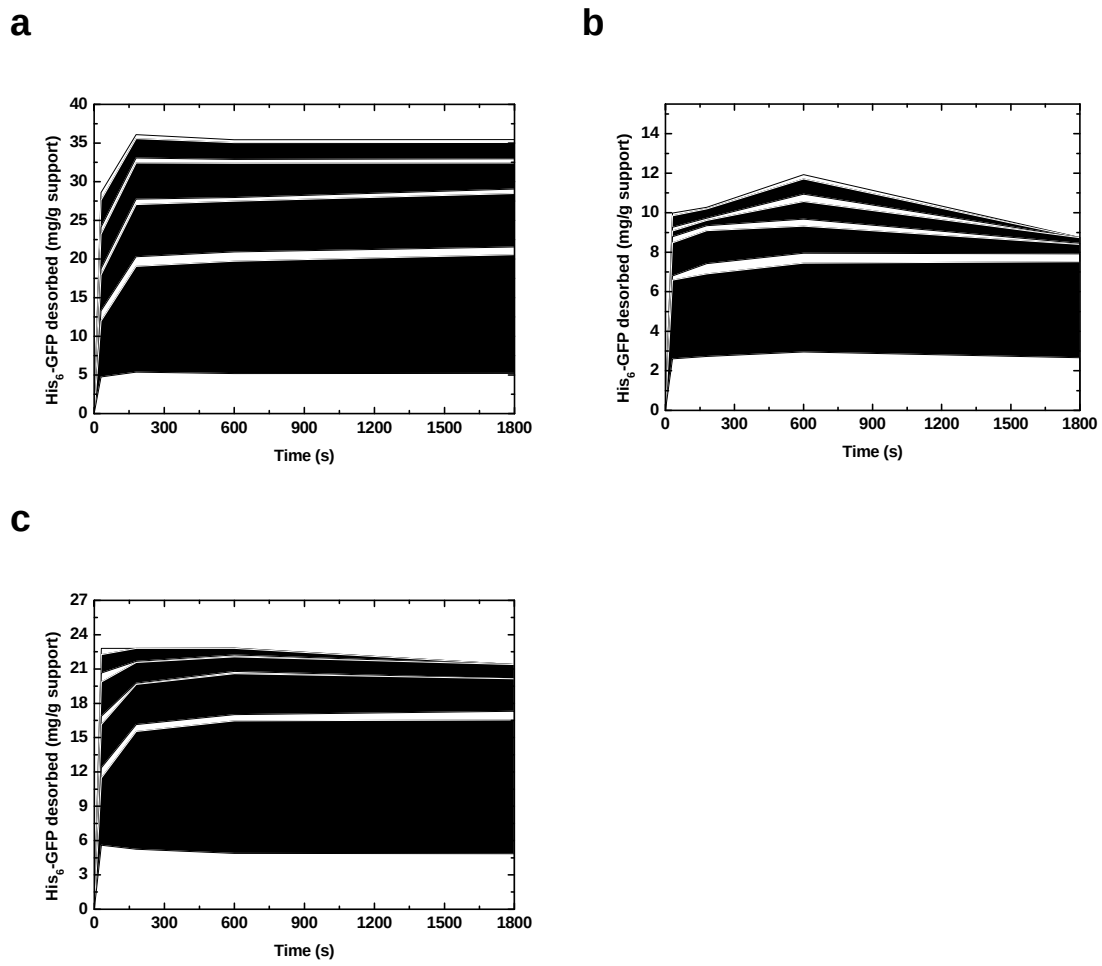

Fig. 6.16 Kinetics of thermally mediated eluted elution from Cu^{2+} charged **(a)** $p(VI)_{21}$ – 4.6 Å, **(b)** $p(NIPAAm)_{22}$ – 4.6 Å and **(c)** $[p(NIPAAm)_{20} + p(VI)_{20}]$ – 4.6 Å modified M-PVA. Supports contacted with His_6-GFP for 1 h at 22°C magnetically separated, washed once at 22°C (wash 1) by resuspension in binding buffer before subjecting to 8 sequential temperature transitions with fresh binding buffer (washes 2 – 9), i.e. 42 → 22 → 42 → 22 → 42 → 22 → 42 → 22°C, for various times (30 – 1800 s) under binding conditions.The amounts of His_6-GFP bound prior to washing $p(VI)_{21}$, $p(NIPAAm)_{22}$ and $[p(NIPAAm)_{20} + p(VI)_{20}]$ modified M-PVA supports were 40, 27 and 15.5 mg/g respectively. The maximum vertical scale of the plots are set to these values and reflect 100% desorption in each case.

It is noteworthy that in all cases more effective desorption was observed at the higher temperature, and His_6-GFP recovery after 9 washes (8 thermal changes) was very good, i.e. reaching >77% for Cu^{2+} – $p(NIPAAm)_{22}$ – 4.6 Å, >84% for Cu^{2+} – $[p(NIPAAm)_{20} + p(VI)_{20}]$ – 4.6 Å and >90% for Cu^{2+} – $p(VI)_{21}$

– 4.6 Å. It is noticeable that for the mixed brush modified (Fig. 6.15c) and especially pVI grafted (Fig. 6.15a) M-PVA all of 'hot' cycles were more effective than 'cold' wash cycles. For the Cu^{2+} charged $p(VI)_{21}$ – 4.6 Å modified support maximum desorption was reached after just 180 s in every wash cycle and there was no evidence of detached His_6-GFP rebinding to the support at longer times (Fig. 6.16c). Quite different behaviour was exhibited by Cu^{2+} charged [$p(NIPAAm)_{20}$ + $p(VI)_{20}$] – 4.6 Å (Fig. 6.16c) and especially Cu^{2+} – $p(NIPAAm)_{22}$ – 4.6 Å (Fig. 6.16b). Here, maximum His_6-GFP desorption was noted later, at 600 s. Moreover, at longer times the level of free His_6-GFP fell, providing clear evidence of rebinding (esp. noticeable for Cu^{2+} – $p(NIPAAm)_{22}$ – 4.6 Å.

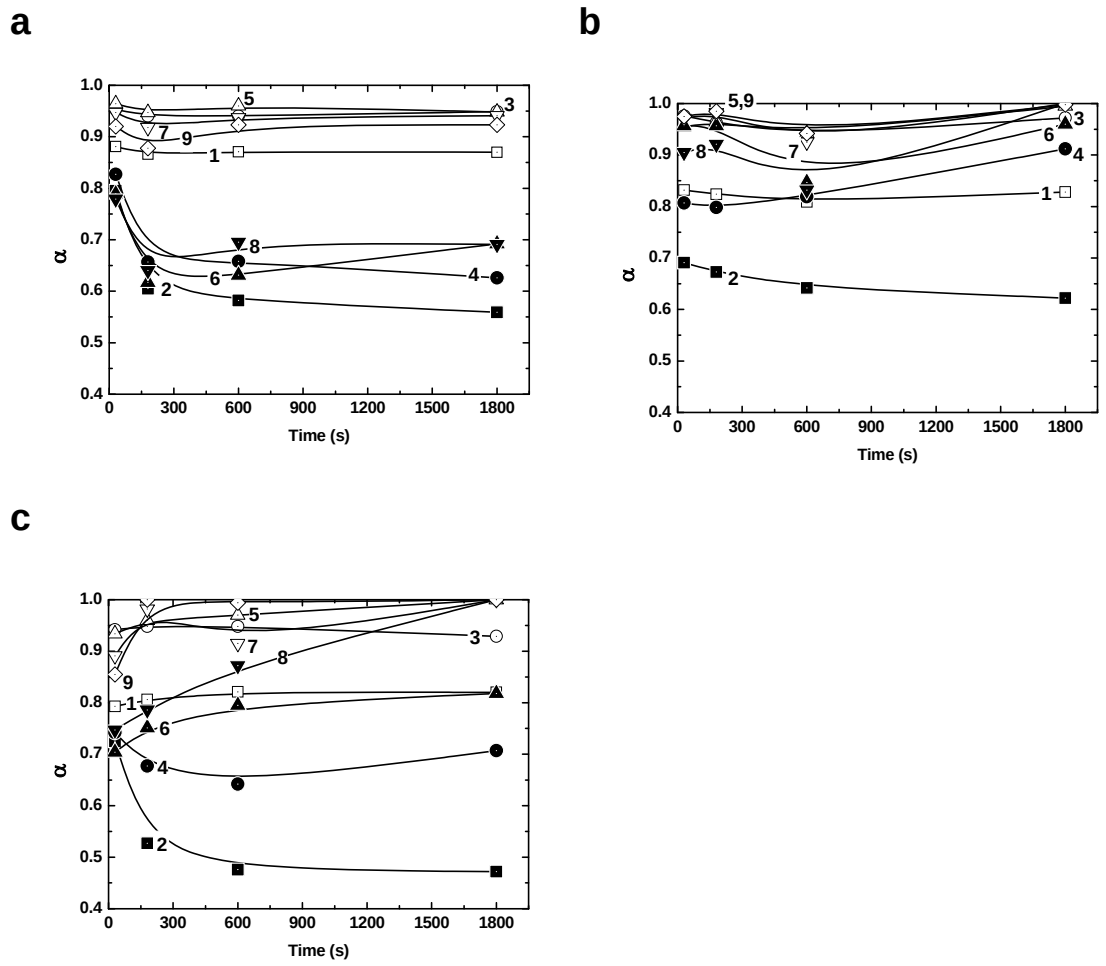

Fig. 6.17 'α vs. time' plots derived from the thermally mediated His_6-GFP elution data presented in Fig. 6.13**.** Panel: (a) Cu^{2+} charged $p(VI)_{21}$ – 4.6 Å; (b) Cu^{2+} charged $p(NIPAAm)_{22}$ – 4.6 Å; and (c) Cu^{2+} charged [$p(NIPAAm)_{20}$ + $p(VI)_{20}$] – 4.6 Å modified M-PVA. Symbols: Low (22°C) and high (42°C) temperature washes are indicated by open and filled symbols respectively; Wash number: 1 (□); 2 (■); 3 (○); 4 (●); 5 (△);6 (▲); 7 (▽); 8 (▼); and 9 (◇).

The superior performance of the Cu^{2+} – $p(VI)_{21}$ – 4.6 Å M-PVA material in the thermally mediated elution study (Fig. 6.16) is clarified by reference to α vs time plots (Fig. 6.17) derived from the same data. In stark contrast to the simliar α values recorded earlier for the binding of His_6-GFP to Cu^{2+} – Chelating Sepharose Fast Flow during 'cold' (α = 0.996) and and 'hot' (α = 0.985) transitions (Fig. 6.8b), at all times points beyond 180 s (Fig. 6.17a), α values during the 'hot' washes were significantly lower ($0.56 < \alpha < 0.69$)

than those during the 'cold' ones ($0.87 < \alpha < 0.96$). Moreover, α remained relatively constant throughout the 8 temperature transitions of the experiment.

For the first 'hot' wash, α values for Cu^{2+} – $p(NIPAAm)_{22}$ – 4.6 Å (Fig. 6.17b) were comparable to those for Cu^{2+} – $p(VI)_{21}$ – 4.6 Å (Fig. 6.17a), but as the support was cycled through further temperature transitions the difference in α values for 'hot' and 'cold' washes was lost. A similar, but less pronounced pattern was revealed for the Cu^{2+} charged mixed brush material, $[p(NIPAAm)_{20} + p(VI)_{20}]$ – 4.6 (Fig. 6.17c). The effectiveness of the 'hot' washes in desorbing His_6-GFP fell progressively with each new transition as α rose from 0.47 – 0.53 in the first, through 0.68 – 0.71 in the second, and 0.75 – 0.82 in the third, finally reaching 0.79 – 1.0 in the last.

Taken collectively, the data for Cu^{2+} – $p(VI)_{21}$ – 4.6 Å clearly hint at a support material that can be used repeatedly, whereas those featuring pNIPAAm containing brushes evidently cannot.

6.5. **Conclusions**

Studies with Cu^{2+} charged Chelating Sepharose Fast Flow (fixed or immobile Cu^{2+}-IDA ligands) confirmed little/no elution by temperature switching under binding conditions. In stark contrast, work with polymer brush modified supports (mobile Cu^{2+} coordinating brush layers) demonstrated significant thermally mediated elution.

Opposite to earlier observations with thermoresponsive anion (Liu, 2009) and cation (Müller *et al.,* 2013) exchange media fashioned in our laboratories of effective protein desorption only occurring when the temperature is lowered,

for the Cu^{2+} charged metal affinity polymers in this work more powerful elution was observed during the 'hot' transition. The best thermally mediated elution of His_6-GFP was demonstrated by the Cu^{2+}charged homo pVI brush modified M-PVA. The optimal mode of operation for this support would likely be room temperature adsorption followed by elution at an elevated temperature determined by the thermal stability of the target binding species. For Cu^{2+} charged pVI, the large difference in partition coefficient at 22 and 42°C *cf.* that observed for Cu^{2+} charged Sepharose Fast Flow can be explained by the synergistic effects of heating on: (i) the intrinsic binding strength of the target protein for its coordinated Cu^{2+} ligand; coupled with (ii) chain elongation, which increases the ligand spacing, hence reducing the tightness of binding. By contrast, in supports featuring pNIPAAm chains, the latter undergo collapse on heating. This chain collapse opposes the inherent thermodynamic weakening of 'Cu^{2+} – target protein' interactions, by reducing the spacing, effectively raising the ligand density.

Contrary to the thermoresponsive ion-exchange matrices detailed previously (Liu, 2009; Müller et al., 2013), the overall conclusion here regarding the utility of smart thermoresponsive polymers such as pNIPAAm in combination with immobilised metal affinity surfaces is that it is flawed. While changing the thermoresponsive polymer to one lacking a nitrogen centre and possessing a significantly lower LCST (e.g. newer PEG based alternatives; Lutz et al., 2006; Lutz and Hoth, 2006; Magnusson *et al.,* 2008; Müller *et al.,* 2013) should reduce non-specific binding, uncouple immobilised metal affinity adsorption from gross brush extension and collapse, and minimise thermal denaturation and unfolding at the support surface, the overriding problem is that shifting to

low temperature to effect brush extension is strongly counteracted by significantly increased binding strength. In this particular instance use of pVI alone appears to be the best option. This metal chelating polymer is temperature sensitive, but displays normal rather than inverse temperature solubility behaviour.

6.6. **References**

Adrados, B.P., Galaev, I.Y. Nilsson, K. and Mattiasson, B. (2001), Size exclusion behavior of hydroxypropylcellulose beads with temperature-dependent porosity, *J. Chromatogr. A* 930: 73-78.

E. Ayano, E. Y. Okada, Y., Sakamoto, C., Kanazawa, H., Kikuchi, A., Okano, T. (2006a), Study of temperature-responsibility on the surfaces of a thermo-responsive polymer modified stationary phase, *J. Chromatogr. A* 1119: 51-57.

Ayano, E., Nambu, K., Sakamoto, C. Kanazawa, K., Kikuchi, K. Okano, T. (2006b), Aqueous chromatography system using pH- and temperature-responsive stationary phase with ion-exchange groups, *J. Chromatogr. A* 1119: 58-65.

Balamurugan S., Mendez S., Balamurugan S. S., O'Brien, M. J and Lopez G.P. (2003), Thermal response of poly(*N*-isopropylacrylamide) brushes probed by surface plasmon resonance, *Langmuir,* 19: 2545-2549.

Baulin V. A., Halperin A. (2003), Signatures of a concentration-dependent Flory χ parameter: Swelling and collapse of coils and brushes, *Macromol. Theory Simul,* 12: 549-559.

Bradford, M.M. (1976), A rapid and sensitive method for the quantitation of microgram quantities of protein utilizing the principle of protein-dye binding, *Anal. Biochem.* 72, 248-254.

Brooks, D.E. and Müller, W. (1996), Size-exclusion phases and repulsive protein-polymer interaction/recognition, *J. Mol. Recognit.* 9: 697–700.

Brooks, D.E., Haynes, C.A., Hritcu, D., Steels, B.M. and Müller, W. (2000), Size-exclusion chromatography does not require pores, *Proc. Natl. Acad. Sci. (USA)* 97: 7064-7067.

Brown, G.N. (2009), *Advances magnetic particle based bioprocessing*, PhD thesis, University of Birmingham, UK.

Brown, G.N., Müller, C., Theodosiou, E., Franzreb, M. and Thomas, O.R.T. (2013), Multi-cycle recovery of lactoferrin and lactoperoxidase from crude whey using fimbriated high-capacity magnetic cation exchangers and a novel 'rotor-stator' high-gradient magnetic separator, *Biotechnol. Bioeng.* 110(6): 1714-1725.

Chang, C., Wei, H., Wu, D.-Q., Yang, B., Chen, N., Cheng, S.-X., Zhang, X.-Z. and Zhuo, R.-X. (2011), Thermo-responsive shell cross-linked PMMA-b-P(NIPAAm-co-NAS) micelles for drug delivery, *Int. J. Pharmaceut.* 420: 333–40.

Clementi, M.E., Condo, S.G., Castagnola, M. and Giardina, B. (1994), Hemoglobin function under extreme life conditions, *Eur. J. Biochem.* 223: 309–317.

Digel, I., Maggakis-Kelemen, C., Zerlin, K.F., Linder, P., Kasischke, N., Kayser, P., Porst, D., Temiz Artmann, A. and Artmann, G.M. (2006), Body temperature-related structural transitions of monotremal and human haemoglobin, *Biophys. J.* 91: 3014-2021.

Du H, Wickramasinghe R. and Qian X. (2010), Effects of salt on the lower critical solution temperature of poly (N-isopropylacrylamide), *J. Phys. Chem. B.* 114(49): 16594-16604.

Finette, G.M.S., Mao, Q.-M. and Hearn, M.T.W. (1997), Comparative studies on the isothermal characteristics of proteins adsorbed under batch equilibrium conditions to ion-exchange, immobilised metal ion affinity and dye affinity matrices with different ionic strength and temperature conditions, *J. Chromatogr. A* 763(1-2): 71-90.

Galaev I.Y., Kumar A., Agarwal R., Gupta M.N. and Mattiasson, B. (1997), Imidazole - a new ligand for metal affinity precipitation. Precipitation of Kunitz soybean trypsin inhibitor using Cu(II)-loaded copolymers of *1*-Vinylimidazole with *N*-Vinylcaprolactam or *N*-Isopropylacrylamide, *Appl. Biochem. Biotechnol*, 68: 121-133.

Galaev, I.Y. and. Mattiasson, B. (1999), 'Smart' polymers and what they could do in biotechnology and medicine, *Trends Biotechnol.* 17: 335-340.

Gekko, K. and Hasegawa, Y. (1986), Compressibility-structure relationship of globular proteins, *Biochemistry* 25: 6563-6571.

Gewehr, M., Nakamura, K., Ise, N. and Kitano, H. (1992), Gel permeation chromatography using porous glass beads modified with temperature-responsive polymers, *Die Makromolekulare Chemie* 193: 249-256.

Hemdan, E.S. and Porath, J. (1985), Development of immobilized metal affinity chromatography: III. Interaction of oligopeptides with immobilized nickel iminodiacetate, *J. Chromatogr. A* 323(2): 265-272.

Hochuli, E. (1988), Large-scale chromatography of recombinant proteins, *J. Chromatogr.* 444: 293-302.

Hoffman, A.S. and Stayton, P. (2004), Bioconjugates of smart polymers and proteins: synthesis and applications, *Macromol. Symp.* 207: 139-151.

Hosoya, K., Sawada, E., Kimata, K., Araki, T., Tanaka, N. and Fréchet, J.M.J. (1994), In situ surface-selective modification of uniform size macroporous polymer particles with temperature-responsive poly-N-isopropylacrylamide, *Macromolecules* 27: 3973-3976.

Hosoya, K., Kimata, K., Araki, T., Tanaka, N. and Fréchet, J.M.J (1995), Uniform-size hydrophobic polymer-based separation media selectively modified with a hydrophilic external polymeric layer, *Anal. Chem.* 67: 1907-1911.

Hoffman, C. (2002), *Einsatz magnetischer Separationverfahren zur biotechnologischen Produktaufarbeitung*, PhD thesis, University Fridericiana Karlsruhe, Karlsruhe, Germany.

Hritcu D., Muller W. and Brooks D.E. (1999), Poly(styrene) latex carrying Cerium(IV)-initiated terminally attached cleavable chains: Analysis of grafted chains and model of the surface layer, *Macromolecules*, 32: 565-573.

Hu, T., You, Y., Pan, C.Y. and Wu, C. (2002), The coil-to-globule-to-brush transition of linear thermally sensitive poly(*N*-isopropylacrylamide) chains grafted on a spherical microgel, *J. Phys. Chem. B*, 106*:* 6659-6662.

Hummel, D.O., Göttgens, S., Neuhoff, U. and Düssel, H.-J. (1995), Linear-temperature programmed pyrolysis of thermoresistant polymers – mass and FT-IR spectrometries. Part 3. Poly(1,4-phenylene terephthalamide) and aromatic polyimides, *J. Analyt. Appl. Pyrol.* 33: 195-212.

Hutchens, W.T. and Yip, T.-T. (1991), Protein interactions with surface-immobilized metal ions: Structure-dependent variations in affinity and binding capacity with temperature and urea concentration, *J. Inorg. Biochem.* 42(2): 105-118.

Ista, L.K., Perez-Luna, V.H., Lopez, G.P., Pérez-luna, V.H. and López, G.P. (1999), Surface-grafted, environmentally sensitive polymers for biofilm release. *Appl. Enviiron. Microbiol.* 65: 1603-1609.

Jagschies, G. (2008), Where is biopharmaceutical manufacturing heading? An analysis of current and upcoming industry challenges, BioPharm Inter. 21 (October) 72-77.

Janzen, R., Unger, K.K., Müller, W. and Hearn, M.T.W. (1990), Adsorption of proteins on porous and nonporous poly(ethyleneimine) and tentacle-type anion-exchangers, *J. Chromatogr.* 522: 77-93.

Kanazawa, H., Kashiwase, Y., Yamamoto, K., Matsushima, Y., Kikuchi, A., Sakurai, Y. and Okano, T. (1997), Temperature-responsive liquid chromatography. 2. Effects of hydrophobic groups in N-isopropylacrylamide copolymer-modified silica, *Anal. Chem.* 69: 823-30.

Kanazawa, H., and Okano, T. (2011), Temperature-responsive chromatography for the separation of biomolecules, *J. Chromatogr. A* 1218: 8738-8747.

Kanazawa, H., Yamamoto, K., Matsushima, Y., Takai, N., Kikuchi, A., Sakurai, Y. and Okano, T. (1996), Temperature-responsive chromatography using poly(N-isopropylacrylamide)-modified silica, *Anal. Chem. 68*: 100-105.

Kanazawa, H., Nishikawa, M., Mizutani, A., Sakamoto, C., Morita-Murase, Y., Nagata, Y., Kikuchi, A. and Okano, T. (2008), Aqueous chromatographic system for separation of biomolecules using thermoresponsive polymer modified stationary phase, *J. Chromatogr. A* 1191: 157-161.

Kikuchi, A., Okuhara, M., Karikusa, F., Sakurai, Y. and Okano, T. (1998),Two-dimensional manipulation of confluently cultured vascular endothelial cells using temperature-responsive poly(*N*-isopropylacrylamide)-grafted surfaces, *J. Biomater. Sci. Polym. Ed.* 9: 1331-1348.

Kizhakkedathu, J.N., Jones N.R. and Brooks E.D. (2004), Synthesis of well-defined environmentally responsive polymer brushes by aqueous ATRP, *Macromolecules* 37: 734-743.

Kobayashi, J., Kikuchi, A., Sakai, K. and Okano, T. (2002), Aqueous chromatography utilizing hydrophobicity- modified anionic temperature-responsive hydrogel for stationary phases, *J. Chromatogr. A* 958: 109-119.

Kobayashi, J., Kikuchi, A., Sakai, K. and Okano, T. (2003), Cross-linked thermoresponsive anionic polymer grafted surfaces to separate bioactive basic peptides, *Anal. Chem.* 75: 3244-3249.

Kondo, A., Oku, S., Murakami, F. and Higashitani, K. (1993), Conformational changes in protein molecules upon adsorption to ultrafine particles, *Colloid Surface* 1: 197-201.

Kubota, K., Fujishige, S. and Ando, I. (1990), Single-chain transition of poly(N-isopropylacrylamide) in water, *J. Phys. Chem.* 94: 5154-5158.

Kumar A., Galaev, I. Y. and Mattiasson, B. (1998a), Affinity precipitation of -amylase inhibitors from wheat meal by metal chelate affinity binding using Cu(II)-loaded copolymers of 1-vinylimidazole with *N*-isopropylacrylamide, *Biotechnol. Bioeng.* 59(6): 695-704.

Kumar A., Galaev, I.Y. and Mattiasson, B. (1998b), Isolation and separation of α-amylase inhibitors I-1 and I-2 from seeds of ragi (Indian finger millet, *Eleusine coracana*) by metal chelate affinity precipitation, *Bioseparation* 7: 129-136.

Kumar A., Galaev, I.Y. and Mattiasson, B. (1999), Metal chelate affinity precipitation: a new approach to protein purification, *Bioseparation* 7: 185-194.

Li, Y., Agrawal, A., Sakon, J. and Beitle, R.R. (2001), Characterization of metal affinity of green fluorescent protein and its purification through salt promoted, immobilized metal affinity chromatography. *J. Chromatogr. A* 909: 183-190.

Liu, H. (2009), *Application of new materials and tools in bioseparations*, PhD thesis, University of Birmingham, UK.

Luo, X., Goh, S.H., Lee, S.Y. and Huan, C.H.A. (1999), Spectroscopic studies of interactions in complexes of poly(1-vinylimidazole) with poly(styrenesulfonic acid) or the zinc salt of poly(styrenesulfonate), *Macromol. Chem. Phys.* 200: 874-880.

Lutz. J-F., Akdemir, Ö. and Hoth, A. (2006), Point by point comparison of two thermsensitive polymers exhibiting a similar LCST: Is the age of poly(NIPAM) over? *J. Am. Chem. Soc.* 128: 13046-13047.

Lutz. J-F. and Hoth, A. (2006) Preparation of ideal PEG analogues with a tunable thermosensitivity by controlled radical copolymerization of 2(-2-methoxyethoxy) methacrylate and oligo(ethylene glycol) methacrylate, *Macromolecules* 39: 893-896.

Luzinov, I., Minko, S. and Tsukruk, V.V. (2004), Adaptive and responsive surfaces through controlled reorganization of interfacial polymer layers, *Progr.Polym. Sci.* 29: 635–698.

Magnusson, J.P, Khan, A., Pasparakis, G., Saeed, A.O., Wang, W. and Alexander, C. (2008), Ion-sensitive “isothermal” responsive polymers prepared in water, *J. Am. Chem. Soc.* 130: 10582-10853.

Maharjan, P., Hearn, M.T.W., Jackson, W.R., De Silva, K. and Woonton, B.W. (2009), Development of a temperature-responsive agarose-based ion-exchange chromatographic resin, *J. Chromatogr. A* 1216: 8722-8729.

Matsuda, N, Shimizu, T., Yamato, M. and Okano, T. (2007), Tissue engineering based on cell sheet technology, *Adv. Mater.* 19: 3089-3099.

Mino, G. and Kaizerman, S. (1958), A new method for the preparation of graft copolymers. Polymerization initiated by ceric ion redox systems, *J. Polym. Sci.* 31: 242-243.

Müller, T.K.H., Cao, P., Ewert, S., Wohlgemuth, J., Liu, H., Willett, T.C., Theodosiou, E., Thomas, O.R.T. and Franzreb, M. (2013), Integrated system for temperature-controlled FPLC comprising improved copolymer modified beaded agarose adsorbents and a travelling cooling zone reactor (TCZR) arrangement', *J. Chromatogr. A*, 1285: 97-109.

Müller, W. (1986), New phase supports for liquid-liquid partition chromatography of bio-polymers in aqueous poly(ethyleneglycol)-dextran systems – synthesis and application for the fractionation of DNA restriction fragments. *Eur. J. Biochem.* 155(1):213-222.

Müller, W. (1990), New ion exchangers for the chromatography of biopolymers, *J. Chromatogr.*, 510: 133-140.

Nagase, K., Kobayashi, J., Kikuchi, A., Akiyama, Y., Kanazawa, H., Annaka, M. and Okano, T. (2010), Preparation of Thermoresponsive Anionic Copolymer Brush Surfaces for Separating Basic Biomolecules, *Biomacromolecules* 11: 215-223.

Odian, G. and Kho, J. H. T. (1970), Ceric ion initiated graft polymerization onto poly(vinyl alcohol), *J. Macromol. Sci. Chem.* A4(2): 317-330.

Okano, T., Yamada, N., Okuhara, M., Sakai, H. and Sakurai, Y. (1995), Mechanism of cell detachment from temperature-modulated, hydrophilic-hydrophobic polymer surfaces, *Biomaterials 16:* 297-303.

Okano, T., Yamada, N., Sakai, H. and Sakurai, Y. (1993), A novel recovery system for cultured cells using plasma-treated polystyrene dishes grafted with poly(N-isopropylacrylamide), *J.Biomed. Mater. Res.* 27: 1243-1251.

Omer, M., Haider, S., and Park, S.-Y. (2011), A novel route for the preparation of thermally sensitive core-shell magnetic nanoparticles, *Polymer 52*: 91-97.

O'Brien, S.M., Sloane, R.P., Thomas, O.R.T. and Dunnill, P. (1997), Characterisation of non-porous magnetic chelator supports and their use to recover polyhistidine-tailed T4 lysozyme from a crude *E. coli* extract. *J. Biotechnol.* 54: 53-67.

Pei, Y., Chen, J., Yang, L., Shi, L., Tao, Q., Hui, B. and Li, J. (2004), The effect of pH on the LCST of poly(N-isopropylacrylamide) and poly(N-isopropylacrylamide-co-acrylic acid), *J. Biomater. Sci. Polym. Ed.* 15(5): 585-94.

Pitfield, I.D. (1992), *Perflurocarbon chromatographic supports*, PhD thesis, University of Cambridge, UK.

Plunkett, K.N., Xi, Z., Moore, J.S. and Leckband, D.E. (2006), PNIPAM chain collapse depends on the molecular weight and grafting density, *Langmuir*, 22: 4259-4266.

Przybycien, T.M., Pujar,N.S., Steele, L.M. (2004), Alternative bioseparation operations: Life beyond packed-bed chromatography, Curr. Opin. Biotechnol. 15: 469-478.

Sakamoto, C., Okada, Y., Kanazawa, H., Ayano, E., Nishimura, T., Ando, M., Kikuchi, A. and Okano, T. (2004), Temperature- and pH-responsive aminopropylsilica ion-exchange columns grafted with copolymers of N-isopropylacrylamide, *J. Chromatogr. A* 1030: 247-253.

Scatchard, G. (1949), The attraction of proteins for small molecules and ions, *Ann. New York Acad. Sci.* 51: 660-672.

Scheyhing, C.H., Meersman, F., Ehrmann, M.A., Heremans, K. and Vogel, R.F. (2002), Temperature-pressure stability of green fluorescent protein: a Fourier transform infrared spectroscopy study, *Biopolymers 65:* 244-253.

Schild, H.G. (1992), Poly(N-isopropylacrylamide): experiment, theory and application, *Progr. Polym. Sci.* 17: 163-249.

Takezawa, T., Mori, Y. and Yoshizato, K. (1990), Cell culture on a thermo-responsive polymer surface, *Bio/Technology* 8: 854-856.

Taylor, L.D. and Cerankowski, L.D. (1975), Preparation of films exhibiting a balanced temperature dependence to permeation by aqueous solutions – a study of lower consolute behaviour, *J. Polym. Sci. Part A: Polym. Chem.* 13: 2551-2570.

Teal, H.E., Hu, Z. and Root, D.D. (2000), Native purification of biomolecules with temperature-mediated hydrophobic modulation liquid chromatography, *Anal. Biochem.* 283: 159-165.

Todd, R.J., Haymore, B.L. and Arnold, F.H. (1991) Cu(II)-binding properties of a synthetic metal binding cytochrome *c*: His-X-His in an -helix, *Protein – Struct. Funct. Genet.* 10: 156-161.

Toomey, R. and Tirrell. M. (2008), Functional polymer brushes in aqueous media from self-assembled and surface-initiated polymers, *Annu. Rev. Phys. Chem.*, 59:493-517.

Tretinnikov, O.N., Sushko, N.I. and Zagorskaya, A. (2013), Detection and quantitative determination of the crystalline phase in poly(vinyl alcohol) cryogels by ATR FTIR spectroscopy, *Polym. Sci. A* 55(2): 91-97.

Willett, T.C. (2009), *Magnetic adsorbents displaying switchable ion-exchange behaviour*, PhD thesis, University of Birmingham, UK.

Wu T., Zhang Y., Wang X. and Liu S. (2008), Fabrication of hybrid silica nanoparticles densely grafted with thermoresponsive poly(*N*-isopropylacrylamide) brushes of controlled thickness via surface-initiated atom transfer radical polymerization, *Chem. Mater.* 20: 101-109.

Yakushiji, T., Sakai, K., Kikuchi, A., Aoyagi, T., Sakurai, Y. and Okano, T. (1999), Effects of cross-linked structure on temperature-responsive hydrophobic interaction of PINAAm hydrogel modified surfaces with steroids, *Anal. Chem.* 71: 1125-1130.

Yim, H., Kent M.S., Mendez, S., Balamurugan, S., Balamurugan, S.S., Lopez G.P. and Satija S. (2004), Temperature-dependent conformational change of PNIPAM grafted chains at high surface density in water, *Macromolecules* 37: 1994-1997.

Yoshizako, H., Akiyama, Y., Yamanaka, H., Shinohara, Y., Hasegawa, Y., Carredano, E., Kikuchi, A. and Okano, T. (2002), Regulation of protein binding toward a ligand on chromatographic matrixes by masking and force-releasing effects using thermoresponsive polymer, *Anal. Chem.* 74: 4160-4166.

Zhang, X.-Z., Yang, Y.-Y., Chung, T.-S. and Ma, K.-X. (2001), Preparation and characterization of fast response macroporous poly(N-isopropylacrylamide) hydrogels, *Langmuir* 17: 6094-6099.

Zhang, Y., Furyk, S., Sagle, L.B., Cho, Y., Bergbreiter, D.E. and Cremer, P.S. (2007), Effects of Hofmeister anions on the LCST of pNIPAM as a function of molecular weight, *J. Phys. Chem. C Nanomater. Interfaces* 111(25): 8916-8924.

Zourna, K. (2009), *Smart magnetic affinity adsorbents*, PhD thesis, University of Birmingham, UK.

Zhu P.W. and Napper D.H. (1994), Experimental observation of coil-to-globule type transitions at interfaces, *J. Colloid Interface Sci.,* 164: 489-494.

Zhu P.W. and Napper D.H. (1997), Conformational transitions of poly(*N*-isopropylacrylamide) chains loopily absorbed at the surfaces of poly(*N-tert*-butylacrylamide) latex particles in water, *J. Phys. Chem. B* 101: 3155-3160.

Zhu, X., Yan, C., Winnik, F.M. and Leckband, D. (2007), End-grafted low-molecular-weight PNIPAM does not collapse above the LCST, *Langmuir,* 23: 162-169.

Zhulina, E.B., Borisov, O.V., Pryamitsyn, V.A. and Birshtein, T.M. (1991), Coil-globule type transitions in polymers. 1. Collapse of layers of grafted polymer chains, *Macromolecules* 24: 140-149.

7. General conclusions and future work

Escherichia coli has been extensively researched and widely used for production recombinant proteins. It offers great advantages in terms of economically and procedure complexity to compete with other cell lines (i.e. yeasts, plants, insect cells and mammalian cells). For biopharmaceutical industry, antibodies own invaluable properties for applications in both diagnosis and therapeutic uses. Nearly half century ago, the first mouse monoclonal antibody was made but was limited by human immunogenicity for its therapeutic use. To date, by the advance of genetic engineering, we are not only able to produce humanised monoclonal antibody but also the antibody fragment in various forms. However, the problem remains unresolved are the optimisation of up-stream fermentation and down-stream purifications. Increase products titre is always a goal to pursue during fermentation stage, but the quality of products often being forgotten, which cause hugely issue when comes to down-stream purifications. Several parameters were altered during fermentation to directing desired protein into periplasm of *E.coli* as the periplasm provides the conditions required for appropriate disulphide bond formation and protein folding. Subsequently dramatically ease the following protein extraction and conditioning, by reducing purification steps to increase final production yields.

In Chapter 2, employing lab scale fermentation (5 L) with CLD048 *E.coli* to produce antibody fragment (Anti-HEWL Fab, so called Fab D1.3) demonstrates that in this particular case, *E.coli* was not able to grow and produce recombinant antibody fragment simultaneously, as the result most of

products were leaked into culture broth which leads to another problematic issue for clarify and purify the proteins. Lower the cultivation temperature was the first strategy applied to slow down cell growth therefore prolonged the protein synthesis phase after induction. Induce at various biomass conditions (i.e. OD~1 or 20) seemed to effect on the final yield as well. Induction with lower [IPTG] (0.02 μM) resulted in low production yield, but higher [IPTG] (0.1~0.2 mM) caused cell lysis in the end of fermentation. In the optimal fermentation condition (i.e. batch No.7, induction with 0.2 mM of [IPTG] at OD~20, cultivation temperature decreased from 25°C to 20°C upon induction) has shown partially controlling the majority of Fab D1.3 into desired compartment (periplasm, OS1), also increased overall titre nearly 26 fold (1.849 mg/L cf. 48.06 mg/L) and solubility (24% cf. 60%) compared with the initial result (batch No.1).

Chapter 3 was extended the results obtained in chapter 2 fermentations. Through systematically conditioning/release experiments followed by chromatography purification (HiTrap SP_XL and HiTrap rProtein G) effectively release and purify Fab D1.3 from either directly culture broth or OS1 (periplasmic fraction). Because of the high ionic strength (ca. 35mS/cm) and heavily contaminated extract, conditioning (i.e. pH adjustment and dilutions) was necessary for the subsequent chromatographic step, which leads massive Fab loss during the pH adjustment possibly due to protein aggregation, along with gradually precipitation observed when samples were left overnight at 4°C fridge. As the result, the feedstock was not able to process on chromatography.

A33 Fab′ was successfully produced and extracted by heat treatment in chapter 4 (~300 mg/L, 12.5% of total protein in periplasmic space). We then extended the studies to optimise the Fab release by heat treatment. In large scale, using 1:1 ratio for extracting periplasmic proteins seemed to be the optimal condition, which would ensure the solution and cell mixing properly during extraction process.

Newly developed protein separation technique was employed in chapter 5 benchmarking with commercial available chromatography column (i.e. HiTrap rProtein G and Fractogel EDM SO_3) The results of this study identify CME as a viable means of performing continuous purification of target macromolecules from complex biological feedstocks at relatively low cost.

A preliminary study in chapter 6 confirmed that Cu^{2+} charged Chelating Sepharose Fast Flow (fixed immobile Cu^{2+}-IDA ligands) had very little elution by temperature switching under conditions that favour binding. Meanwhile, the idea for applying the smart thermoresponsive polymers (such as pNIPAAm) in combination with immobilised metal affinity surfaces is not a successful combination. This was because of charging thermoresponsive polymer with Cu^{2+} also give the pNIPAAm the ability to bind with rich histidine proteins which causing non-specific binding. For the future selection of using thermoresponsive polymer would be to one lacking a nitrogen centre and possessing a significantly lower LCST, thus would reduce non-specific binding, uncouple immobilised metal affinity adsorption from gross brush extension and collapse, and minimise thermal denaturation and unfolding at the support surface.

Clearly, future application of the developed generic fermentation improving method in this thesis is of interest. Further studies are to be done to demonstrate exploitation of the effectors of *E.coli* fermentation in producing antibody fragments in this thesis for selective accumulation and release to ease the subsequently downstream purification processes. The influence of upstream changes (i.e. medium composition, timing of induction, phase of growth) on the optimal release is to be investigated. Given the marked changes that can occur in composition of cell envelopes under different growth regimes it will be interesting to see which release method could match with newly developed magnetic separation technique to smooth the transition between upstream and downstream and optimise the whole recombinant protein production process.

8. Appendix

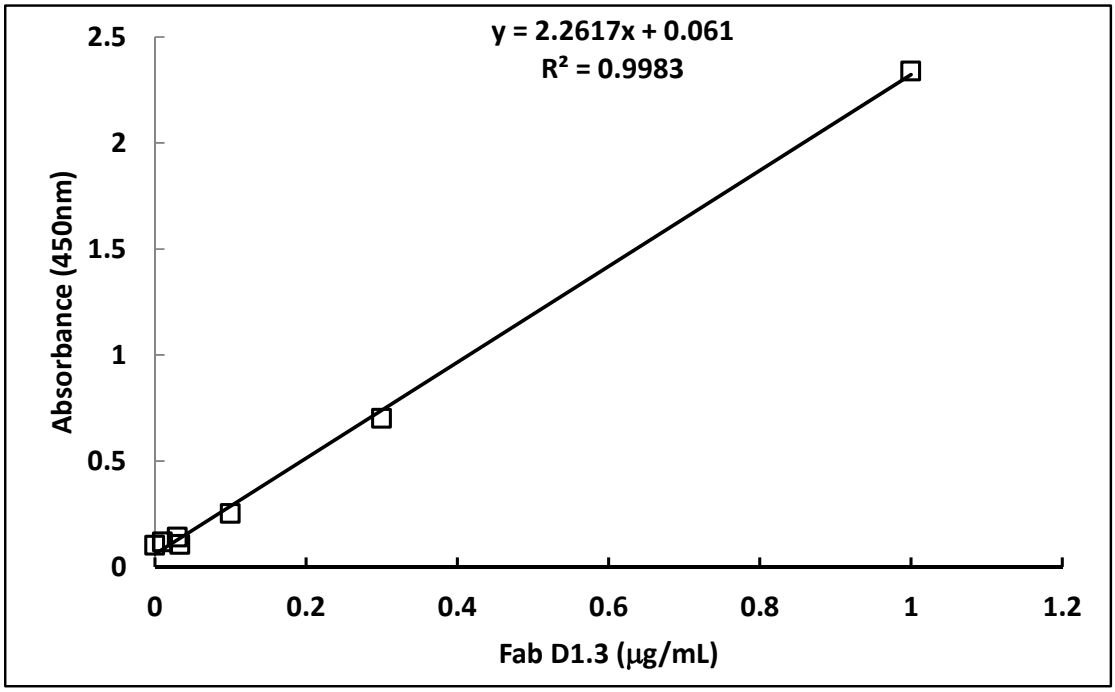

Fig. 8.1 Calibration curve used for calculation of Fab D1.3 concentration in the samples by ELISA.

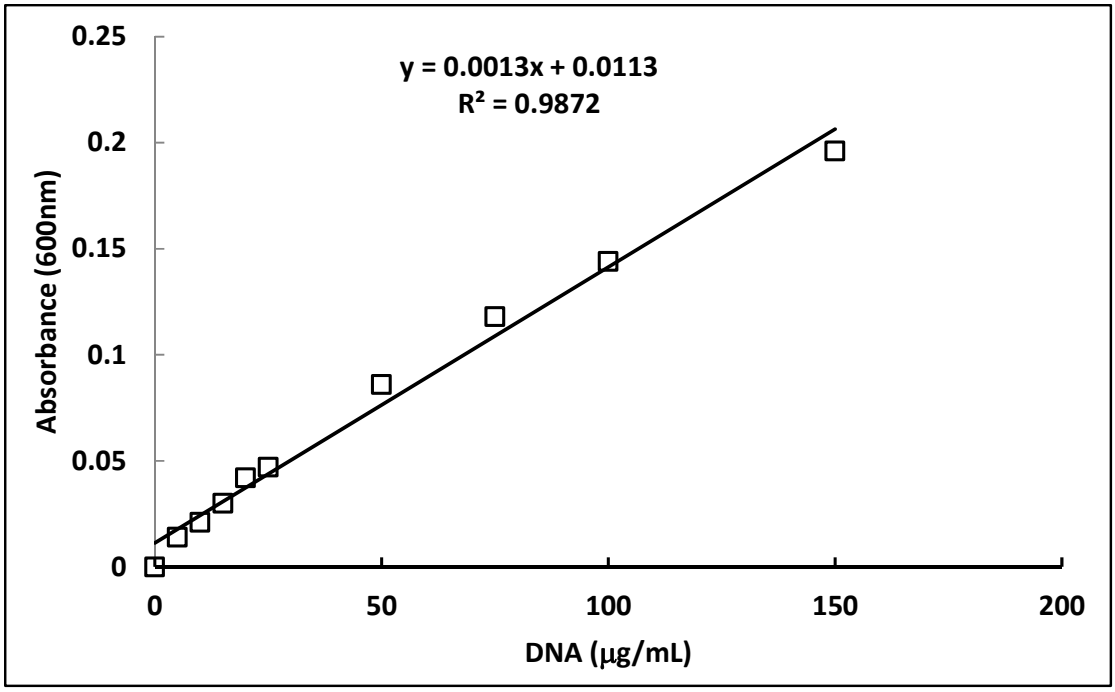

Fig. 8.2 Calibration curve used for calculation of DNA concentration in the samples by DPA assay

.

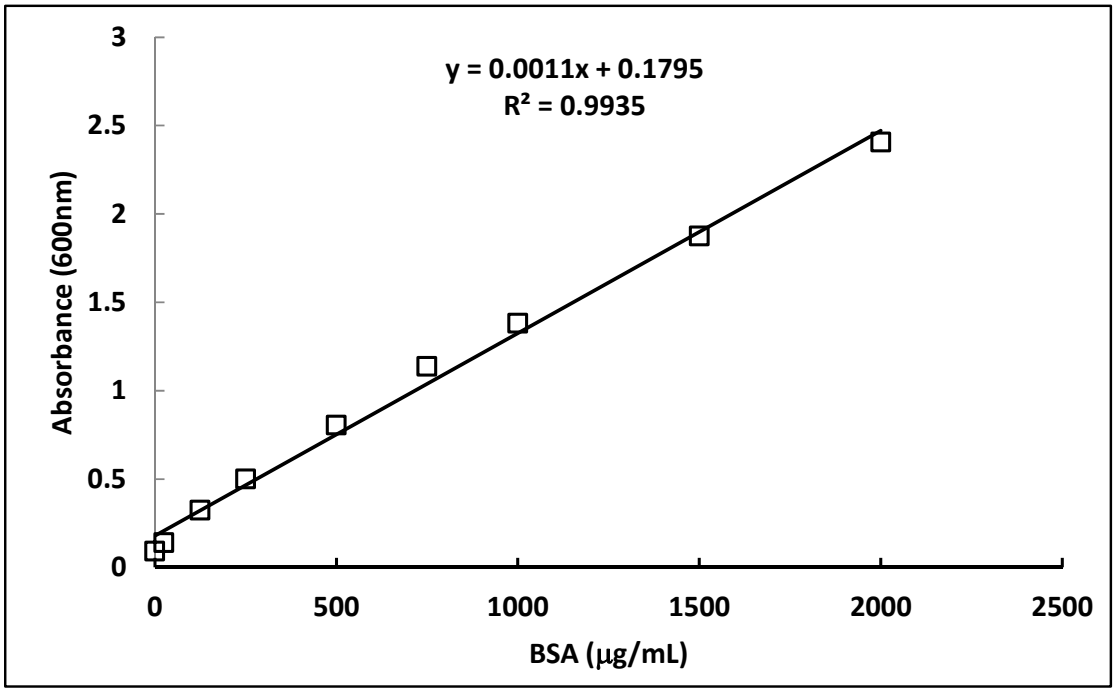

Fig. 8.3 Calibration curve used for calculation of total protein concentration in the samples by BCA assay.

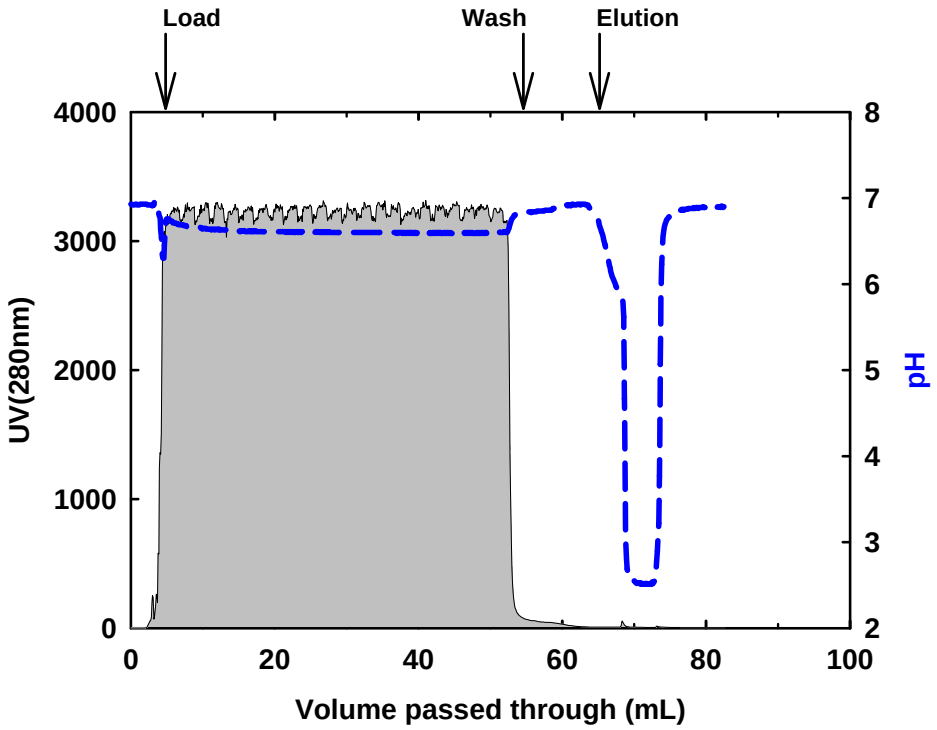

Fig. 8.4 Chromatogram for the purification of Fab D1.3 from culture broth (conductivity ~ 35 mS/cm) on a HiTrap rProtein G column.

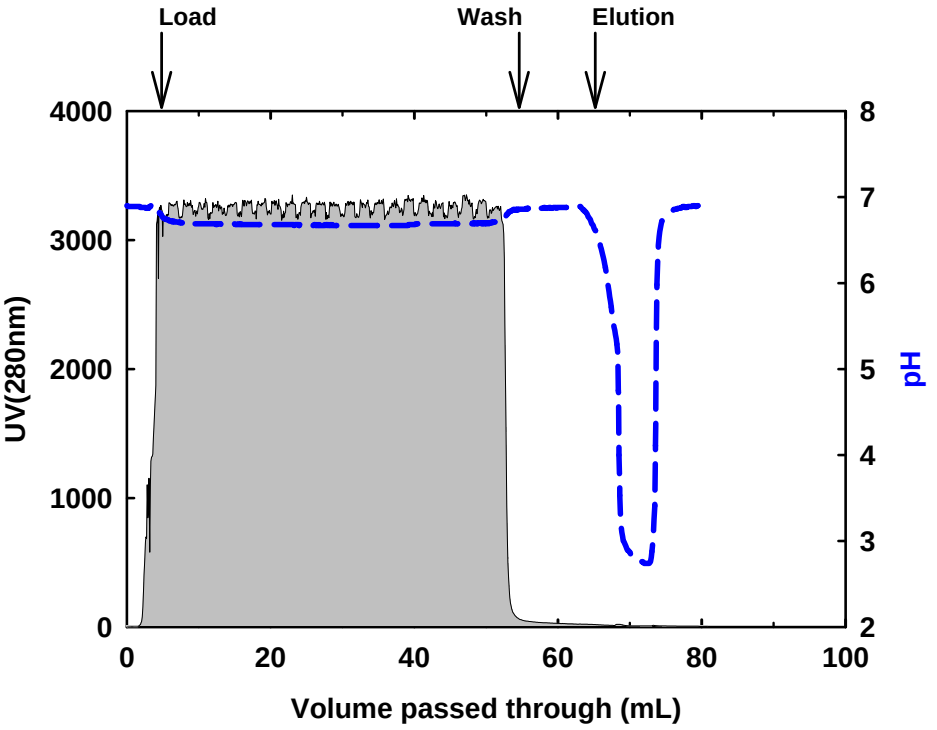

Fig. 8.5 Chromatogram for the purification of Fab D1.3 from benzonase pre-treated culture broth (conductivity ~ 35 mS/cm) on a HiTrap rProtein G column.

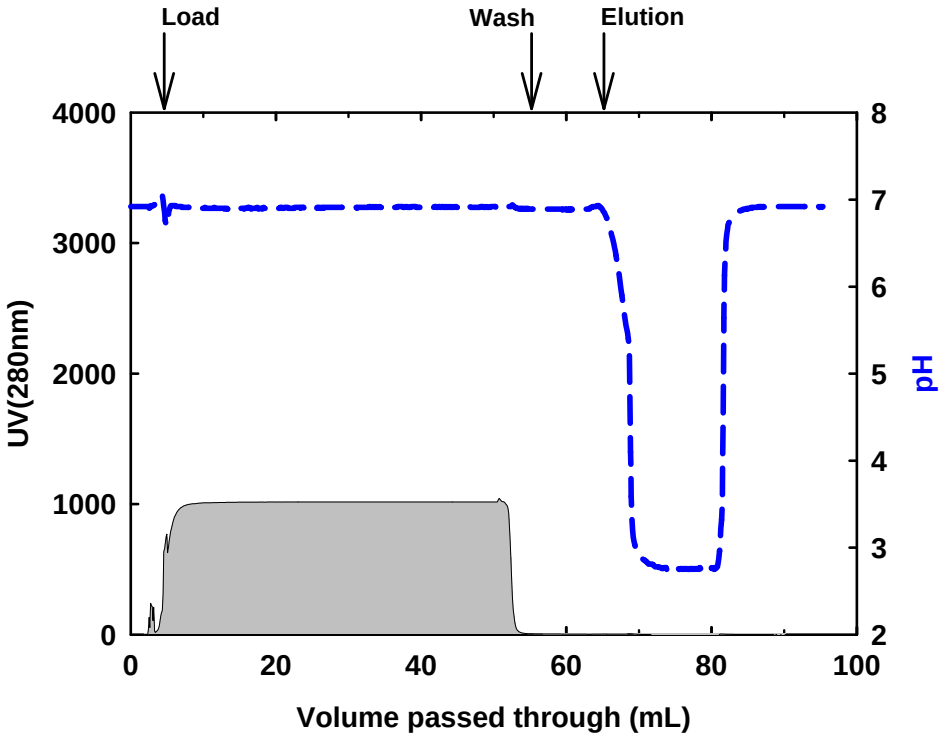

Fig. 8.6 Chromatogram for the purification of Fab D1.3 from 5 times diluted culture broth (conductivity ~ 10mS/cm) on a HiTrap rProtein G column.